Jorge Alves Audino

Evolução da margem do manto em Pteriomorphia (Mollusca: Bivalvia): um modelo para compreensão da macroecologia do bentos marinho

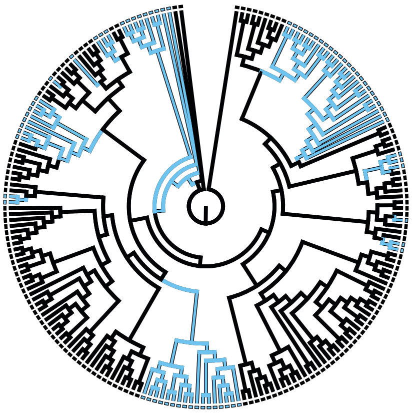

Evolution of the mantle margin in Pteriomorphia (Mollusca: Bivalvia): insights into the macroecology of the marine benthos

São Paulo

2019

Jorge Alves Audino

Evolução da margem do manto em Pteriomorphia (Mollusca: Bivalvia): um modelo para compreensão da macroecologia do bentos marinho

Evolution of the mantle margin in Pteriomorphia (Mollusca: Bivalvia): insights into the macroecology of the marine benthos

São Paulo

2019

Jorge Alves Audino

Evolução da margem do manto em Pteriomorphia (Mollusca: Bivalvia): um modelo para compreensão da macroecologia do bentos marinho

Evolution of the mantle margin in Pteriomorphia (Mollusca: Bivalvia): insights into the macroecology of the marine benthos

Tese apresentada ao Instituto de Biociências da Universidade de São Paulo, para a obtenção de Título de Doutor em Ciências Biológicas, na Área de Zoologia.

Orientador: Prof. Dr. José Eduardo Amoroso
Rodriguez Marian

São Paulo
2019

Ficha catalográfica elaborada pelo Serviço de Biblioteca do Instituto de Biociências da USP,
com os dados fornecidos pelo autor no formulário:
http://www.ib.usp.br/biblioteca/ficha-catalografica/ficha.php

Audino, Jorge Alves
Evolução da margem do manto em Pteriomorphia (Mollusca: Bivalvia) : ampliando o conhecimento sobre macroecologia e diversificação do bentos marinho / Jorge Alves Audino ; orientador José Eduardo Amoroso Rodriguez Marian. -- São Paulo, 2019.

289 f.

Tese (Doutorado) - Instituto de Biociências da Universidade de São Paulo, Departamento de Zoologia.

1. Bivalves. 2. Convergência evolutiva. 3. Filogenia. 4. Microscopia. 5. Ocelos. I. Marian, José Eduardo Amoroso Rodriguez , orient. II. Título.

Bibliotecária responsável pela estrutura da catalogação da publicação:
Elisabete da Cruz Neves – CRB – 8/6228

AGRADECIMENTOS

Gostaria de agradecer a todos aqueles que contribuíram para o desenvolvimento desta tese de doutorado. O árduo trabalho de quatro anos de pesquisa, aqui apresentado, é também fruto do apoio de muitas pessoas e instituições.

Gostaria de agradecer ao Programa de Pós-Graduação em Ciências Biológicas (Zoologia), área de concentração Zoologia, pela oportunidade e desenvolvimento do doutorado. Ao Instituto de Biociências da Universidade de São Paulo (IB-USP), pela infraestrutura fundamental para realização do projeto de pesquisa, bem como pelas disciplinas do curso. Agradeço ao Centro de Biologia Marinha (CEBIMar-USP), pela utilização da infraestrutura de excelência e pronto atendimento para o desenvolvimento das atividades de coleta e pesquisa. Registro também meus agradecimentos a *Iowa State University*, especialmente ao *Department of Ecology, Evolution, and Organismal Biology*, pela realização do estágio no exterior com total suporte e tranquilidade.

Agradeço à Fundação de Amparo à Pesquisa do Estado de São Paulo (FAPESP) pela disponibilização do auxílio financeiro indispensável para realização da pesquisa, nas formas de bolsa regular (2015/09519-4), reserva técnica e bolsa para estágio de pesquisa no exterior (BEPE 2017/01365-3). Agradeço também à Coordenação de Aperfeiçoamento de Pessoal de Nível Superior – Brasil (CAPES), código 001, pelo auxílio financeiro nos primeiros meses de doutorado.

Agradeço as seguintes coleções científicas cujo material de pesquisa foi fundamental para o desenvolvimento do doutorado: Coleção de Bivalvia do Museu de Zoologia “Prof. Adão José Cardoso” da UNICAMP (ZUEC-BIV, Campinas, SP), *Harvard Museum of Comparative Zoology* (MCZ, Cambridge, EUA), Museu de Zoologia da USP (MZUSP, São Paulo, SP), *Santa Barbara Museum of Natural History* (SBMNH, Santa Barbara, EUA), *Smithsonian National Museum of Natural History* (USNM, Washington, EUA). Aproveito também para registrar meus agradecimentos ao gentil apoio dos curadores das coleções que prontamente me auxiliaram: Dra. Ellen Strong, Dr. Flávio Passos, Dr. Gonzalo Giribet, Dr. Luis Simone, e Dr. Paul Valentich-Scott.

A *American Malacological Society*, agradeço o auxílio financeiro disponibilizado em 2015 para participação no simpósio *Early Career Malacologists* durante o *American Malacological Society 81st Annual Meeting*. Agradeço também a *Malacological Society of London* pela premiação *Sir Charles Maurice Yonge Award – Early Career Research Grant* e pelo auxílio financeiro disponibilizado para participação no *84th American Malacological Society Meeting*.

Ao Prof. Dr. José Eduardo Amoroso Rodriguez Marian, exprimo meus incontáveis agradecimentos. Sempre pude contar com seu apoio, dedicação e disponibilidade. Sinto-me profundamente honrado e orgulhoso de poder trabalhar com alguém exemplo de ética, profissionalismo e rigor. Obrigado por me ensinar a decidir pelo correto e adequado, ao invés do fácil ou conveniente. Obrigado pela minha formação como pessoa e pesquisador.

À Profa. Dra. Jeanne Serb, devo profundos agradecimentos por me aceitar em estágio no exterior e trilhar comigo uma promissora parceria de pesquisas. Agradeço plenamente a confiança depositada em mim, ao tratamento acolhedor, e a todo suporte para minha estadia e pesquisa em Iowa.

Ao Prof. Dr. Álvaro Esteves Migotto, pela colaboração com estudos de material *in vivo* e auxílio para registros de vídeos e fotografias. Expresso meu agradecimento ao minucioso e paciente suporte que foi indispensável para obtenção de parte das imagens da presente pesquisa.

Ao Prof. Dr. André Morandini e Prof. Dr. Daniel Lahr, pela gentil disponibilização de seus laboratórios e microscópios para registro fotográfico.

Ao Prof. Dr. Alberto Ribeiro, pela permissão de uso do Laboratório de Biologia Celular e Microscopia Eletrônica e Confocal do IB-USP, suas instalações e equipamentos.

Ao M. Sc. Waldir Caldeira e a Geol. Sheila Carmo, pelo gentil auxílio nas preparações de microscopia eletrônica e confocal, assim como pela operação dos microscópios.

Aos técnicos do Departamento de Zoologia, Sr. Ênio Mattos e Biol. Phillip Lenktaitis, pelos incontáveis auxílios em microscopia, pela operação do microscópio eletrônico de varredura, e por fazer do Laboratório de Histologia um ambiente tão agradável.

Ao Laboratório de Biologia e Evolução de Mollusca por todo o apoio e cooperação, especialmente no agradável convívio com M. Sc. Licia Oliveira, M. Sc. Lígia Apostólico e M. Sc. Luiza Saad.

Ao Laboratório de Sistemática e Biogeografia de Insecta, por toda alegria, suporte, café e companheirismo. Agradeço ao apoio de M. Sc. Darlan Redü, M. Sc. Deyvis Garcia, M. Sc. Filipe Gudin, Biol. Letícia de Paula, M. Sc. Lucas de Campos, M. Sc. Marcelo Santis, M. Sc. Rodrigo Dios, e Dr. Thalles Pereira. Muito obrigado por proporcionarem momentos tão felizes (e muitas vezes fundamentais) ao dia a dia. Reforço também meus agradecimentos ao M. Sc. Lucas de Campos pela valiosa ajuda nas atividades de campo e pela amizade.

A todos os meus familiares, agradeço imensamente pela compreensão e torcida. Mesmo após tanto anos de estudo e pesquisa, os votos de confiança e sucesso sempre estiveram comigo,

assim como um apoio incondicional. Em especial, minha mãe Maria Heloisa A. Audino, meu pai Marcos C. F. Audino, e minha irmã Catarina A. Audino, não tenho palavras para agradecer todo o apoio, vibração e carinho.

À minha esposa, Biol. Mayra Sato, expresso minha total e mais profunda gratidão. Muito obrigado por me mostrar todos os dias a importância da empatia, paciência e dedicação. Obrigado por ser um exemplo de luta, conquista e seriedade em momentos difíceis. Agradeço principalmente ao incondicional apoio que me fez manter a calma e a alegria do dia a dia. Com todo o meu amor, obrigado.

ÍNDICE

INTRODUÇÃO GERAL

INTRODUÇÃO GERAL

1. INTRODUÇÃO

Questões macroevolutivas concentram elementos cruciais para a Biologia Evolutiva ao explorar associações entre diversidade fenotípica e paisagens adaptativas (Simpson, 1953; Schluter, 2000). A compreensão de como fatores ecológicos similares podem levar a fenótipos análogos em táxons independentes é fundamental para o estudo da evolução dos organismos (Losos, 2011; Serb *et al.*, 2017). Neste contexto, a evolução repetida de caracteres em linhagens independentes, *i.e.*, convergência evolutiva (Agrawal, 2017), em associação com fatores ambientais similares sugere possíveis adaptações, além de auxiliar na compreensão da evolução fenotípica sob regimes seletivos semelhantes (Harvey & Pagel, 1991; Losos, 2011; Mahler *et al.*, 2017). Enquanto diversos táxons de vertebrados são utilizados como modelos para estudos de irradiação evolutiva e convergência (Losos & Mahler, 2010), invertebrados são proporcionalmente menos estudados, de modo que padrões ecomorfológicos ainda permanecem amplamente subestimados.

Os Pteriomorphia são bivalves marinhos que representam modelos promissores em investigações de convergência e irradiação evolutiva devido à ampla diversidade morfológica e ecológica. Por serem animais bentônicos com diferentes hábitos de vida e com atributos fenotípicos supostamente associados a esses hábitos, esse grupo de bivalves representa um importante modelo para se explorar questões macroevolutivas no bentos marinho. O clado Pteriomorphia reúne ostras, mexilhões, vieiras, entre outros bivalves, e agrupa atualmente 23 famílias em cinco ordens (Bieler *et al.*, 2014), correspondendo a 20% da diversidade atual de bivalves (Combosch & Giribet, 2016). A classificação atual de Pteriomorphia encontra-se sumarizada no Anexo 1.

O monofiletismo de Pteriomorphia foi corroborado em diversas análises filogenéticas, utilizando diferentes amostragens taxonômicas e dados morfológicos e moleculares (Steiner & Hammer, 2000; Giribet & Wheeler, 2002; Matsumoto, 2003; Bieler *et al.*, 2014; Gonzalez *et al.*, 2015; Lemer *et al.*, 2016; Sun & Gao, 2017). Contudo, as relações entre famílias e ordens ainda é pouco consensual e intensamente debatida, o que se configura em um fator limitante para se compreender questões relacionadas à homologia de caracteres morfológicos e à evolução fenotípica.

Os bivalves Pteriomorphia apresentam hábitos de vida variados, podendo ser classificados em duas categorias principais, *i.e.*, epifaunais e infaunais, conforme o posicionamento do corpo em relação ao substrato (Stanley, 1975). Bivalves epifaunais vivem sobre substrato consolidados, como rochas, corais e outros fragmentos, geralmente com o auxílio do bisso, formado por filamentos de grande resistência secretados pelo animal e que garantem sua adesão a superfícies sólidas. Já bivalves semi-infaunais e infaunais possuem o hábito de se enterrar em substratos não-consolidados, deixando a região posterior do corpo exposta, acima da superfície. Em Pteriomorphia, a suposta condição ancestral de escavadores superficiais foi substituída por hábitos epifaunais na maioria das linhagens, contribuindo para a irradiação evolutiva do grupo (Stanley, 1972). Em Ostreida, as ostras (Ostreidae) cimentam uma das valvas sobre substratos consolidados, enquanto muitos Pteriidae vivem fixados pelo bisso a diferentes tipos de substrato (Tëmkin, 2006). Os Pinnidae representam uma exceção, sendo todos animais semi-infaunais, vivendo parcialmente enterrados em substrato não-consolidado com auxílio de um longo e volumoso bisso (Yonge, 1953). Em Pectinida e Limida, a diversidade de hábitos epifaunais é notável, incluindo espécies vágeis, além de espécies cimentantes, como em Spondylidae (Waller, 2006). Os mexilhões, típicos representantes da ordem Mytilida, são epifaunais, vivendo fixos sobre rochas e outros materiais por meio de um forte bisso; contudo, muitas linhagens do clado apresentam hábito perfurador ou semi-infaunal (Distel, 2000). Finalmente, a ordem Arcida também abrange diversas linhagens de bivalves epifaunais e infaunais (Oliver & Holmes, 2006).

Como brevemente exemplificado acima, a irradiação evolutiva da maioria das linhagens de Bivalvia é caracterizada pela ocupação de diferentes zonas adaptativas, o que está possivelmente relacionado à ampla diversificação morfológica do grupo (Giribet, 2008). Estudos anatômicos identificaram supostas associações entre diferentes modos de vida e possíveis adaptações morfológicas, relacionadas principalmente ao formato e estrutura das valvas, organização da musculatura adutora e presença de especializações do manto (Stanley, 1972; Yonge, 1983; Oliver & Holmes, 2006; Morton, 2015). Contudo, a maioria dessas hipóteses não foi testada em um contexto filogenético ou por métodos comparativos. Recentemente, entretanto, esse tipo de abordagem foi empregado na investigação da evolução morfológica e ecológica de alguns clados de bivalves, como Pectinidae, Mytilidae e Galeommatidae, corroborando a existência de inúmeras convergências evolutivas associadas a contextos ecológicos similares (Alejandrino, Puslednik, & Serb, 2011; Lorion *et al.*, 2013; Li, Ó Foighil, & Strong, 2016; Serb *et al.*, 2017).

Considerando o contexto apresentado acima, a margem do manto (ou palial) dos bivalves representa uma promissora fonte de dados fenotípicos, pois está intimamente associada ao uso de habitats e também à diversificação taxonômica (Yonge, 1983). O manto é um órgão formado pelos lobos direito e esquerdo, unidos dorsalmente, e responsável pela secreção da concha, além de delimitar a cavidade do manto, onde localizam-se os ctenídios (brânquias) (Carter *et al.*, 2012). Em sua porção mais distal, junto à borda da valva, a margem do manto organiza-se em pregas que podem variar com relação à forma e à função. De modo generalizado, a margem do manto é tipicamente composta por três pregas, sendo a principal região de interação com o meio externo (Yonge, 1983). Por isso, é considerada um elemento chave na compreensão da irradiação evolutiva dos bivalves e na conquista de novos nichos ecológicos (Yonge, 1983). Um exemplo clássico corresponde aos sifões, estruturas formadas a partir da fusão de pregas do manto e que permitem a comunicação e fluxo de água com o ambiente em animais que vivem enterrados no sedimento (Yonge, 1957).

A plasticidade e diversidade da margem do manto inclui estruturas especializadas como glândulas e células secretoras que atuam na limpeza, adesão, lubrificação e até mesmo perfuração do substrato (Morton & Scott, 1980; Morton, 1982). Além disso, tentáculos também são comuns na margem do manto de Limidae, Pectinidae, Ostreidae e Pteriidae, onde podem desempenhar funções sensoriais, secretoras e defensivas (Gilmour, 1967; Morton, 1973; Moir, 1977; Mikkelsen & Bieler, 2003). Órgãos fotorreceptores ocorrem na margem do manto de vários grupos de bivalves, representando um elemento de grande interesse em estudos evolutivos e anatômicos (Morton, 2008). Apesar do extenso conhecimento sobre a morfologia da margem do manto em bivalves infaunais, principalmente quanto à descrição dos sifões e graus de fusão (Yonge, 1957, 1983; Sartori *et al.*, 2008), a escassez de informações para a mesma região em bivalves epifaunais é notável.

No caso de Pteriomorphia, a carência de informações comparativas e sistematizadas sobre a morfologia do manto no grupo representa uma importante lacuna em estudos anatômicos e evolutivos. Contudo, diversas linhas de evidência apontam para a correlação de estruturas paliais e a diversificação de hábitos de vida. Por exemplo, o surgimento independente de fotorreceptores em pregas paliais de diversas linhagens de bivalves é amplamente reconhecido como um caso de convergência evolutiva (Serb & Eernisse, 2008; Morton, 2008). A evolução de pregas paliais hipertrofiadas também parece estar fortemente associada ao hábito epifaunal em muitos grupos de bivalves (Yonge, 1983). O desenvolvimento de estruturas tentaculares no manto, assim como alguns graus de fusão, também são apontados como convergentes (Gilmour, 1967; Morton, 1973; Yonge, 1983). Portanto, a margem do manto reúne caracteres morfológicos de grande potencial na compreensão de adaptações e convergências evolutivas em Bivalvia, sendo um elemento chave em Pteriomorphia dada sua diversidade de forma e função.

Em um contexto mais amplo, a margem do manto dos bivalves concentra estruturas em contato primário com o ambiente externo, da mesma forma que os lofóforos em briozoários, coroa de tentáculos em cnidários, e região anterior do corpo em poliquetas tubículas (Gilmour, 1978; Dauer, 1985; Nielsen & Riisgård, 1998). Todas as regiões descritas podem ser consideradas correspondentes, pois possuem concentração de órgãos sensoriais, combinados com ação ciliar, produção de muco e outras secreções, além de auxiliarem na obtenção de alimento, proteção e circulação de água. Desse modo, a margem do manto de bivalves também representa um potencial modelo no estudo sobre a diversificação de forma e funções de regiões corpóreas associadas à interação com o ambiente, particularmente em animais sésseis do bentos marinho.

2. OBJETIVOS

Investigar a diversidade morfológica da margem do manto em Pteriomorphia, por meio de abordagens comparativas e funcionais, a fim de inferir a evolução dessa região e testar hipóteses de convergências associadas à diversificação do grupo no bentos marinho. De modo mais específico, a presente pesquisa e seus respectivos objetivos estiveram organizados de acordo com as seguintes perguntas:

1. Qual a diversidade morfológica da margem do manto em Pteriomorphia?

Objetivo: Sistematizar o conhecimento sobre a margem do manto para diferentes níveis taxonômicos quanto à anatomia, morfologia funcional e diversidade.

2. Como foi a evolução dessa diversidade?

Objetivo: Estudar a evolução da margem palial por meio da reconstrução de estados ancestrais de caracteres do manto, de modo a inferir mudanças de estado ao longo da filogenia do grupo.

3. De que modo a diversificação de forma e função da margem do manto está associada à evolução de Pteriomorphia no bentos marinho?

Objetivo: Fornecer bases sólidas para proposição e teste de hipóteses de homologia e convergência de estruturas do manto e sua eventual correlação com o modo de vida dos representantes de Pteriomorphia.

4. Quais aspectos funcionais estão vinculados à diversidade morfológica?

Objetivo: Compreender a anatomia funcional da margem do manto e estruturas associadas em espécies representantes das principais famílias de Pteriomorphia, fornecendo subsídios anatômicos para compreensão dos padrões encontrados no estudo evolutivo.

3. METODOLOGIA GERAL

Para contemplar seus objetivos, a pesquisa foi divida em três frentes de estudos: (1) inferência filogenética de Pteriomorphia com base em dados moleculares; (2) avaliação e descrição da diversidade palial com base em espécimes depositados em coleções, como base para o levantamento de caracteres, reconstrução de estados ancestrais e testes de correlação com hábitos de vida; e (3) estudo anatômico detalhado da margem do manto em exemplares coletados, para compreensão da base funcional das estruturas envolvidas.

De acordo com a abordagem proposta, a primeira frente do estudo objetivou a inferência filogenética de Pteriomorphia como ferramenta para a subsequente análise da evolução fenotípica. A segunda frente de estudo vincula-se às perguntas 1 a 3, possuindo um componente mais abrangente e comparativo, associado ao levantamento da diversidade morfológica e dos hábitos de vida. Considerando explicitamente o contexto filogenético, o reconhecimento de padrões na morfologia do manto possibilitou o teste de correlações entre os atributos fenotípicos observados e aspectos da biologia dos táxons. O terceiro componente da pesquisa foi dirigido à pergunta 4, e se propôs a explicar os padrões encontrados a partir da compreensão da base funcional das estruturas envolvidas, envolvendo análises anatômicas detalhadas.

3.1. Inferência filogenética

Para a inferência filogenética de Pteriomorphia, foram utilizadas 187 espécies de 19 famílias de Pteriomorphia, considerando as sequências nucleotídicas de cinco genes, *i.e.*, 16S rRNA, COI mtDNA, 18S rRNA, 28S rRNA e histona H3, obtidas no *Genbank*. Mais informações a respeito da amostragem taxonômica e do conjunto de dados moleculares estão detalhadas na metodologia dos capítulos 2, 6 e 7, que incluem análises filogenéticas. De modo geral, alinhamentos foram gerados no MAFFT sob o método L-INS-i (Katoh & Standley, 2013), a seleção de modelos de evolução nucleotídica foi realizada por meio do ModelFinder (Kalyaanamoorthy *et al.*, 2017) e as buscas de árvores foram conduzidas sob máxima verossimilhança no IQ-TREE (Nguyen *et al.*, 2014). Quando possível, tempos de divergência foram estimados por inferência Bayesiana a partir de dados fósseis, utilizando-se o modelo *fossilized birth-death model* no software RevBayes (Höhna *et al.*, 2016). Mais informações a respeito da amostragem taxonômica, dados fósseis e outros parâmetros de análise estão descritos nos capítulos 6 e 7.

3.2. Diversidade e evolução da margem do manto em Pteriomorphia.

As espécies de interesse nesta frente de estudo abrangeram a diversidade de Pteriomorphia, bem como as variações dentro de cada família. O material de pesquisa foi obtido em coleções científicas via empréstimo ou visita, incluindo materiais analisados no exterior. No total, foram observados exemplares de 209 espécies depositados nas seguintes coleções: MCZ (*Harvard Museum of Comparative Zoology*, Cambridge, EUA), MZSP (Museu de Zoologia da USP), SBMNH (*Santa Barbara Museum of Natural History*, Santa Barbara, EUA), USNM (*Smithsonian National Museum of Natural History*, Washington, EUA), e ZUEC-BIV (Coleção de Bivalvia do Museu de Zoologia “Prof. Adão José Cardoso” da UNICAMP).

3.2.1. Caracterização morfológica

A morfologia geral da margem do manto foi avaliada nas espécies de interesse, com ênfase na obtenção de informações sobre os seguintes caracteres: 1) morfologia geral (*e.g.*, pigmentação e variação ao longo do eixos corpóreos); 2) pregas do manto (*e.g.*, número de pregas, morfologia, tamanho relativo); 3) fusão palial (pontos de fusão ao longo da margem do manto); 4) estruturas paliais associadas (*e.g.*, tentáculos e órgãos fotorreceptores.). O estudo foi realizado por meio de dissecções em etanol e observações sob estereomicroscópio.

3.2.2. Reconstrução da evolução da margem do manto

Os caracteres de interesse foram codificados e organizados em matrizes com base na observação dos espécimes provenientes de coleções científicas. Estados de caráter foram atribuídos aos terminais com base em observações das espécies correspondentes. Em espécies não observadas, e no caso de não haver informação na literatura, os estados foram assinalados como equivalentes aos de espécies congenéricas analisadas.

Reconstruções de estado ancestral foram conduzidas sob máxima verossimilhança. Dois possíveis modelos foram considerados, *i.e.*, o modelo MK1 (Markov *k*-state), que assume taxas iguais para transições de estado, e o modelo AsymmMK (asymmetrical Markov *k*-state), que permite que as taxas de transição sejam diferentes. A razão de verossimilhança (*likelihood ratio*) foi utilizada para verificar qual modelo se ajustava melhor aos dados apresentados, definindo assim o modelo adotado na análise (Pagel, 1994; Maddison & Maddison, 2018).

Testes de correlação foram aplicados quando dois caracteres binários, com múltiplas transições ao longo da filogenia, pareciam estar associados. Hipóteses de correlação foram aceitas sempre que o modelo de oito parâmetros (hipóteses de evolução dependente) apresentou melhor desempenho ($p<0,05$) do que o modelo de quatro parâmetros (hipóteses de evolução independente), considerando as diferenças em *loglikelihood* dos modelos (Pagel, 1994). Reconstruções de estado ancestral e testes de correlação foram realizados no software Mesquite (Maddison & Maddison, 2018).

3.3. Anatomia detalhada e funcional da margem do manto

Esta frente de estudo foi dedicada a compreender a base funcional das estruturas da margem do manto, empregando análises anatômicas detalhadas. Indivíduos das espécies de interesse foram coletados no Canal de São Sebastião (SP) nas regiões infra, meso e supra litoral de costões rochosos. A coleta, manutenção e demais procedimentos com animais vivos foram realizados com apoio da infraestrutura e equipe técnica do Centro de Biologia Marinha da Universidade de São Paulo (CEBIMar-USP). Foram obtidas amostras do manto de 12 espécies, listadas na Tabela 1, contemplando 7 famílias de Pteriomorphia.

Tabela 1. Espécies coletadas no Canal de São Sebastião (SP) e cujas amostras da margem do manto foram processadas para diferentes técnicas de microscopia: histologia e histoquímica (Hist), microscopia eletrônica de varredura (MEV) e microscopia confocal (MC). Algumas amostras não foram processadas para microscopia confocal devido ao excesso de pigmentação no manto, o que inviabilizaria a análise.

Família	**Espécie**	**Autor**	**Hist**	**MEV**	**MC**
Arcidae	*Arca imbricata*	Bruguière, 1789	✓	✓	
Arcidae	*Barbatia candida*	(Helbling, 1779)	✓	✓	✓
Mytilidae	*Brachidontes exustus*	(Linnaeus, 1758)	✓	✓	
Mytilidae	*Leiosolenus bisulcatus*	(d'Orbigny, 1853)	✓	✓	
Mytilidae	*Perna perna*	(Linnaeus, 1758)	✓	✓	
Noetiidae	*Arcopsis adamsi*	(Dall, 1886)	✓	✓	✓

Ostreidae	*Ostrea equestris*	Say, 1834	✓	✓	✓
Pinnidae	*Pinna carnea*	Gmelin, 1791	✓	✓	✓
Pteriidae	*Isognomon bicolor*	(Adams, 1845)	✓	✓	✓
Pteriidae	*Pinctada imbricata*	Röding, 1798	✓	✓	✓
Pteriidae	*Pteria colymbus*	Röding, 1798	✓	✓	✓
Spondylidae	*Spondylus ictericus*	Reeve, 1856	✓	✓	✓

3.3.1. Fixação do material para estudos de microscopia

Antes da fixação, os indivíduos foram anestesiados adicionando-se solução de cloreto de magnésio a 7,5% à água do mar (proporção 1 anestésico: 3 água do mar), sob refrigeração, por um período de até 3h (conforme o tamanho dos indivíduos). Esse procedimento foi realizado com o objetivo de se reduzir as contrações musculares observadas durante a fixação. Indivíduos diminutos foram fixados inteiramente, enquanto que indivíduos maiores tiveram sua margem do manto dissecada e posteriormente fixada. Dois tipos de solução fixadora foram empregados: (1) amostras para microscopia confocal foram fixadas em solução de paraformaldeído a 4% em tampão PB a 1,0M (tampão fosfato com osmolaridade ajustada para 1000mOsm e pH 7.2) por duas horas e em seguida lavadas e mantidas em tampão PB com 0,1% de NaN_3; (2) amostras destinadas à histologia e microscopia eletrônica foram fixadas em solução de Karnovsky modificada (paraformaldeído a 2% e glutaraldeído a 2,5% em solução tampão de cacodilato de sódio a 0,1M, com osmolaridade ajustada para 1000mOsm e pH 7.4) por três horas e em seguida lavadas e mantidas em tampão cacodilato de sódio a 0,1M.

3.3.2. Histologia e histoquímica

A partir da metodologia de fixação descrita anteriormente, as amostras da margem do manto de espécimes coletados foram submetidas ao procedimento descrito a seguir. Após desidratação em série alcoólica ascendente até etanol a 100%, as amostras foram incluídas em resina à base de glicol-metacrilato da marca “Leica” (“Leica Historesin Kit”), seguindo-se instruções do fabricante. Cortes seriados de 3 μm a 4 μm de espessura foram obtidos e montados em lâminas. Foram empregados os métodos de coloração descritos na Tabela 2. Todas as lâminas produzidas foram posteriormente preparadas em meio de montagem apropriado (“Entellan”) com lamínula.

Tabela 2. Métodos de coloração empregados nos estudos histológicos da margem do manto. Referências utilizadas para os métodos: Humason, 1962; Behmer, Tolosa, & Freitas Neto, 1976; Bancroft & Stevens, 1982; Pearse, 1985; Junqueira & Carneiro, 1995.

Método de coloração	**Objetivo**
Hematoxilina de Mayer e eosina Y	Coloração para análise geral
Azul de Toluidina e fucsina Básica	Coloração para análise geral
Azul de Alcian	Identificação de mucopolissacarídeos ácidos
PAS	Identificação de mucopolissacarídeos
PAS + azul de Alcian	Diferenciar os tipos de mucopolissacarídeos
Preto de Sudão B	Identificação de agregados lipídicos
Tricromo de Mallory	Evidenciar musculatura, tecido conjuntivo e glândulas
Tricromo de Gomori	Evidenciar musculatura, tecido conjuntivo e glândulas
Azul de bromofenol	Evidenciar proteínas básicas
Amarelo naftol	Evidenciar aminoácidos e peptídeos

3.3.3 Microscopia Eletrônica de Varredura

Para microscopia eletrônica de varredura, as amostras foram submetidas à segunda fixação com OsO_4 a 1% em solução tampão de cacodilato de sódio a 0.1M durante 30 minutos, depois lavadas com ácido tânico em solução tampão por 15 minutos e, então, mantidas em nova solução de OsO_4 por 15 minutos. Após a segunda fixação, todas as amostras foram então desidratadas até etanol a 100% em série alcoólica ascendente, submetidas ao ponto crítico com CO_2 como fluido transicional (Balzers CPD 030), montadas em *stubs* e metalizadas com ouro (Balzers CPD 050). O material resultante foi analisado no Microscópio Eletrônico de Varredura do Instituto de Biociências da USP (ZEISS SIGMA VP).

3.3.4. Microscopia Confocal de Varredura a Laser

Amostras para microscopia confocal foram incialmente mantidas em solução tampão com Triton X-100 a 2% (PBT) *overnight* para aumento de permeabilidade dos tecidos. Para marcação muscular (fibras de actina), as amostras foram incubadas em *Alexa Flour 488 Phalloidin* em PBT por 24 horas no escuro. Para marcação de cílios e fibras nervosas (filamentos de tubulina), as amostras foram incubadas em *Alexa Flour 488 Anti-tubulin* em PBT por 24 horas no escuro. Em seguida, as amostras foram lavadas em três banhos de 15 minutos cada com solução tampão (PB) e então montadas em lâmina e lamínula utilizando meio de montagem *Anti-Fading Diamond Pro* (Molecular Probes) com DAPI para marcação nuclear. As lâminas foram mantidas sob refrigeração até análise no Microscópio Confocal de Varredura a Laser do IB-USP (ZEISS LSM 880). Planos ópticos foram registrados ao longo do eixo z e digitalmente agrupados pelo método de projeção de máxima intensidade. Demais ajustes forem realizados com o software ZEN Lite (ZEISS).

4. ORGANIZAÇÃO DA TESE

Além da presente "Introdução geral" e das "Considerações Finais", a tese está organizada em oito capítulos estruturados como artigos científicos e redigidos em inglês. Cada capítulo aborda um conjunto de questões e hipóteses específicas que, somadas, permitem compreender a diversidade e evolução da margem do manto nos bivalves Pteriomorphia.

Capítulo 1. Evolutionary significance of the mantle margin in pteriomorphian bivalves

O capítulo compreende uma ampla revisão sobre a margem do manto nos moluscos bivalves, com ênfase nos Pteriomorphia. O conhecimento sobre essa região anatômica é avaliado, considerando publicações em diferentes áreas, incluindo morfologia, genética e fisiologia. Ao longo da revisão, são apresentadas diferentes evidências que suportam a margem do manto como uma região de grande potencial para estudos evolutivos, principalmente devido à relação entre ecologia e morfologia funcional. De modo complementar, Pteriomorphia é indicado como clado modelo para diferentes investigações, principalmente focadas em evolução convergente e diversificação de órgãos sensoriais. Em suma, o capítulo fornece uma introdução ao tema da tese e explora os fundamentos teóricos que subsidiam os demais capítulos.

O capítulo foi publicado na revista *American Malacological Bulletin*.

Capítulo 2. On the evolution of mantle photoreceptor organs in Pteriomorphia (Mollusca: Bivalvia)

O capítulo explora a diversidade e evolução de órgãos fotorreceptores em Pteriomorphia. A abordagem filogenética compreende a maior amostragem taxonômica do grupo atualmente, incluindo 187 espécies de 19 famílias. A margem do manto foi analisada em 209 espécies (com base em indivíduos preservados em coleções) para avaliação da presença, tipo e distribuição de órgãos fotorreceptores. Com base na hipótese filogenética inferida, estudos de reconstrução de estado ancestral foram conduzidos para avaliar a evolução dos órgãos fotorreceptores, assim como dos hábitos de vida. Os dados obtidos para Pteriomorphia sistematizam informações morfofuncionais e evolutivas, fornecendo evidências robustas para hipóteses de homologia e convergência de órgãos fotorreceptores no clado.

Capítulo 3. Form and function of tentacles in pteriomorphian bivalves

O capítulo apresenta dados detalhados da anatomia de tentáculos de Pteriomorphia por meio de histologia, microscopia eletrônica e confocal. Foram consideradas amostras de indivíduos coletados de seis espécies de quatro famílias de Pteriomorphia (*i.e.*, Ostreidae, Pinnidae, Pteriidae e Spondylidae), com ênfase em observações de musculatura, inervação, ciliação e atividade secretora. Os dados obtidos para a diversidade de tentáculos do clado, em conjunto com informações da literatura, permitem o reconhecimento de padrões anatômicos e funcionais, bem como a proposição de hipóteses de homologia.

Capítulo 4. The evolution of tentacles untangled: revealing tentacle homology and convergence in epifaunal bivalves

O capítulo aborda a evolução de tentáculos em Pteriomorphia, com base na hipótese filogenética inferida para o clado, apresentada no segundo capítulo. O estudo morfológico foi realizado com base em exemplares preservados de coleções científicas, totalizando 121 espécies de 13 famílias que possuem tentáculos na margem do manto. As observações focaram no tipo, localização e distribuição de tentáculos na margem do manto. O estudo de morfologia comparada, combinada à reconstrução de estados ancestrais, permitiu testar hipóteses de homologia dos tentáculos em Pteriomorphia, revelando atributos homólogos bem como homoplásticos.

Capítulo 5. Comparative and functional anatomy of the mantle margin in ark clams and relatives (Bivalvia: Arcoidea) supports association between morphology and life habits

O capítulo apresenta um estudo anatômico detalhado de representantes de quatro famílias da ordem Arcida (*i.e.*, Arcidae, Cucullaeidae, Glycymerididae e Noetiidae). Com base em dados de histologia, microscopia eletrônica e confocal, a margem do manto foi estudada nesses animais, com ênfase em funções secretoras e sensoriais. Dados de morfologia geral para 27 espécies provenientes de coleções complementam a análise. Os resultados obtidos revelam padrões morfofuncionais e possíveis associações a diferentes hábitos de vida.

O capítulo foi publicado na revista *Journal of Zoology*.

Capítulo 6. Ark clams and relatives (Bivalvia: Arcida) show convergent morphological evolution associated with lifestyle transitions in the marine benthos

O capítulo aborda a evolução da margem do manto na ordem Arcida, com base em hipóteses filogenéticas geradas para 54 espécies de seis famílias que compõem clado, além de uma árvore datada a partir de dados fósseis. A margem do manto foi estudada em 64 espécies provenientes de museus, permitindo ampla caracterização da região e das estruturas associadas. Métodos filogenéticos comparativos foram empregados para avaliar a evolução das estruturas da margem do manto, bem como sua associação com hábitos de vida.

O capítulo foi publicado na revista *Biological Journal of the Linnean Society*.

Capítulo 7. Phylogeny and anatomy of marine mussels (Mytilidae) reveal convergent evolution of siphon traits in association with similar ecology

O capítulo explora a evolução da margem do manto na família dos mexilhões (Mytilidae) com base em anatomia comparada e funcional, além de métodos filogenéticos comparativos. Foram utilizadas 32 espécies a fim de inferir a filogenia do grupo, incluindo uma árvore datada a partir de dados fósseis. A margem do manto foi estudada em 43 espécies (23 gêneros) com base em espécimes preservados provenientes de coleções. Dados de anatomia detalhada também foram investigados por meio de microscopia integrativa para quatro espécies coletadas. Resultados da morfologia comparada e funcional são discutidos no contexto filogenético e revelam diferentes aspectos da evolução da margem do manto em associação a transições entre hábitos de vida.

Capítulo 8. Detailed and comparative anatomy reveal further unusual mantle specializations in pen shells (Mollusca: Bivalvia: Pinnidae)

O capítulo apresenta dados de morfologia comparada da margem do manto para 10 espécies dos três gêneros (*Atrina*, *Pinna* e *Streptopinna*) que compõe a família Pinnidae. Além disso, a margem do manto foi detalhadamente estudada em *Pinna carnea* (espécime coletado) por meio de microscopia eletrônica de varredura e histologia. Os dados obtidos revelam padrões morfofuncionais em Pinnidae, além de informações inéditas a respeito da composição e atividade secretora do manto. Um nova estrutura glandular é descrita para a margem do manto.

Referências bibliográficas

Agrawal AA. 2017. Toward a predictive framework for convergent evolution: Integrating natural history, genetic mechanisms, and consequences for the diversity of life. *The American Naturalist* 190: S1–S12.

Alejandrino A, Puslednik L, Serb JM. 2011. Convergent and parallel evolution in life habit of the scallops (Bivalvia: Pectinidae). *BMC Evolutionary Biology* 11.

Bancroft J, Stevens A. 1982. *Theory and Practice of Histological Techniques*. New York, NY: Churchill Livingstone.

Behmer OA, Tolosa EMC, Freitas Neto AG. 1976. *Manual de técnicas para microscopia normal e patológica*. São Paulo: Edusp.

Bieler R, Mikkelsen PM, Collins TM, Glover EA, González VL, Graf DL, Harper EM, Healy J, Kawauchi GY, Sharma PP, Staubach S, Strong EE, Taylor JD, Tëmkin I, Zardus JD, Clark S, Guzmán A, McIntyre E, Sharp P, Giribet G. 2014. Investigating the Bivalve Tree of Life – an exemplar-based approach combining molecular and novel morphological characters. *Invertebrate Systematics* 28: 32.

Carter JG, Harries PJ, Malchus N, Sartori AF, Anderson LC, Bieler R, Bogan AE, Coan EV, Cope JC, Cragg S. 2012. Illustrated glossary of the Bivalvia. *Treatise Online*: 1–209.

Combosch DJ, Giribet G. 2016. Clarifying phylogenetic relationships and the evolutionary history of the bivalve order Arcida (Mollusca: Bivalvia: Pteriomorphia). *Molecular Phylogenetics and Evolution* 94: 298–312.

Dauer DM. 1985. Functional morphology and feeding behavior of *Paraprionospio pinnata* (Polychaeta: Spionidae). *Marine Biology* 85: 143–151.

Distel DL. 2000. Phylogenetic relationships among Mytilidae (Bivalvia): 18S rRNA data suggest convergence in mytilid body plans. *Molecular Phylogenetics and Evolution* 15: 25–33.

Gilmour THJ. 1967. The defensive adaptations of *Lima hians* (Mollusca, Bivalvia). *Journal of the Marine Biological Association of the United Kingdom* 47: 209–221.

Gilmour THJ. 1978. Ciliation and function of the food-collecting and waste-rejecting organs of lophophorates. *Canadian Journal of Zoology* 56: 2142–2155.

Giribet G. 2008. Bivalvia. *Phylogeny and Evolution of the Mollusca*. Berkeley: University of California Press, 105–141.

Giribet G, Wheeler W. 2002. On bivalve phylogeny: a high-level analysis of the Bivalvia (Mollusca) based on combined morphology and DNA sequence data. *Invertebrate Biology* 121: 271–324.

Gonzalez VL, Andrade SCS, Bieler R, Collins TM, Dunn CW, Mikkelsen PM, Taylor JD, Giribet G. 2015. A phylogenetic backbone for Bivalvia: an RNA-seq approach. *Proceedings of the Royal Society B: Biological Sciences* 282: 20142332–20142332.

Harvey PH, Pagel MD. 1991. *The comparative method in evolutionary biology*. Oxford: Oxford university press.

Höhna S, Landis MJ, Heath TA, Boussau B, Lartillot N, Moore BR, Huelsenbeck JP, Ronquist F. 2016. RevBayes: Bayesian phylogenetic inference using graphical models and an interactive model-specification language. *Systematic Biology* 65: 726–736.

Humason GL. 1962. *Animal tissue techniques*. San Francisco & London: W. H. Freeman and Company.

Junqueira LC, Carneiro J. 1995. *Histologia Básica*. Guanabara Koogan.

Kalyaanamoorthy S, Minh BQ, Wong TK, von Haeseler A, Jermiin LS. 2017. ModelFinder: fast model selection for accurate phylogenetic estimates. *Nature methods* 14: 587.

Katoh K, Standley DM. 2013. MAFFT multiple sequence alignment software version 7: improvements in performance and usability. *Molecular Biology and Evolution* 30: 772–780.

Lemer S, González VL, Bieler R, Giribet G. 2016. Cementing mussels to oysters in the pteriomorphian tree: A phylogenomic approach. *Proceedings of the Royal Society B: Biological Sciences* 283: 20160857.

Li J, Ó Foighil D, Strong EE. 2016. Commensal associations and benthic habitats shape macroevolution of the bivalve clade Galeommatoidea. *Proceedings of the Royal Society B: Biological Sciences* 283: 20161006.

Lorion J, Kiel S, Faure B, Kawato M, Ho SYW, Marshall B, Tsuchida S, Miyazaki JI, Fujiwara Y. 2013. Adaptive radiation of chemosymbiotic deep-sea mussels. *Proceedings of the Royal Society B: Biological Sciences* 280: 20131243–20131243.

Losos JB. 2011. Convergence, adaptation, and constraint. *Evolution* 65: 1827–1840.

Losos JB, Mahler DL. 2010. Adaptive radiation: the interaction of ecological opportunity, adaptation, and speciation. *Evolution after Darwin: the first 150 years*. Sunderland, MA: Sinauer.

Maddison WP, Maddison DR. 2018. Mesquite: a modular system for evolutionary analysis. Version 3.51 http://www.mesquiteproject.org.

Mahler DL, Weber MG, Wagner CE, Ingram T. 2017. Pattern and process in the comparative study of convergent evolution. *The American Naturalist* 190: S13–S28.

Matsumoto M. 2003. Phylogenetic analysis of the subclass Pteriomorphia (Bivalvia) from mtDNA COI sequences. *Molecular Phylogenetics and Evolution* 27: 429–440.

Mikkelsen PM, Bieler R. 2003. Systematic revision of the western Atlantic file clams, *Lima* and *Ctenoides* (Bivalvia: Limoida: Limidae). *Invertebrate Systematics* 17: 667.

Moir AJG. 1977. Ultrastructural studies on the ciliated receptors of the long tentacles of the giant scallop, *Placopecten magellanicus* (Gmelin). *Cell and Tissue Research* 184: 367–380.

Morton B. 1973. The biology and functional morphology of *Galeomma* (*Paralepida*) *takii* (Bivalvia: Leptonacea). *Journal of Zoology* 169: 133–150.

Morton B. 1982. Functional morphology of *Bathyarca pectunculoides* (Bivalvia: Arcacea) from a deep Norwegian fjord with a discussion of the mantle margin in the Arcoida. *Sarsia* 67: 269–282.

Morton B. 2008. The evolution of eyes in the Bivalvia: New insights. *American Malacological Bulletin* 26: 35–45.

Morton B. 2015. Evolution and adaptive radiation in the Mytiloidea (Bivalvia): clues from the pericardial–posterior byssal retractor musculature complex. *Molluscan Research* 35: 227–245.

Morton B, Scott PJB. 1980. Morphological and functional specializations of the shell, musculature and pallial glands in the Lithophaginae (Mollusca: Bivalvia). *Journal of Zoology* 192: 179–203.

Nguyen LT, Schmidt HA, von Haeseler A, Minh BQ. 2014. IQ-TREE: a fast and effective stochastic algorithm for estimating maximum-likelihood phylogenies. *Molecular biology and evolution* 32: 268–274.

Nielsen C, Riisgård H. 1998. Tentacle structure and filter-feeding in *Crisia eburnea* and other cyclostomatous bryozoans, with a review of upstream-collecting mechanisms. *Marine Ecology Progress Series* 168: 163–186.

Oliver PG, Holmes AM. 2006. The Arcoidea (Mollusca: Bivalvia): a review of the current phenetic-based systematics. *Zoological Journal of the Linnean Society* 148: 237–251.

Pagel M. 1994. Detecting correlated evolution on phylogenies: a general method for the comparative analysis of discrete characters. *Proc. R. Soc. Lond. B* 255: 37–45.

Pearse AGE. 1985. *Histochemistry, theoretical and applied*. London: Churchill Livingstone.

Sartori AF, Printrakoon C, Mikkelsen PM, Bieler R. 2008. Siphonal structure in the Veneridae (Bivalvia: Heterodonta) with an assessment of its phylogenetic application and a review of venerids of the Gulf of Thailand. *The Raffles Bulletin of Zoology* 18: 103–125.

Schluter D. 2000. *The ecology of adaptive radiation*. Oxford: Oxford University Press.

Serb JM, Eernisse DJ. 2008. Charting evolution's trajectory: Using molluscan eye diversity to understand parallel and convergent evolution. *Evolution: Education and Outreach* 1: 439–447.

Serb JM, Sherratt E, Alejandrino A, Adams DC. 2017. Phylogenetic convergence and multiple shell shape optima for gliding scallops (Bivalvia: Pectinidae). *Journal of Evolutionary Biology* 30: 1736–1747.

Simpson GG. 1953. *The major features of evolution*. New York, NY: Columbia University Press.

Stanley SM. 1972. Functional morphology and evolution of byssally attached bivalve mollusks. *Journal of Paleontology* 46: 165–212.

Stanley SM. 1975. Adaptive themes in the evolution of the Bivalvia (Mollusca). *Annual Review of Earth and Planetary Sciences* 3: 361–385.

Steiner G, Hammer S. 2000. Molecular phylogeny of the Bivalvia inferred from 18S rDNA sequences with particular reference to the Pteriomorphia. *Geological Society, London, Special Publications* 177: 11–29.

Sun W, Gao L. 2017. Phylogeny and comparative genomic analysis of Pteriomorphia (Mollusca: Bivalvia) based on complete mitochondrial genomes. *Marine Biology Research* 13: 255–268.

Tëmkin I. 2006. Morphological perspective on the classification and evolution of Recent Pterioidea (Mollusca: Bivalvia). *Zoological Journal of the Linnean Society* 148: 253–312.

Waller TR. 2006. Phylogeny of families in the Pectinoidea (Mollusca: Bivalvia): importance of the fossil record. *Zoological Journal of the Linnean Society* 148: 313–342.

Yonge CM. 1953. Form and Habit in *Pinna carnea* Gmelin. *Philosophical Transactions of the Royal Society B: Biological Sciences* 237: 335–374.

Yonge CM. 1957. Mantle fusion in the Lamellibranchia. *Pubblicazioni della Stazione Zoologica di Napoli* 29: 151–171.

Yonge CM. 1983. Symmetries and the role of the mantle margins in the bivalve Mollusca. *Malacological Review* 16: 1–10.

Anexo 1. Classificação atual dos bivalves Pteriomorphia segundo a plataforma de dados *MolluscaBase* (2019) do *World Register of Marine Species* (http://www.marinespecies.org/).

PTERIOMORPHIA Beurlen, 1944
- **Ordem Arcida Gray, 1854**
  - Superfamília Arcoidea Lamarck, 1809
    - Família Arcidae Lamarck, 1809
    - Família Cucullaeidae Stewart, 1930
    - Família Glycymerididae Dall, 1908 (1847)
    - Família Noetiidae Stewart, 1930
    - Família Parallelodontidae Dall, 1898
  - Superfamília Limopsoidea Dall, 1895
    - Família Limopsidae Dall, 1895
    - Família Phylobryidae F. Bernard, 1897
- **Ordem Limida Moore, 1952**
  - Superfamília Limoidea d'Orbigny, 1846
    - Família Limidae d'Orbigny, 1846
- **Ordem Mytilida Férussac, 1822**
  - Superfamília Mytiloidea Rafinesque, 1815
    - Família Mytilidae Rafinesque, 1815
- **Ordem Ostreida Férussac, 1822**
  - Superfamília Ostreoidea Rafinesque, 1815
    - Família Ostreidae Rafinesque, 1815
    - Família Gryphaeidae Vyalov, 1936
  - Superfamília Pinnoidea Leach, 1819
    - Família Pinnidae Leach, 1819
  - Superfamília Pterioidea Gray, 1847 (1820)
    - Família Malleidae Lamarck, 1818
    - Família Pteriidae Gray, 1847 (1820)
    - Família Pulvinitidae Stephenson, 1941
- **Ordem Pectinida Gray, 1854**
  - Superfamília Anomioidea Rafinesque, 1815
    - Família Anomiidae Rafinesque, 1815
    - Família Placunidae Rafinesque, 1815
  - Superfamília Dimyoidea P. Fischer, 1886
    - Família Dimyidae P. Fischer, 1886
  - Superfamília Pectinoidea Rafinesque, 1815
    - Família Entoliidae Teppner, 1922
    - Família Pectinidae Rafinesque, 1815
    - Família Propeamussiidae Abbott, 1954
    - Família Spondylidae Gray, 1826
  - Superfamília Plicatuloidea Gray, 1857
    - Família Plicatulidae Gray, 1857

CHAPTER 1

On the evolutionary significance of the mantle margin in pteriomorphian bivalves

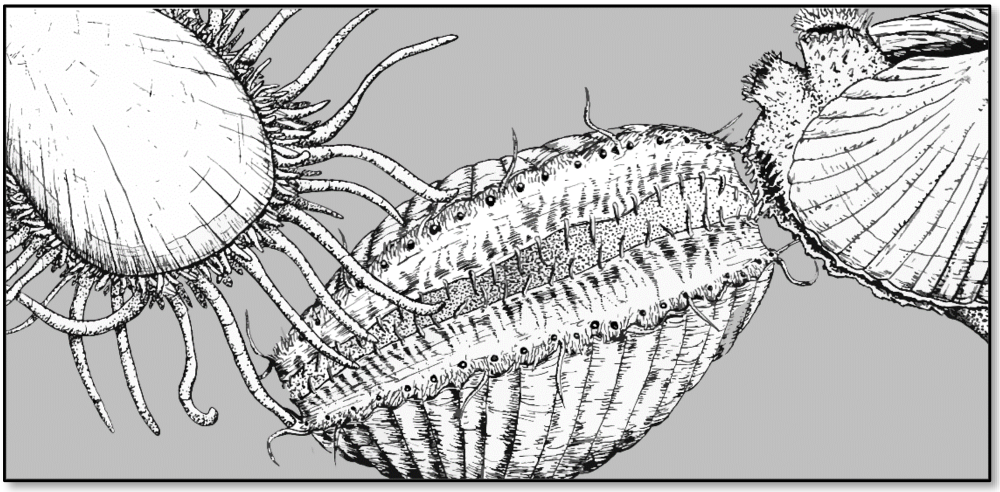

CHAPTER 1

On the evolutionary significance of the mantle margin in pteriomorphian bivalves

---

Abstract

The bivalve mantle margin comprises the free portion of the pallial lobes, and often bears muscular, sensory or secretory structures located on extensions of the mantle, called mantle folds. In the bivalve Infraclass Pteriomorphia, which underwent an extensive adaptive radiation in epifaunal habitats, the mantle margin exhibits an enormous diversity in mantle fold organization and associated structures. The present work reviews the current knowledge of the mantle margin in Pteriomorphia and discusses how the mantle margin can be used as a model for investigating the evolution of the marine epifaunal benthos as many species in this community have undergone similar selective pressures and developed comparable morphological adaptations, such as ciliated tentacular organs. Herein, we stress how additional investigations are necessary to cover the huge diversity seen in this taxonomic group. Given the scarcity of broad comparative studies of bivalves, including Pteriomorphia, the homology of their pallial features is still not clear. Moreover, although it is suspected that mantle margin diversification is correlated with transitions in pteriomorphian life habits, no hypotheses have been tested within a phylogenetic framework. To address these questions requires extensive comparative analyses of mantle margin diversity in Pteriomorphia that focuses on: 1) genetic expression and molecular dynamics in the mantle margin; 2) mantle margin morphogenesis, 3) assessment and test of hypotheses on homology, convergent and parallel evolution of mantle margin characters, and 4) testing possible correlations between mantle margin morphological diversity and lifestyle transitions. In a broader sense, by using Pteriomorphia as a model clade, we will gain insight into the macroecology of the marine epifauna.

Keywords: Anatomy, epifaunal, homology, life habit, mantle folds

This is the accepted version of the following article: *On the evolutionary significance of the mantle margin in pteriomorphian bivalves*, which has been published in final form at *American Malacological Bulletin* 34(2):148-159 (2016), https://doi.org/10.4003/006.034.0212

The molluscan mantle is an organ that encloses the animal viscera and secretes the shell. The mantle margin corresponds to the free portion of the mantle and it is characterized by tissue extensions named mantle (or pallial) folds (Stasek and Mcwilliams 1973). The huge morphological and functional diversity of this anatomical region is evidenced by a variety of muscular, sensory and secretory structures exhibited across the molluscan taxa. For example, in the Aculifera, the mantle margin is greatly reduced, with either minute folds in the small pallial cavity of Caudofoveata (Stasek and Mcwilliams 1973), or with three mantle folds in the Polyplacophora, where the inner and outer folds are reduced while the middle fold is enlarged. The hypertrophy of the middle fold in chitons forms the girdle, a typical structure of the group that might cover the shell plates, and also bears cuticle, spicules or scales (Beedham and Trueman 1967, Stasek and Mcwilliams 1973).

In the Conchifera, the presence of three mantle folds is claimed to be the common condition, although diversity in number, function and form of this organ represents a challenge for identifying broader patterns (Stasek and Mcwilliams 1973). In the monoplacophoran *Neopilina galathea* Lemche, 1957 (Lemche and Wingstrand 1959) and in the cephalopod *Nautilus pompilius* Linnaeus, 1758 (Westermann *et al*. 2005), the mantle margin displays the typical three-fold pattern. Differently, a single projection is commonly present in gastropods and scaphopods, although in some cases the mantle margin is shaped into distinct folds (Hyman 1967, Stasek and Mcwilliams 1973, Steiner 1998).

Mantle margin diversity and functions in the Bivalvia

In bivalves, the mantle is an organ formed by left and right lobes located beneath the valves and united dorso-medially by an isthmus, defining the mantle cavity (Carter *et al*. 2012). The periostracum – the organic shell outer layer secreted by glands located in the mantle margin – serves as a reference to identify the mantle folds according to their position. The folds are numbered consecutively inward and outward from the periostracal groove (Waller 1978). Consequently, the bivalve mantle margin is frequently divided into three folds, i.e., first inner fold (IF-1, also named “middle fold” in the literature), second inner fold (IF-2, or simply “inner fold”) and outer fold (OF) (Waller 1978; Yonge 1983). While the three-fold pattern is largely present among bivalves, numerous exceptions have been described, including four mantle folds in Veneridae (Ansell 1961, Hillman and Shuster 1966, Sartori and Mikkelsen 2008), a duplicated outer fold (OF-1 and OF-2) with a single inner fold in Arcidae (Waller 1980, Morton and Peharda 2008), and a duplication of the first inner fold in Donacidae (Passos and Domaneschi 2004).

Functional morphology of the bivalve mantle margin typically suggests major roles for each mantle fold (Yonge 1983). Just like the outer epithelium of the mantle, OF is involved in periostracum and shell formation via protein matrix secretion and extracellular calcification process (Timmermans 1969, Taylor 1973, Saleuddin and Petit 1983, Furuhashi *et al*. 2009). IF-1 frequently bears sensorial structures, and IF-2 is a muscular projection. Nevertheless, despite these general roles, a huge diversity of functions is seen in specific structures and regions of the mantle folds. For instance, muscular control of the water current, cleansing, mucus secretion and protection are examples of roles commonly displayed by this region (Yonge 1983, Prezant 1990). A remarkable case of mantle margin specialization occurs in the Tridacnidae, where the inner folds are fused and hypertrophied, bearing symbiont zooxanthellae (Yonge 1982). In the anomalodesmatan Lyonsiidae and Laternulidae, unique arenophilic mantle glands are present in the mantle margin, adjacent to the periostracal groove, being responsible for adhesion of foreign material (Prezant 1981, Morton 1987a, Sartori *et al*. 2006, Sartori *et al.* 2009). Even a plethora of photosensitive organs – varying from simple eyespots to complex camera-type eyes – has been described for the mantle folds of different bivalve families (Morton 2008).

Mantle marginal fusion is spread across multiple bivalve lineages, mostly resulting in siphons and pallial apertures (Yonge 1948). Such structures, which might be formed by the mantle folds in different ways (Yonge 1957), contribute to the water flow into and out of the mantle cavity even when the animal is buried deep within the sediment (Zwarts and Wanink 1989). When the mantle margin bears associated structures, such as papillae, tentacles and glands, they are commonly concentrated in the siphons (Yonge 1983, Fishelson 2000, Sartori *et al.* 2008). While mantle fusion and siphon formation are considered key features in the radiation of the infaunal habits in bivalves (Yonge 1948, Stanley 1968), the diverse free mantle margin of pteriomorphians might be associated with the diversity of epifaunal habits observed in this taxonomic group (Stanley 1975).

Pteriomorphia as a model group for investigating the evolution of the epifaunal benthos

Who are the pteriomorphian bivalves?

The Pteriomorphia is a diverse clade comprising marine, mostly byssate epifaunal bivalves, including economically important groups such as mussels, oysters, scallops, pearl oysters, and also ark clams, file clams and their numerous relatives. Asymmetries in the adductor muscles (heteromyarian or monomyarian), reduction of foot and inequilateral, asymmetric shells are among diagnostic morphological features of pteriomorphian bivalves

(Giribet 2008). In addition, this group has been traditionally recognized by anatomical and embryonic characters, separating them from the putative basal Protobranchia and the remaining bivalves grouped in the Heteroconchia (Waller 1998, Bieler and Mikkelsen 2006).

Pteriomorphia was recovered monophyletic in several phylogenetic analyses, with some internal groups showing consistent affinities (Waller 1998, Steiner and Hammer 2000, Matsumoto 2003, Giribet and Wheeler 2005, Xue *et al.* 2009, Sharma *et al.* 2012, Bieler *et al*. 2014; González *et al*. 2015), although relationships between some families and orders are still contentious (Fig. 1). The diversity of the clade is also reflected in the variety of habitat occupancy, lifestyles and morphology (Stanley 1972, 1977) spread across four main clades, frequently recognized as the orders Arcida, Mytilida, Ostreida and Pectinida (Carter *et al.* 2011; Bieler *et al.* 2014).

Benthic lifestyles are surprisingly diverse in bivalves, and include a variety of substrata and habits (e.g., burrowing, perforating, free-living, cementing). The superficial burrowing habit has been claimed as the ancestral condition for the bivalve mode of life based on anatomical and fossil evidence, thus implying a shallow infaunal lifestyle in the origin and early diversification of Bivalvia (Stanley 1972). In this case, the transition to hard-substratum epifaunal attachment in the Pteriomorphia would involve multiple changes in morphological and ecological adaptive traits and a subsequent diversification of epifaunal habitats (Yonge 1962, Stanley 1972, Harper and Skelton 1993). However, infaunal and semi-infaunal burrower species are nested within Pteriomorphia, and probably represent cases of reversion (Stanley 1972, Oliver and Holmes 2006).

A detailed look at the lifestyles of pteriomorphians reveals a plethora of habits spreading across lineages. In Mytilida, most mussels (Mytiloidea) are byssally attached to hard or soft substrata, living in epifaunal or semi-infaunal conditions, also known as epibyssate and endobyssate habits, respectively (Stanley 1972, Distel 2000). Unlike most mussels, the Lithophaginae represent a special case in Mytilidae, with species capable of perforation, boring into hard-substrata such as corals (Morton and Scott 1980, Owada 2007). Diverse lifestyles are shown in the Arcida (Arcoidea and Limopsoidea), with endobyssate and epibyssate bivalves living on hard or soft substrata (Oliver and Holmes 2006). Differently, Ostreida exhibit exclusively epifaunal habits, with species of oysters (Ostreoidea), pearl oysters (Pteroidea) and relatives living byssally attached or cemented to hard-substrata (Tëmkin 2006a, 2010). The pen shells (Pinnidae) live as semi-infaunal bivalves, but byssally attached to soft sediments (Yonge 1953). In Pectinida (Anomioidea, Dimyoidea, Limoidea, Pectinoidea and Plicatuloidea), diversification of epifaunal lifestyles are remarkable, habits varying from free-living, byssally attached and even cemented (Yonge 1936, Waller 2006, Alejandrino *et al*. 2011, Serb *et al*. 2011).

In summary, a deep connection between mantle margin and modes of life might have played crucial roles in the diversification and evolution of bivalves. In particular, Pterimorphia represents a suitable clade for further studies because of its monophyletic status, large variation in free mantle margin organization and plethora of epifaunal lifestyles. Notwithstanding, epifaunal habits with similar morphological and ecological conditions are not restricted to bivalves. Many epifaunal invertebrate taxa share similar patterns of sensorial perception and occupancy in substrata, which makes the pteriomorphian bivalves suitable models for broader comparative questions, shedding some light into selective forces driving diversification of epifaunal benthos and morphological evolution.

Targeting studies for mantle margin investigations

The evolution of the bivalve mantle margin represents a challenge and the ancestral condition for several pallial features is highly speculative (Waller 1978, 1980, Tëmkin 2006a, Morton and Peharda 2008). In the following sections, we briefly review papers that have used Pteriomorphia as a model group in molecular, anatomical or developmental studies of the mantle margin. We then evaluate and discuss the potential of these integrative approaches for elucidating the evolution of Pteriomorphia and the macroecology of epifaunal benthos.

Molecular dynamics in the mantle margin

Genome sequencing and gene expression studies (transcriptomics) have served as an important approach to investigate the function and evolution of the mantle margin and its structures. For example, a combination of the complete genome sequence and transcriptomic data from different organs of *Crassostrea gigas* (Thunberg, 1793) has allowed the exploration of key aspects of molluscan biology, such as the genes responsible for shell formation, stress adaptation and immune response in the mantle (Zhang *et al.* 2012). Interestingly, genomic data from both oyster (Ostreidae) and pearl oyster (Pteriidae) have identified multiple gene family expansions, with frequent duplication of genes responsible for shell formation. These data provide the first implication that dynamic genomic evolution might be associated with adaptations to a sessile lifestyle in the intertidal zone (Takeushi et al. 2016).

In the last decades, the progressive expansion of gene expression (transcriptomics) databases has allowed for major comparisons among genetic data and functional implications. Transcriptomics comprises sequencing RNA transcripts from target tissues, identifying known and novel genes involved in a variety of functions and activities. Functional annotations can be made via comparisons to protein databases, such as Gene Ontology (GO), describing gene products according to their associated biological processes, cellular components and molecular functions (Ashburner *et al.* 2000). Additional databases includes EuKaryotic Orthologous Groups (KOG) and pathway mapping analysis using the Kyoto Encyclopedia of Genes and Genomes (KEGG), which are employed to categorize unigenes according to their diverse biological functions and to identify candidate genes involved in specific processes (Kanehisa *et al.* 2008). In pteriomorphians, a comparative transcriptomic analysis of four *Pinctada* Röding, 1798 species provided a fine example of how functional transcriptomics can improve our knowledge of protein synthesis, cellular activities and growth factors, also serving as background for future studies (Huang *et al.* 2013).

As a consequence of such advances, new insights were gained into the evolution of the bivalve mantle. Shell formation is doubtless the main function associated to the mantle organ in molluscs. Not surprisingly, recent studies have focused on genes involved in biomineralization and pigmentation by means of mantle transcriptomics. In *Pinctada maxima* (Jameson, 1901), biomineralization was investigated for gene expression according to five mantle regions, showing both novel and similar to previously described transcripts associated with organic and inorganic processes of shell formation (Gardner *et al.* 2011). Transcriptomic analysis of mantle tissue from *Mytilus edulis* Linnaeus, 1758 revealed transcripts encoding putative shell matrix proteins with similar sequences of previously characterized proteins of other bivalves and gastropods (Freer *et al.* 2014). Additionally, a combination of genomic, transcriptomic and proteomic approaches for *Pinctada* species was able to annotate several shell matrix proteins, expanding resources for comparative studies on the bivalve “biomineralization toolkit” (Joubert *et al.* 2010, Miyamoto *et al.* 2013). Similarly, mantle transcriptomic analyses of the scallops *Mizuhopecten yessoensis* (Jay, 1857) and *Chlamys farreri* Jones and Preston, 1904 were carried out in order to investigate shell color variation and shell formation, contributing to understanding the molecular mechanisms underlying both processes (Shi *et al.* 2013, Ding *et al.* 2015, Sun *et al.* 2015).

Apart from shell and matrix secretion, transcriptomics were also useful to understand how some genes are involved in sensorial activities in the mantle. A pioneer study on molluscan photosensory systems was conducted with transcriptomic analysis of scallop pallial eyes, revealing transcripts involved in the phototransduction pathways and the circadian clock, and also identifying candidate genes potentially involved in sensory reception (Pairett and Serb 2013). In addition, duplication of opsin genes (light-sensitive proteins from photoreceptor cells) might have occurred in the ancestor of scallops and oysters, while divergent sequences and ortholog-specific retention suggest functional differences (Serb *et al*. 2013).

In summary, recent advances in bivalve genomic and transcriptomic approaches provided outstanding contributions to functional and evolutionary issues. Additional studies focusing on different organs and varied taxa are still necessary to better understand the functions performed by the mantle, and its responses to environmental stress, as well as to gain insight into adaptations associated to different lifestyles.

Anatomy

Pteriomorphia concentrates not only the diversification of bivalve epifaunal habits, but also the major diversity of pallial structures, which are located in the mantle folds (Fig. 2). The number of folds is variable, especially in the Arcida, where multiple conditions may be present (Morton 1982a) (Fig. 3). In this group, the mantle margin exhibits an extraordinary diversity in fold organization, organs and functions, which are still poorly known for many subtaxa. For example, in some species of *Arca* Linnaeus, 1758 the mantle margin has only one inner fold, and the outer fold is enlarged, acting as a pallial curtain (=veil) (Waller 1980). In some cases, the outer fold is also duplicated, forming the second outer fold (=pallial skirt, OF-2,), which represents an unusual condition given the general three-fold pattern (Waller 1980, Yonge 1983, Morton and Peharda 2008) (Fig. 3). Within Pteriomorphia, four folds have also been described for *Pulvinites exempla* (Hedley, 1914) (Pulvinitidae), a group phylogenetically distant from ark clams, possibly representing a case of convergent evolution (Tëmkin 2006b). Additionally, a second outer mantle fold was also found in some pteriids, such as *Isognomon legumen* (Gmelin, 1791), *Isognomon radiatus* (Anton, 1838), *Pteria brevialata* (Dunker, 1872) and *Pteria colymbus* (Röding, 1798) (Harper and Morton 1992, Morton 1995, Tëmkin 2006a).

A major role performed by the mantle margin is secretory, including shell and periostracum formation (Wilbur and Saleuddin 1983). Anatomical studies concerning shell and protein matrix secretion generated detailed information for several pteriomorphian bivalves, including insights into the calcification process and shell microstructure (Bevelander and Nakahara 1969, Waller 1980, Ubukata 1997, Checa 2005). Periostracum thickness was also evaluated as a potential factor affecting the evolution of shell morphology and habitat occupancy in some bivalve clades (Harper 1997). Detailed anatomical studies of the outer epithelium of the mantle were conducted for *Mytilus edulis* (Bubel 1973), *Ostrea edulis* Linnaeus, 1758 (Beedham 1958) and arcoids (Waller 1980, Reindl and Haszprunar 1996), while data on mantle cell characterization, proliferation and regeneration is available for pteriids (Jabbour-Zahab *et al.* 1992, Acosta-Salmón and Southgate 2005, Fang *et al.* 2008).

Aside from mucins involved in shell and periostracum secretion, other types of mucins are produced by the mantle margin, and they play roles in feeding, protection and cleansing activities (Prezant 1990). Histochemical characterization of secretory regions in mantle folds and types of mucus are available for *Nodipecten nodosus* (Linnaeus, 1758), *Pinna carnea* Gmelin, 1791, *Pinctada margaritifera* (Linnaeus, 1758) and *Pinctada maxima* (Yonge 1953, Dix 1972, Jabbour-Zahab *et al.* 1992, Audino *et al.* 2015a). A detailed mapping of mucocyte distribution for the pallial surface was provided for the mussel *Mytilus edulis* and the scallop *Placopecten magellanicus* (Gmelin, 1791), suggesting different mantle rejection pathways with similar use of acid mucopolysaccharides secretion for transport of particles (Beninger and St-Jean 1997). Specializations in form and function of mantle glands are also found, several groups displaying various types of mucus performing distinct roles. For instance, enlarged pallial glands in *Bathyarca* Kobelt, 1891 *(*Arcidae), posterior to the adductor muscle, comprise secretory cells possibly acting to bind and remove waste materials from the mantle cavity (Morton 1982a, Oliver and Allen 1980). In the mantle of Lithophaginae, pallial glands are responsible for chemically boring hard substrata using a modified shell-resorbing mechanism (Morton and Scott 1980, Morton 1982b, Kleemann 1990). Overall, data on mantle secretory activity is poorly known for most taxa, which at present prevents the identification of secretion patterns and the understating of the evolutionary significance of mucins.

Sensorial and secretory functions are also performed by pallial tentacular organs located at the inner mantle folds (Yonge 1983, Waller 1976, Tëmkin 2006a). While tentacles are restricted to IF-2 in Pinnidae, as described for *Pinna carnea* (Yonge, 1953), tentacular structures are found on both inner folds of Ostreidae, Pteriidae, Limidae, Pectinidae, Anomiidae and other families (Waller 1976, Tëmkin 2006a). While in scallops and relatives (Pectinida) tentacles are simple, long projections, they are branched in some pteriids (Waller 1976, Tëmkin 2006a, Audino *et al.* 2015b). In general, tentacles are briefly described in morphological studies and little is known about their structural organization, musculature, innervation or cilia types and distribution. However, fine anatomical details of pallial tentacles were described for the scallops *Nodipecten nodosus* (Audino *et al*. 2015b) and *Placopecten magellanicus* (Moir 1977), and for the file clam *Limaria hians* (Gmelin, 1791) (Gilmour 1963, 1967, Owen and McCrae 1979).

Diversity of form and function in the mantle margin also includes pallial curtains, largely present in pteriomorphians, and even a few cases of pallial fusion. Mantle curtains have long been recognized as flap-shaped extensions of the mantle margin, being present in Arcidae, Ostreidae, Pectinidae and several other families (Nelson 1938, Waller 1980, Yonge 1983), but lack of detailed information about their structure (*e.g.*, mantle fold contribution) and function prevents a broader comparative analysis. In Pteriomorphia, fusions along the mantle margin are uncommon, except for mussels that exhibit a posterior fusion point of the inner folds, forming an excurrent aperture (Waller 1978, Narchi *et al.* 1997). Some other apparently relevant characteristics of the pteriomorphian mantle margin include pigmentation, presence of papillae, variation in fold proportions and presence of photoreceptor organs.

The inner and outer mantle folds of numerous bivalves commonly bear photoreceptor cells and light sensitive organs. The complex pallial eyes formed in the middle mantle fold of scallops (Pectinidae) are doubtless the most studied optical structure in bivalves. For a long time, those curious organs were investigated with respect to their anatomy, physiology, optical properties, development and molecular basis (Dakin 1910, Land 1966, Hamilton and Koch 1996,Morton 2000a, Wilkens 2006,Speiser and Johnsen 2008, Pairett and Serb 2013, Audino *et al*. 2015c). The scallop eyes are camera-type organs bearing cornea, lens, a double retina and a reflector layer that acts as a mirror, which is responsible for producing a focus on the retina (Land 1966, Speiser and Johnsen 2008, Malkowsky and Götze 2014). Pallial eyes are also found in the Limidae; in *Ctenoides mitis* (Lamarck, 1807), they are lens-bearing organs, open to the environment and located in the middle mantle fold (Morton 2000b). Interestingly, the disco clam *Ctenoides ales* (Finlay, 1927) has silica spheres in the inner mantle fold acting as a broadband reflector, although its function remains uncertain (Dougherty *et al*. 2014). In the Arcoidea, two outer folds may be present (OF-1 and OF-2) with eyespots formed by pigmented cups and compound eyes frequently present in the OF-1 (Fig. 3). For example, photoreceptors are organized in pigmented cups beneath the periostracum in *Barbatia virescens* (Reeve, 1844) and *Anadara notabilis* (Röding, 1798) (Morton 1987b, Nilsson 1994). Simple ocelli are also found in Pteroidea, including pigmented cups devoid of lens in OF-1 of *Isognomon* Lightfoot, 1786 (Tëmkin 2006). Alternatively, compound eyes (unique in the Mollusca) formed by multiple facets are present in the arcoidean genera *Arca*, *Glycymeris* da Costa, 1778 and *Barbatia* Gray, 1842 (Waller 1980, Morton and Peharda 2008, Morton and Puljas 2015).

Developmental studies

Developmental studies using bivalves, especially pteriomorphians, have focused on several aspects of individual growth, shell development and ecological influences. In fact, Pteriomorphia exhibit an advantage as a model group for developmental studies, because several species of oysters, pearl oysters, mussels and scallops are worldwide cultivated, thus representing a real potential for experimental studies on morphogenesis.

Even though bivalve larvae have been extensively studied, bivalve organogenesis is still scarcely understood, but progress has been achieved for structures such as gills, muscles and shell (*e.g.*, Voronezhskaya *et al*. 2008, Cannuel *et al*. 2009, Wurzinger-Mayer *et al*. 2014, Audino *et al*. 2015d). The anatomy of the mantle margin of *Ostrea edulis* larvae has already been investigated, but information for other groups are restricted, fragmentary or lacking (Elston 1980).

In a recent investigation of the mantle margin of the scallop Nodipecten nodosus, the first insights into mantle margin formation were obtained (Audino et al. 2015a). Initially unfolded, the margin becomes bilobed during larval development. After metamorphosis, an outgrowth process is responsible for the emergence of the middle mantle fold from the outer surface of the inner fold (Audino *et al*. 2015a), corroborating a previous hypothesis on inner fold differentiation (Morton and Peharda 2008). It is not yet clear if this is a shared process among bivalves, additional comparative data being still necessary, especially for members from Arcida and Mytilida, given that mantle margin conformation in these latter cases is considerably different from the scallop pattern.

Homology of mantle margin components

Identifying homologies is central to morphological evolution and comparative anatomical studies and, in the case of the bivalve mantle margin, very little is known in this respect. Even the homology of the bivalve three-fold pattern is doubtful in the light of the numerous exceptions described so far (Waller 1978, Morton and Peharda 2008), the only undoubtedly homologous structure being the periostracal gland, making this structure a reference for comparisons (Waller 1978). Considering these limitations, a descriptive system based on the relative position of mantle folds was proposed (Waller 1978) (Fig. 3). In this case, mantle folds are numbered relative to the periostracal groove, preventing implicit homology hypotheses due to functional interpretations (Waller 1978). In the Arcoidea, number and organization of mantle folds were intensively debated, leading to a hypothesis assuming a two-fold mantle margin as the plesiomorphic state (Morton and Peharda 2008); this hypothesis, however, deserves testing within a phylogenetic framework.

Photoreceptor organs are also at the center of debates on homology at different taxonomic levels. Mantle photoreceptor cells and eyes have apparently evolved independently in the mantle margin of several distantly related bivalve taxa (Morton 2008, Salvini-Plawen

2008). These organs are largely regarded as not homologous structures with very similar endpoints (Morton 2008, Serb and Eernisse 2008). However, other mantle structures lack hypotheses of homology, mainly constrained by scarce anatomical data and lack of information for numerous taxa. For example, similar compound eyes are typically found in the Arcidae and in the close related Glycymerididae (Morton and Puljas 2015), but homology/homoplasy hypotheses have yet to be proposed and tested, since more data on anatomy, development and phylogenetic are still needed.

In general, mantle folds and their associated structures, such as tentacles, represent a challenge to understand putative ancestral conditions and homologies. For example, tentacle morphology of scallops (Pectinidae) shows several anatomical similarities compared to those present in file clams (Limidae) (Gilmour 1967, Moir 1977, Owen and McCrae 1979, Audino *et al*. 2015b). Additionally, simple tentacles are also present in phylogenetically close families, such as Spondylidae, Anomiidae and Propeamussidae, thus arising the logical hypothesis that middle fold tentacles would be present at least in the ancestor of Pectinoidea. At least for Pteriidae, tentacle morphology has been discussed in an evolutionary perspective, and these organs were considered homologous within the family (Tëmkin 2006a). Nevertheless, homology of tentacular structures in higher taxonomic levels cannot presently be assessed, since data from more close and distant pteriomorphian relatives should be considered and tested for congruence within a phylogenetic framework (see example in Fig. 4). As previously pointed out, the homology assessment for mantle characters still requires a broad survey of the mantle anatomy in the Pteriomorphia (Tëmkin 2006a).

Morphological convergence and parallelism

The evolutionary history of bivalves resulted in a high level of morphological similarities that still remain unclear. While convergent pathways lead to similar structures or functions in distantly related taxa with different ancestral conditions, parallel processes implies similar ancestral morphologies evolving by the same trajectories to a similar secondary condition (*e.g.*, Serb and Eernisse 2008). For example, similar body plans and shell shapes seem to have evolved by evolutionary convergence in different lineages of mytilids (Distel 2000) and scallops (Serb *et al.* 2011; Mynhardt *et al.* 2014), respectively.

Mantle margin diversity in Pteriomorphia provides an excellent framework to understand how convergent and parallel mechanisms have underlined the evolution of mantle characters. The presence of similar structures in several closely or distantly related taxa, as well as the same morphological function performed by different structures, are common cases in the pteriomorphian mantle margin (Waller 1976, Yonge 1983, Morton 2008). In addition, the clade is suitable to evaluate how some mantle characters such as mantle fold number and presence of tentacles have evolved, thus contributing to evolutionary and adaptive issues previously pointed out but still unclear (Tëmkin 2006a).

Correlation between lifestyle transitions and morphological changes and innovations

Lifestyle transitions were apparently remarkably abundant during Pteriomorphia diversification, and efforts to understand how and when these transitions occurred represent a key issue in the study of the evolution of the clade. For instance, an investigation with scallops has recently revealed how different lifestyles – such as the swimming habit – have had multiple origins by convergent evolution (Alejandrino *et al*. 2011, Serb *et al*. 2011). Also, phylogenetic analysis of the Pterioidea with subsequent mapping of substrata types suggested "epifaunal habit on rocks" as the ancestor lifestyle in pterioid bivalves, with a single origin of epizoic life on sessile cnidarians (Tsubaki *et al.* 2011). These results yielded significant hypotheses that should be analyzed under different perspectives and integrated into a major evolutionary scenario for pteriomorphian morphology and ecology.

Numerous lines of evidence suggest correlation between mantle margin and modes of life in bivalve evolution, although significant efforts are necessary to clarify these issues (Yonge 1962, Stanley 1972, Mynhardt *et al.* 2014). In infaunal bivalves, siphon formation and different levels of mantle fusion are considered adaptive features in this type of habit (Yonge 1957, Stanley 1968, Sartori and Mikkelsen 2008). In epifaunal bivalves, a pallial curtain is frequently present, mainly associated with the formation of functional apertures for water flow (Nelson 1938, Waller 1980, Yonge 1983). Similarly, numerous tentacular organs are distributed along the mantle margin of epifaunal species (Waller 1976). Despite such observations, patterns of covariation in habits of life and mantle margin morphology still lacks phylogenetic support and more comparative data. Again, the Pteriomorphia represent a suitable model for such issue due to their diversity in lifestyle transitions and mantle margin structure. A recent investigation on the evolution of the pallial eye and habitats in scallops revealed a tendency of changes in ocular traits according to depth (Malkowsky and Götze 2014). Hypotheses on morphological innovations of the mantle margin related to habit shifts could be tested under a phylogenetic framework, providing a major explanatory context, in a broader evolutionary sense, potentially being able to support more specific hypotheses on the association between habit, ecology and mantle morphology in bivalve lineages.

Macroecology of the marine epifauna

In the light of the anatomical organization frequently displayed by the marine benthos, several characters of the pteriomorphian mantle margin are functionally similar to other animals that live in close relationship with the marine substratum. For example, the bivalve mantle margin concentrates sensory organs that interact with the surrounding environment, just like the lophophores of bryozoans and the tentacular crowd of cnidarians and sessile polychaetes. All those organs, despite clearly not homologous, exhibit, for example, ciliary mechanisms that perform a variety of roles, such as sensory perception and food capture (Gilmour 1978, Orrhage 1980, Nielsen and Riisgard 1998). In a broader sense, the evolutionary significance of the mantle margin in Pteriomorphia might reveal insightful aspects of the evolution of the marine epifauna, leading to hypotheses on convergent pathways influenced by similar lifestyles.

Acknowledgments

The authors acknowledge funding provided by FAPESP (São Paulo Research Foundation; 2015/09519-4). The authors thank Jingchun Li and Alvin Alejandrino for invitation to the *Early Career Malacologists Symposium of the American Malacological Society 81st Annual Meeting*. JAA acknowledges the support of the American Malacological Society through a Travel Award to the 81st Annual Meeting and a Best Student Presentation Award in the same event. The following scientific collections have provided support: “Museu de Zoologia da Universidade de São Paulo” (MZUSP) and “Coleção de Bivalves da Universidade Estadual de Campinas” (ZUEC-BIC, Unicamp). The authors thank Prof. Jeanne M. Serb for invaluable contributions to the manuscript, and also the comments from an anonymous reviewer.

Literature cited

Acosta-Salmón, H., P. C. Southgate. 2005. Mantle regeneration in the pearl oysters *Pinctada fucata* and *Pinctada margaritifera*. *Aquaculture* **246**: 447–453.

Alejandrino, A., L. Puslednik, J. M. Serb. 2011. Convergent and parallel evolution in life habit of the scallops (Bivalvia: Pectinidae). *BMC Evolutionary Biology* **11**: 164.

Amaral, V. S., L. R. L. Simone. 2014. Revision of genus *Crassostrea* (Bivalvia : Ostreidae) of Brazil. *Journal of the Marine Biological Association of the United Kingdom* **94**: 811–836.

Ansell, A. D. 1961. The functional morphology of the British species of Veneracea (Eulamellibranchis). *Journal of Marine Biological Association of the United Kingdom* **41**: 489–515.

Ashburner, M., C. A. Ball, J. A. Blake, D. Botstein, et al. 2000. Gene Ontology: Tool for the unification of biology. The Gene Ontology Consortium. *Nature Genetics* **25**: 25–29.

Audino, J. A., J. E. A. R. Marian, A. Wanninger, S. G. B. C. Lopes. 2015a. Mantle margin morphogenesis in *Nodipecten nodosus* (Mollusca: Bivalvia): New insights into the development and the roles of bivalve pallial folds. *BMC Developmental Biology* **15**: 22.

Audino, J. A., J. E. A. R. Marian, A. Wanninger, S. G. B. C. Lopes. 2015b. Anatomy of the pallial tentacular organs of the scallop *Nodipecten nodosus* (Linnaeus, 1758) (Bivalvia: Pectinidae). *Zoologischer Anzeiger* **258**: 39–46.

Audino, J. A., J. E. A. R. Marian, A. Wanninger, S. G. B. C. Lopes. 2015c. Development of the pallial eye in *Nodipecten nodosus* (Mollusca : Bivalvia): Insights into early visual performance in scallops. *Zoomorphology* **134**: 403–415.

Audino, J. A., J. E. A. R. Marian, A. Kristof, A. Wanninger. 2015d. Inferring muscular ground patterns in Bivalvia: Myogenesis in the scallop *Nodipecten nodosus*. *Frontiers in Zoology* **12**: 34.

Beedham, G. E., E. R. Trueman. 1967. The relalionship of the mantle and shell of the Polyplacophora in comparison with that of other Mollusca. *Journal of Zoology* **151**: 215–231.

Beedham, G. E. 1958. Observations on the mantle of the Lamellibranchia. *Quarterly Journal of Microscopical Science* **99**: 181–197.

Beninger, P. G., S. D. St-Jean. 1997. The role of mucus in particle processing by suspension-feeding marine bivalves: Unifying principles. *Marine Biology* **129**: 389–397.

Bevelander, G., H. Nakahara. 1969. An electron microscope study of the formation of the nacreous layer in the shell of certain bivalve molluscs. *Calcified Tissue Research* **3**: 84–92.

Bieler, R., P. M. Mikkelsen, T. M. Collins, E. A. Glover, et al. 2014. Investigating the Bivalve Tree of Life - An exemplar-based approach combining molecular and novel morphological characters. *Invertebrate Systematics* **28**: 32–115.

Bieler, R., P. M. Mikkelsen. 2006. Bivalvia - A look at the branches. *Zoological Journal of the Linnean Society* **148**: 223–235.

Bubel. A. 1973. An electron-microscope study of periostracum formation in some marine bivalves. I. The Origin of the Periostracum. Marine Biology **20**: 213–221

Cannuel, R., P. G. Beninger, H. McCombie, P. Boudry. 2009. Gill development and its functional and evolutionary implications in the blue mussel *Mytilus edulis* (Bivalvia: Mytilidae). *Biological Bulletin* **217**: 173–188.

Carter, J. G., C. R. Altaba, L. C. Anderson, R. Araujo, et al. 2011. A synoptical classification of the Bivalvia (Mollusca). *Paleontological Contributions* **4**: 1–47.

Carter, J. G., P. J. Harries, N. Malchus, A. F. Sartori, et al. 2012. Illustrated glossary of the Bivalvia. *Treatise Online* **48**: 1–209.

Checa, A. G., A. B. Rodríguez-Navarro, F. J. Esteban-Delgado. 2005. The nature and formation of calcitic columnar prismatic shell layers in pteriomorphian bivalves. *Biomaterials* **26**: 6404–6414

Dakin, W. J. 1910. The eye of *Pecten*. *Quarterly Journal of Microscopical Science* **55**: 49–112.

Ding J., L. Zhao, Y. Chang, W. Zhao, Z. Du, Z. Hao. 2015. Transcriptome sequencing and characterization of japanese scallop *Patinopecten yessoensis* from different shell color lines. PLoS ONE **10**(2): e0116406.

Distel, D. L. 2000. Phylogenetic relationships among mytilidae (Bivalvia): 18S rRNA data suggest convergence in mytilid body plans. *Molecular Phylogenetics and Evolution* **15**: 25–33.

Dix, T. 1972. Histochemistry of mantle and pearl sac secretory cells in *Pinctada maxima* (Lamellibranchia). *Australian Journal of Zoology* **20**: 359–368.

Dougherty, L. F., S. Johnsen, R. L. Caldwell, N. J. Marshall. 2014. A dynamic broadband reflector built from microscopic silica spheres in the "disco" clam *Ctenoides ales*. *Journal of the Royal Society Interface* **11**: 98.

Elston, R. 1980. Functional anatomy, histology and ultrastructure of the soft tissues of the larval American oyster, *Crassostrea virginica. Proceedings of the National Shellfisheries Association* **70**: *65–93.*

Fang, Z., Q. Feng, Y. Chi, L. Xie, R. Zhang. 2008. Investigation of cell proliferation and differentiation in the mantle of *Pinctada fucata* (Bivalve, Mollusca). *Marine Biology* **153**: 745–54

Fishelson, L. 2000. Comparative morphology and cytology of siphons and siphonal sensory organs in selected bivalve molluscs. *Marine Biology* **137**: 497–509.

Freer, A., S. Bridgett, J. Jiang, M. Cusack. 2014. Biomineral proteins from *Mytilus edulis* mantle tissue transcriptome. *Marine Biotechnology* **16**: 34–45.

Furuhashi, T., C. Schwarzinger, I. Miksik, M. Smrz, A. Beran. 2009. Molluscan shell evolution with review of shell calcification hypothesis. *Comparative biochemistry and physiology Part B: Biochemistry and molecular biology* **154**: 351–371.

Gardner, L. D., D. Mills, A. Wiegand, D. Leavesley, A. Elizur. 2011. Spatial analysis of biomineralization associated gene expression from the mantle organ of the pearl oyster *Pinctada maxima*. *BMC genomics* **12**(1): 1.

Gilmour, T. 1963. A note on the tentacles of *Lima hians* (Gmelin) (Bivalvia). *Journal of Molluscan Studies* **35**: 82–85.

Gilmour, T. 1967. The defensive adaptations of *Lima hians* (Mollusca, Bivalvia). *Journal of Marine Biological Association of the United Kingdom* **47**: 209–221.

Gilmour, T. 1978. Ciliation and function of the food-collecting and waste-rejecting organs of lophophorates. *Canadian Journal of Zoology* **56**: 2142–2155.

Giribet, G., W. Wheeler. 2005. On bivalve phylogeny: a high-level analysis of the Bivalvia (Mollusca) based on combined morphology and DNA sequence data. *Invertebrate Biology* **121**: 271–324.

Giribet, G. 2008. Bivalvia. *In*: Ponder, W. F., and D. R. Lindberg, eds., *Phylogeny and Evolution of the Mollusca*. University of California Press, California. Pp. 105–142.

González, V. L., S. C. S. Andrade, T. M. Collins, C. W. Dunn, P. M. Mikkelsen, J. D. Taylor, G. Giribet. 2015. A phylogenetic backbone for Bivalvia : An RNA-seq approach. *Proceedings of the Royal Society B Biological Sciences* **282**: 1801.

Hamilton, P. V., K. M. Koch. 1996. Orientation toward natural and artificial grassbeds by swimming bay scallops, *Argopecten irradians* (Lamarck, 1819). *Journal of Experimental Marine Biology and Ecology* **199**: 79–88.

Harper, E. M. 1997. The molluscan periostracum: An important constraint in bivalve evolution. *Palaeontology* **40**: 71–98.

Harper, E. M., B. Morton. 1992. The biology of *Isognomon legumen* (Gmelin, 1791) (Bivalvia: Pterioida) at Cape D'Aguilar, Hong Kong, with special reference to predation by muricids. *In*: B. Morton, ed., *Proceedings of the Third International Workshop on the Malacofauna of Hong Kong and and Southern China, Hong Kong, 13 April − 1 May 1992*. Hong Kong University Press, Hong Kong. Pp. 405–425.

Harper, E. M., P. W. Skelton. 1993. The Mesozoic Marine Revolution and epifaunal bivalves. *Scripta Geologica, Special Issue* **2**: 127–153.

Hillman, R. E., C. N. J. Shuster. 1966. A comment on the origin of the fourth fold in the mantle of the quahog, *Mercenaria mercenaria*. *Chesapeake Science* **7**: 112–113.

Huang, X. D., M. Zhao, W. G. Liu, Y. Y. Guan, et al. 2013. Gigabase-scale transcriptome analysis on four species of pearl oysters. *Marine biotechnology* **15**(3): 253–264.

Hyman, L. H. 1967. *The Invertebrates, vol. 6: Mollusca*. McGraw-Hill, New York.

Jabbour-Zahab, R., D. Chagot. 1992. Mantle histology, histochemistry and ultrastructure of the pearl oyster *Pinctada margaritifera* (L.). *Aquatic Living Resources* **5**: 287–298.

Joubert, C., D. Piquemal, B. Marie, L. Manchon, et al. 2010. Transcriptome and proteome analysis of *Pinctada margaritifera* calcifying mantle and shell: Focus on biomineralization. *BMC Genomics* **11**: 613.

Kanehisa, M., Araki, M., Goto, S., Hattori, et al. 2008. KEGG for linking genomes to life and the environment. *Nucleic Acids Research* **36**: D480–D484.

Kleemann, K. 1990. Evolution of chemically-boring Mytilidae (Bivalvia). *In*: Morton, B., ed, *The Bivalvia: Proceedings of a Memorial Symposium in Honour of Sir Charles Maurice Yonge, Edinburgh 1986*. Hong Kong University Press, Hong Kong. Pp 111–124.

Land, M. F. 1966. A multilayer interference reflector in the eye of the scallop, *Pecten maximus*. *Journal of Experimental Biology* **45**: 433–447.

Lemche, H., K. Wingstrand. 1959. The anatomy of *Neopilina galatheae*, 1957 (Mollllusca, Tryblidiacea). *Galathea Report* **3**: 9–71.

Malkowsky, Y., M. C. Götze. 2014. Impact of habitat and life trait on character evolution of pallial eyes in Pectinidae (Mollusca: Bivalvia). *Organisms Diversity and Evolution* **14**: 173–185.

Matsumoto, M. 2003. Phylogenetic analysis of the subclass Pteriomorphia (Bivalvia) from mtDNA COI sequences. *Molecular Phylogenetics and Evolution* **27**: 429–440.

Miyamoto, H., H. Endo, N. Hashimoto, K. Limura, et al. 2013. The diversity of shell matrix proteins: Genome-wide investigation of the pearl oyster, *Pinctada fucata*. *Zoological science* **30**(10): 801–816.

Moir, A. J. 1977. Ultrastructural studies on the ciliated receptors of the long tentacles of the giant scallop, *Placopecten magellanicus* (gmelin). *Cell and Tissue Research* **184**: 367–380.

Morton, B. 1982a. Functional morphology of *Bathyarca pectunculoides* (Bivalvia: Arcacea) from a deep Norwegian fjord with a discussion of the mantle margin in the Arcoida. *Sarsia* **67**: 269–282.

Morton, B. 1982b. The mode of life and functional morphology of *Gregariella coralliophaga*

(Gmelin, 1791) (Bivalvia: Mytilacea) with a discussion on the evolution of the boring Lithophaginae and adaptive radiation in the Mytilidae. *In*: Morton, B., and C. K. Tseng, eds., *Proceedings of the First International Marine Biological Workshop: The Marine Flora and Fauna of Hong Kong and Southern China, Hong Kong, 1980*. Hong Kong University Press, Hong Kong. Pp. 875–895

Morton, B. 1987a. The mantle margin and radial mantle glands of *Entodesma saxicola* and *E. inflata* (Bivalvia: Anomalodesmata: Lyonsiidae). *Journal of Molluscan Studies* **53**: 139–151.

Morton, B. 1987b. The pallial photophores of *Barbatia virescens* (Bivalvia, Arcacea). *Journal of Molluscan Studies* **53**: 241–244.

Morton, B. 1995. The biology and functional morphology of *Pteria brevialata* (Bivalvia: Pterioidea), epizoic on gorgonians in Hong Kong. *Journal of Zoology* **236**: 223–241.

Morton, B. 2000a. The function of pallial eyes within the Pectinidae, with a description of those present in *Patinopecten yessoensis*. *Geological Society of London, Special Publications* **177**: 247–255.

Morton, B. 2000b. The pallial eyes of *Ctenoides floridanus* (Bivalvia: Limoidea). *Journal of Molluscan Studies* **66**: 449–455.

Morton, B. 2008. The evolution of eyes in the Bivalvia: New Insights. *American Malacological Bulletin* **26**: 35–45.

Morton, B., M. Peharda. 2008. The biology and functional morphology of *Arca noae* (Bivalvia: Arcidae) from the Adriatic Sea, Croatia, with a discussion on the evolution of the bivalve mantle margin. *Acta Zoologica* **89**: 19–28.

Morton, B., S. Puljas. 2015. The ectopic compound ommatidium-like pallial eyes of three species of Mediterranean (Adriatic Sea) *Glycymeris* (Bivalvia: Arcoida). Decreasing visual acuity with increasing depth? *Acta Zoologica (Stockholm)* **00**: 000–000.

Morton, B., P. J. B. Scott. 1980. Morphological and functional specializations of the shell, musculature and pallial glands in the Lithophaginae (Mollusca: Bivalvia). *Journal of Zoology* **192**(2): 179–203.

Mynhardt, G., A. Alejandrino, L. Puslednik, J. Corrales, J. M. Serb. 2014. Shell shape convergence masks biological diversity in gliding scallops: Description of *Ylistrum* n. gen.(Pectinidae) from the Indo-Pacific Ocean. *Journal of Molluscan Studies* **80**(4): 400–411.

Narchi, W., M. S. Galvão-bueno. 1997. Anatomia funcional de *Perna perna* (Linné) (Bivalvia, Mytilldae). Revista Brasileira de Zoologia **14**: 135–168. [In Portuguese]

Nelson, T. C. 1938. The feeding mechanism of the oyster. I. On the pallium and the branchial chambers of *Ostrea virginica*, *O. edulis* and *O. angulata*, with comparisons with other species of the genus. *Journal of Morphology* **63**: 1–61.

Nielsen, C., H. U. Riisgard. 1998. Tentacle structure and filter-feeding in *Crisia eburnea* and other cyclostomatous bryozoans, with a review of upstream-collecting mechanisms. *Marine Ecology Progress Series* **168**: 163–186.

Nilsson, D. E. 1994. Eyes as optical alarm systems in fan worms and ark clams. *Philosophical Transactions of the Royal Society B: Biological Sciences* **346**: 195–212.

Oliver, G., J. A. Allen. 1980. The functional and adaptive morphology of the deep-sea species of the Arcacea (Mollusca: Bivalvia) from the Atlantic. *Philosophical Transactions of the*

Royal Society of London B: Biological Sciences **291**(1045): 45–76.

Oliver, P. G., A. M. Holmes. 2006. The Arcoidea (Mollusca: Bivalvia): A review of the current phenetic-based systematics. *Zoological Journal of the Linnean Society* **148**: 237–251.

Orrhage, L. 1980. On the structure and homologues of the anterior end of the polychaete families Sabellidae and Serpulidae. *Zoomorphology* **96**: 113–167.

Owada, M. 2007. Functional morphology and phylogeny of the rock-boring bivalves *Leiosolenus* and *Lithophaga* (Bivalvia: Mytilidae): A third functional clade. *Marine Biology* **150**: 853–860.

Owen, G., J. M. McCrae. 1979. Sensory cell/gland cell complexes associated with the pallial tentacles of the bivalve *Lima hians* (Gmelin), with a note on specialized cilia on the pallial curtains. *Philosophical Transactions of the Royal Society B: Biological Sciences* **287**: 45–62.

Pairett, A. N., J. M. Serb. 2013. *De novo* assembly and characterization of two transcriptomes reveal multiple light-mediated functions in the scallop eye (Bivalvia: Pectinidae). *PLoS ONE* **8**: e69852.

Passos, F. D., O. Domaneschi. 2004. Biologia e anatomia funcional de *Donax gemmula* Morrison (Bivalvia, Donacidae) do litoral de São Paulo, Brasil. *Revista Brasileira de Zoologia* **21**: 1017–1032. [In Portuguese]

Prezant, R. S. 1981. The arenophilic radial mantle glands of the Lyonsiidae (Bivalvia, Anomalodesmata) with notes on lyonsiid evolution. *Malacologia* **20**(2): 267–289.

Prezant, R. S. 1990. Form, function and phylogeny of bivalve mucins. *In*: Morton, B., ed, *The Bivalvia: Proceedings of a Memorial Symposium in Honour of Sir Charles Maurice Yonge, Edinburgh 1986*. Hong Kong University Press, Hong Kong. Pp 83–95.

Reindl, S., G. Haszprunar. 1996. Fine structure of caeca and mantle of arcoid and limopsoid bivalves (Mollusca: Pteriomorpha). *The Veliger* **39**: 101–116.

Salvini-Plawen, L. Von. 2008. Photoreception and the polyphyletic evolution of photoreceptors (with special reference to Mollusca). *American Malacological Bulletin* **26**: 83–100.

Sartori, A. F., E. M. Harper. 2009. Sticky bivalves from the Mesozoic: Clues to the origin of the anomalodesmatan arenophilic system. *Lethaia* **42**(4): 486–494.

Sartori, A. F., C. Printrakoon, P. M. Mikkelsen, R. Bieler. 2008. Siphonal structure in the Veneridae (Bivalvia : Heterodonta) with an assessment of its phylogenetic application and a review of venerids of the gulf of Thailand. *The Raffles Bulletin of Zoology* ***18***: 103–125.

Sartori, A. F., F. D. Passos, O. Domaneschi. 2006. Arenophilic mantle glands in the Laternulidae (Bivalvia: Anomalodesmata) and their evolutionary significance. *Acta Zoologica* **87**: 265–272.

Saleuddin, A. S. M., H. P. Petit. 1983. The mode of formation and the structure of the periostracum. ln: Wilbur, J. M., ed., *The Mollusca*. Academic Press, New York. Pp. 199–231.

Serb, J. M., A. Alejandrino, E. Otárola-Castillo, D. C Adams. 2011. Morphological convergence of shell shape in distantly related scallop species (Mollusca: Pectinidae). *Zoological Journal of the Linnean Society* **163**: 571–584.

Serb, J. M., D. J. Eernisse. 2008. Charting evolution’s trajectory: Using molluscan eye diversity to understand parallel and convergent evolution. *Evolution: Education and Outreach* **1**: 439–447.

Serb, J. M., A. J. Porath-Krause, A. N. Pairett. 2013. Uncovering a gene duplication of the photoreceptive protein, opsin, in scallops (Bivalvia: Pectinidae). *Integrative and Comparative Biology* **53**: 68–77.

Sharma, P. P., V. L. González, G. Y. Kawauchi, S. C. Andrade, et al. 2012. Phylogenetic analysis of four nuclear protein-encoding genes largely corroborates the traditional classification of Bivalvia (Mollusca). *Molecular Phylogenetics and Evolution* **65**(1): 64–74.

Shi, M., Y. Lin, G. Xu, L. Xie, X. Hu, Z. Bao, R. Zhang. 2013. Characterization of the Zhikong scallop (*Chlamys farreri*) mantle transcriptome and identification of biomineralization-related genes. *Marine biotechnology* **15**(6): 706–715.

Simone, L. R. L., P. M. Mikkelsen, R. Bieler. 2015. Comparative anatomy of selected marine bivalves from the Florida Keys, with notes on Brazilian congeners (Mollusca: Bivalvia). *Malacologia* **58**: 1–127.

Speiser, D. I., S. Johnsen. 2008. Comparative morphology of the concave mirror eyes of scallops (Pectinoidea). *American Malacological Bulletin* **26**: 27–33.

Stanley, S. M. 1968. Post-Paleozoic adaptive radiation of infaunal bivalve molluscs: A consequence of mantle fusion and siphon formation. *Journal of Paleontology* **42**: 214–229.

Stanley, S. M. 1972. Functional morphology and evolution of byssally attached bivalve mollusks. *Journal of Paleontology* **46**: 165–212.

Stanley, S. M. 1975. Adaptive themes in the evolution of the Bivalvia (Mollusca). *Annual Review of Earth and Planetary Sciences* **3**: 361–385.

Stasek, C. R., W. R. Mcwilliams. 1973. The comparative morphology and evolution of the molluscan mande edge. *The Veliger* **16**: 1–19.

Steiner, G. S. 1998. Point of view phylogeny of Scaphopoda (Mollusca) in the light of new anatomical data on the Gadilinidae and some problematica, and a reply to Reynolds. *Zoologica Scripta* **27**: 73–82.

Steiner, G., S. Hammer. 2000. Molecular phylogeny of the Bivalvia inferred from 18S rDNA sequences with particular reference to the Pteriomorphia. *Geological Society, London, Special Publications* **177**: 11–29.

Sun, X., A. Yang, B. Wu, L. Zhou, Z. Liu. 2015. Characterization of the mantle transcriptome of Yesso scallop (*Patinopecten yessoensis*): Identification of genes potentially involved in biomineralization and pigmentation. *PLOS One* **10**(4): e0122967.

Takeuchi, T., R. Koyanagi, F. Gyoja, M. Kanda, et al. 2016. Bivalve-specific gene expansion in the pearl oyster genome: Implications of adaptation to a sessile lifestyle. *Zoological letters* **2**: 3.

Taylor, J. D. 1973. The structural evolution of the bivalve shell. *Palaeontology* **16**(3): 519–534.

Tëmkin, I. 2006a. Morphological perspective on the classification and evolution of recent Pterioidea (Mollusca: Bivalvia). *Zoological Journal of the Linnean Society* **148**: 253–312.

Tëmkin, I. 2006b. Anatomy, shell morphology, and microstructure of the living fossil *Pulvinites exempla* (Hedley, 1914) (Mollusca: Bivalvia: Pulvinitidae). *Zoological Journal of the*

Linnean Society **148**: 523–552.

Tëmkin, I. 2010. Molecular phylogeny of pearl oysters and their relatives (Mollusca, Bivalvia, Pterioidea). *BMC Evolutionary Biology* **10**: 342.

Timmermans, L. P. 1968. Studies on shell formation in molluscs. *Netherlands Journal of Zoology* **19**(4): 413–523.

Tsubaki, R., Y. Kameda, M. Kato. 2011. Pattern and process of diversification in an ecologically diverse epifaunal bivalve group Pterioidea (Pteriomorphia, Bivalvia). *Molecular phylogenetics and evolution* **58**(1): 97–104.

Ubukata, T. 1997. Mantle kinematics and formation of commarginal shell sculpture in Bivalvia. *Paleontological Research* **1**(2): 132–143.

Voronezhskaya, E. E., L. P. Nezlin, N. A. Odintsova, J. T. Plummer, R. P. Croll. 2008. Neuronal development in larval mussel *Mytilus trossulus* (Mollusca: Bivalvia). *Zoomorphology* **127**: 97–110.

Waller, T. R. 1976. The behavior and tentacle morphology of pteriomorphian bivalves: A motion-picture study. *Bulletin of the American Malacological Union* **1975:** 7–13.

Waller, T. R. 1978. Morphology, morphoclines and a new classification of the Pteriomorphia (Mollusca: Bivalvia). *Philosophical Transactions of the Royal Society B: Biological Sciences* **284**: 345–365.

Waller, T. R. 1980. Scanning electron microscopy of shell and mantle in the order Arcoida (Mollusca: Bivalvia). *Smithsonian Contributions to Zoology* **313**: i-iii, 1–58.

Waller, T. R. 1998. Origin of the molluscan class Bivalvia and a phylogeny of major groups. In: Johnston P. A., J. W. Haggart, eds., *Bivalves: An Eon of Evolution - Palaeobiological studies honoring Norman D. Newell*. University of Calgary Press, Calgary. Pp. 1–45.

Waller, T. R. 2006. Phylogeny of families in the Pectinoidea (Mollusca: Bivalvia): Importance of the fossil record. *Zoological Journal of the Linnean Society* **148**: 313–342.

Westermann, B., H. Schmidtberg, K. Beuerlein. 2005. Functional morphology of the mantle of *Nautilus pompilius* (Mollusca, Cephalopoda). *Journal of Morphology* **264**: 277–285.

Wilbur, K. M., A. S. M. Saleuddin. 1983. Shell formation. *In*: Saleuddin, A. S. M., and K. M. Wilbur, eds., *The Mollusca, Vol. 4. Physiology*. Academic Press, New York. Pp. 235–287.

Wilkens, L. A. 2006. Neurobiology and behavior of the scallop. *In*: S. E. Shumway, G. J. Parsons, eds, *Scallops: Biology, Ecology and Aquaculture*. Elsevier, Amsterdan. Pp. 317–356.

Wurzinger-Mayer, A., J. R. Shipway, A. Kristof, T. Schwaha, S. M. Cragg, A. Wanninger. 2014. Developmental dynamics of myogenesis in the shipworm *Lyrodus pedicellatus* (Mollusca: Bivalvia). *Frontiers in Zoology* **11**: 90.

Xue, D. X., H. Y. Wang, T. Zhang, S. P. Zhang, F. S. Xu. 2012. 基于 28S rRNA 基因片段的翼形亚纲 (Bivalvia: Pteriomorphia) 系统发育的初步研究. *Oceanologia et Limnologia Sinica* **43**: 348–356. [In Chinese]

Yonge, C. M. 1936. The evolution of the swimming habit in the Lamellibranchia. *Mémoires du Musée Royal d'Histoire Naturelle de Belgique* **3**: 77–100.

Yonge, C. M. 1948. Formation of Siphons in Lamellibranchia. *Nature* **161**: 198–199.

Yonge, C. M. 1953. Form and Habit in *Pinna carnea* Gmelin. *Philosophical Transactions of the Royal Society B: Biological Sciences* **237**: 335–374.

Yonge, C. M. 1957. Mantle fusion in the Lamellibranchia. *Pubblicazioni Stazione Zoologica di Napoli* **29**: 151–171.

Yonge, C. M. 1962. On the primitive significance of the byssus in the Bivalvia and its effects in evolution. *Journal of Marine Biological Association of the United Kingdom* **42**: 113–125.

Yonge, C. M. 1982. Functional morphology and evolution in the Tridacnidae (Mollusca: Bivalvia: Cardiacea). *Records of the Australian Museum* **33**: 735–777.

Yonge, C. M. 1983. Symmetries and the role of the mantle margins in the bivalve Mollusca. *National Wildlife* **16**: 1–10.

Zhang, G., X. Fang, X. Guo, L. Li, R. Luo, et al. 2012. The oyster genome reveals stress adaptation and complexity of shell formation. *Nature* **490**(7418): 49–54.

Zwarts, L., J. Wanink. 1989. Siphon size and burying depth in deposit-and suspension-feeding benthic bivalves. *Marine Biology* **100**(2): 227–240.

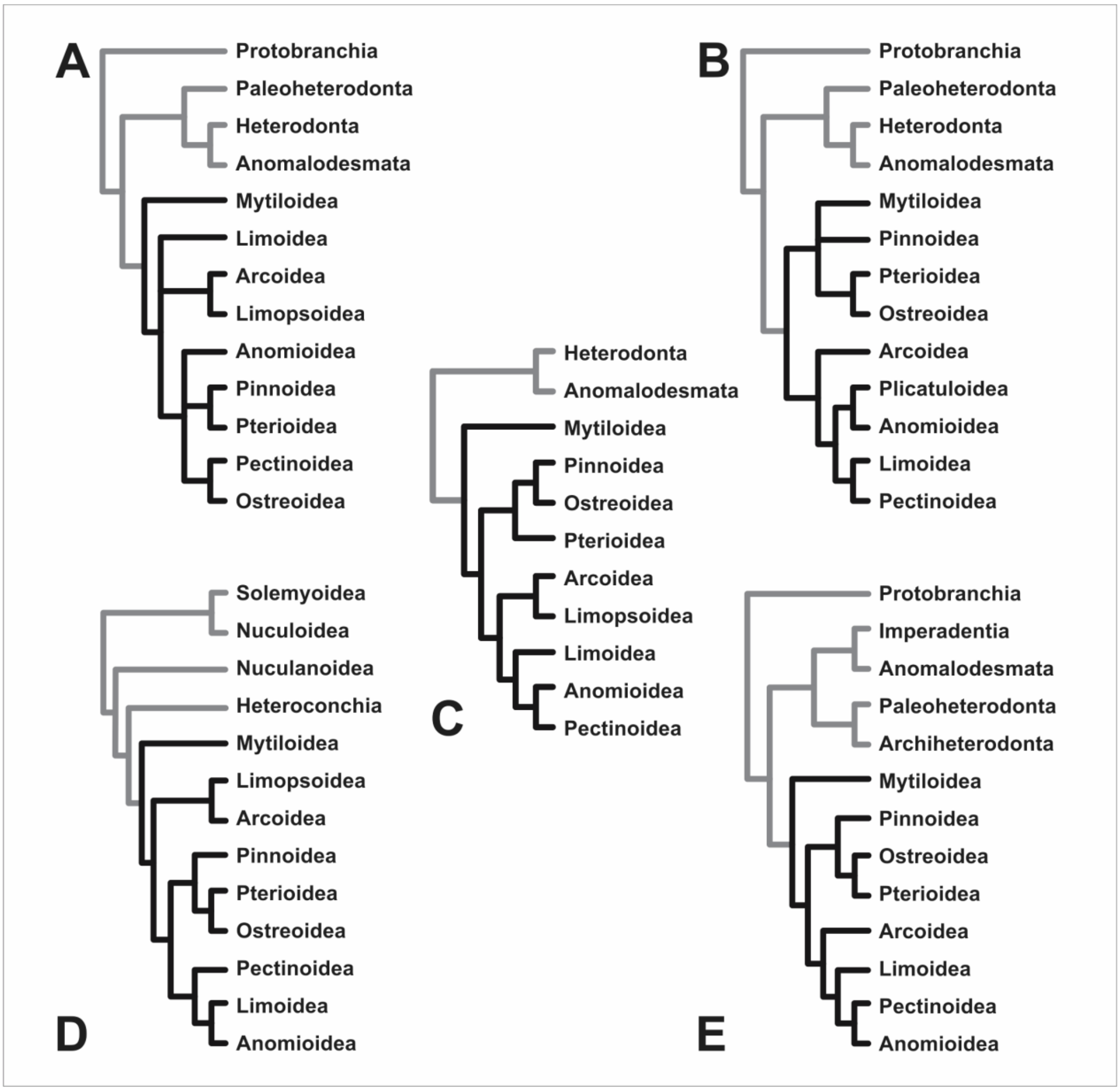

Figure1. Hypotheses for the internal relationships of Pteriomorphia (black branches) based on molecular and/or morphological data. **A.** Waller (1998). **B.** Steiner and Hammer (2000). **C.** Matsumoto (2003). **D.** Giribet and Wheeler (2002). **E.** Bieler *et al*. (2014).

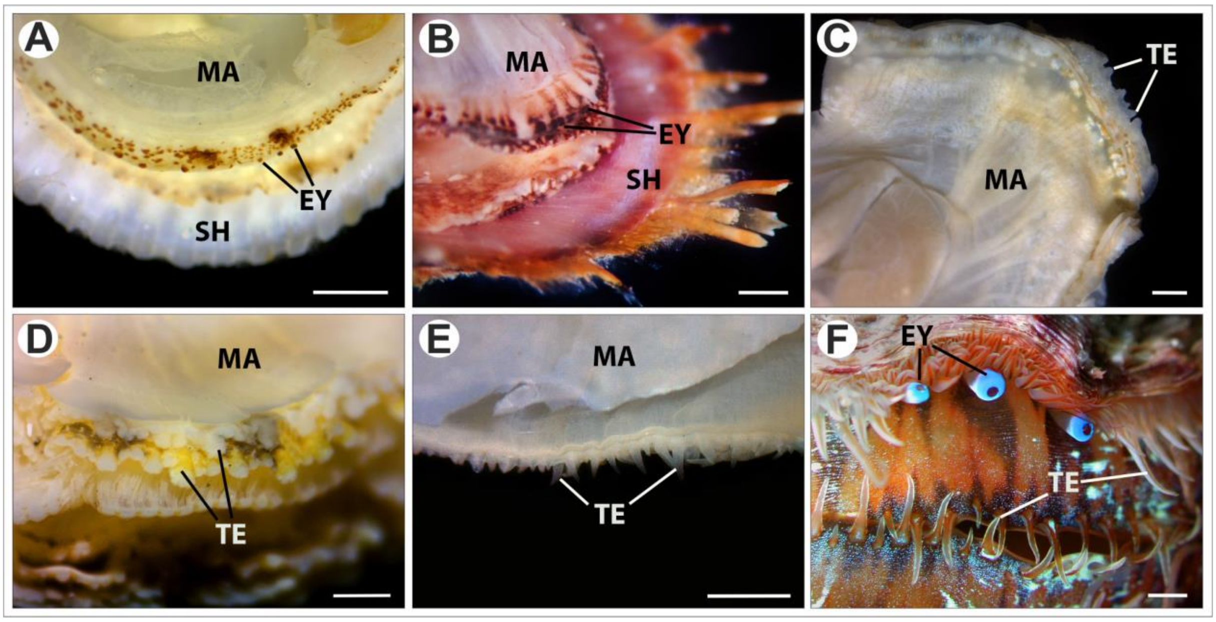

Figure 2. Mantle margin morphology in selected pteriomorphian species. Scale bars: 1mm. **A.** *Glycymeris pectinata* (Gmelin, 1791) (ZUEC-BIV 2198). **B.** *Barbatia cancellaria* (Lamarck, 1819) (MZUSP 48857). **C.** *Atrina seminuda* (Lamarck, 1819) (ZUEC-BIV 2135). **D.** *Pteria hirundo* (Linnaeus, 1758) (ZUEC-BIV 1401). **E.** *Anomia simplex* d'Orbigny, 1853 (ZUEC-BIV 1423). **F.** *Nodipecten nodosus* (specimen from Audino *et al*. 2015a). Abbreviations: EY, pallial eyes; MA, mantle; SH, shell; TE, pallial tentacles.

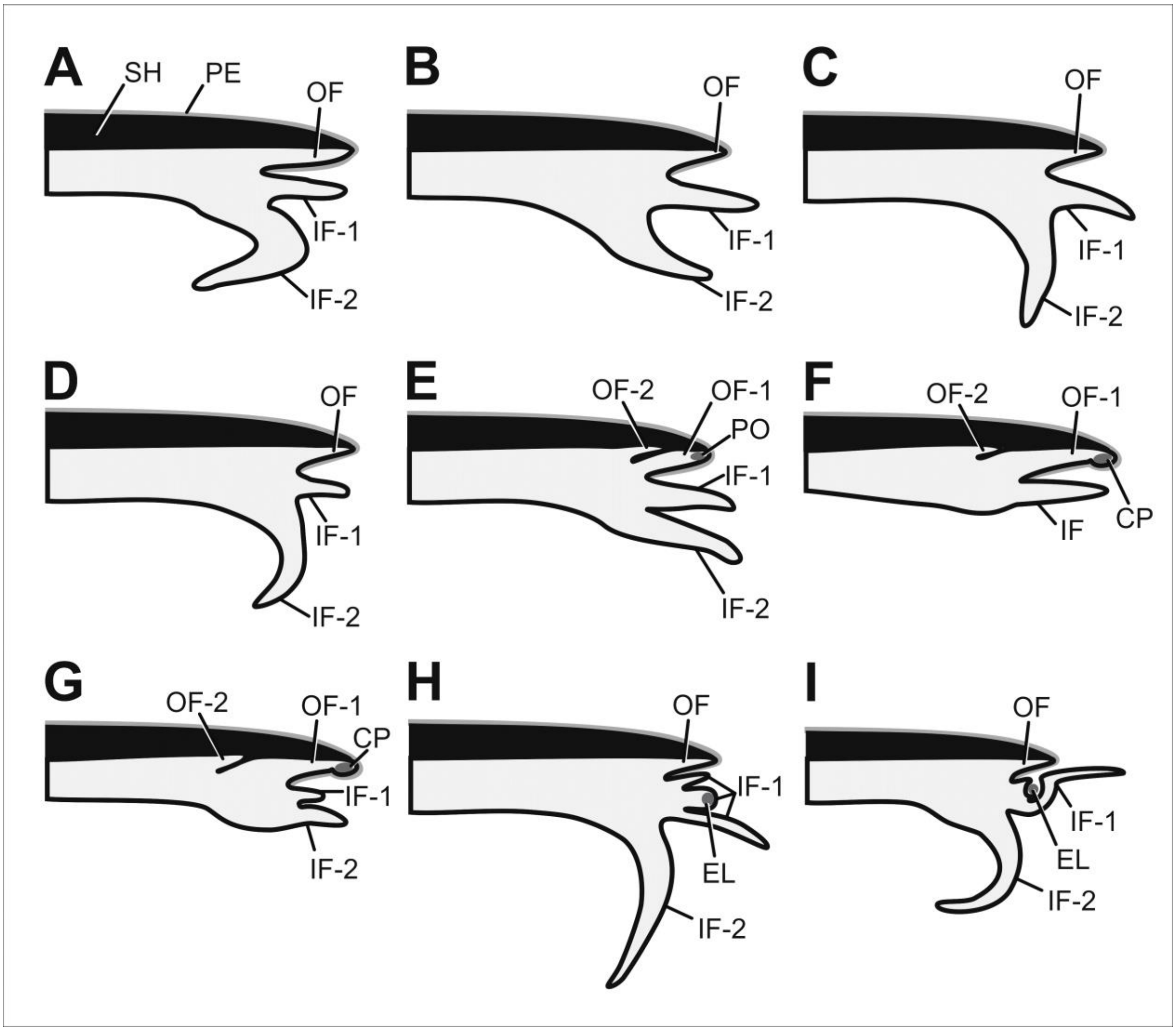

Figure 3. Morphological diversity of the mantle margin in the Pteriomorphia illustrated in cross-section. **A.** *Brachidontes exustus* (Linnaeus, 1758) (Myilidae) (Redrawn after Simone *et al.* 2015). **B.** *Crassostrea mangle* Amaral & Simone, 2014 (Ostreidae) (Redrawn after Amaral and Simone 2014). **C.** *Pinna carnea* Gmelin, 1791 (Pinnidae) (Redrawn after Yonge 1953). **D.** *Pinctada margaritifera* (Pteriidae) (Redrawn after Jabbour-Zahab and Chagot 1992). **E.** *Isognomon radiatus* (Pteriidae) (Redrawn after Tëmkin 2006a). **F.** *Glycymeris bimaculata* (Poli, 1795) (Glycymerididae) (Redrawn after Morton and Puljas 2015). **G.** *Barbatia cancellaria* (Arcidae) (Redrawn after Morton 1982). **H.** *Nodipecten nodosus* (Pectinidae) (Redrawn after Audino et al. 2015d). **I.** *Ctenoides mitis* (Limidae) (Redrawn after Morton 2000b). Abbreviations: CP, compound pallial eye; EL, pallial eye bearing lens; IF, inner mantle fold; IF-1, first inner fold; IF-2, second inner fold; OF, outer mantle fold; OF-1, first outer fold; OF-2, second outer fold; PE, periostracum; PO, pallial ocellus (pigmented cup); SH, shell.

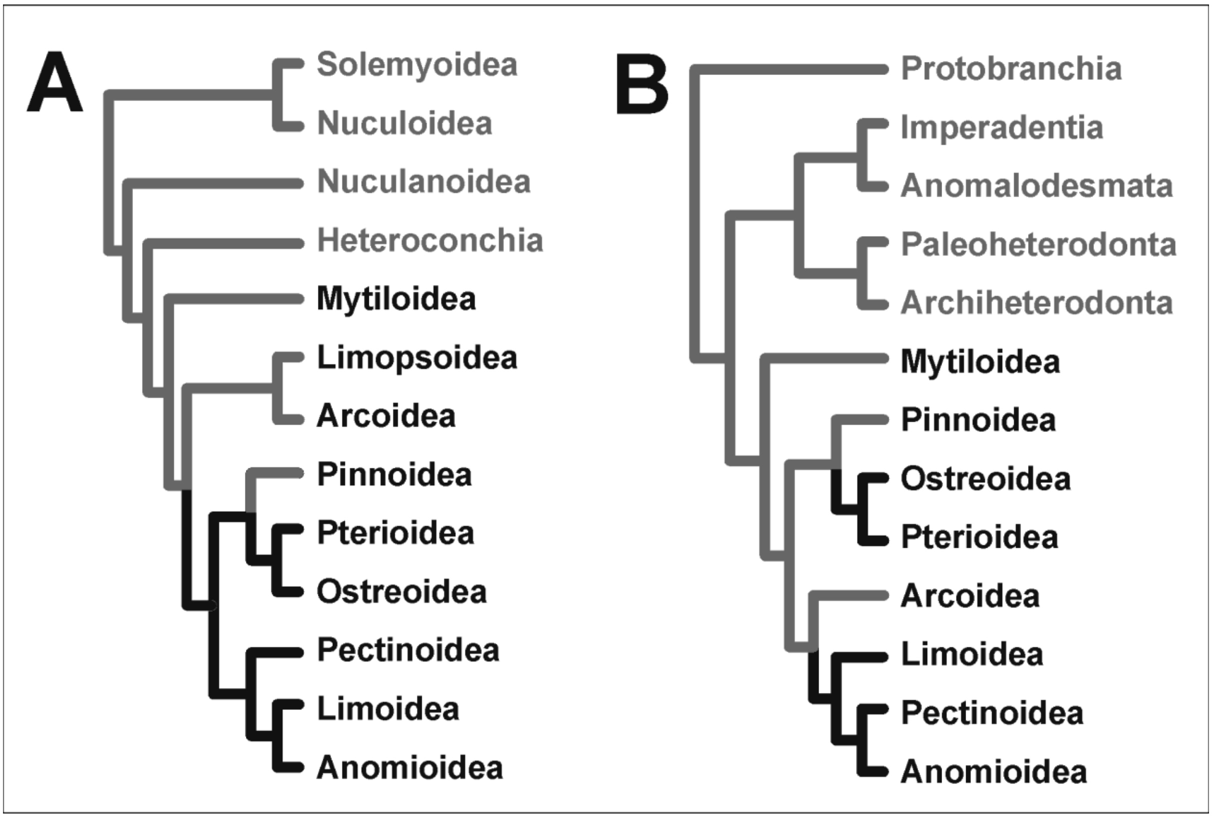

Figure 4. Competitive hypotheses for the evolution of tentacles (black branches) in the middle mantle margin (IF-1) within Pteriomorphia. **A.** In this particular topology (Giribet and Wheeler 2002), the tentacles from the middle mantle fold would have arisen once in the ancestor of all pteriomorphians excluding the Arcida (Arcoidea + Limopsoidea) and Mytilida (Mytiloidea). Subsequently, tentacles would have been lost in the branch leading to Pinnoidea (pen shells). **B.** Other phylogenetic scenarios (*e.g.*, Bieler *et al*. 2014), however, may impose different reconstructions of ancestral character state. For example, tentacles might have evolved twice independently in Pteriomorphia, specifically in the clades Pterioidea+Ostreoidea and Limoidea+Pectinoidea+Anomioidea. Consequently, the tentacles found in both clades would not be homologous, being originated by convergent evolution.

CHAPTER 2

On the evolution of mantle photoreceptor organs in Pteriomorphia (Mollusca: Bivalvia)

CHAPTER 2

On the evolution of mantle photoreceptor organs in Pteriomorphia (Mollusca: Bivalvia)

Abstract

Bivalves exhibit a wide range of photoreceptor organs, making them suitable models for investigations on eye evolution. In particular, pteriomorphian bivalves (e.g., oysters, scallops, and ark clams) display a remarkable diversity of photoreceptor organs and ecologies. The present study evaluated the morphology and distribution of eyes in Pteriomorphia, as well as their history of lifestyle transitions to determine 1) how many times eyes have evolved, and 2) whether lifestyles transitions influenced photoreceptor evolution. The phylogenetic approach is based on five sequences (16S rRNA, 18S rRNA, 28S rRNA, COI mtDNA, and histone H3; from the Genbank), including 185 species of 19 pteriomorphian families. Morphological data were acquired for 162 preserved species and lifestyles were compiled from the literature. The present phylogenetic analysis of Pteriomorphia, which has the greatest taxonomic sampling to date, recovered most families as monophyletic and organized in four orders across two main clades (Arcida+Pectinida and Ostreida+Mytilida). Photoreceptor organs have arisen exclusively in epifaunal lineages, at least six times independently. They comprise five types (i.e., pigmented caps, pigmented cups, compound eyes, concave mirror eyes, and invaginated eyes) and are present in 11 families. Transitions to byssally crevice-dwelling habit seem associated with convergent gains of eyespots. Once photoreceptor organs have arisen, multiple secondary losses occurred in lineages that shifted to infaunal habits. The observed patterns suggest that phototaxis, posture control, and alarm responses represent the main light-guided behaviors driving eye evolution in pteriomorphians. Altogether, our results provide a robust basis to explore macroevolutionary patterns of photoreception in marine benthic invertebrates.

Keywords: eye, convergence, macroecology, morphology, phylogeny, habit, transition.

Introduction

Photoreceptor organs are among key systems in comparative studies focused on understanding multi-level diversity and complex trait evolution (Land and Nilsson 2012; Oakley and Speiser 2015). Accordingly, central questions in eye evolution were explored through the application of numerous approaches, including comparative anatomy, phylogenetic diversification, genetic regulation, and ecological studies of visual guided behaviors (Arendt 2003; Nilsson 2013). For example, substantial contributions were obtained by means of genetic experiments and comparative genomics to understand the origin and evolution of simple photoreceptor organs and complex image forming eyes (Gehring 2014). Common use and independent recruitment of genetic components, such as the master control gene Pax6, suggest the homology of different eye-types at the molecular level and subsequent diversification by divergent, parallel, or convergent evolution (Vopalensky and Kozmik 2009; Gehring 2014).

Model organisms have been playing a crucial role in eye investigation to explore functional bases and evolutionary patterns of eye diversification, but there are plenty of other promising model animals to explore (Serb and Eernisse 2008). Marine invertebrates, for instance, display a plethora of photoreceptor organs, including clades with high diversity of eye types and visual mechanisms (Cronin 1986; Land and Nilsson 2012). For example, extinct and extant arthropod groups experienced a wide diversification of visual systems, including numerous variations in compound eyes and optical mechanisms (Oakley 2003; Nilsson and Kelber 2007; Strausfeld et al. 2016). In polychaetes, a wide diversity of photoreceptor organs is found among sessile worms, varying from single ocelli to compound eyes (Nilsson 1994; Purschke et al. 2006; Bok et al. 2016, 2017).

Mollusks are regarded as models to understand functional anatomy and convergent evolution of photoreceptor systems (Serb and Eernisse 2008). Different photoreceptor organs have evolved in most molluscan classes, resulting in an unusual diversity of systems and optical properties in the phylum. For instance, visual ecology was extensively investigated in cephalopods, demonstrating high visual acuity in coleoids, such as squids and octopuses, which have camera-type eyes (Sivak 1982; Sweeney et al. 2007). Comparative analyses of Pax genes across metazoans show unique patterns underlying eye diversity and plasticity in cephalopods (Navet et al. 2017). At the genetic level, the acquisition of multiple splicing variants of Pax-6 is responsible for the development of this eye type, resulting in an extreme case of morphological convergence with vertebrate eyes (Yoshida et al. 2014). In addition, phylogenetic comparative data of cephalopods indicates convergent evolution of a corneal membrane in different demersal lineages (Lindgren et al. 2012).

Bivalve mollusks display a wide range of photoreceptor organs, including cephalic larval eyespots, ctenidial eyespots, and mantle eyes (Morton 2008). The latter comprise different types of organs, varying from simple pigmented photoreceptor cells to complex camera-type eyes (Morton 2008; Wilkens 2008). The most familiar example are the eyes found in the mantle of scallops (Pectinidae), which are generally conspicuous as bright, repeated structures (Dakin 1910). These concave mirror eyes have been extensively investigated through anatomical, developmental, and even opsin characterization studies (Land 1965; Speiser and Johnsen 2008; Serb et al. 2013; Audino et al. 2015; Palmer et al. 2017). Other intriguing bivalve mantle eyes include lens-bearing eyespots in giant clams (Tridacnidae) (Wilkens 1986; Land 2003) and camera-type eyes in *Laternula* (Laternulidae) (Adal and Morton 1973). Interestingly, most lineages of bivalves bearing mantle photoreceptor organs are included in a clade named Pteriomorphia (Morton 2008), which encompasses many epifaunal bivalves, such as scallops, oysters, ark clams, and mussels.

Eyes in Pteriomorphia vary from simple eyespots to more elaborate structures, such as the invaginated eyes of file clams (Limidae) (Morton 2000a), the compound eyes of ark clams (Arcidae) (Waller 1980; Morton and Peharda 2008), and the aforementioned mirror eyes of scallops (Pectinidae). Recent progresses in the understanding of eye evolution in bivalves were obtained for ark clams and relatives (Arcida), in which a correlation was found between eye loss and infaunalization (Audino et al. 2019), and for Pectinidae, in which the evolution of eye size and components seems related to bathymetric distribution (Malkowsky and Götze 2014).

Even though anatomical information for pteriomorphian eyes are available for selected species the origin and diversification of photoreceptor organs remains unknown for the clade. Phylogenetic comparative studies are helpful to estimate broad patterns of photoreception evolution and the environmental context of eye origins (Oakley and Speiser 2015). In addition, the behavioral drive between sensory systems and natural selection suggest that reconstruction of eye evolution should account for the evolution of corresponding behaviors (Nilsson and Bok 2017), which are ultimately associated with lifestyles and habitat use. Here, we focused on pteriomorphian bivalves to understand how many times photoreceptor organs have evolved and whether lifestyles are evolutionary associated with eye evolution.

Firstly, the present study examined the presence and morphology of photoreceptor organs in pteriomorphian groups to accurately identify its diversity. Then, a phylogenetic hypothesis for Pteriomorphia was inferred to provide a suitable background to investigate eye evolution and possible associations with lifestyles.

Material and Methods

Ecological and morphological investigation

Mantle photoreceptor organs were investigated for presence, type, location, and general morphology in 162 species from 18 families of Pteriomorphia (Table 1). Three species, i.e., *Isognomon bicolor* (C. B. Adams, 1845), *Nodipecten nodosus* (Linnaeus 1759), and *Spondylus ictericus* Reeve, 1856, were collected in São Sebastião's coast (São Paulo State, Brazil), anesthetized, and processed for analyses following the method of Audino et al. (2019). The remaining species were investigated through the analysis of archived specimens (Table 1), which were examined in ethanol under the stereomicroscope. In addition, histological sections were obtained from samples of *Acar dominguensis* (Lamarck, 1819) (Arcidae), *Barbatia cancellaria* (Lamarck, 1819) (Arcidae), *I. bicolor* (Pteriidae), *N. nodosus* (Pectinidae), *Parvamussium pourtalesianum* (Dall, 1886) (Propeamussiidae), and *S. ictericus* (Spondylidae) to provide a general anatomical characterization of each eye type, except for the invaginated eyes. Tissue samples containing photoreceptor organs were completely dehydrated and embedded in resin (Leica Historesin Kit, Germany). Serial sections of 3 µm were stained with toluidine blue and basic fuchsin.

Ecological data on habits of life were compiled from literature for species included in the phylogenetic analysis (Supplementary Table S1). We focused primarily on major lifestyle categories, including epifaunal (above the sediment), semi-infaunal (partially buried in the sediment), and infaunal (buried in the sediment). In addition, other subsets of epifaunal habits were also discriminated, such as cementing and crevice-dwelling, as well as general bathymetric distribution (<1000m for epipelagic and mesopelagic zones, and >1000m for bathypelagic and abyssopelagic zones).

Phylogenetic analysis and character evolution

Molecular data was based on up to five nucleotide sequences (16S rRNA, 18S rRNA, 28S rRNA, COI, and Histone H3) available in *GenBank*. In total, 199 taxa were included in the analysis, including 187 pteriomorphian species and 12 other mollusks as the outgroup (Table 2). Respective accession numbers are listed in Table 2. Missing data correspond to 24% of the dataset with a total of 6,347 bp. Alignments were performed in MAFFT v7.311

under the L-INS-i method (Katoh and Standley 2013) and the best-fit model of sequence evolution was tested in ModelFinder (Kalyaanamoorthy et al. 2017), returning GTR+I+G for our dataset. Tree searches were performed in IQ-TREE (Nguyen et al. 2014) under maximum likelihood and bootstrap values were generated after 100 replicates.

To investigate eye evolution and lifestyle shifts, traits were coded, and states were assigned to terminals. States for unobserved sequenced species were assigned based on literature information or as equivalent to closest relatives, *i.e.*, congeneric species. Ancestral state reconstruction was performed in Mesquite (Maddison and Maddison 2018) under maximum likelihood. For reconstruction, two models were considered, *i.e.*, the Markov k-state (MK1) and the asymmetrical Markov k-state (AsymmMK). While the former represents one parameter model that assumes equal rates for any transitions, the latter is a two-parameter model that allow different rates (forward and backward transitions). To test which model fitted the data better, a likelihood ratio (LR) test, which follows a chi-square distribution with df=1, was performed (Pagel, 1999, Maddison & Maddison, 2018). The best-fit model is specified for each trait history presented below.

Results

Phylogenetic hypothesis

Our phylogenetic approach includes the greatest taxonomic sampling of Pteriomorphia to date and recovered the clade as monophyletic (Fig. 1). The ML tree indicates four monophyletic orders, *i.e.*, Ostreida, Mytilida, Arcida, and Pectinida organized in two major clades: Arcida + Pectinida and Ostreida + Mytilida (Fig. 1). From the 19 taxonomic valid families included in the analysis, 17 were successfully recovered as clades. The Mytilida is comprised by a single family, Mytilidae, while the Ostreida embraces Ostreoidea (Ostreidae and Gryphaeidae) sister to Pterioidea (Malleidae and Pteriidae), and Pinnidae as the sister group to the remaining Ostreida. Within Arcida, some internal relationships are weakly supported, suggesting caution in their interpretation. All arcidan families were recovered monophyletic but Arcidae, which is polyphyletic. In the Pectinida, a clade comprising Anomiidae, Dimyidae, and Plicatulidae is sister to the remaining groups, with Limidae sister to Pectinoidea (Pectinidae, Propeamussiidae, and Spondylidae). The Propeamussiidae is not monophyletic in our analysis, with *Propeamussium dalli* sister to Spondylidae and *Parvamussium pourtalesianum* sister to Pectinidae.

Evolution and diversity of photoreceptor organs

Ancestral state reconstructions indicate the pteriomorphian ancestor had no eye on its mantle margin (Fig. 2). Subsequently, photoreceptor organs have arisen at least six times independently in the Arcida, Pectinida, and Ostreida (Fig. 2), occurring in 11 families (Table 1). Photoreceptor organs in Pteriomorphia can be categorized in five types according to morphology: 1) pigmented caps, 2) pigmented cups, 3) compound eyes, 4) concave mirror eyes, and 5) invaginated eyes (Fig. 2).

In the Ostreida, photoreceptor organs are restricted to Malleidae and Pteriidae, in which pigmented, photoreceptor cells are arranged in small clusters (Fig. 3C), repeatedly distributed on the outer mantle fold (Fig. 3, Table 1). These pigmented caps were likely present in the ancestor of Malleidae and Pteriidae (i.e., Pterioidea) (Fig. 2). Subsequent losses of eyespots have occurred in different epifaunal genera, such as *Pteria* and *Pinctada*, in *Isognomon ephippium*, and in the infaunal *Malleus malleus* (Fig. 2).

In the Arcida, pigmented cups on the outer mantle fold were present in the ancestor of the clade, representing a single, ancient origin (Fig. 2, dark blue). In most extant taxa, these eyespots are repeated cup-like structures (Fig. 4D) present in the anterior region (Fig. 4A-D) or restricted to the anterodorsal region, as in *Anadara* species (Table 1). Interestingly, pigmented cups were lost in some lineages, such as the semi-infaunal *Bathyarca*, *Limopsis*, and *Trisidus* (Fig. 2). Compound eyes comprise another type of organ present in the clade, formed by multiple units of photoreceptor and pigmented cells in a globular arrangement (Fig. 4E-H), posteriorly located on the outer mantle fold. In our analysis, compound eyes also have a single origin, with three subsequent losses, i.e., in the clades Limopsidae+Philobryidae, *Anadara*+(*Barbatia candida*+*B. lacerata*), and *Bathyarca glomerula* (Fig. 2, light blue, Table 1).

Invaginated eyes occur in the Limidae as small chambers underneath the proximal mantle surface and among the tentacles of the middle fold along its entire extension (Fig. 5A, B). A single origin was reconstructed for the ancestor of *Lima* and *Ctenoides*, with a loss in *Acesta* (Fig. 2). These organs were not observed in the studied species from the limid genera *Acesta*, *Limaria*, and *Limatula* (Table 1).

Concave mirror eyes are complex visual organs formed by a system of lens, retina, and reflector (mirror) layer (Fig. 5D, G, J). These eyes are located at the tip of eyestalks, among tentacles in the middle mantle fold (Fig. 5C-J). In our analysis, the concave mirror eyes have two different origins: in the ancestor of all Pectinidae + *Parvamussium pourtalesianum*, and in the ancestor of Spondylidae (Fig. 2). In the glass scallops

(Propeamussiidae) investigated herein, mirror eyes were only observed in *Cyclopecten subimbrifer*, *Similipecten nanus*, and *Parvamussium pourtalesianum* (Fig. 5C, Table 1). The remaining propeamussiid species do not bear eyes in their mantle margin. In contrast, all scallops (Pectinidae) and thorny oysters (Spondylidae) have numerous mirror eyes. These organs are very similar in morphology and distribution, although pigmentation varies among blue, brown, and black (Fig. 5C-J). In some scallop species from the genus *Euvola*, *Pecten*, and *Argopecten*, eyes are much more numerous on the left mantle lobe, with few units on the right side (Table 1), which usually faces the substrate and supports the body. In the glass scallops *Cyclopecten subimbrifer*, *Similipecten nanus*, and *Parvamussium pourtalesianum*, eyes are restricted to the left side of the body, being absent on the right mantle margin (Table 1).

Lifestyles shifts in Pteriomorphia

According to ancestral state reconstructions, all pteriomorphian bivalves descend from an epifaunal ancestor and the epifaunal habit would be a synapomorphy for the clade, considering the plesiomorphic infaunal condition (Fig. 6A). Photoreceptor organs have exclusively evolved in lineages with ancestral epifaunal habits (Fig. 6A, B). For example, concave mirror eyes are present in the cemented Spondylidae and in the Pectinidae, which includes byssally attached, recessing, swimming and free (unattached) habits. Invaginated eyes had their origin in epifaunal limids living byssally attached in crevices and byssal nests. In addition, eyespots, such as pigmented cups and caps, had their origin in byssate, epifaunal ancestors of different clades, such as Arcida and Pterioidea.

Lifestyle transitions also seem associated with eye evolution. The epibyssate habit on exposed surfaces was likely replaced by convergent adoption of the crevice-dwelling habit in different pteriomorphian lineages, including Limidae, Malleidae, and Pteriidae (particularly *Isognomon*) (Fig. 6C). This habit is characterized by occupation of crevices in hard substrate, such as boulders and corals, by means of byssus attachment, resulting in limited body exposure. Two independent gains of mantle photoreceptor organs, respectively in Limidae and Pterioidea, seems associated with crevice-dwelling habit (Fig. 6B, C).

Secondary losses of pigmented cups and pigmented caps have occurred in lineages that shifted to the semi-infaunal/infaunal habit. This is the case of *Malleus malleus* and semi-infaunal lineages within Arcida, such as *Trisidus*, *Eontia*, *Limopsis*, and *Tegillarca* (Fig. 6B, D). In addition, losses of compound eyes have occurred in some semi-infaunal lineages, such as *Anadara*, and groups occurring in deep waters, such as *Bathyarca* and *Limopsis* (Fig. 2, 6D). Considering a general bathymetric classification (shallow vs. deep waters), the ancestor of Pectinoidea (Pectinidae, Propeamussiidae, and Spondylidae) likely inhabited deep (bathypelagic) waters (Fig. 6E). The evolution of mirror eyes in Spondylidae coincides with occupancy of shallow habits (Fig. 6E, F). Interestingly, an independent gain of mirror eyes is indicated for the clade Pectinidae+*Parvamussium pourtalesianum*, but its hypothetical ancestor likely lived in deep waters (Fig. 6E, F).

Discussion

Phylogenetic relationships within Pteriomorphia

Our results support the monophyly of Pteriomorphia, as previously indicated by numerous phylogenetic analyses of Bivalvia with different taxonomic samplings and molecular data (Steiner and Hammer 2000; Giribet and Wheeler 2002; Sharma et al. 2012; Bieler et al. 2014; Gonzalez et al. 2015; Ozawa et al. 2017). Relationships among pteriomorphian orders and superfamilies were investigated in a few studies and resulted in conflicting hypotheses. Analyses based on COI mtDNA sequences indicated a clade comprised by Pectinida and Arcida, leaving the Mytilida sister to all remaining pteriomorphians (Matsumoto 2003). In a phylogenomic approach for Pteriomorphia, the Mytilida is sister to Ostreida (Pinnoidea + Ostreoidea + Pterioidea) (Lemer et al. 2016), which is similar to our analysis. However, the same analysis recovered Arcida sister to all pteriomorphians, while our results place the clade sister to Pectinida. A different topology was also obtained in a mitogenomic analysis of Pteriomorphia, in which Arcida and Pectinida are grouped together, sister to Mytilida (Sun and Gao 2017).

Despite their large datasets, previous analyses were generally based on a low taxonomic sampling (Lemer et al. 2016, Sun and Gao 2017), which may represent an important constraint (Puslednik and Serb 2008). Our analysis relies on a much broader taxonomic sampling, suggesting two main clades formed by Pectinida + Arcida and Mytilida + Ostreida. The clade formed by Ostreoidea + Pterioidea, sister to Pinnoidea, seems to be consensual (Matsumoto 2003, Lemer et al. 2016). The phylogenetic placement of Arcida and Mytilida are inconsistent in most analyses, highlighting a particular sensitivity to the effects of datasets and taxonomic samplings. The Limoidea was frequently recovered as sister to a clade formed by Pectinoidea, Anomioidea, Dimyoidea, and Plicatuloidea (Xue et al. 2012; Bieler et al. 2014; Lemer et al. 2016), supporting the distinction between Limida and Pectinida as separate orders (Bieler et al. 2014). However, our results indicate the Limoidea is placed within Pectinida, sister to Pectinoidea, as also recovered elsewhere (Combosch et al. 2016). Therefore, we argue that Pectinida is formed by the superfamilies Pectinoidea, Limoidea, Anomioidea, Plicatuloidea, and Dimyoidea, which does not support the order Limida sensu Bieler et al. (2014).

Phylogenetic hypotheses for most pteriomorphian families and superfamilies were produced in the last decades based on morphology and mostly on molecular data. The superfamily Pectinoidea was studied based on fossil data (Waller 2006), while the phylogeny of Pectinidae was resolved by molecular sequences (Puslednik and Serb 2008; Alejandrino et al. 2011). Our results contribute to understand the relationships within Pectinoidea, suggesting the Propeamussiidae is not monophyletic. In the Ostreida, phylogenetic relationships were investigated for Pterioidea (Tëmkin 2010; Tsubaki et al. 2011), Ostreoidea (Salvi et al. 2014), Ostreidae (Raith et al. 2016), and Pinnidae (Lemer et al. 2014). Similarly to our results, the phylogenetic placement of *Isognomon* within Pteriidae was previously recovered by (Tëmkin 2010), leaving the Malleidae sister to the remaining pearl oysters (Pteriidae). While the phylogenetics of Arcida are highly debatable and controversial, the polyphyletic nature of the family Arcidae and the controversial placement of Glycymerididae have been demonstrated by several comprehensive studies (Feng et al. 2015; Combosch and Giribet 2016, Audino et al. 2019; present study).

Morphological diversity of bivalve photoreceptor organs

In an extensive review of photoreceptor organs in Bivalvia, three categories were proposed based on the location in the mantle margin, i.e., on the outer, middle, or inner mantle fold (Morton 2008). In addition, the evolution of these organs was tentatively explored in that study, although further details on phylogenetic and taxonomic diversity were not available at that time. Our results should elucidate this gap in bivalve knowledge, revealing origins and evolutionary patterns across Pteriomorphia.

Eyespots in Pteriidae and Malleidae include pigmented, photoreceptor cells organized in clusters along the outer mantle fold. The presence of these structures in Malleidae is comparatively described for the first time, revealing numerous pigmented caps in *Malleus albus*, *Malleus candeanus*, *Malleus regula*, but not in *Malleus malleus*. These organs are also present in *Isognomon* species (except for *Isognomon ephippium*), and were previously reported for *Isognomon spathulatus* (Tëmkin and Printrakoon 2016), *Isognomon legumen* (Harper and Morton 1994), and *Isognomon radiatus* (Tëmkin 2006). In *Pteria brevialata*, putative mantle photoreceptors were described based on histological sections, comprehending eosinophilic cells (possibly photosensory) scattered along the outer mantle fold (Morton 1995). Nevertheless, pigmented eyespots were not observed in the *Pteria* species analyzed herein and, in accordance with Tëmkin (2006), we argue that although those eosinophilic cells in *P. brevialata* may have a role in photoreception, their interpretation as ocelli lacks evidence. Considering the ancestral reconstruction hypothesis, cap eyespots may have been present in the ancestor of Pterioidea, with a subsequent loss in *Pteria*. Therefore, the eosinophilic cells described in *P. brevialata* may represent a vestigial or reduced tissue of a plesiomorphic photoreceptor organ.

In the Arcida, the presence of pigmented cups is relatively well known for *Barbatia virescens* (Morton 1987) and *Barbatia candida* (Audino and Marian 2018). The histological organization of pigmented caps was described for *Philobrya munita* (Morton 1978), although further details were not available for the remaining Philobryidae. Compound eyes are common organs among arcidan species, with anatomical details available for the genera *Arca, Barbatia*, and *Glycymeris* (Waller 1980; Morton and Peharda 2008; Morton and Puljas 2016; Audino and Marian 2018). As described herein, compound eyes are restricted to the posterior region of the mantle, while pigmented cups are more frequent in the anterior and anterodorsal region (Table 1).

Considering the position of the animals, the posterior region of the mantle is more exposed to the surrounding environment in both infaunal and epifaunal bivalves while the anterior region is usually closer to the substrate. Such a pattern of distribution may be related to different light-guided behaviors for each type of photoreceptor organ, as discussed in the next section.

The concave mirror eyes of scallops are curious organs that have received great scientific attention since past centuries (Hickson 1880; Dakin 1910). Mirror eyes are present in all Pectinidae and Spondylidae, with detailed studies available for selected species, including comparative anatomy and visual properties relative to image formation (Dakin 1928; Land 2000; Speiser and Johnsen 2008; Speiser et al. 2011; Malkowsky and Jochum 2014; Audino et al. 2015; Palmer et al. 2017). Interestingly, mirror eyes do not occur in all Propeamussiidae, as indicated by our survey (Table 1) and by the eyeless *Propeamussium lucidum* (Morton and Thurston 1989). A more comprehensive analysis of Propeamussiidae is still required to understand the anatomy of these animals and the taxonomic distribution of eyes. Unfortunately, these very small bivalves occur in deep waters and soft parts are rarely preserved, making the previous requirement a difficult task.

Mantle eyes in Limidae are invaginated structures located on the middle mantle fold and embedded in connective tissue beneath the epithelium. Electrophysiological properties were investigated in the photosensory cells of *Ctenoides scabra* (Nasi 1991), while functional insights related to visual capabilities were obtained for *Ctenoides ales* (Dougherty et al. 2017). In *Ctenoides mitis*, eye capsules have cornea, lens, and an organized retina (Morton 2000a); a similar morphology is present in *C. ales* (Dougherty et al. 2017). Invaginated eyes were also reported for *C. miamiensis, C. obliquus, C. planulatus* (Mikkelsen and Bieler 2003), as well as for *C. mitis* and *C. scaber*, both included in this study. This type of eyes is also present in the genus *Lima*, such as in *Lima caribaea* (Mikkelsen and Bieler 2003), but previous descriptions also include lensless cup-shaped organs in *Lima squamosa* and *Lima lima* (Hesse 1900; Dakin 1928; Waller 1975). Based on possible anatomical differences, such as lens presence, it has been previously suggested that invaginated eyes in *Ctenoides* and *Lima* actually comprise two different types (Morton 2000a). Our phylogenetic data suggests that photoreceptor organs have evolved just once in the clade because we have treated all cases as having the same state – unfortunately, it was not possible to obtain histological sections from the analyzed Limidae. Therefore, further histological investigation is required to elucidate the organization of invaginated eyes in different limid genera, and to verify the uniqueness of this eye type. In addition, eyes were not observed in *Limaria inflata* and *Limaria hians* (Hesse 1900), or in any studied species from the genera *Acesta*, *Limaria*, and *Limatula* (Table 1). Additional investigation should check if they represent secondary losses of invaginated eyes.

In our study, mantle eyes were not observed in the Anomiidae, i.e., in *Anomia*, *Heteranomia*, and *Pododesmus*. Nevertheless, a striking exception do exist in *Enigmonia aenigmatica*, a limpet-like bivalve which inhabits mangroves (Yonge 1977). In this species, pigmented eyespots with lens were described on the mantle epithelia, except in the region of the mantle margin and folds (Morton 2008). These cluster of photosensory and pigmented cells are scattered on the mantle beneath the shell, which is relatively thin and translucent, allowing light detection (Yonge 1977; Morton 2008).

Photoreception evolution in bivalves

Ancestor state reconstructions of discrete traits are useful to estimate the origin of both simple and complex features, as well as possible evolutionary patterns (Cunningham et al. 1998; Pagel 1999). Nevertheless, photoreceptor systems frequently include complex traits, and scoring them as binary characters frequently hampers the inference of the evolutionary history of their components (Oakley and Speiser 2015). Aware of these limitations, we consider the present phylogenetic approach a significant progress in the understanding of the evolution of photoreceptor organs in bivalves, particularly to estimate their origins and general historical patterns.

The evolution of photoreceptor organs in Pteriomorphia is marked by multiple origins of different types of eyes with distinct optic properties and locations. Our results do not support previous assumptions on eye sophistication, i.e., a transition from outer to middle mantle fold eyes as the bivalve lineages become more derived (Morton 2000a). Nevertheless, more improved optic conditions are indeed present in organs formed on the middle mantle fold (i.e., invaginated eyes and mirror eyes) compared to eyespots from the outer mantle fold. This apparent trend could be explained by the presence of the periostracum layer that covers the photoreceptor organs on the outer mantle fold, while eyes on the middle fold have no such optic constraint (Morton 2008).

Eyes have evolved exclusively in epifaunal lineages of pteriomorphian bivalves. Therefore, if present in extant semi-infaunal/infaunal lineages (e.g., *Anadara* spp.), they are always plesiomorphic, i.e., have originated in an epifaunal ancestor. Our results show some similarities between eye and lifestyle evolution. For example, numerous losses of photoreceptor organs occurred independently in semi-infaunal/infaunal lineages, and byssate lineages that shifted to the crevice-dwelling habit acquired some type of photoreceptor organs. Accordingly, previous analyses suggested correlation between eye losses and shifts to infaunal habits in Arcida (Audino et al. 2019). The loss of eyes in association with infaunal habits leaves an open question whether eye loss is a result of relaxed selection when the epifaunal condition is replaced or positive selection in the infaunalization context (see Audino et al. 2019). In the Pterioidea, comparative studies demonstrated the importance of habit and substrate type for taxonomic diversification and ecological radiation (Yonge 1968; Tsubaki et al. 2011). Our data reinforce such conclusion, supported by the shift to the crevice-dwelling habit and the evolution of eyespots in Pterioidea. This habit of living in crevices involve a combination of behavioral and morphological adaptations enabling the use of likely inaccessible locations, which ultimately help avoid predation in the benthos (Harper and Skelton 1993; Harper and Morton 1994). In this case, the pigmented cap eyespots may help find adequate crevices and aid in body positioning using light clues.

The adaptive roles of concave mirror eyes are still debatable, and the investigation of the evolution of such a complex structure is far from being exhausted. In a previous attempt to explore the evolutionary connection between lifestyle and mirror eyes in Pectinidae, light sensitive compartments of the retina were revealed to be associated with different depth ranges (Malkowsky and Götze 2014). In addition, a tendency in eye reduction is exhibited by shallow to deep water species (Malkowsky and Götze 2014). Our results suggest convergent gain of mirror eyes in Spondylidae associated with occupancy of photic zones from an eyeless deep-sea ancestor (*i.e.*, a propeamussiid-like ancestor from the bathypelagic zone). Conversely, mirror eyes in Pectinidae and *Parvamussium pourtalesianum* would already be present in a deep-sea ancestor. Considering these results, depth does not seem to act as a selective force driving mirror eye evolution, as previously suggested (Morton 2001; Malkowsky and Götze 2014). Nevertheless, phylogenetic and morphological efforts, particularly the increase of Propeamussiidae taxonomic sampling, are critically necessary to elucidate the intriguing evolutionary scenario proposed here for mirror eyes.

In a comprehensive revision of the evolution of low-resolution vision in animals, Nilsson and Bok (2017) argued about the driving force of behavioral tasks acting on the evolution of photoreceptors organs from simple photoreception to vision. The authors highlighted the importance of reconstructing the behavioral drive associated with the corresponding eye diversification. The ecological features presented here provide insights to explore bivalve eye evolution linked to corresponding behaviors, from the perspective of a byssally attached, epifaunal ancestor. For example, morphological and ecological features indicate that the pigmented cups of arcidans may detect local changes in light intensity, possibly related to simple phototaxis, enabling selective positioning and attachment on hard substrate (Morton 1987; Audino and Marian 2018). In a different way, protective and alarm responses are regarded as the main behaviors triggered by compound eyes in ark clams (Nilsson 1994). The crevice-dwelling habit in *Malleu*s and *Isognomon* may be associated with simple phototaxis behavior and positioning control by directional photoreception provided by the pigmented cups. A convergent lifestyle in Limidae may also have been associated with body orientation using low-resolution vision and alarm responses by optical inputs in the photoreceptor system (invaginated eyes) (Dougherty et al. 2017). Concave mirror eyes, by their turn, are potentially associated with habitat positioning behaviors using low resolution vision in scallops, as well as alarm responses (Morton 2000b; Speiser and Johnsen 2008). However, acquisition of such eye type in Spondylidae remains controversial considering the cementing (sessile) habit of the clade (Dakin 1928; Morton 2000b). Altogether, our study suggests that phototaxis (or even area taxis), posture control, and alarm responses represent the three main behaviors driving eye evolution in pteriomorphian bivalves, which were likely associated with epifaunal habit diversification in this clade.

Acknowledgments

This study is part of the first author's Doctorate's thesis through the Graduate Program in Zoology of the Institute of Biosciences (University of São Paulo). We acknowledge the grants 2015/09519-4 and 2017/01365-3 provided by the São Paulo Research Foundation (FAPESP). This study was financed in part by the Coordenação de Aperfeiçoamento de Pessoal de Nível Superior - Brasil (CAPES) - Finance Code 001. We also thank the following institutions that provided materials for this study: Center for Marine Biology (CEBIMar), Museum of Comparative Zoology (MCZ), Museum of Zoology "Prof. Adão José Cardoso" of the University of Campinas (ZUEC), Museum of Zoology of the University of São Paulo (MZSP), Santa Barbara Museum of Natural History (SBMNH), and Smithsonian National Museum of Natural History (USNM). This is a contribution of NP-BioMar (Research Center for Marine Biodiversity – USP).

References

Adal MN, Morton B. 1973. The fine structure of the pallial eyes of *Laternula truncata* (Bivalvia: Anomalodesmata: Pandoracea). Journal of Zoology 170:533–56.

Alejandrino A, Puslednik L, Serb JM. 2011. Convergent and parallel evolution in life habit of the scallops (Bivalvia: Pectinidae). BMC Evolutionary Biology 11:164.

Arendt D. 2003. Evolution of eyes and photoreceptor cell types. International Journal of Developmental Biology 47:563–71.

Audino JA, Marian JEAR. 2018. Comparative and functional anatomy of the mantle margin in ark clams and their relatives (Bivalvia: Arcoidea) supports association between morphology and life habits. Journal of Zoology 305:149–62.

Audino JA, Marian JEAR, Wanninger A, Lopes SGBC. 2015. Development of the pallial eye in *Nodipecten nodosus* (Mollusca: Bivalvia): insights into early visual performance in scallops. Zoomorphology 134:403–15.

Audino JA, Serb JM, Marian JEAR. 2019. Ark clams and relatives (Bivalvia: Arcida) show convergent morphological evolution associated with lifestyle transitions in the marine benthos. Biological Journal of the Linnean Society doi 10.1093/biolinnean/blz017

Bieler R, Mikkelsen PM, Collins TM, Glover EA, González VL, Graf DL, Harper EM, Healy J, Kawauchi GY, Sharma PP, Staubach S, Strong EE, Taylor JD, Tëmkin I, Zardus JD, Clark S, Guzmán A, McIntyre E, Sharp P, Giribet G. 2014. Investigating the Bivalve Tree of Life – an exemplar-based approach combining molecular and novel morphological characters. Invertebrate Systematics 28:32.

Bok MJ, Capa M, Nilsson D-E. 2016. Here, there and everywhere: The radiolar eyes of fan worms (Annelida, Sabellidae). Integrative and Comparative Biology 56:784–95.

Bok MJ, Porter ML, ten Hove HA, Smith R, Nilsson D-E. 2017. Radiolar eyes of serpulid worms (Annelida, Serpulidae): Structures, function, and phototransduction. The Biological Bulletin 233:39–57.

Combosch DJ, Giribet G. 2016. Clarifying phylogenetic relationships and the evolutionary history of the bivalve order Arcida (Mollusca: Bivalvia: Pteriomorphia). Molecular Phylogenetics and Evolution 94:298–312.

Combosch DJ. et al. 2017. A family-level tree of life for bivalves based on a Sanger-sequencing approach. Molecular Phylogenetics and Evolution 107:191–208.

Cronin TW. 1986. Photoreception in marine invertebrates. American Zoologist 26:403–15.

Cunningham CW, Omland KE, Oakley TH. 1998. Reconstructing ancestral character states: a critical reappraisal. Trends in Ecology & Evolution 13:361–66.

Dakin WJ. 1910. The eye of *Pecten*. Quarterly Journal of Microscopical Science 55:49–112.

Dakin WJ. 1928. The eyes of *Pecten*, *Spondylus*, *Amussium* and allied lamellibranchs, with a short discussion on their evolution. Proc R Soc Lond B 103:355–65.

Dougherty LF, Dubielzig RR, Schobert CS, Teixeira LB, Li J. 2017. Do you see what I see? Optical morphology and visual capability of ‘disco’ clams (*Ctenoides ales*). Biology Open bio.024570.

Feng Y, Li Q, Kong L. 2015. Molecular phylogeny of Arcoidea with emphasis on Arcidae species (Bivalvia: Pteriomorphia) along the coast of China: Challenges to current classification of arcoids. Molecular Phylogenetics and Evolution 85:189–96.

Gehring WJ. 2014. The evolution of vision. Wiley Interdisciplinary Reviews: Developmental Biology 3:1–40.

Giribet G, Wheeler W. 2002. On bivalve phylogeny: a high-level analysis of the Bivalvia (Mollusca) based on combined morphology and DNA sequence data. Invertebrate Biology 121:271–324.

Gonzalez VL, Andrade SCS, Bieler R, Collins TM, Dunn CW, Mikkelsen PM, Taylor JD, Giribet G. 2015. A phylogenetic backbone for Bivalvia: an RNA-seq approach. Proceedings of the Royal Society B: Biological Sciences 282:20142332–20142332.

Harper EM, Morton B. 1994. The biology of *Isognomon legumen* (Gmelin, 1791) (Bivalvia: Pterioida) at Cape D’Aguilar, Hong Kong, with special reference to predation by muricids. In: Proceedings of the Third International Workshop on the Malacofauna of Hong Kong and Southern China, Hong Kong, 13 April—1 May 1992. Vol. 3. Hong Kong: Hong Kong University Press. p. 405–425.

Harper EM, Skelton PW. 1993. The Mesozoic Marine Revolution and epifaunal bivalves. Scripta Geologica, Special Issue 2:127–153.

Hesse R. 1900. Untersuchungen über die Orange der Lichtempfindung bei niederen Thieren. VI. Die Augen einiger Mollusken. Zeitschrift für Wissenschaftliche Zoologische 68:379–477.

Hickson SJ. 1880. Memoirs: The Eye of *Pecten*. Journal of Cell Science s2-20:443–55.

Kalyaanamoorthy S, Minh BQ, Wong TK, von Haeseler A, Jermiin LS. 2017. ModelFinder: fast model selection for accurate phylogenetic estimates. Nature methods 14:587.

Katoh K, Standley DM. 2013. MAFFT multiple sequence alignment software version 7: improvements in performance and usability. Molecular biology and evolution 30:772–80.

Land MF. 1965. Image formation by a concave reflector in the eye of the scallop, *Pecten maximus*. The Journal of Physiology 179:138–53.

Land MF. 2000. Eyes with mirror optics. Journal of Optics A: Pure and Applied Optics 2:R44–50.

Land MF. 2003. The spatial resolution of the pinhole eyes of giant clams (*Tridacna maxima*). Proceedings of the Royal Society B: Biological Sciences 270:185–88.

Land MF, Nilsson D-E. 2012. Animal eyes. Oxford: Oxford University Press.

Lemer S, Buge B, Bemis A, Giribet G. 2014. First molecular phylogeny of the circumtropical bivalve family Pinnidae (Mollusca, Bivalvia): Evidence for high levels of cryptic species diversity. Molecular Phylogenetics and Evolution 75:11–23.

Lemer S, González VL, Bieler R, Giribet G. 2016. Cementing mussels to oysters in the pteriomorphian tree: a phylogenomic approach. Proceedings of the Royal Society B: Biological Sciences 283:20160857.

Lindgren AR, Pankey MS, Hochberg FG, Oakley TH. 2012. A multi-gene phylogeny of Cephalopoda supports convergent morphological evolution in association with multiple habitat shifts in the marine environment. BMC Evolutionary Biology 12:129.

Maddison WP, Maddison DR. 2018. Mesquite: a modular system for evolutionary analysis. Version 3.51 http://www.mesquiteproject.org. (http://www.mesquiteproject.org).

Malkowsky Y, Götze M-C. 2014. Impact of habitat and life trait on character evolution of pallial eyes in Pectinidae (Mollusca: bivalvia). Organisms Diversity & Evolution 14:173–85.

Malkowsky Y, Jochum A. 2014. Three-dimensional reconstructions of pallial eyes in Pectinidae (Mollusca: Bivalvia). Acta Zoologica 96:167–73.

Matsumoto M. 2003. Phylogenetic analysis of the subclass Pteriomorphia (Bivalvia) from mtDNA COI sequences. Molecular Phylogenetics and Evolution 27:429–40.

Mikkelsen PM, Bieler R. 2003. Systematic revision of the western Atlantic file clams, *Lima* and *Ctenoides* (Bivalvia: Limoida: Limidae). Invertebrate Systematics 17:667.

Morton B. 1978. The biology and functional morphology of *Philobrya munita* (Bivalvia: Philobryidae). Journal of Zoology 185:173–96.

Morton B. 1987. The pallial photophores of *Barbatia virescens* (Bivalvia: Arcacea). Journal of Molluscan Studies 53:241–43.

Morton B. 1995. The biology and functional morphology of *Pteria brevialata* (Bivalvia: Pterioidea), epizoic on gorgonians in Hong Kong. Journal of Zoology 236:223–41.

Morton B. 2000a. The pallial eyes of *Ctenoides floridanus* (Bivalvia: Limoidea). Journal of Molluscan Studies 66:449–55.

Morton B. 2000b. The function of pallial eyes within the Pectinidae, with a description of those present in *Patinopecten yessoensis*. Geological Society, London, Special Publications 177:247–55.

Morton B. 2001. The evolution of eyes in the Bivalvia. Oceanography and Marine Biology: An Annual Review 39:165–205.

Morton B. 2008. The evolution of eyes in the Bivalvia: New insights. American Malacological Bulletin 26:35–45.

Morton B, Peharda M. 2008. The biology and functional morphology of *Arca noae* (Bivalvia: Arcidae) from the Adriatic Sea, Croatia, with a discussion on the evolution of the bivalve mantle margin. Acta Zoologica 89:19–28.

Morton B, Puljas S. 2016. The ectopic compound ommatidium-like pallial eyes of three species of Mediterranean (Adriatic Sea) *Glycymeris* (Bivalvia: Arcoida). Decreasing visual acuity with increasing depth? Acta Zoologica 97:464–74.

Morton B, Thurston MH. 1989. The functional morphology of *Propeamussium lucidum* (Bivalvia: Pectinacea), a deep-sea predatory scallop. Journal of Zoology 218:471–96.

Nasi E. 1991. Electrophysiological properties of isolated photoreceptors from the eye of *Lima scabra*. The Journal of General Physiology 97:17–34.

Navet S, Buresi A, Baratte S, Andouche A, Bonnaud-Ponticelli L, Bassaglia Y. 2017. The Pax gene family: Highlights from cephalopods. PLOS ONE 12:e0172719.

Nguyen L-T, Schmidt HA, von Haeseler A, Minh BQ. 2014. IQ-TREE: a fast and effective stochastic algorithm for estimating maximum-likelihood phylogenies. Molecular Biology and Evolution 32:268–74.

Nilsson D-E. 1994. Eyes as optical alarm systems in fan worms and ark clams. Philosophical Transactions: Biological Sciences 346:195–212.

Nilsson D-E. 2013. Eye evolution and its functional basis. Visual Neuroscience 30:5–20.

Nilsson D-E, Bok MJ. 2017. Low-resolution vision—at the hub of eye evolution. Integrative and Comparative Biology 57:1066–70.

Nilsson D-E, Kelber A. 2007. A functional analysis of compound eye evolution. Arthropod Structure & Development, Origin and Evolution of Arthropod Visual Systems (Part II) 36:373–85.

Oakley TH. 2003. On homology of arthropod compound eyes. Integrative and Comparative Biology 43:522–30.

Oakley TH, Speiser DI. 2015. How complexity originates: The evolution of animal eyes. Annual Review of Ecology, Evolution, and Systematics 46:237–60.

Ozawa G, Shimamura S, Takaki Y, Yokobori S, Ohara Y, Takishita K, Maruyama T, Fujikura K, Yoshida T. 2017. Updated mitochondrial phylogeny of Pteriomorph and Heterodont Bivalvia, including deep-sea chemosymbiotic *Bathymodiolus* mussels, vesicomyid clams and the thyasirid clam *Conchocele cf. bisecta*. Marine Genomics 31:43–52.

Pagel M. 1999. Inferring the historical patterns of biological evolution. Nature 401:877–84.

Palmer BA, Taylor GJ, Brumfeld V, Gur D, Shemesh M, Elad N, Osherov A, Oron D, Weiner S, Addadi L. 2017. The image-forming mirror in the eye of the scallop. Science 358:1172–75.

Purschke G, Arendt D, Hausen H, Müller MCM. 2006. Photoreceptor cells and eyes in Annelida. Arthropod Structure & Development, Origin and Evolution of Arthropod Visual Systems (Part I) 35:211–30.

Puslednik L, Serb JM. 2008. Molecular phylogenetics of the Pectinidae (Mollusca: Bivalvia) and effect of increased taxon sampling and outgroup selection on tree topology. Molecular Phylogenetics and Evolution 48:1178–88.

Raith M, Zacherl DC, Pilgrim EM, Eernisse DJ. 2016. Phylogeny and species diversity of gulf of California oysters (Ostreidae) inferred from mitochondrial DNA. American Malacological Bulletin 33:263–83.

Salvi D, Macali A, Mariottini P. 2014. Molecular phylogenetics and systematics of the bivalve family Ostreidae based on rRNA sequence-structure models and multilocus species tree. PLoS ONE 9:e108696.

Serb JM, Eernisse DJ. 2008. Charting evolution’s trajectory: Using molluscan eye diversity to understand parallel and convergent evolution. Evolution: Education and Outreach 1:439–47.

Serb JM, Porath-Krause AJ, Pairett AN. 2013. Uncovering a gene duplication of the photoreceptive protein, opsin, in scallops (Bivalvia: Pectinidae). Integrative and Comparative Biology 53:68–77.

Sharma PP, González VL, Kawauchi GY, Andrade SCS, Guzmán A, Collins TM, Glover EA, Harper EM, Healy JM, Mikkelsen PM, Taylor JD, Bieler R, Giribet G. 2012. Phylogenetic analysis of four nuclear protein-encoding genes largely corroborates the traditional classification of Bivalvia (Mollusca). Molecular Phylogenetics and Evolution 65:64–74.

Sivak JG. 1982. Optical properties of a cephalopod eye (the short finned squid, *lllex illecebrosus*). Journal of Comparative Physiology 147:323 327.

Speiser DI, Johnsen S. 2008. Comparative morphology of the concave mirror eyes of scallops (Pectinoidea). American Malacological Bulletin 26:27–33.

Speiser DI, Loew ER, Johnsen S. 2011. Spectral sensitivity of the concave mirror eyes of scallops: potential influences of habitat, self-screening and longitudinal chromatic aberration. Journal of Experimental Biology 214:422–31.

Steiner G, Hammer S. 2000. Molecular phylogeny of the Bivalvia inferred from 18S rDNA sequences with particular reference to the Pteriomorphia. Geological Society, London, Special Publications 177:11–29.

Strausfeld NJ, Ma X, Edgecombe GD, Fortey RA, Land MF, Liu Y, Cong P, Hou X. 2016. Arthropod eyes: The early Cambrian fossil record and divergent evolution of visual systems. Arthropod Structure & Development 45:152–72.

Sun W, Gao L. 2017. Phylogeny and comparative genomic analysis of Pteriomorphia (Mollusca: Bivalvia) based on complete mitochondrial genomes. Marine Biology Research 13:255–68.

Sweeney AM, Haddock SHD, Johnsen S. 2007. Comparative visual acuity of coleoid cephalopods. Integrative and Comparative Biology 47:808–14.

Tëmkin I. 2006. Morphological perspective on the classification and evolution of Recent Pterioidea (Mollusca: Bivalvia). Zoological Journal of the Linnean Society 148:253–312.

Tëmkin I. 2010. Molecular phylogeny of pearl oysters and their relatives (Mollusca, Bivalvia, Pterioidea). BMC Evolutionary Biology 10:342.

Tëmkin I, Printrakoon C. 2016. Morphology and taxonomy of *Isognomon spathulatus* (Reeve, 1858), a cryptic bivalve from the mangroves of Thailand. Zootaxa 4107:141.

Tsubaki R, Kameda Y, Kato M. 2011. Pattern and process of diversification in an ecologically diverse epifaunal bivalve group Pterioidea (Pteriomorphia, Bivalvia). Molecular Phylogenetics and Evolution 58:97–104.

Vopalensky P, Kozmik Z. 2009. Eye evolution: common use and independent recruitment of genetic components. Philosophical Transactions of the Royal Society B: Biological Sciences 364:2819–32.

Xue DX, Wang HY, Zhang T, Zhang SP, Xu FS. 2012. Phylogenetic analysis of the subclass Pteriomorphia (Bivalvia) based on partial 28S rRNA sequence. Oceanologia et Limnologia Sinica 43(2):348–356.

Waller TR. 1975. The behavior and tentacle morphology of pteriomorphian bivalves: a motion-picture study. Bulletin of the American Malacological Union 7–13.

Waller TR. 1980. Scanning electron microscopy of shell and mantle in the order Arcoida (Mollusca: Bivalvia). Smithsonian Contributions to Zoology 1–58.

Waller TR. 2006. Phylogeny of families in the Pectinoidea (Mollusca: Bivalvia): importance of the fossil record. Zoological Journal of the Linnean Society 148:313–42.

Wilkens LA. 1986. The visual system of the giant clam *Tridacna* : Behavioral adaptations. The Biological Bulletin 170:393–408.

Wilkens LA. 2008. Primary inhibition by light: A unique property of bivalve photoreceptors. American Malacological Bulletin 26:101–9.

Yonge CM. 1968. Form and habit in species of *Malleus* (including the “hammer oysters”) with comparative observations on *Isognomon isognomon*. The Biological Bulletin 135:378–405.

Yonge CM. 1977. Form and evolution in the anomiacea (Mollusca: Bivalvia) *Pododesmus*, *Anomia*, *Patro*, *Enigmonia* (Anomiidae): *Placunanomia*, *Placuna* (Placunidae fam. nov.). Philosophical Transactions of the Royal Society of London B, Biological Sciences 276:453–523.

Yoshida M, Yura K, Ogura A. 2014. Cephalopod eye evolution was modulated by the acquisition of Pax-6 splicing variants. Scientific Reports 4:4256.

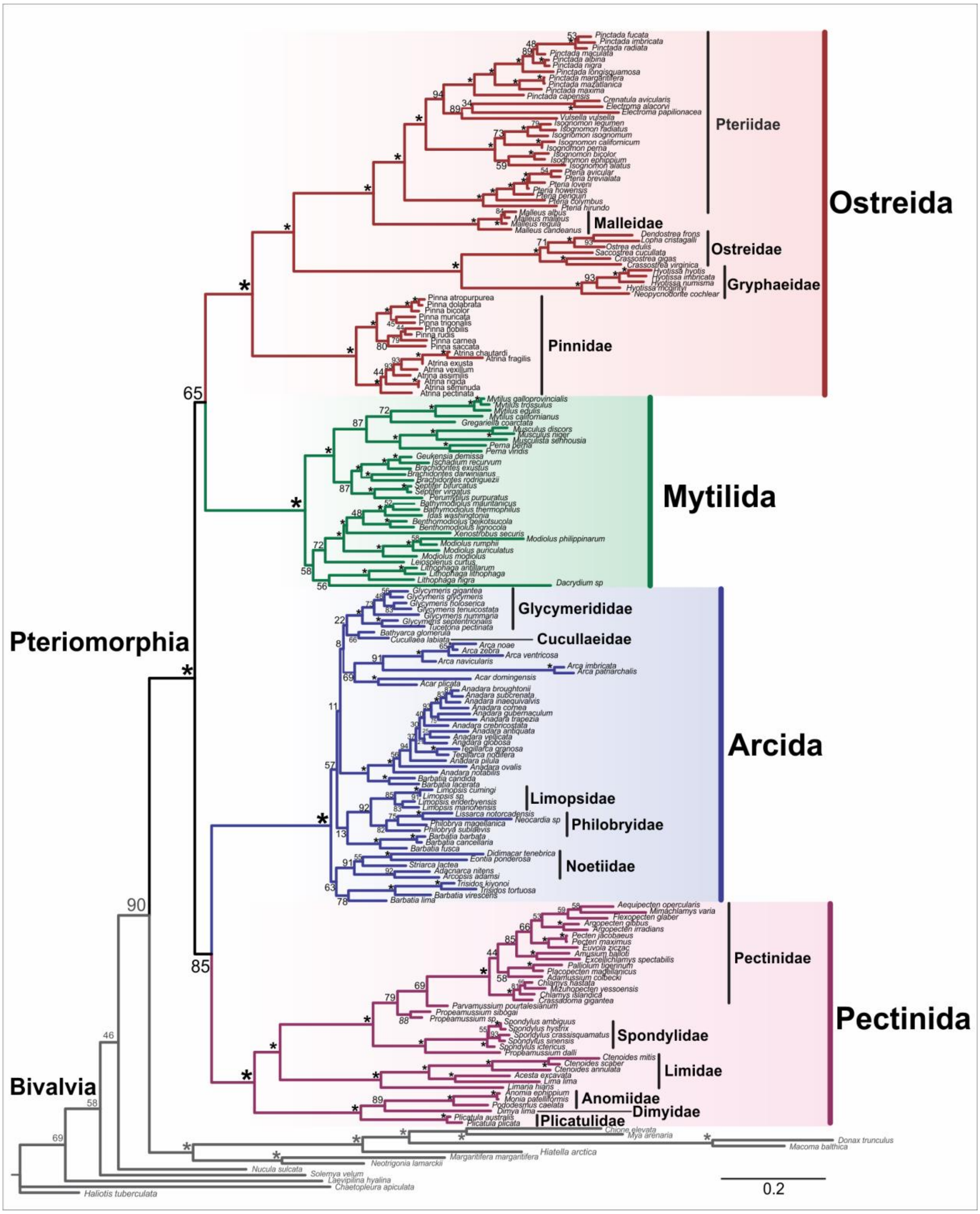

Figure 1. Pteriomorphia phylogeny. Maximum likelihood phylogeny of Pteriomorphia based on five nucleotide sequences (16S rRNA, 18S rRNA, 28S rRNA, COI, and H3). Internal nodes are indicated with respective bootstrap values; asterisks represent bootstrap ≥ 95. Most families were recovered monophyletic and organized in four orders across two main clades (Arcida+Pectinida and Ostreida+Mytilida).

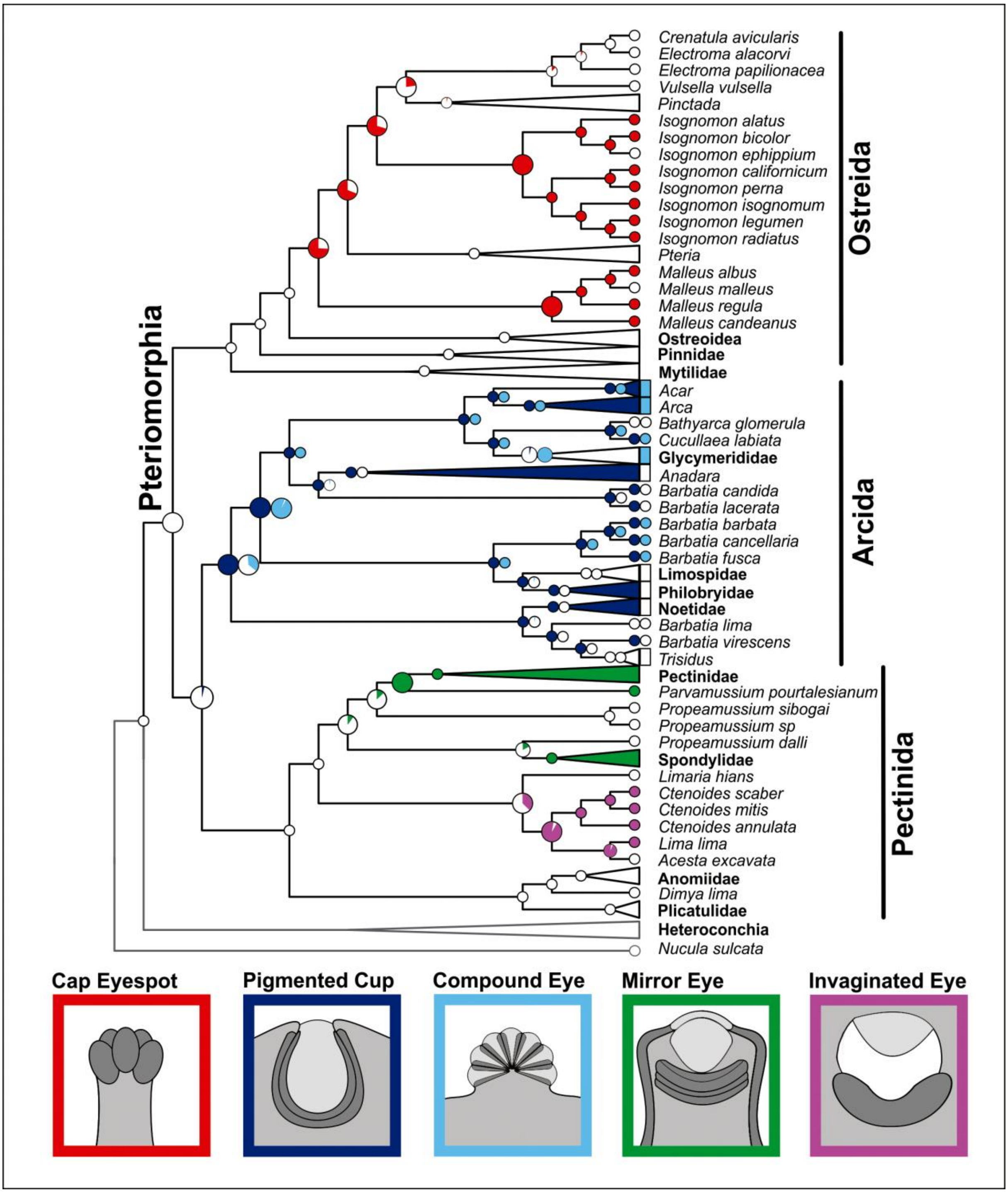

Figure 2. Evolution of photoreceptor organs. Summary of ancestral state reconstructions for photoreceptor organs within Pteriomorphia based on maximum likelihood. Pie charts indicate the proportional likelihood scores for presence and absence states. The five types of photoreceptor organs are depicted and color coded. The MK1 model was applied for the history of concave mirror eyes, while the remaining types were reconstructed under the AsymmMK model. Compound eyes (light blue) had their reconstruction indicated at the right side of respective nodes and terminals to prevent overlaying the reconstruction of pigmented cups, a different type of photoreceptor organ also present in most arcidans. Eyeless clades were intentionally collapsed to facilitate data presentation.

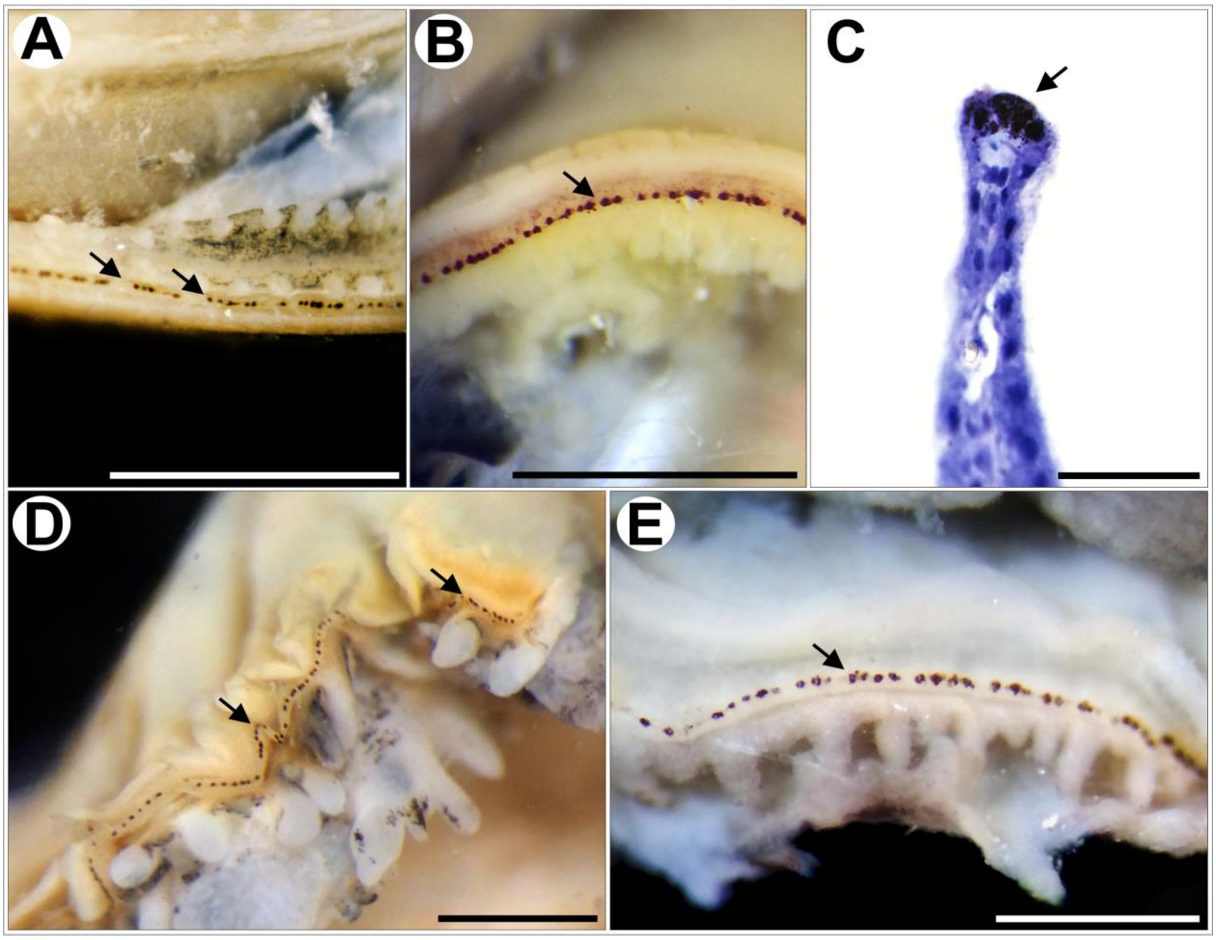

Figure 3. Photoreceptor organs in Ostreida. Pigmented caps (arrows) in *Isognomon* (Pteriidae, A-C) and *Malleus* (Malleidae, D-E). Scale bars = 0,5 mm (50 µm in C). **A.** *Isognomon alatus* (MZSP89628). **B.** *Isognomon radiatus* (USNM803357). **C.** *Isognomon bicolor* (collected specimen); sagittal section. **D.** *Malleus regula* (MCZ379030). **E.** *Malleus candeanus* (MCZ340681).

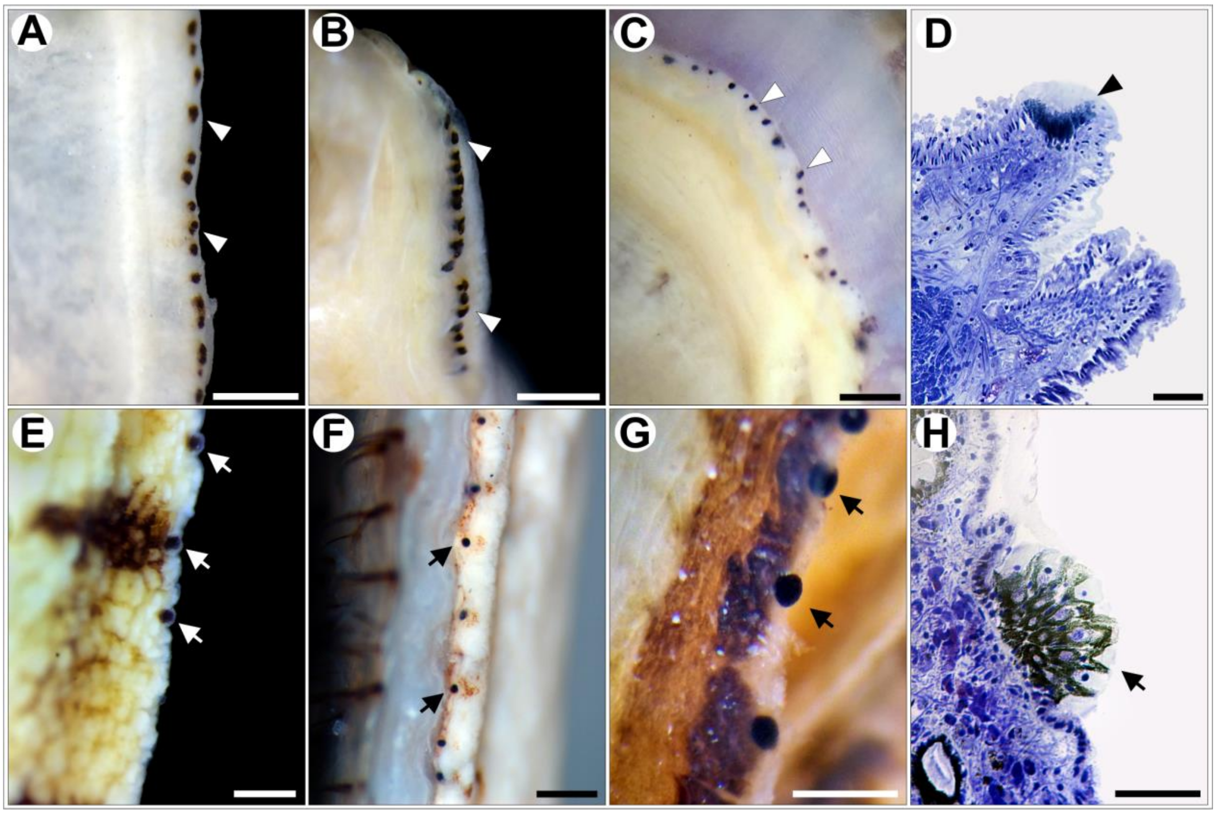

Figure 4. Photoreceptor organs in Arcida. Pigmented cups (arrowheads) in A-D and compound eyes (arrows) in E-H. Scale bars = 0,5 mm (in D and H scale bar = 20 μm). **A.** *Acar gradata* (USNM796185). **B.** *Anadara antiquata* (USNM802329). **C.** *Barbatia barbata* (MCZ378867). **D.** *Barbatia cancellaria* (MZSP48857); sagittal section. **E.** *Cucullaea labiata* (USNM746883). **F.** *Glycymeris undata* (MZSP91983). **G.** *Arca noae* (USNM1086014). **H.** *Acar dominguensis* (MZSP118292); sagittal section.

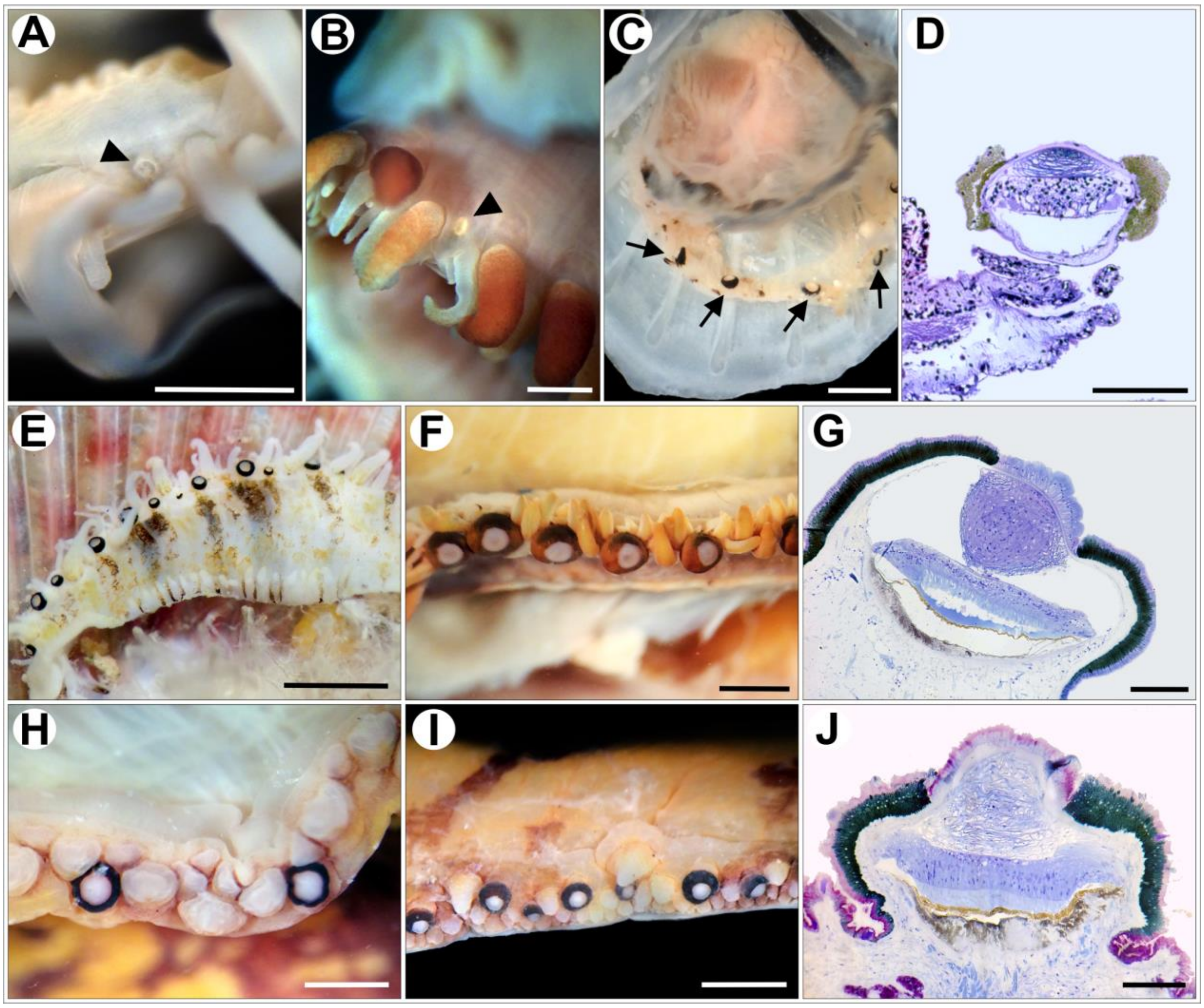

Figure 5. Photoreceptor organs in Pectinida. Invaginated eyes (arrowheads) in Limidae (A-B) and concave mirror eyes (arrows) in Propeamussiidae (C, D), Pectinidae (E-G), and Spondylidae (H-J). Scale bars = 1mm (in D, G, J scale bar = 100 µm). **A.** *Ctenoides floridanus* (USNM664306). **B.** *Lima lima* (USNM754383). **C.** *Parvamussium pourtalesianum* (USNM856965). **D.** *Parvamussium pourtalesianum* (USNM856965); sagittal section. **E.** *Chlamys varia* (MCZ378918). **F.** *Pecten jacobaeus* (USNM1086023). **G.** *Nodipecten nodosus* (collected specimen); sagittal section. **H.** *Spondylus americanus* (USNM833744). **I.** *Spondylus senegalensis* (USNM1086035). **J.** *Spondylus ictericus* (collected specimen); sagittal section.

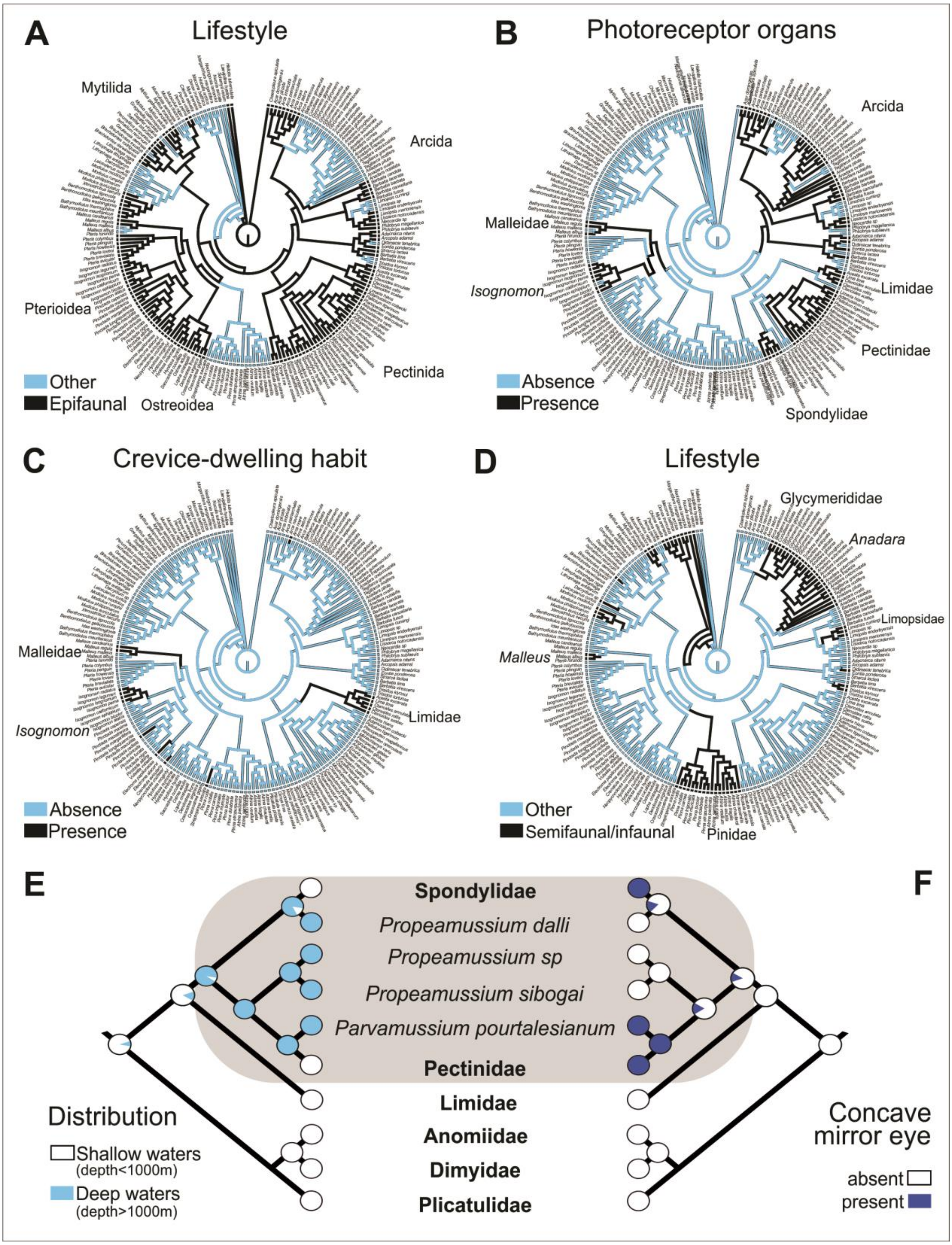

Figure 6. Lifestyles and photoreceptor organs evolution in Pteriomorphia. Maximum likelihood reconstructions applying the AsymmMK model in E and the MK1 model in A-D, and F. **A.** Ancestral state reconstruction (ASR) of the epifaunal habit in Pteriomorphia, indicating an epifaunal ancestor for the clade and secondary shifts across different lineages. **B.** Summary of ASR for photoreceptor organs within Pteriomorphia, showing five independent origins and numerous secondary losses. **C.** ASR for the crevice-dwelling habit, showing five independent transitions to this habit in epifaunal groups.

D. ASR for the semi-infaunal/infaunal habits, showing secondary transitions to these habits within Pteriomorphia. There is an apparent correspondence to events of eye loss, i.e., four of these transitions coincide with the loss of photoreceptor organs (compare to B). **E.** ASR of the bathymetric distribution of Pectinida, suggesting the ancestor of Pectinoidea (grey box) likely inhabited deep waters. Shallow waters were secondary occupied by Spondylidae and Pectinidae. **F.** ASR of concave mirror eyes in Pectinoidea, as indicated in Figure 2. The evolution of concave mirror eyes in Spondylidae displays a similar history to the secondary occupancy of shallow habitats.

Tables

Table 1. Pteriomorphian taxa investigated for eye presence and morphology. Catalog numbers and collections are listed. Type of photoreceptor organ and location are also provided. Abbreviations: MCZ – Museum of Comparative Zoology, ZUECBIV – Museum of Zoology “Prof. Adão José Cardoso” of the University of Campinas, MZSP – Museum of Zoology of the University of São Paulo, USNM – Smithsonian National Museum of Natural History, SBMNH – Santa Barbara Museum of Natural History. Absence of photoreceptor organ is indicated by “–”.

Taxa	**Catalogue number**	**Photoreceptor organ**	**Location and distribution**
Anomiidae			
Anomia simplex	ZUECBIV1423, USNM804291 USNM804325, MCZ280425	–	–
Heteranomia squamula	USNM871362, MCZ300656	–	–
Pododesmus macrochisma	SBMNH361457	–	–
Pododesmus rudis	USNM850821, USNM847837	–	–
Arcidae			
Acar dominguensis	MZSP118292	Pigmented cups Compound eyes	Outer fold, anterior mantle region Outer fold, posterior mantle region
Acar gradata	USNM796185	Pigmented cups Compound eyes	Outer fold, anterior mantle region Outer fold, posterior mantle region
Acar plicata	MZSP115322	Pigmented cups Compound eyes	Outer fold, anterior mantle region Outer fold, posterior mantle region
Anadara antiquata	MZSP99848	Pigmented cups	Outer fold, anterodorsal mantle region
Anadara baughmani	USNM803522	Pigmented cups	Outer fold, anterodorsal mantle region
Anadara broughtonii	USNM802331	Pigmented cups	Outer fold, anterodorsal mantle region
Anadara chemnitzii	MZSP43259, ZUECBIV4870	Pigmented cups	Outer fold, anterodorsal mantle region
Anadara ferruginea	SBMNH81002	Pigmented cups	Outer fold, anterodorsal mantle region
Anadara floridana	USNM847847	Pigmented cups	Outer fold, anterodorsal mantle region

Anadara grandis	USNM803487	Pigmented cups	Outer fold, anterodorsal mantle region
Anadara inaequivalvis	MZSP55060	Pigmented cups	Outer fold, anterodorsal mantle region
Anadara notabilis	MZSP84987, MZSP84886	Pigmented cups	Outer fold, anterodorsal mantle region
Anadara transversa	USNM801135, MCZ359001	Pigmented cups	Outer fold, anterodorsal mantle region
Anadara trapezia	SBMNH10187	Pigmented cups	Outer fold, anterodorsal mantle region
Arca imbricata	MZSP95208, MZSP109869	Pigmented cups Compound eyes	Outer fold, anterior mantle region Outer fold, posterior mantle region
Arca navicularis	USNM719071, MCZ378833	Pigmented cups Compound eyes	Outer fold, anterior mantle region Outer fold, posterior mantle region
Arca noae	USNM1086014	Pigmented cups Compound eyes	Outer fold, anterior mantle region Outer fold, posterior mantle region
Arca patriarchalis	MZSP99765	Pigmented cups Compound eyes	Outer fold, anterior mantle region Outer fold, posterior mantle region
Arca ventricosa	MZSP55027	Pigmented cups Compound eyes	Outer fold, anterior mantle region Outer fold, posterior mantle region
Arca zebra	MZSP101688	Pigmented cups Compound eyes	Outer fold, anterior mantle region Outer fold, posterior mantle region
Barbatia barbata	MCZ378867	Pigmented cups Compound eyes	Outer fold, anterior mantle region Outer fold, posterior mantle region
Barbatia cancellaria	MZSP32336, MZSP48857	Pigmented cups Compound eyes	Outer fold, anterior mantle region Outer fold, posterior mantle region
Barbatia fusca	SBMNH349329, USNM847011	Pigmented cups Compound eyes	Outer fold, anterior mantle region Outer fold, posterior mantle region
Barbatia lima	MZSP71135	–	–
Barbatia virescens	MZSP71367, MCZ378874	Pigmented cups	Outer fold, anterodorsal mantle region
Bathyarca corpulenta	SBMNH349320	–	–
Bathyarca pectunculoides	MCZ348402	–	–
Bentharca asperula	MCZ348399	–	–
Lunarca ovalis	MZSP84823, USNM803532	Pigmented cups	Outer fold, anterodorsal mantle region
Tegillarca granosa	MZSP55596, MCZ378820	–	–

Trisidos kiyonoi	SBMNH97422, SBMNH97423	–	–
Cucullaeidae			
Cucullaea labiata	USNM746883	Pigmented cups Compound eyes	Outer fold, anterior mantle region Outer fold, posterior mantle region
Dimyidae			
Dimya argentea	USNM855224	–	–
Glycymerididae			
Glycymeris decussata	MZSP91966	Compound eyes	Outer fold, posteroventral mantle region
Glycymeris gigantea	MCZ378989	Compound eyes	Outer fold, posteroventral mantle region
Glycymeris glycymeris	USNM794960	Compound eyes	Outer fold, posteroventral mantle region
Glycymeris holoserica	MCZ378984	Compound eyes	Outer fold, posteroventral mantle region
Glycymeris longior	MZSP91201, ZUECBIV78	Compound eyes	Outer fold, posteroventral mantle region
Glycymeris nummaria	MCZ378985	Compound eyes	Outer fold, posteroventral mantle region
Glycymeris tenuicostata	MCZ378982	Compound eyes	Outer fold, posteroventral mantle region
Glycymeris undata	MZSP91983	Compound eyes	Outer fold, posteroventral mantle region
Tucetona pectinata	MZSP91971, ZUECBIV2198	Compound eyes	Outer fold, posteroventral mantle region
Gryphaeidae			
Hyotissa hyotis	MCZ378999	–	–
Hyotissa mcgintyi	MZSP118279, USNM804282	–	–
Hyotissa numisma	USNM803328	–	–
Hyotissa sinensis	SBMNH141713	–	–
Neopicnodonte cochlear	MCZ379076	–	–
Limidae			
Acesta mori	MCZ384449	–	–
Acesta oophaga	USNM1263635	–	–

Acesta sphoni	SBMNH424265	–	–
Ctenoides mitis	USNM664306, MCZ378941	Invaginated eyes	Middle fold; entire mantle extension
Ctenoides scaber	USNM833716, MCZ376728	Invaginated eyes	Middle fold; entire mantle extension
Lima lima	USNM754383	Invaginated eyes	Middle fold; entire mantle extension
Limaria fragilis	USNM700291, USNM78784	–	–
Limaria hians	MCZ371725	–	–
Limaria orbignyi	SBMNH19892	–	–
Limaria pelucida	ZUECBIV2130, USNM850805	–	–
Limatula celtica	MCZ357556	–	–
Limatula hodgsoni	USNM882395	–	–
Limatula pygmaea	ZUECBIV2207	–	–
Limatula setifera	USNM850807	–	–
Limatula subovata	ZUECBIV5733, MCZ357577	–	–
Limopsidae			
Limopsis aurita	ZUECBIV2248, MCZ348438	–	–
Limopsis cristata	MZSP104154, MCZ348410	–	–
Limopsis galatheae	MCZ348437	–	–
Limopsis lilliei	MZSP90647, USNM904585	–	–
Limopsis marionensi	USNM760835, USNM886526	–	–
Limopsis sulcata	USNM832925	–	–
Limopsis tenella	USNM807040	–	–
Malleidae			
Malleus albus	MZSP55595	Pigmented caps	Outer fold; entire mantle extension
Malleus candeanus	USNM847920, MCZ340681	Pigmented caps	Outer fold; entire mantle extension

Malleus malleus	USNM802338	–	–
Malleus regula	MCZ379030	Pigmented caps	Outer fold; entire mantle extension
Noetiidae			
Arcopsis adamsi	MZSP19724, ZUECBIV1153	Pigmented cups	Outer fold, anterior mantle region
Didimacar tenebrica	SBMNH80722	Pigmented cups	Outer fold, anterior mantle region
Eontia ponderosa	SBMNH235066, USNM803530	–	–
Sheldonella bisulcata	MZSP26911	–	–
Striarca lactea	USNM857645, MCZ379156	Pigmented cups	Outer fold, anterior mantle region
Ostreidae			
Crassostrea gigas	USNM836263	–	–
Crassostrea virginica	USNM804279	–	–
Dendostrea folium	USNM802346	–	–
Dendostrea frons	USNM804288, MCZ378951	–	–
Lopha cristagalli	USNM793723	–	–
Ostrea edulis	USNM836256, MCZ379114	–	–
Ostrea equestris	USNM801030	–	–
Ostrea permolis	USNM850800	–	–
Pustulostrea australis	USNM787959	–	–
Saccostrea cucullata	SBMNH345722	–	–
Saccostrea palmula	USNM796192	–	–
Striostrea prismatica	SBMNH212884	–	–
Pectinidae			
Adamussium colbecki	USNM886965	Concave mirror eyes	Middle fold; entire mantle extension
Aequipecten glyptus	USNM803317	Concave mirror eyes	Middle fold; entire mantle extension

Aequipecten opercularis	MCZ371755	Concave mirror eyes	Middle fold; entire mantle extension
Argopecten gibbus	USNM801015, MCZ319455	Concave mirror eyes	Middle fold; entire mantle extension (mainly left side)
Argopecten irradians	MCZ278251	Concave mirror eyes	Middle fold; entire mantle extension
Chlamys hastata	USNM739716	Concave mirror eyes	Middle fold; entire mantle extension
Chlamys islandica	MCZ319213	Concave mirror eyes	Middle fold; entire mantle extension
Crassadoma gigantea	SBMNH466682	Concave mirror eyes	Middle fold; entire mantle extension
Delectopecten vitreus	USNM757159	Concave mirror eyes	Middle fold; entire mantle extension
Euvola raveneli	USNM801009	Concave mirror eyes	Middle fold; entire mantle extension (mainly left side)
Euvola ziczac	USNM833726	Concave mirror eyes	Middle fold; entire mantle extension (mainly left side)
Flexopecten glaber	MCZ371469	Concave mirror eyes	Middle fold; entire mantle extension
Gloripallium pallium	USNM701201	Concave mirror eyes	Middle fold; entire mantle extension
Lindapecten muscosus	USNM855448	Concave mirror eyes	Middle fold; entire mantle extension
Mimachlamys munda	USNM855527, USNM855529	Concave mirror eyes	Middle fold; entire mantle extension
Mimachlamys varia	MCZ378918	Concave mirror eyes	Middle fold; entire mantle extension
Mirapecten mirificus	USNM886347	Concave mirror eyes	Middle fold; entire mantle extension
Palliolum tigerinum	MCZ376695	Concave mirror eyes	Middle fold; entire mantle extension
Pecten jacobaeus	USNM1086023	Concave mirror eyes	Middle fold; entire mantle extension (mainly left side)
Pedum spondyloideum	USNM793736	Concave mirror eyes	Middle fold; entire mantle extension
Placopecten magellanicus	USNM829091, MCZ319444	Concave mirror eyes	Middle fold; entire mantle extension
Spathochlamys benedicti	USNM804647	Concave mirror eyes	Middle fold; entire mantle extension
Zygochlamys patagonica	USNM886527	Concave mirror eyes	Middle fold; entire mantle extension
Pinnidae			
Atrina inflata	MZSP55029	–	–
Atrina maura	USNM828614	–	–

Atrina rigida	USNM847971	–	–
Atrina seminuda	ZUECBIV2135	–	–
Atrina serrata	USNM801651	–	–
Atrina vexillum	USNM793718	–	–
Pinna carnea	MZSP29040, USNM804284	–	–
Pinna muricata	USNM836526, MCZ238056	–	–
Pinna rudis	MZSP114038	–	–
Pinna saccata	USNM793744, USNM780031	–	–
Philobryidae			
Adacnarca nitens	MZSP90616, USNM886551	–	–
Lissarca notorcardensis	MZSP87826, USNM899485	–	–
Neocardia sp.	USNM881121, MCZ378927	Pigmented cups	Outer fold, anterior mantle region
Philobrya sublaevis	MZSP90645, USNM882353	–	–
Plicatulidae			
Plicatula gibbosa	USNM801020, USNM801022	–	–
Propeamussiidae			
Catillopecten eucymatus	MCZ361432	–	–
Cyclopecten subimbrifer	ZUECBIV5702	Concave mirror eyes	Middle fold; entire mantle extension (left side only)
Parvamussium cancellatum	USNM803323, USNM856966	–	–
Parvamussium pourtalesianum	ZUECBIV2265, USNM856965	Concave mirror eyes	Middle fold; entire mantle extension (left side only)
Propeamussium dalli	USNM803326, USNM856943	–	–
Propeamussium lucidum	MCZ361413	–	–
Propeamussium meridionale	USNM897961	–	–
Propeamussium sp	USNM803320, USNM856941	–	–

Similipecten nanus	ZUECBIV2269, USNM803327	Concave mirror eyes	Middle fold; entire mantle extension (left side only)
Pteriidae			
Electroma alacorvi	USNM700050, USNM801689	–	–
Electroma papilionacea	USNM616482	–	–
Isognomon alatus	MZSP89628, USNM836243	Pigmented caps	Outer fold; entire mantle extension
Isognomon bicolor	ZUECBIV2123	Pigmented caps	Outer fold; entire mantle extension
Isognomon ephippium	USNM701010	–	–
Isognomon isognomum	MZSP54988	Pigmented caps	Outer fold; entire mantle extension
Isognomon perna	MZSP71186, MZSP11583	Pigmented caps	Outer fold; entire mantle extension
Isognomon radiatus	USNM803357	Pigmented caps	Outer fold; entire mantle extension
Pinctada albina	USNM755664	–	–
Pinctada imbricata	ZUECBIV2383	–	–
Pinctada maculata	USNM801689	–	–
Pinctada margaritifera	USNM836493	–	–
Pinctada mazatlantica	SBMNH42703	–	–
Pinctada radiata	MZSP106549	–	–
Pteria brevialata	MZSP55575, USNM836352	–	–
Pteria colymbus	USNM801027	–	–
Pteria hirundo	MZSP10885, ZUECBIV1401	–	–
Pteria penguim	USNM801027	–	–
Vulsella minor	USNM896263	–	–
Vulsella vulsella	MZSP896263	–	–
Spondylidae			
Spondylus americanus	USNM833744, USNM804280	Concave mirror eyes	Middle fold; entire mantle extension

Spondylus senegalensis	USNM1086035	Concave mirror eyes	Middle fold; entire mantle extension
Spondylus squamosus	USNM793728	Concave mirror eyes	Middle fold; entire mantle extension

Table 2. Taxa included in the phylogenetic analyses, with respective accession numbers for nucleotide sequences available in the *GenBank* database.

Taxa	16S rRNA	18S rRNA	28S rRNA	COI	Histone H3
Anomiidae					
Anomia ephippium	KX713191	AY377636	AJ307556	KF369195	
Monia patelliformis	KC429261	KC429342	KC429441		KC429179
Pododesmus caelata		AJ389650	AJ307555		
Arcidae					
Acar dominguensis				FJ480593	KT757861
Acar plicata		AJ389630	AJ307533	FJ480453	AF416856
Anadara antiquata		JN974491	JN974542	HQ258850	JN974592
Anadara broughtonii		JN974489	JN974541	HQ258847	JN974590
Anadara cornea		JN974499	DQ343860	HQ258856	JN974600
Anadara crebricostata		JN974495	JN974547	HQ258859	JN974596
Anadara globosa		JN974484	JN974535	HQ258861	JN974584
Anadara gubernaculum		JN974493	JN974544	HQ258857	JN974594
Anadara inaequivalvis		JN974497	JN974548	AB076937	JN974598
Anadara notabilis		KT757768	KT757816	AF416828	KT757863
Anadara pilula		JN974507	JN974558	HQ258862	JN974608
Anadara subcrenata		JN974501	DQ343861	HQ258851	JN974602
Anadara trapezia	KX713189	KT757770	KT757817	KX713443	KT757865
Anadara vellicata		JN974487	JN974539	HQ258848	JN974588
Arca imbricata		AY654986	KT757820	AF253494	AY654989
Arca navicularis		JN974517	KT757821	HQ258822	JN974618
Arca noae	KX713192	KC429325	KT757822	KC429090	KC429160
Arca patriarchalis		JN974527	JN974576		JN974627
Arca ventricosa				AB076935	AF416854
Arca zebra		KT757776	KT757824		AF416864
Barbatia barbata	KC429244	KC429326	KT757825	KC429091	KC429161
Barbatia cancellaria		KT757779	KT757827		
Barbatia candida		KT757784	KT757831	AF253487	AF416849
Barbatia fusca		JN974526	JN974575		JN974626
Barbatia lacerata		JN974509	JN974560	HQ258826	JN974610
Barbatia lima		JN974511	JN974563	HQ258837	JN974612
Barbatia virescens		JN974524	KT757835	HQ258840	JN974624
Bathyarca glomerula		KT757790	KT757837		KT757880
Lunarca ovalis				GQ166571	AF416844

Tegillarca granosa	KJ607173	JN974505	KT757857	HQ258867	JN974606
Tegillarca nodifera		JN974503	JN974554	HQ258869	JN974604
Trisidos kiyonoi		JN974522	JN974571	HQ258846	JN974622
Trisidos tortuosa	KX713263	KT757811	KT757858		KT757899
Cucullaeidae					
Cucullaea labiata		JN974513	JN974565	KJ774477	JN974614
Dimyidae					
Dimya lima	KX713213	KC429344	KX713375		KC429181
Glycymerididae					
Glycymeris gigantea		KT757794	KT757841		KT757883
Glycymeris glycymeris	KC429246	KC429328	KC429421	KC429093	KC429163
Glycymeris holoserica		KT757796	KT757843		KT757885
Glycymeris nummaria		KT757798	KT757845	KX785178	KT757887
Glycymeris septentrionalis		KT757799	KT757846	KF643645	KT757888
Glycymeris tenuicostata		KT757800	KT757847		KT757889
Tucetona pectinata	KX713264	KT757812	KT757859	KX713507	KT757900
Gryphaeidae					
Hyotissa hyotis	AY548883	AJ389632	KC847156	GQ166583	HQ329258
Hyotissa imbricata	KC847136		KC847157	AB076917	
Hyotissa mcgintyi	KC429254	KC429336	AY376596		KC429171
Hyotissa numisma	AY376598	AJ389633	AF137035		
Neopicnodonte cochlear	JF496758		AF137034	AB076939	
Limidae					
Acesta excavata	AM494898	GQ240893		AM494908	
Ctenoides annulatus	EU379439				EU379493
Ctenoides mitis	EU379440	KT757792	KT757839		KT757881
Ctenoides scaber	KC429256	KC429338	KC429433	KC429100	
Lima lima	KC429257	KC429339	KC429434	KC429101	KC429174
Limaria hians	JF808185	AF120534		AF120650	AY070152
Limopsidae					
Limopsis cumingi		KT757802		AB076930	
Limopsis enderbyensis		AJ422057	AY321301		
Limopsis marionensi		AJ422058	AY321303		
Limopsis sp.	KC429247	KC429329	KC429422		KC429164
Malleidae					
Malleus albus	KC429252	KC429334	HQ329464	KC429097	KC429169
Malleus candeanus	HQ329411	HQ329351	HQ329465		HQ329279

Malleus malleus	HQ329412	HQ329352	HQ329466		HQ329280
Malleus regula	HQ329414	HQ329353	HQ329467		HQ329283
Mytilidae					
Bathymodiolus mauritanicus	HF545083	AY649828	FJ890504	FJ890502	HF545126
Bathymodiolus thermophilus	KF611760	AF221638	GU966640	GQ473715	KF720623
Benthomodiolus lignocola	KF611733	AF221648		AY275545	HF545156
Benthomodiolus geikotsucola	HF545049	AB679345	HF545023	AB679346	HF545149
Brachidontes darwinianus			KC844370	KC844414	
Brachidontes exustus	KX71319	KT757791	KT757838	AY621838	
Brachidontes rodriguezii		DQ640530	KC844362	KC844477	
Dacrydium sp.	KX713210	KX713285	KX713372	KX713456	KX713529
Geukensia demissa	U68772	L33450	AY622004	GQ282963	
Gregariella coarctata		AJ414641	AJ307538		
Idas washingtonia	HF545073	AF221645		AY275546	
Ischadium recurvum	KT959477		AY622009	AY621933	
Leiosolenus curtus	JQ267791	AB201235	AB103123	AB076944	LC004203
Lithophaga antillarum	KX713229	KX713308	KX713397		KX713550
Lithophaga lithophaga	JF496757	AF120530		AF120644	
Lithophaga nigra		AF124209	AB103127		
Modiolus auriculatus		AJ389644	AJ307537	GQ480317	
Modiolus modiolus	KF611732	AF124210	EF526455	HM884246	
Modiolus philippinarum		AB201232		KY705073	LC004218
Modiolus rumphii	KC429248	KC429330	KC429423	KC429094	KC429165
Musculista senhousia		AB201231		HQ891093	
Musculus discors	KR827553	AF124206		KF643642	KP113647
Musculus niger		KX713316	KX713404	KF644120	
Mytilus californianus	AF317544	L33449		U68777	AY267745
Mytilus edulis	KC429249	KC429331	KC429424	KF644190	KC429166
Mytilus galloprovincialis	AF317543	L33452	AB105357	AB076943	AY267748
Mytilus trossulus	U22879	L33453		KF643612	AY267747
Perna perna	DQ923882	DQ640520		KU743163	
Perna viridis	AB265680	EF613234		DQ917584	
Perumytilus purpuratus	JQ390293	KJ453820	KJ598046	KF661934	
Septifer bifurcatus		KJ453815	KJ453831		
Septifer virgatus	AB372228	KJ453817	KJ453832	AB076941	
Xenostrobus securis	AB372227	EF186014		JF430154	
Noetiidae					

Arcopsis adamsi	KC429245	KC429327	KC429419	KC429092	KC429162
Didimacar tenebrica		JN974515	JN974566	HQ258870	JN974616
Eontia ponderosa	KC429245	KT757793	KT757840	AF416834	AF416860
Striarca lactea	JF496761	AF120531	KT757855	AF120646	
Ostreidae					
Crassostrea gigas	AF280611	AB064942	AF137051	DQ417691	HQ009488
Crassostrea virginica	KC429253	KC429335	KC429429	FJ743529	KC429170
Dendostrea frons	AF052070		AF137039	AB084109	
Lopha cristagalli	AF052066	AJ389635	AF137038	AB076908	
Ostrea edulis	AF052068	L49052	AF137047	AF120651	AY070151
Saccostrea cucullata	AB748902	AJ389634	AJ344329	AB721961	
Pectinidae					
Adamussium colbecki	HM600752	AJ242534	FJ263652		EU379491
Aequipecten opercularis	EU379462	AJ310482	AJ307543	KR084493	EU379516
Amusium balloti	HM540095		HM540093		EU379488
Argopecten gibbus	EU379443	AF074389	HM622697		EU379496
Argopecten irradians	EU379446	L11265	HM622700	GU120020	EU379486
Chlamys hastata	FJ263648	L49049	FJ263658		FJ263667
Chlamys islandica	FJ263646	L11232	FJ263656		FJ263666
Crassadoma gigantea	EU379444	L49050	FJ263654		EU379498
Euvola ziczac	EU379484		HM630509		EU379539
Excellichlamys spectabilis	HM630458	AJ389648	AJ307544	AB076911	HM630463
Flexopecten glaber	GU320272	AJ389662	AJ307545		HQ197860
Mimachlamys varia	EU379482	L49051	AJ307546	EU523666	EU379536
Mizuhopecten yessoensis	FJ263649	EU660798	HM630386	GU119990	HM630385
Palliolum tigerinum	JQ611453	JQ611497			JQ611562
Pecten jacobaeus	AJ245394	AY070112		AY377728	AY070153
Pecten maximus	KC429258	L49053	HM630545	KC429102	EU379508
Placopecten magellanicus	EU379452	X53899	FJ263657		EU379506
Pinnidae					
Atrina assimilis	KJ365681	KJ365873	KJ366133	KJ366470	
Atrina chautardi	KJ365675	KJ365892	KJ366174	KJ366416	
Atrina exusta	KJ365674	KJ365962	KJ366262	KJ366439	
Atrina fragilis	DQ663474		KJ366257	KJ366406	
Atrina pectinata	KJ365657	KJ365829	KJ366108	HQ449360	
Atrina rigida	HQ329397	KJ365786	KJ366041	KJ366328	HQ329248
Atrina seminuda	HQ329398	HQ329324			HQ329249

Atrina vexillum	JN182778	KJ365836	KJ366264	HQ449380	
Pinna atropurpurea	KJ365564	KJ365801	KJ366081	KJ481930	
Pinna bicolor	KJ365682	KJ365837	KJ366116	JN182725	
Pinna carnea	KC429255	HQ329375	KJ366067	KJ366325	KC429172
Pinna dolabrata	KJ365590	KJ365934	KJ366236		
Pinna muricata	KJ365568	KJ365752	KJ366259	KJ366324	
Pinna nobilis	DQ663473	KJ365983	KJ366274		
Pinna rudis	KJ365521	KJ365749	KJ366028	KJ366482	
Pinna saccata	KJ365577	AB594353	KJ366083	KJ366453	
Pinna trigonalis	KJ365661	KJ365948		KJ366451	
Philobryidae					
Adacnarca nitens		KP340836	KT757815		KT757862
Lissarca notorcardensis			EF192520	KF612434	
Neocardia sp.		KT757804	KT757850	KX713486	KT757891
Philobrya magellanica		KP340835	KP340812		
Philobrya sublaevis		KP340845	KT757853		KT757895
Plicatulidae					
Plicatula australis		AF229626	AB102737		KC429178
Plicatula plicata		AJ389651	AJ307539		
Propeamussiidae					
Parvamussium pourtalesianum	EU379465		HM600741		EU379519
Propeamussium dalli	EU379470		HM600740		EU379524
Propeamussium sibogai	HM600755		HM600748		HM600735
Propeamussium sp	KC429259	KC429340	KC429437	KC429103	KC429176
Pteriidae					
Crenatula avicularis	HQ329399	HQ329325	HQ329440		HQ329251
Electroma alacorvi	HQ329400	AJ389641	HQ329442		HQ329252
Electroma papilionacea		HQ329327	HQ329441		HQ329253
Isognomon alatus	KC429251	KC429333	HQ329446	KC429096	KC429168
Isognomon bicolor	HQ329406	HQ329332	HQ329447		HQ329260
Isognomon californicum		HQ329333	HQ329448		HQ329261
Isognomon ephippium		HQ329334	HQ329449		HQ329262
Isognomon isognomum		AF229621	HQ329451		HQ329264
Isognomon legumen		KT757801	KT757848	AB076950	KT757894
Isognomon perna		AB594386	AB594433	AB076918	
Isognomon radiatus	HQ329408	HQ329338	HQ329453		HQ329266
Pinctada albina	HQ329415	AB214453	AB214468	AB261165	HQ329286

Pinctada capensis	HQ329416	HQ329359	HQ329474		HQ329288
Pinctada fucata	HQ329419	AY028625	HQ329476	GQ355871	HQ329290
Pinctada imbricata	HQ329421	AB214456	AB214471	KP455060	HQ329291
Pinctada longisquamosa	HQ329424	HQ329367	HQ329481		HQ329295
Pinctada maculata	AB214440	AB214455	AB214470	AB261166	
Pinctada margaritifera	HQ329425	AB214451	AB214466	AB259166	HQ329296
Pinctada maxima	KF284042	AB214450	AB214465	JQ990784	
Pinctada mazatlantica	HQ329427	HQ329371	HQ329485		HQ329298
Pinctada nigra	HQ329428	AB214454	AB214469		HQ329301
Pinctada radiata	KF284053	AB214457	AB214472	GQ355876	
Pteria avicular		HQ329389	HQ329491		HQ329304
Pteria brevialata	HQ329434	AB594356	AB594405		
Pteria colymbus	HQ329432	HQ329384	HQ329495		HQ329307
Pteria hirundo	KC429250	KC429332	KC429425	AF120647	KC429167
Pteria howensis		HQ329393	HQ329504		HQ329320
Pteria loveni	HQ329436	HQ329380	HQ329500	AB076925	HQ329313
Pteria penguim	EF031242	AB591837	HQ329496		HQ329314
Vulsella vulsella		HQ329395	HQ329509		HQ329322
Spondylidae					
Spondylus ambiguus	KC429260	KC429341			KC429177
Spondylus crassisquamatus		AJ389646	AJ307542		
Spondylus hystrix		AJ389647	AJ307561		
Spondylus ictericus	EU379477		HM600742		EU379531
Spondylus sinensis		AF229629	AB102750		
Outgrup					
Chione elevata	KC429298	KC429387	KC429495	KC429136	KC429219
Donax trunculus	EF417551	KC429395	KC429503	KC429143	KC429226
Hiatella arctica	KC429286	KC429375	KC429480	KC429127	KC429208
Macoma balthica	KC429303	KC429393	KC429501	KC429141	KC429224
Margaritifera margaritifera	KC429265	AF229612	KC429443	AF303316	KC429185
Mya arenaria	KC429313	AF120560	KC429515	KF644013	KC429235
Neotrigonia lamarckii	KC429262	KC429345	KC429443	KC429105	KC429182
Nucula sulcuta	KC984679	AF207642	KC984815	KC984746	KC984777
Nuculana minuta	KC984679	AF120529	DQ279961	AF120643	KC984765
Solemya velum	DQ280028	AF120524	KC984796	KC984745	KC429159
Yoldia limatula		AF120528	KC429411	AF120642	KC429156
Antalis entalis	DQ280027	AY377636	AY145388	AY260816	DQ280000

Chaetopleura apiculata	AY377590	DQ279936	AY145398	KP254304	AY377741
Haliotis tuberculata	AY650168			AY377729	AY377775
Laevipilina hyalina	FJ449543	FJ445774	FJ445777	FJ445781	FJ445778

Supplementary material

Table S1. Lifestyles of pteriomorphian species compiled from the literature. Abbreviations: BO=borer (in hard substrate, such as wood or limestone), CD=crevice-dweller, CE=cemented, D=deep waters (>1000 m for bathypelagic and abyssopelagic zones), EB=epibiotic (fixed on other organisms), EF=epifaunal, IF=infaunal, NB=nest-building (usually with byssus, mucus, and grains), S=shallow waters (<1000m for epipelagic and mesopelagic zones), SF=semi-infaunal.

Taxa	Lifestyles	Substrate	Relative depth	References
Anomiidae Rafinesque, 1815				
Anomia chinensis Philippi 1850	EF, CE	rock, shells and debris	S	Tsi and Ma 1982, Ong Che and Morton 1991, Scott 1994, Leung and Morton 2000
Anomia ephippium (Linnaeus, 1758)	EF, CE	hard substrate	S	Yonge 1973
Anomia simplex d'Orbigny, 1853	EF, CE	hard substrate	S	Turgeon et al. 2009
*Monia umbonata (*Gould, 1861)	EF, CE	dead coral heads	S	Dudgeon and Morton 1982
Arcidae Lamarck 1809				
Acar domingensisi (Lamarck, 1819)	EF	rocks	S	Simone and Chichverkrun 2004
Acar plicata (Dillwyn, 1817)	EF	mud, rubble, shell-hash, under corals	S	Kilburn 1983, Leung and Morton 2000
Anadara antiquata (Linnaeus, 1758)	EF/SF	muddy sand, attached to rock or coral fragments	S	Evseev and Lutaenko 1998, Broom 1985, Kilburn 1983
Anadara broughtonii (Schrenck, 1867)	IF	mud	S	Broom 1985, Oliver and Holmes 2006
Anadara cornea (Reeve, 1844)	IF	mud, sand	S	Broom 1985, Tsi and Ma 1982, Li and Gao 1985, Morton 1986
Anadara ferruginea (Reeve, 1844)	IF	coarse sand, fine sand, and silty clay	S	Tsi and Ma 1982, Scott 1994, Morton 1994, Leung and Morton 1997, Nicholson and Morton 2000
Anadara gubernaculum (Reeve, 1844)	IF	sand, silty sand	S	Evsee and Lutaenko 1998, Oliver and Holmes 2006
Anadara inequivalvis (Bruguière, 1789)	IF	sand, muddy sand	S	Broom 1985, Tsi and Ma 1982, Scott 1994, Nicholson and Morton 2000
Anadara notabilis (Röding, 1798)	IF	sand	S	Rocha and Martins 1998, Oliver and

				Holmes 2006, Turgeon et al. 2009
Anadara ovalis (Bruguiére, 1789)	IF	sand	S	Oliver and Holmes 2006, Alexander 2007, Turgeon et al. 2009
Anadara pilula (Reeve, 1843)	IF	sand, silty sand	S	Norte-Campos et al. 2005, Oliver and Holmes 2006
Anadara subcrenata (Lischke, 1869)	IF	mud, muddy sand	S	Broom 1985, Oliver and Holmes 2006
Anadara trapezia (Deshayes, 1839)	IF	sandy mudflats	S	Sullivan 1960, Oliver and Holmes 2006
Anadara vellicata (Reeve, 1844)	IF	silty sand	S	Evsee and Lutaenko 1998, Oliver and Holmes 2006
Arca imbricata Bruguière, 1789	EF	rocks	S	Oliver and Holmes 2006, Turgeon et al. 2009
Arca navicularis Bruguière, 1789	EF	under rocks and on coral heads	S	Kilburn 1983
Arca noae Linnaeus, 1758	EF	rocks	S	Thomas 1996, Oliver and Holmes 2006, Morton and Peharda 2008
Arca patriarchalis Röding, 1798	EF	dead corals	S	Dudgeon and Morton 1982
Arca ventricosa (Lamarck, 1819)	EF	coral heads	S	Kilburn 1983, Oliver and Holmes 2006
Arca zebra (Swainson, 1833)	EF	rocks	S	Oliver and Holmes 2006, Turgeon et al. 2009
Barbatia barbata (Linnaeus, 1758)	EF	rocks	S	Thomas 1996, Oliver and Holmes 2006, Turgeon et al. 2009
Barbatia cancellaria (Lamarck, 1819)	EF	rocks	S	Simone and Chichverkrun 2004
Barbatia candida (Helbling, 1779)	EF	rocks	S	Simone and Chichverkrun 2004, Turgeon et al. 2009
Barbatia fusca (Bruguière, 1789)	EF	coral heads	S	Sanpanich 2011, Tsi and Ma 1982, Oliver and Holmes 2006
Barbatia lacerata (Bruguière, 1789)	EF	corals and rocks	S	Oliver et al. 2004
Barbatia lima (Reeve, 1844)	EF	rocks	S	Scott 1994, Leung and Morton 2000
Barbatia setigera (Reeve, 1844)	EF	coarse sand	S	Kilburn 1983
Barbatia virescens (Reeve, 1844)	EF	rocks, piers and boulders	S	Morton 1987, Britton 1990, Taylor and Morton 1996, Harper and Morton 1997
Bathyarca glomerula (Dall, 1881)	SF	soft sediments	D	Oliver and Allen 1980, Turgeon et al. 2009

Bathyarca pectunculoides (Scacchi, 1835)	SF	muddy shell gravel	D	Morton 1982, Oliver and Allen 1980
Tegillarca granosa (Linnaeus, 1758)	IF	muddy sand	S	Evsee and Lutaenko 1998, Broom 1985, Morton 1986
Tegillarca nodifera (Martens, 1860)	IF	mud, sand, soft clay bottom	S	Evsee and Lutaenko 1998
Trisidos kiyonoi (Makiyama, 1931)	SF	gravelly sand, coarse sand	S	Scott 1994
Trisidos semitorta (Lamarck, 1819)	SF	coarse sand and shell hash	S	Savazzi 1984, Tsi and Ma 1982, Morton 1983, Leung and Morton 2000
Trisidos tortuosa (Linnaeus, 1758)	SF	fine muddy sand	S	Kilburn 1983, Savazzi 1984
Cucullaeidae Stewart, 1930				
Cucullaea labiata (Lightfoot, 1786)	SF	sand and corals	S	Morton 1981, Oliver and Holmes 2006, Sanpanich 2011
Dimyidae Fischer, 1886				
Dimya lima Bartsch, 1913	EF, CE	hard substrate	S	Yonge 1973
Glycymerididae Dall, 1908 (1847)				
Glycymeris gigantea (Reeve, 1843)	SF	Coarse shell gravel, sand, mud, stones	S	Thomas 1995, 1996, Oliver and Holmes 2006
Glycymeris glycymeris (Linnaeus, 1758)	SF	Coarse shell gravel, sand, mud, stones	S	Thomas 1995, 1996, Oliver and Holmes 2006
Glycymeris holoserica (Reeve, 1843)	SF	Coarse shell gravel, sand, mud, stones	S	Thomas 1995, 1996, Oliver and Holmes 2006
Glycymeris nummaria (Linnaeus, 1758)	SF	Coarse shell gravel, sand, mud, stones	S	Thomas 1995, 1996, Oliver and Holmes 2006
Glycymeris septentrionalis (Middendorff, 1849)	SF	Coarse shell gravel, sand, mud, stones	S	Thomas 1995, 1996, Oliver and Holmes 2006
Glycymeris tenuicostata (Reeve, 1843)	SF	Coarse shell gravel, sand, mud, stones	S	Thomas 1995, 1996, Oliver and Holmes 2006
Tucetona pectinata (Gmelin, 1791)	SF	Coarse shell gravel, sand, mud, stones	S	Turgeon et al. 2009
Gryphaeidae Vyalov, 1936				
Hyotissa hyotis (Linnaeus, 1758)	EF, CE	hard substrate	S	Turgeon et al. 2009, Lam and Morton 2009
Hyotissa mcgintyi (Harry, 1985)	EF, CE	hard substrate	S	Turgeon et al. 2009, Lam and Morton

				2009
Hyotissa sinensis (Gmelin, 1791)	EF, CE	shell hash and rubble	S	Morris 1985, Scott 1994, Lam and Morton 2003
Neopycnodonte cochlear (Poli, 1795)	EF, CE	rocks	S	Turgeon et al. 2009, Johnson et al. 2013
Limidae d’Orbigny, 1846				
Acesta excavata (Fabricius, 1779)	EF	rocks	S	Gagnon and Haedrich 2003
Ctenoides annulatus (Lamarck, 1819)	EF, CD	coral crevices	S	Zuschin and Piller 1997
Ctenoides mitis (Lamarck, 1807)	EF, CD	coral crevices and ledges	S	Turgeon et al. 2009, Pearce and LaBarbera 2009, Mikkelsen and Bieler 2003
Ctenoides scaber (Born, 1778)	EF, CD	coral rubbles and rocks	S	Turgeon et al. 2009, Dukeman et al. 2005, Mikkelsen and Bieler 2003
Lima lima (Linnaeus, 1758)	EF, CD	coral galleries, gravel to rocks	S	Morton 1979, Dudgeon and Morton 1982, Zuschin and Piller 1997, Malkowsky and Götze 2014
Limaria hians (Gmelin, 1791)	EF, CD, NB	rocks and corals, nests	S	Merrill and Turner 1963
Limopsidae Dall, 1895				
Limopsis aurita (Brocchi, 1814)	EF/SF	rocks, soft sediments, mud	S-D	Oliver and Allen 1980
Limopsis cristata Jeffreys, 1876	SF	soft sediments	S-D	Oliver and Allen 1980, Morton 2012, Linse 2014
Limopsis tenella Jeffreys, 1876	SF	soft sediments	D	Oliver and Allen 1980
Limopsis galathea Knudsen, 1970	SF	soft sediments	D	Oliver and Allen 1980
Limopsis minuta (Philippi, 1836)	SF	gravel	S-D	Oliver and Allen 1980, Turgeon et al. 2009
Limopsis marionensis E. A. Smith, 1885	EF, EB	rocks and associated with sponges	S-D	Cattaneo-Vietti et al. 2000, Narchi et al. 2002, Pörtner et al. 1999
Malleidae Lamarck, 1818				
Malleus albus Lamarck, 1819	SF	muddy sand	S	Yonge 1968
Malleus candeanus(d'Orbigny, 1853)	EF, CD	corals, rocks	S	Boss and Moore 1967
Malleus malleus (Linnaeus, 1758)	SF	coarse sand	S	Yonge 1968, Tsubaki et al. 2011
Malleus regula (Forsskål in Niebuhr, 1775)	EF, CD	rocks	S	Tsubaki et al. 2011, Ubukata 2003

Mytilidae Rafinesque, 1815				
Adula diengensis (Dall, 1911)	EF	free-living, mud flats, crevices		Soot-Ryen 1955, Ockelmann and Dinesen 2009
Amygdalum watsoni (E. A. Smith, 1885)	IF, NB	soft mud, byssal nest	S	Lee and Morton 1985
Arcuatula elegans (Gray, 1828)	IF, NB	mud, in a gelatinous byssal net	S	Morton 1980, Lee and Morton 1985, Leung and Morton 1997, 2000
Arcuatula senhausia (Benson, 1842)	IF, NB	sand and mudflats, in a byssal nest	S	Morton 1974
Aulacomya atra (Molina, 1782)	EF	rocks and mussels	S	Soot-Ryen 1955
Bathymodiolus brooksi Gustafson, R. D. Turner, Lutz & Vrijenhoek, 1998	EF	cold seeps	D	Duperron et al. 2007
Bathymodiolus childressi Gustafson, R. D. Turner, Lutz & Vrijenhoek, 1998	EF	cold seeps	D	Duperron et al. 2007
Bathymodiolus mauritanicus Cosel, 2002	EF	hydrocarbon seeps	D	Turgeon et al. 2009, Lorion et al. 2010
Bathymodiolus thermophilus Kenk & B. R. Wilson, 1985	EF	hydrothermal vents	D	Lorion et al. 2010
Benthomodiolus geikotsucola Okutani & Miyazaki, 2007	EF	bone	D	Lorion et al. 2010
Benthomodiolus lignocola Dell, 1987	EF	bone, wood	D	Lorion et al. 2010
Botula fusca (Gmelin, 1791)	BO	dead coral	S	Lee and Morton 1985, Huang et al. 1992, Turgeon et al. 2009
Brachidontes darwinianus (d'Orbigny, 1842)	EF	hard substrate, rocks	S	Tanaka 2005, Trovant et al. 2013
Brachidontes exustus (Linnaeus, 1758)	EF	hard substrate	S	Turgeon et al. 2009
Brachidontes rodriguezii (d'Orbigny, 1842)	EF	hard substrate	S	Trovant et al. 2013
Crenella decussata (Montagu, 1808)	IF	soft substrate	S	Turgeon et al. 2009, Morton 1974
Dacrydium elegantulum Soot-Ryen, 1955	IF, NB	nest of sand grains and bottom materials, mud	D	Turgeon et al. 2009, Mattson and Waren 1977, Salas 1996
Geukensia demissa (Dillwyn, 1817)	SF	mud	S	Owada 2007
Gregariella coralliophaga (Gmelin, 1791)	BO	rock pools, vacated bore holes in dead corals	S	Scott 1980, Morton 1982, Lee and Morton 1985, Turgeon et al. 2009
Idas washingtonia (Bernard, 1978)	EF	sunken wood	D	Samadi et al. 2007
Ischadium recurvum (Rafinesque, 1820)	EF	hard substrate, oyster reef	S	Turgeon et al. 2009

Leiosolenus curtus (Lischke, 1874)	BO	calcareous sandstone	S	Owada 2015
Lioberus castaneus (Say, 1822)	EF	hard substrate	S	Turgeon et al. 2009
Lithophaga antillarum (d'Orbigny, 1853)	BO	coral, limestone	S	Turgeon et al. 2009
Lithophaga lithophaga (Linnaeus, 1758)	BO	limestone	S	Morton and Scott 1980
Lithophaga nigra (d'Orbigny, 1853)	BO	coral, limestone	S	Turgeon et al. 2009
Modiolus americanus (Leach, 1815)	EF/SF	hard substrate, seagrass	S	Stanley 1970, Strömgren 1976, Savazzi 1994, Turgeon et al. 2009
Modiolus auriculatus Kraus, 1848	EF	rocks, rocky sand, seagrass, attached to pilings	S	Huang et al 1992, Hazek et al. 2014
Modiolus modiolus (Linnaeus, 1758)	EF/SF	sand, mud and rocks	S	Stanley 1972, Dinesen and Morton 2014
Modiolus philippinarum (Hanley, 1843)	SF	sand and mudflats	S	Savazzi 1984, Lee and Morton 1995, Sanpanich 2011
Modiolus rumphii (Philippi, 1847)	SF	sand	S	Stanley 1972
Musculus discors (Linnaeus, 1767)	IF, NB	sandy mud, byssal nest among algae	S	Aitken and Fournier 1993, Merrill and Turner 1963
Musculus lateralis (Say, 1822)	EF/SF, NB	coarse silt, hard substrate, byssal nest	S	Pires-Vanin et al. 2014, Turgeon et al. 2009, Bertran 1971
Musculus niger (Gray, 1824)	IF, NB	silty sand	S	Aitken and Fournier, 1993
Mytilisepta bifurcata (Conrad, 1837)	EF	hard substrate, rocks	S	Seed and Richardson 1999
Mytilus edulis Linnaeus, 1758	EF	hard substrate	S	Stanley 1972
Mytilus galloprovincialis (Lamarck, 1819)	EF	rocks and pilings	S	Britton 1990, Lee and Morton 1985, Morton 1987
Perna perna (Linnaeus, 1758)	EF	hard substrate	S	Turgeon et al. 2009
Perna viridis (Linnaeus, 1758)	EF	hard substrate, rocks and pilings	S	Tsi and Ma 1982, Lee and Morton 1985, Morton 1986, Taylor 1993, Leung and Morton 2000
Perumytilus purpuratus (Lamarck, 1819)	EF	hard substrate	S	Trovant et al. 2013
Septifer bilocularis (Linnaeus, 1758)	EF	dead corals, on pilings, rocks	S	Lee and Morton 1995, Huang et al 1992, Sanpanich 2011
Septifer virgatus (Wiegmann, 1837)	EF	pier pilings, corals heads, rocks	S	Dudgeon and Morton 1982, Lee and Morton 1985, Taylor and Morton 1996

Xenostrobus securis (Lamarck, 1819)	EF	rocky substrates	S	Colgan and Costa 2013
Noetiidae Stewart, 1930				
Arcopsis adamsi (Dall, 1886)	EF	rocks on sand	S	Oliver and Järnegren 2004
Didimacar tenebrica (Reeve, 1844)	EF	rocks and boulders	S	Oliver 1990, Scott 1994, Harper and Morton 1997, Leung and Morton 2000
Noetia ponderosa (Say, 1822)	IF	soft sediments	S	Oliver and Holmes 2006, Turgeon et al. 2009
Striarca symmetrica (Reeve, 1844)	EF	rocks and dead corals	S	Oliver 1985, Harper and Morton 1997, Vongpanich and Matsukuma 2004
Striarca lactea (Linnaeus, 1758)	EF	rocks, under boulders, among gravel	S	Oliver and Cosel 1992
Ostreidae Rafinesque, 1815				
Crassostrea gigas (Thunerg, 1793)	EF, CE	hard substrate	S	Lam and Morton 2009
Crassostrea virginica (Gmelin, 1791)	EF, CE	hard substrate	S	Turgeon et al. 2009
Dendostrea frons (Linnaeus, 1758)	EF, CE	hard substrate	S	Turgeon et al. 2009
Lopha cristagalli (Linnaeus, 1758)	EF, CE	hard substrate	S	Lam and Morton 2009
Ostrea edulis Linnaeus, 1758	EF, CE	hard substrate	S	
Saccostrea cucullata (Born, 1778)	EF, CE	pier pilings, rocks, crevices, mangroves	S	Taylor 1990, Morton 1990, Lam and Morton 2009
Pectinidae Rafinesque, 1815				
Adamussium colbecki (E. A. Smith, 1902)	EF	sand	S	Cattaneo-Vietti et al. 2000, Brand 2006, Alejandrino et al. 2011
Aequipecten opercularis (Linnaeus, 1758)	EF	sand to gravel	S	Brand 2006, Alejandrino et al. 2011, Malkowsky and Götze 2014
Argopecten gibbus (Linnaeus, 1758)	EF	soft substrate	S	Brand 2006, Alejandrino et al. 2011
Argopecten irradians (Lamarck, 1819)	EF	soft substrate	S	Brand 2006, Alejandrino et al. 2011
Chlamys hastata (G. B. Sowerby II, 1842)	EF	gravel to rocks	S	Alejandrino et al. 2011, Malkowsky and Götze 2014
Chlamys islandica (Müller, 1776)	EF	gravel to rocks	S	Malkowsky and Götze 2014
Crassadoma gigantea (Gray, 1825)	EF, CE	hard substrate	S	Alejandrino et al. 2011
Euvola ziczac (Linnaeus, 1758)	EF	soft substrate	S	Turgeon et al. 2009

Excellichlamys spectabilis (Reeve, 1853)	EF	corals, coral rubbles	S	Dijkstra 1998
Flexopecten glaber (Linnaeus, 1758)	EF	rocky, sandy and muddy bottoms	S	Schejter and Bremec 2007, Malkowsky and Götze 2014
Mimachlamys varia (Linnaeus, 1758)	EF	rocks and corals	S	Brand 2006, Alejandrino et al. 2011, Malkowsky and Götze 2014
Mizuhopecten yessoensis (Jay, 1857)	EF	sand and muddy sand	S	Brand 2006, Alejandrino et al. 2011, Malkowsky and Götze 2014
Palliolum tigerinum (O. F. Müller, 1776)	EF	mud, muddy sand with gravel and rocks	S	Janssen and Dijkstra 1996, Malkowsky and Götze 2014
Pecten jacobaeus (Linnaeus, 1758)	EF	sand and muddy sand	S	Brand 2006, Alejandrino et al. 2011, Malkowsky and Götze 2014
Pecten maximus (Linnaeus, 1758)	EF	sand and muddy sand	S	Brand 2006, Alejandrino et al. 2011, Malkowsky and Götze 2014
Placopecten magellanicus (Gmelin, 1791)	EF	soft substrate	S	Brand 2006, Alejandrino et al. 2011
Ylistrum balloti (Bernardi, 1861)	EF	soft substrate	S	Alejandrino et al. 2011
Pinnidae Leach, 1819				
Atrina assimilis (Reeve, 1858)	SF	soft sediments	S	Yonge 1953
Atrina chautardi (Nicklès, 1953)	SF	soft sediments	S	Yonge 1953
Atrina exusta (Gmelin, 1791)	SF	soft sediments	S	Yonge 1953
Atrina fragilis (Pennant, 1777)	SF	sand	S	Yonge 1953, Fryganiotis et al. 2013
Atrina pectinata (Linnaeus, 1767)	SF	coral, sand, seagrass	S	Sanpanich 2011, Yang et al. 2015
Atrina rigida (Lightfoot, 1786)	SF	soft sediments, seagrass	S	Turgeon et al. 2009, Munguia 2007
Atrina seminuda (Lamarck, 1819)	SF	soft sediments, seagrass	S	Turgeon et al. 2009
Atrina vexillum (Born, 1778)	SF	sand and mud	S	Morton 1987
Pinna atropurpurea G. B. Sowerby I, 1825	SF	sand and mud	S	Wu 1985
Pinna bicolor Gmelin, 1791	SF	sand and mud	S	Tsu and Ma 1982, Morton 1987
Pinna carnea Gmelin, 1791	SF	sand, seagrass	S	Turgeon et al. 2009, Yonge 1953
Pinna dolabrata Lamarck, 1819	SF	soft sediments	S	Yonge 1953
Pinna muricata (Linnaeus, 1758)	SF	soft sediment	S	Tsubaki et al. 2011
Pinna nobilis Linnaeus, 1758	SF	sand, seagrass	S	Yonge 1953
Pinna rudis Linnaeus, 1758	SF	sand, seagrass, among	S	Turgeon et al. 2009

		rocks		
Pinna trigonalis Pease, 1861	SF	soft sediments	S	Yonge 1953
Streptopinna saccata (Linnaeus, 1758)	SF, CD	embedded in living and dead coral	S	Tsubaki et al. 2011
Phylobryidae Bernard, 1897				
Adacnarca nitens Pelseneer, 1903	EF, EB	sand, rocks, hydrozoans, bryozoans, sponges, ascidians and gorgonacians	S	Cattaneo-Vietti et al. 2000, Higgs et al. 2009
Lissarca notorcardensis Melvill & Standen, 1907	EF, EB	spines of cidaroid sea urchins	S	Brey et al. 1993, Linse et al. 2007
Neocardia sp. Sowerby III, 1892	EF, EB	associated with phytals	S	Lasiak 1999
Philobrya munita (Finlay, 1930)	EF, EB	under rocks, attached to algae *Carpophyllum*	S	Morton 1978
Philobrya sublaevis Pelseneer, 1903	EF, EB	algae	S	Cattaneo-Vietti et al. 2000
Plicatulidae Gray, 1857				
Plicatula plicata (Linnaeus, 1767)	EF, CE	dead coral heads	S	Dudgeon and Morton 1982, Jiang and Zhou 1982
Plicatula gibbosa	EF, CE	hard substrate, seagrass	S	Turgeon et al. 2009
Propeamussiidae Abbott, 1954				
Parvamussium pourtalesianum (Dall, 1886)	EF	muddy bottoms	D	Morton and Thurston 1989
Propeamussium dalli	EF	muddy bottoms	D	Morton and Thurston 1989
Propeamussium sp	EF	muddy bottoms	D	Morton and Thurston 1989
Pteriidae Gray, 1847 (1820)				
Crenatula picta (Gmelin, 1791)	EF, EB	embedded in sponges	S	Reid and Porteous 1980, Tsubaki et al. 2011
Electroma alacorvi (Dillwyn, 1817)	EF, EB	associated with living corals	S	Mohammed and Yassien 2008
Isognomon alatus (Gmelin, 1791)	EF	hard substrate	S	Turgeon et al. 2009
Isognomon bicolor (Adams, 1845)	EF	hard substrate	S	Turgeon et al. 2009
Isognomon ephippium (Linnaeus, 1758)	EF	rocks and pilings	S	Tsi and Ma 1982, Huang et al. 1992,

				1999
Isognomon isognomon (Linnaeus, 1758)	EF, CD	rocks	S	Tsubaki et al. 2011, Ubukata 2003
Isognomon legumen (Gmelin, 1791)	EF, CD	boulders, coral heads, pilings and mussel aggregations	S	Dudgeon and Morton 1982, Huang et al. 1992, Morton 1994, Taylor and Morton 1996, Harper and Morton 1997
Isognomon perna (Linnaeus, 1767)	EF, CD	rocks	S	Tsubaki et al. 2011, Ubukata 2003
Isognomon radiatus (Anton, 1838)	EF, CD	corals and rocks	S	Kobluk and Lysenko 1986
Pinctada fucata (Gould, 1850)	EF	rocks	S	Tsubaki et al. 2011
Pinctada imbricata Röding, 1798	EF	hard substrate, rocks, shells	S	Turgeon et al. 2009
Pinctada longisquamosa (Dunker, 1852)	EF	algae and seagrass, rocks	S	Turgeon et al. 2009, Mikkelsen et al. 2004
Pinctada maculata (Gould, 1850)	EF, CD	rocks	S	Tsubaki et al. 2011, Ubukata 2003
Pinctada margaritifera (Linnaeus, 1758)	EF	hard substrate	S	Turgeon et al. 2009
Pteria brevialata (Dunker, 1872)	EF	gorgonian *Hicksonella princeps*	S	Morton 1995, Leung and Morton 1997, 2000
Pteria colymbus Röding, 1798	EF, EB	gorgonians	S	Turgeon et al. 2009
Pteria hirundo (Linnaeus, 1758)	EF, EB	gorgonians	S	Turgeon et al. 2009
Pteria loveni (Dunker, 1879)	EF, EB	gorgonians	S	Tsubaki et al. 2011
Pteria penguin (Röding, 1798)	EF, EB	gorgonians	S	Dudgeon and Morton 1982, Reid and Brand 1985, Tsubaki et al. 2011
Spondylus ducalis Röding, 1798	EF, CE	dead coral heads	S	Dudgeon and Morton 1982
Spondylus tenuis Schreibers, 1793	EF, CE	hard substrate	S	Turgeon et al. 2009
Vulsella vulsella (Linnaeus, 1758)	EF, EB	embedded within the sponge *Ricinia*	S	Reid and Porteous 1980, Dudgeon and Morton 1982, Tsubaki et al. 2011

CHAPTER 3

Form and function of tentacles in pteriomorphian bivalves

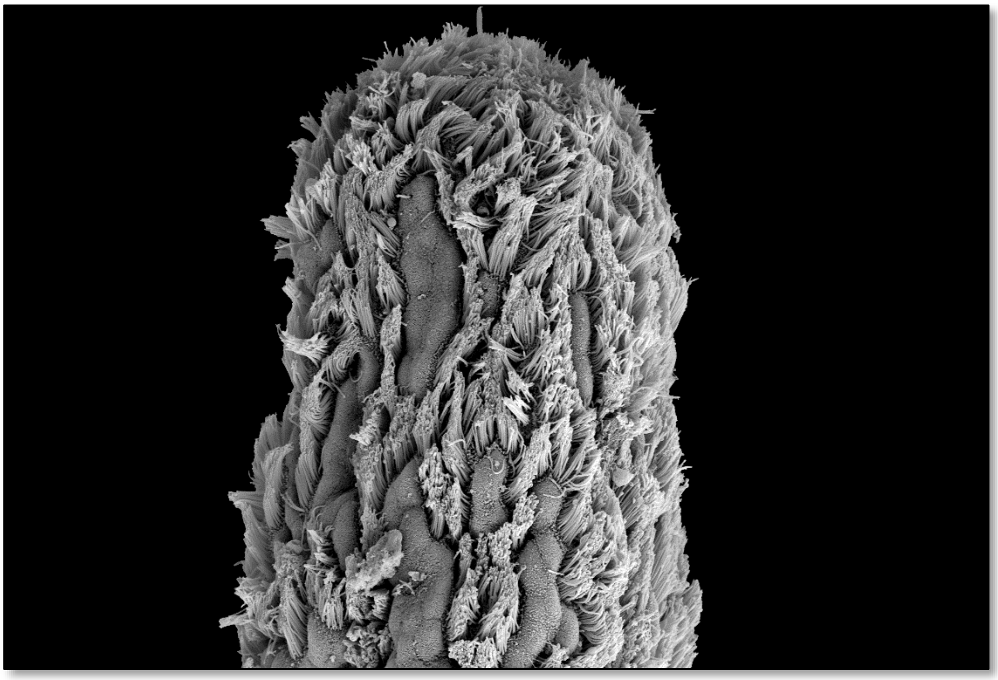

CHAPTER 3

Form and function of tentacles in pteriomorphian bivalves

Abstract

Tentacles are remarkable anatomical structures in benthic invertebrates for their diversity of form and function. In bivalves, tentacular organs are commonly associated with protective, secretory, and sensory roles. However, anatomical details are available for only a few species, rendering the diversity and evolution of bivalve tentacles still obscure. In Pteriomorphia, a clade including oysters, scallops, pearl oysters, and relatives, tentacles are abundant and diverse. We investigated tentacle anatomy in the group to understand variation, infer functions, and investigate patterns in tentacle diversity. Six species from four pteriomorphian families (Ostreidae, Pinnidae, Pteriidae, Spondylidae) were collected and thoroughly investigated under integrative microscopy techniques, including histology, scanning electron microscopy, and confocal microscopy. Tentacles can be divided in middle fold tentacles (MFT) and inner fold tentacles (IFT) according to their position in the mantle margin. While MFT morphology indicates intense secretion of mucosubstances, no evidence for secretory activity was found for IFT. However, both tentacle types have ciliary conditions to promote mucus transportation for cleaning and lubrication. Protective and sensory functions are discussed based on different lines of evidence, including secretion, cilia distribution, musculature, and innervation. Our results support the homology of tentacles in Pteriidae and Ostreidae, considering their morphology, presence of ciliated receptors at the tip of MFT and IFT, and branched innervation pattern of IFT. This is in accordance with recent phylogenetic hypotheses that support the close relationship between both families. In contrast, major structural differences indicate that IFT and MFT are probably not homologous across all pteriomorphians. By applying integrative microscopy, we were able to reveal elements that are essential for the understanding of homology and function when dealing with such plastic phenotypes.

Keywords: anatomy, mantle, microscopy, protective, secretory, sensory.

Introduction

Tentacular organs, including palps, tentacles, and papillae, are among key features in the taxonomy and biology of most invertebrate groups. Tentacles may be generically defined as slender, flexible appendages in animals, usually comprehending contractible extensions of the body (Brusca, Moore, & Shuster, 2016). Despite clearly not homologous among phyla, tentacles have evolved in numerous groups, performing different roles deeply associated with the lifestyle and ecological context of the organism (Audino, Marian, Wanninger, & Lopes, 2015; Schwaha & Wanninger, 2015; Tamberg & Shunatova, 2017). In this context, three main functions can be assigned to tentacular organs, i.e., feeding, protective, and sensory.

In several invertebrate species, tentacles are related to feeding behavior through the collection of food particles by ciliary mechanisms. In sea cucumbers and sipunculans, for example, the oral tentacles are used in nonselective deposit feeding, or water filtering, by means of a combination of hydrostatic pressure, complex musculature, and mucus coating (Cameron & Fankboner, 1984; Pilger, 1982). In most suspension feeders, such as bryozoans, phoronids, entoprocts, and many polychaetes, tentacles are convergently organized in crowns responsible for both water flow and food particle collection by mucociliary transportation (Dubois, Barillé, Cognie, & Beninger, 2005; Nielsen & Riisgård, 1998; Riisgård, 2002; Schwaha & Wanninger, 2015; Tamberg & Shunatova, 2016, 2017).

In cnidarians, tentacle crowns are commonly found around the polyp mouth or at the edge of the umbrella in medusae (Shimizu & Namikawa, 2009). In anemones, corals, and tube anemones, tentacles bear a great diversity of nematocysts and spirocysts, the former used for stinging and capturing prey, while the latter for binding it to the feeding tentacles (Rifkin, 1991; Thorington & Hessinger, 1998). Among cephalopod mollusks, nautilids use a complex adhesive gland system in the digital tentacles to catch and bind the prey (von Byern, Wani, Schwaha, Grunwald, & Cyran, 2012).

Tentacles can also be used in aggressive interactions or protective strategies. In many anemones and antiphatarian corals, specialized tentacles are developed in response to other cnidarian species, frequently resulting in extensive nematocyst discharge (Goldberg, Grange, Taylor, & Zuniga, 1990; Watson & Mariscal, 1983). An alternative form of protection can involve tentacle autotomy, as observed in some medusae, preventing damage caused by tentacle entanglement with prey, predators, or conspecifics (Bickell-Page & Mackie, 1991). In file clams (Limidae), specialized tentacles are thought to be involved in protective responses through secretion of distasteful substances (Gilmour, 1967).

In most mollusks, with the evident exception of cephalopods, tentacles are not directly involved in feeding processes; instead, they participate in sensory roles. In gastropods, for example, cephalic and mantle tentacles are sensory organs associated with the acquisition of olfactory clues involved in a variety of social, feeding, and reproductive behaviors (Croll, 1983; Künz & Haszprunar, 2001).

In many bivalve taxa, multiple tentacles are distributed along the mantle margin, comprising an impressive diversity of form and function (Yonge, 1983). Within Bivalvia, the largest diversity of tentacles is found within the Pteriomorphia. This large clade, which includes oysters, scallops, mussels, and relatives, are characteristic for their numerous tentacles in the mantle margin. In scallops (Pectinidae), long tentacles were thoroughly examined for two species, *Nodipecten nodosus* and *Placopecten magellanicus*, and revealed to be specialized sensory organs (Audino et al., 2015; Moir, 1977). Enormous tentacles are also present in Limidae, possibly performing sensory roles (Gilmour, 1963, 1967). Tentacle morphology and distribution were examined in pearl oysters and relatives (Pterioidea), revealing shared characters, such as tentacle presence on two mantle folds and distribution along the entire mantle margin (Tëmkin, 2006).

Tentacular organs are an interesting system to be explored in the light of multidisciplinary approaches investigating evolutionary novelties and the evolution of complex phenotypes. As illustrated above, tentacles comprise key anatomical features to understand diversification of form and function combined with ecological and taxonomic variation. However, externally they are all superficially similar, which requires a detailed anatomical investigation to detect variation. In this study, we have applied integrative microscopy techniques to investigate the functional anatomy of tentacles in representatives of major pteriomorphian lineages, aiming at understanding variation, inferring functions, and investigating patterns in tentacle diversity.

Material and methods

Taxa sampling

Specimens of pteriomorphians were collected in rocky shores during low tide in São Sebastião's coast (State of São Paulo, Brazil), except for *Pinna carnea* that was collected in sand flats. Mantle margin samples were obtained after dissecting animals previously anesthetized in a 7.5% solution of $MgCl_2$ for 3 h. Samples were obtained for six species: *Isognomon bicolor* (C. B. Adams, 1845), *Pinctada imbricata* Röding, 1798, and *Pteria* *colymbus* (Röding, 1798) (Pteriidae), *Ostrea equestris* Say, 1834 (Ostreidae), *Pinna carnea* Gmelin, 1791 (Pinnidae), and *Spondylus ictericus* Reeve, 1856 (Spondylidae). Limidae and Pectinidae representatives have been previously examined (Audino et al., 2015; Gilmour, 1967) and were not included in our analysis.

For histology and scanning electron microscopy (SEM), fragments of the mantle margin bearing tentacles were fixed for 3 h at 4°C in a modified Karnovsky solution, and stored in cacodylate buffer (Marian, 2012). For confocal laser scanning microscopy (CLSM), samples were fixed in 4% paraformaldehyde for 2 h and stored in 0.1 M phosphate buffer (PB) (Audino & Marian, 2018).

Microscopy techniques

For scanning electron microscopy (SEM), post fixation procedures were conducted as described in Audino et al. (2015). Analysis and image acquisition were performed on a Zeiss DSM 940. For confocal laser scanning microscopy (CLSM), samples were permeabilized in PB containing 2% Triton-X 100 (PBT) overnight. To evidence musculature, samples were incubated in a 1:40 dilution of Alexa Fluor 488 phalloidin (Molecular Probes, USA) in PBT for 24 h at room temperature in the dark. For cilia and nerve investigation, samples were incubated in a 1:400 dilution of alpha-tubulin antibody with Alexa Flour 488 conjugate (Molecular Probes, USA) in the same conditions as described for phalloidin. After three washes of 15 min in PBT, samples were mounted in microscope slides in ProLong Diamond Antifade Mountant with DAPI (Molecular Probes, USA). Analysis was performed on a Zeiss LSM 880 (Zeiss, Germany) and image stacks were digitally merged in the software ZEN lite 2.3 (Zeiss, Germany). In some samples, including *I. bicolor, P. carnea* and *S. ictericus*, intense pigmentation or cilia abundance prevented observation of tentacular nerves.

For histology, samples were completely dehydrated in ethanol and embedded in resin (Leica Historesin Kit, Germany). Serial sections of 4 µm were obtained in a Leica RM2255 microtome (Leica, Germany). To evidence secretory cells, periodic acid-Schiff stain (PAS) and alcian blue (AB) were applied for mucosubstances (Bancroft & Stevens, 1982), and bromophenol blue (BB) was applied for protein aggregates (Pearse, 1985). Other staining methods included hematoxylin and eosin (HE), Gomori trichrome stain, and toluidine blue and basic fuchsin (TF).

Results

In the studied animals, tentacles can be divided in two types according to their location in the mantle margin, i.e., in which mantle fold they are located. Inner fold tentacles (IFT) are marginal projections of the mantle curtain, varying from filiform to flattened structures. Middle fold tentacles (MFT) can be marginal or submarginal projections, usually organized in commarginal rows. Anatomical features of IFT and MFT are described below for each studied species and summarized in Table 1.

Pteria colymbus (Pteriidae)

MFT are marginal structures, filiform and more pigmented (brownish) at the base (Fig. 1A). They display two main sizes – short and long –, short tentacles having ca. 50% of the size of long tentacles (Fig. 1A). MFT are distributed on the entire fold extension, being proportionally larger and more abundant ventrally. Two types of subepithelial secretory cells are abundant in the MFT; one type has granular content with affinity for eosin and BB (Fig. 1B, C), and the other for PAS and AB (Fig. 1D). The tentacle epithelium is covered by tufts of short cilia (Fig. 1E) more densely distributed at the tentacle’s base. A cluster of long cilia is located at the tip of each tentacle (Fig. 1F). MFT are very muscular structures with numerous longitudinal fibers (Fig. 1G) continuous with the mantle radial muscles. Thin fibers also form a delicate transverse musculature (Fig. 1G). MFT are provided with central nerves that branch towards the tip.

IFT are marginal, slightly pigmented, and present along the entire margin. In the anterior and posterior regions, they are filiform, short, appearing as small papillae (Fig. 1A). In contrast, IFT are large and slightly flat in the ventral region, mainly along the inhalant aperture. In this region, some MFT are branched (Fig. 1H), reaching similar length of MFT. Pigmentation is also more intense ventrally, with brown, yellow, and white spots (Fig. 1H). Despite intense secretory activity in the inner mantle fold, gland cells were not identified in the IFT. Each tentacle is densely covered by cilia, both in short not branched (Fig.1I) and large branched tentacles (Fig. 1J, K). Musculature in IFT is similar to MFT, including longitudinal and transverse fibers, although muscle bundles ramify in branched tentacles (Fig. 1L). IFT innervation includes multiple, branching tentacular nerves.

Pinctada imbricata (Pteriidae)

MFT are marginal, filiform, and pigmented at the base (brownish and greyish). They are very similar to those observed in *P. colymbus*, including the presence of short and long tentacles. In the ventral region, MFT are proportionally longer and abundant. Intense secretory activity is observed by subepithelial secretory cells with affinity for PAS and AB (Fig. 2A). Affinity for eosin was also observed in some subepithelial cells, but not for BB. All MFT have a cluster of long cilia at the tips (Fig. 2B), while shorter cilia are sparsely distributed along the tentacle. Longitudinal musculature run along the tentacles (Fig. 2C), but transverse fibers were not observed.

IFT are marginal and slightly pigmented along the entire margin, including white spots. They are larger ventrally, especially along the inhalant aperture, where most of them are branched and slightly flat (Fig. 2D). In general, tissue organization of IFT is similar to the that of the inner fold, except for the absence of secretory cells in the former (Fig. 2E). Tufts of cilia are sparsely distributed on their surface (Fig. 2F, G), and a cilia cluster is present at the tip of each branch (Fig. 2H). Musculature comprises few transverse fibers and more longitudinal muscles, which ramify in branched tentacles. Innervation exhibits an intense branching pattern, even in non-branched tentacles, from the base to the tips. Small nerves directly reach the ciliary tufts, mainly those at the tips where numerous ciliary roots and nerves seems connected (Fig. 2H).

Isognomon bicolor (Pteriidae)

MFT are marginal, filiform, and pigmentation can vary from light to dark grey. Along the entire margin, all tentacles have similar size, although they are proportionally longer and more abundant in the ventral region. Intense secretory activity is present, including subepithelial secretory cells with affinity for eosin and toluidine blue (large granules), but not for PAS or alcian blue (Fig. 3A-C). Epithelial secretory cells are evidenced by TF and AB (Fig. 3C). Tentacles are densely covered by cilia at the base, but tufts are largely scarce on the inner surface (i.e., the surface opposed to the valve) (Fig. 3D). A cluster of cilia is located at the tip (Fig. 3E). Musculature includes transverse and longitudinal fibers, the latter being more developed than the former (Fig. 3F). Innervation was not observed.

IFT are marginal, slightly flat, and dark pigmented, although pigmentation is less intense than in the inner fold. They are present along the entire margin, being longer ventrally and not branched. Secretory cells are lacking, and cilia cover the surface of the tentacles, being more concentrated distally (Fig. 3G). Musculature includes longitudinal and transverse fibers. A branched innervation seems present, with nerves reaching the long ciliary roots at the tip (Fig. 3H).

Ostrea equestris (Ostreidae)

MFT are submarginal, filiform, and pigmented with brownish to grayish spots. Tentacle position on the inner surface of the fold (i.e., the surface of the fold opposed to the valve) includes distal and proximal commarginal rows. Shorter tentacles are located on the distal row, near to the edge, while longer tentacles are proximal. In the ventral region, MFT are proportionally larger and more abundant, particularly along the inhalant aperture. Short and long tentacles show intense secretory activity, as indicated by subepithelial and epithelial secretory cells. Two types of subepithelial secretory cells are present. Cells with more sparsely distributed granules were stained in dark blue with toluidine blue (Fig. 4A) and had affinity for BB (Fig. 4C); those with more densely distributed granules stained in light blue with toluidine blue (Fig. 4A) and had a strong affinity for eosin (Fig. 4B). Weak affinity for PAS and AB was observed. MFT have abundant tufts of cilia on the epithelium and a dense cluster at the tip (Fig. 4D, F). MFT are very muscular, mainly formed by longitudinal fibers (Fig. 4E). Tentacle innervation is provided by branching nerves from the base reaching the ciliary rootlets, which are more evident at the apical tufts (Fig. 4F).

IFT are marginal (Fig. 4G), filiform, usually lightly pigmented and have a similar size compared to MFT. Along the margin, IFT are larger ventrally and not branched. Secretory cells were not detected. Cilia on tentacle surface are distributed in numerous longitudinal rows (Fig. 4H, I), forming a dense cluster at the tip (Fig. 4J). Tentacle musculature is mainly formed by longitudinal fibers, with no evidence of transverse fibers (Fig. 4K). Innervation includes multiple branching nerves from the base to the tip.

Pinna carnea (Pinnidae)

Only IFT are present. They are marginal, slightly flat, and pigmentation includes tiny yellow, brown, and whitish spots (Fig. 5A). MFT occurs only in the posterior region, being larger along the inhalant and exhalant apertures (Fig. 5A). Secretory cells were not detected in sections, although droplets of possible mucosubstances were observed interspersed with the short cilia that cover the entire tentacle surface (Fig. 5B, C). Musculature is formed by longitudinal and transverse fibers (Fig. 5D). Innervation was not observed.

Spondylus icterícus (Spondylidae)

MFT are submarginal, filiform, and slightly pigmented with yellow and whitish spots (Fig. 6A). Brown and white pigmentation are more intense on the outer surface, i.e., the side that faces the valve. MFT are located on the inner surface of the fold, occupying proximal to distal positions (Fig. 6B). Some tentacles are replaced by eyes at the tip of eyestalks (Fig. 6A). Extremely long tentacles are also present in a proximal position on the fold, being much longer than the surrounding tentacles (Fig. 6A). MFT are uniformly distributed on the entire margin, with not evident difference in density or size according to the body regions. The epithelium contains numerous secretory cells stained by PAS and alcian blue (Fig. 6C), with low affinity for TF and none for BB or eosin. Long tentacles show sparse tufts of cilia on the epithelium, while the remaining tentacles have cilia organized in longitudinal rows (Fig. 6D, E). Droplets of mucosubstances were observed on the cilia rows, being secreted by the adjacent glandular epithelium (Fig. 6F). Musculature and innervation could not be investigated by confocal microscopy, but histological sections indicate abundance of longitudinal muscles, transverse fibers, and a central tentacular nerve.

IFT are very small marginal projections, similar to papillae (Fig. 6A). They are uniformly distributed along the entire margin, being unpigmented and translucid. Secretory activity was not detected. Short cilia cover all tentacle surface while long cilia are present in sparsely distributed tufts (Fig. 6G, H). Despite their small size, IFT are provided with longitudinal muscles and tiny transverse fibers (Fig. 6I). Innervation was not observed.

Discussion

Comparative anatomy of bivalve tentacles

Although always occurring in the mantle margin, tentacle location greatly varies among bivalves. Tentacles can occur on the middle mantle fold, inner mantle fold, or even on both (Yonge, 1983). All species studied herein have tentacles on both mantle folds, except for *Pinna carnea*, which has tentacles only on the inner fold. In addition, tentacles can be distributed along the entire mantle margin or be restricted to some regions. The first condition is observed in most studied species, with tentacle distribution following the mantle extension. Nevertheless, tentacles are much abundant and larger ventrally in the case of pteriid and ostreid species. The second condition is illustrated by *Pinna carnea*, with tentacles restricted to the posterior region, bordering the inhalant and exhalant apertures (Yonge, 1953).

In infaunal and semi-infaunal bivalves, IFT are common on the siphons as sensory and protective structures distributed close to their apertures (Yonge, 1983). A great diversity in shape and number of siphonal tentacles was described for infaunal bivalves from the families Veneridae, Donacidae, and Tellinidae, which have multiple branched tentacles on the inhalant siphon (Fishelson, 2000; Narchi, 1972; Piffer, Arruda, & Passos, 2011; André F Sartori & Domaneschi, 2005; André Fernando Sartori, Printrakoon, Mikkelsen, & Bieler, 2008; Vitonis, Zaniratto, Machado, & Passos, 2012). Despite the absence of a siphon, a similar condition is present in *Pteria colymbus* and *Pinctada imbricata*, because both species have developed, branched tentacles restricted to the ventral, inhalant region. Carnivorous bivalves from the order Anomalodesmata also bear siphonal tentacles, (e.g., *Cardiomya cleryana*; (Machado, Morton, & Passos, 2017)). More rarely, tentacles can also occur in the anterior portion of the pedal opening, as observed in Cyammiidae (Passos & Machado, 2014).

In the Galeommatidae, a bivalve family of commensal or free-living small bivalves, tentacles show a high degree of specialization. In many species, when the mantle is fully extended, the shell is almost completely covered by the middle fold (Lützen & Nielsen, 2005; Morton, 1973). In the exposed surface of this fold, numerous tentacles and papillae can be present, their number, size, pigmentation, and tip morphology showing considerable variation (Lützen & Nielsen, 2005).

Among the Pteriomorphia, tentacles have been studied in detail only for a few species, although general observations were described for many groups (Waller, 1975). In file clams (Limidae), MFT pigmentation ranges from white translucid to intense red. In these bivalves, they vary from short to extremely long structures, sometimes annulated, and always restricted to the middle fold, where they are usually densely distributed (Allen, 2004; Gilmour, 1963, 1967; Mikkelsen & Bieler, 2003). In scallops (Pectinidae) and thorny oysters (Spondylidae), the middle mantle fold bears tentacles formed on the inner surface (i.e., the surface of the fold opposed to the valve), also including very long tentacles (Audino et al., 2015; Dakin, 1928b; Moir, 1977). Tentacles on the inner mantle fold are also common in scallops; given that they are located along the margin, they are named “guard tentacles” of the mantle cavity aperture (Audino et al., 2015; Dakin, 1909; Drew, 1906). Although previous studies have not recorded IFT in Spondylidae (Dakin, 1928a), our data for *Spondylus ictericus* show robust evidence for their presence. Possibly due to their extremely small size or preservation artifacts, they have passed unnoticed in previous investigations.

Pearl oysters and relatives (Pterioidea) are another pteriomorphian lineage with numerous tentacles on both middle and inner mantle folds, with also variation in size and pigmentation (Tëmkin, 2006). Our data for the pteriids *Isognomon bicolor*, *Pinctada imbricata*, and *Pteria colymbus* are in accordance with the general pattern of tentacle distribution in the middle and inner folds, and also with the presence of branched tentacles in the latter two genera. Interestingly, our results for *Ostrea equestris* show great similarity to Pteriidae in respect to general increase of IFT size and abundance towards the ventral region (inhalant aperture), as also observed in *Crassostrea* spp. (Amaral & Simone, 2014). In contrast to pteriids, MFT are submarginal in *Crassostrea* and *Ostrea*, with proximal (long) and distal (short) tentacles (Amaral & Simone, 2014; present study).

Tentacle functions and anatomical patterns

Tentacle organs are related to food manipulation in most marine invertebrate groups, mainly those depending on seawater filtration to obtain food particles. Alternatively, in the case of bivalves, other roles are played by the them, including defense against predators and sensory functions (Yonge, 1983). The increase of tentacular size towards the inhalant and exhalant regions is a common trend for many bivalve groups, especially for those with siphons (Sartori et al., 2008). Even for bivalves with free mantle margins (i.e., devoid of siphons), the position of the inner mantle fold of inhalant and exhalant regions may be muscularly adjusted to conform/protect the mantle cavity (Owen & McCrae, 1979). Tentacles are supposed to prevent the entrance of large particles into the mantle cavity, especially in turbulent environments, where large particles can disturb the water flow through the gills and obstruct the mantle cavity. Our results show abundant musculature in the IFT, regardless of their size or of the presence of lateral branches. IFT muscles should allow for fine adjustments in tentacle position, possibly protecting the mantle cavity apertures. In contrast to previous hypotheses on tentacles as non-specialized extensions of the mantle margin (Waller, 1975), our data is in accordance with studies on Pterioidea arguing for the structural and functional complexity of those structures (Tëmkin, 2006). As described herein, elongated IFT at the inhalant region are observed in Ostreidae, Pteriidae, and Pinnidae, as well as in most siphoned bivalves. A similar pattern is also observed in many mussel species (Mytilidae), where the inhalant aperture is protected by lobules on the inner fold (Audino et al. in prep).

In particular cases, tentacles can also play defensive roles against potential predators. For example, *Limaria hians* (former *Lima hians*, Limidae) can autotomize parts of its tentacles, or even the entire organ, with subsequent release of distasteful mucus to avoid predation (Gilmour, 1963, 1967). In the phylogenetically distant Galeommatidae, anatomical data on *Galeomma takii* also suggest autotomy and secretion as similar defensive mechanisms. When stimulated, papillae on the middle fold, which almost completely cover the shell, are capable of autotomy, secreting a noxious substance (Morton, 1973).

Even though defensive tentacles were not observed in the investigated species, secretory activity is largely present. Our results show that secretion of mucosubstances is an important role performed exclusively by MFT, including neutral (PAS-positive) and acidic polysaccharides (alcian blue-positive) and basic glycoproteins (bromophenol blue-positive), secreted by subepithelial and epithelial secretory cells. Similar results were obtained for other Pteriidae, with acidophilic secretory cells and neutral glycoproteins secretion in the MFT of *Pinctada margaritifera* (Jabbour-Zahab, Chagot, Blanc, & Grizel, 1992). The diversity and production of mucous by the tentacles are expected to keep these organs constantly clean by the agglutination of undesirable particles or even small organisms, propelling them for rejection (Beninger & St-Jean, 1997; Prezant, 1990). Another evidence reinforcing this hypothesis is the short, densely distributed cilia covering the surface of MFT in the studied species, which is likely associated with mucociliary transportation (Sleigh, 1989; Sleigh, Blake, & Liron, 1988).

Secretory activity in MFT was also shown for *Nodipecten nodosus* (Audino et al., 2015), including acidic and neutral mucins, which shows great similarity to our data for *Spondylus ictericus*. In the case of *N. nodosus*, cilia are densely distributed on the tentacle surface (Audino et al., 2015). In contrast, *S. ictericus* exhibits longitudinal rows of cilia along the MFT that are supposed to promote mucus propulsion, which is supported by secretory evidence in adjacent areas.

Despite intense secretory activity in the inner mantle fold of many bivalve species (Audino & Marian, 2018; Jabbour-Zahab et al., 1992; Richardson, Runham, & Crisp, 1981), IFT show little or no evidence of secretory cells in the species investigated herein. Nevertheless, our results indicate these organs should be able to propel the mucus secreted proximally in the fold, possibly helping to lubricate the mantle margin. Droplets of possible mucosubstance observed in the tentacles of *P. carnea* and cilia distribution in the pteriids and in *O. equestris* species support this hypothesis. Moreover, ciliary rows observed in *O. equestris* and ciliary patches in the pteriids match the conditions to provide mucociliary transportation of mucus rafts required for cleansing and lubrication (Sleigh, 1989).

Bivalve tentacles are also regarded as sensory organs due to putative mechano- and chemoreceptors organized in ciliary cells. Nevertheless, both functional types can hardly be distinguished based exclusively on morphological criteria (Owen & McCrae, 1979). Scallops and limids are, by far, the most investigated examples of bivalve having specialized sensory tentacles. In *Placopecten magellanicus* and *Nodipecten nodosus*, ciliary tufts, supposedly acting as mechanoreceptors, are distributed on papillae at the distal portion of long, exploratory tentacles (Audino et al., 2015; Moir, 1977). Ciliary papillae were not observed on the MFT of *Spondylus ictericus*, a representative of a phylogenetically close family to Pectinidae. However, ciliary tufts are regularly distributed on the surface of the distal portion of long tentacles, and they are most likely related to sensory perception.

Sensory ciliated receptors are also common at the tip of siphons and on siphonal tentacles, as observed in Donacidae and Tellinidae (Hodgson & Fielden, 1984; Vitonis et al., 2012), and on papillae along the middle fold, as in *Mysella charcoti* (Lasaeidae) (Passos, Domaneschi, & Sartori, 2005). In the present study, a dense ciliary cluster was consistently observed at the tip of MFT in *Isognomon bicolor*, *Ostrea equestris*, *Pinctada imbricata*, and *Pteria colymbus*. These results suggest the presence of putative sensory receptors at the tip of MFT as a shared pattern between Pteriidae and Ostreidae.

Ciliated receptors were also observed at the tip of IFT in the pteriid and ostreid species studied herein, which suggests that these structures play important sensory roles in addition to the protection of the mantle cavity aperture. The extensive innervation associated with ciliated receptors supports this hypothesis. However, lack of data for other species prevent further conclusions on innervation patterns. In the pteriid and ostreid species studied, MFT innervation is characterized by a branching pattern throughout the tentacle, resulting in numerous small nerves running along the organ and reaching the ciliated receptors. This suggests another common pattern shared by Pteriidae and Ostreidae, which is distinct, for example, from tentacle innervation in the pectinid *N. nodosus*, in which a single central nerve emits very tiny projections to the epithelium (Audino et al., 2015).

Although the evolutionary origin and history of tentacles during Pteriomorphia radiation are still speculative, our results support the homology of MFT and IFT in Pteriidae and Ostreidae, considering their ventral morphology, presence of ciliary clusters at the tip, and branched innervation pattern. Even though information for additional taxa would be important to support such a conclusion, our results are in accordance with phylogenetic hypotheses that recover the sister relationship between Ostreoidea and Pterioidea (Tëmkin, 2010; Lemer et al., 2016). In contrast, profound anatomical differences, such as tentacle innervation, cilia organization, and distribution in the mantle margin, indicate IFT and MFT are not homologous across Pteriomorphia. Given that tentacle diversification may be associated with similar selective pressures, as suggested by the recurrent evolution of protective IFT in numerous bivalve lineages (Sartori et al., 2008; Vitonis et al., 2012), evolutionary convergence should also be considered when exploring tentacle evolution in Pteriomorphia.

Just like most benthic invertebrates, bivalves have evolved numerous types of tentacles associated with diverse functions. The detailed anatomical analysis of pallial tentacles in selected representatives of pteriomorphian bivalves revealed possible shared characters for the clades Pteriidae and Ostreidae, as well as the first anatomical description of tentacles in Spondylidae and Pinnidae. In conclusion, by applying integrative microscopy to study the structure and infer the functional morphology of such diverse organs, we were able to reveal elements that are essential for the understanding of homology when dealing with such plastic phenotypes.

Acknowledgements

The authors acknowledge funding provided by the grant 2015/09519-4, São Paulo Research Foundation (FAPESP). This study was financed in part by the Coordenação de Aperfeiçoamento de Pessoal de Nível Superior - Brasil (CAPES) - Finance Code 001. This study is part of the first author’s Doctorate’s thesis through the Graduate Program in Zoology of the Institute of Biosciences (University of São Paulo). The authors thank the Center for Marine Biology (CEBIMar–USP), the technical staff, and Prof. Alvaro Migotto for the invaluable support in the collection and analysis of live specimens used in this study. The authors also thank the Laboratory of Cell Biology (IB-USP) for providing the facilities for confocal microscopy analysis and technical assistance. This is a contribution of NP-BioMar (Research Center for Marine Biodiversity – USP).

References

Allen, J. A. (2004). The Recent species of the genera *Limatula* and *Limea* (Bivalvia, Limacea) present in the Atlantic, with particular reference to those in deep water. *Journal of Natural History, 38,* 2591–2653.

Amaral, V. S. D., & Simone, L. R. L. (2014). Revision of genus Crassostrea (Bivalvia: Ostreidae) of Brazil. *Journal of the Marine Biological Association of the United Kingdom, 94,* 811–836.

Audino, & Marian, J. E. A. R. (2018). Comparative and functional anatomy of the mantle margin in ark clams and their relatives (Bivalvia: Arcoidea) supports association between morphology and life habits. *Journal of Zoology, 305,* 149–162.

Audino, Marian, J. E. A. R., Wanninger, A., & Lopes, S. G. B. C. (2015). Anatomy of the pallial tentacular organs of the scallop *Nodipecten nodosus* (Linnaeus, 1758) (Bivalvia: Pectinidae). *Zoologischer Anzeiger - A Journal of Comparative Zoology, 258,* 39–46.

Bancroft, J., & Stevens, A. (1982). *Theory and Practice of Histological Techniques*. New York, NY: Churchill Livingstone.

Beninger, P. G., & St-Jean, S. D. (1997). The role of mucus in particle processing by suspension-feeding marine bivalves: unifying principles. *Marine Biology, 129,* 389–397.

Bickell-Page, L. R., & Mackie, G. O. (1991). Tentacle autotomy in the hydromedusa *Aglantha digitale* (Cnidaria): an ultrastructural and neurophysiological analysis. *Philosophical Transactions of the Royal Society of London. Series B: Biological Sciences, 331*, 155–170.

Brusca, R. C., Moore, W., & Shuster, R. M. (2016). *Invertebrates* (3rd ed.). Sunderland, MA: Sinauer Associates.

Cameron, J. L., & Fankboner, P. V. (1984). Tentacle structure and feeding processes in life stages of the commercial sea cucumber *Parastichopus californicus* (Stimpson). *Journal of Experimental Marine Biology and Ecology*, *81*, 193–209.

Croll, R. P. (1983). Gastropod chemoreception. *Biological Reviews, 58*, 293–319.

Dakin, W. J. (1909). *Pecten*. London: Williams & Norgate.

Dakin, W. J. (1928a). The anatomy and phylogeny of *Spondylus*, with a particular reference to the lamellibranch nervous system. *Proceedings of the Royal Society B: Biological Sciences*, *103*, 337–354.

Dakin, W. J. (1928b). The eyes of *Pecten*, *Spondylus*, *Amussium* and allied lamellibranchs, with a short discussion on their evolution. *Proceedings of the Royal Society B: Biological Sciences, 103*, 355–365.

Drew, G. A. (1906). *The habits anatomy, and embryology of the giant scallop. (Pecten tenuicostatus, Mighels)*. Orono: University of Maine Studies.

Dubois, S., Barillé, L., Cognie, B., & Beninger, P. (2005). Particle capture and processing mechanisms in *Sabellaria alveolata* (Polychaeta: Sabellariidae). *Marine Ecology Progress Series*, *301*, 159–171.

Fishelson, L. (2000). Comparative morphology and cytology of siphons and siphonal sensory organs in selected bivalve molluscs. *Marine Biology*, *137*, 497–509.

Gilmour, T. H. J. (1963). A note on the tentacles of *Lima hians* (Gmelin)(Bivalvia). *Journal of Molluscan Studies*, *35*, 82–85.

Gilmour, T. H. J. (1967). The defensive adaptations of *Lima hians* (Mollusca, Bivalvia). *Journal of the Marine Biological Association of the United Kingdom*, *47*, 209–221.

Goldberg, W. M., Grange, K. R., Taylor, G. T., & Zuniga, A. L. (1990). The structure of sweeper tentacles in the black coral *Antipathes fiordensis*. *The Biological Bulletin*, *179,* 96–104.

Hodgson, A. N., & Fielden, L. J. (1984). The structure and distribution of peripheral ciliated receptors in the bivalve molluscs *Donax serra* and *D. sordidus*. *Journal of Molluscan Studies, 50*, 104–112.

Jabbour-Zahab, R., Chagot, D., Blanc, F., & Grizel, H. (1992). Mantle histology, histochemistry and ultrastructure of the pearl oyster *Pinctada margaritifera* (L.). *Aquatic Living Resources, 5*, 287–298.

Künz, E., & Haszprunar, G. (2001). Comparative ultrastructure of gastropod cephalic tentacles: Patellogastropoda, Neritaemorphi and Vetigastropoda. *Zoologischer Anzeiger - A Journal of Comparative Zoology*, *240*, 137–165.

Lützen, J., & Nielsen, C. (2005). Galeommatid bivalves from Phuket, Thailand. *Zoological Journal of the Linnean Society*, *144*, 261–308.

Machado, F. M., Morton, B., & Passos, F. D. (2017). Functional morphology of *Cardiomya cleryana* (d'Orbigny, 1842) (Bivalvia: Anomalodesmata: Cuspidariidae) from Brazilian waters: new insights into the lifestyle of carnivorous bivalves. *Journal of the Marine Biological Association of the United Kingdom, 97*, 447–462.

Marian, J. E. A. R. (2012). Spermatophoric reaction reappraised: Novel insights into the functioning of the loliginid spermatophore based on *Doryteuthis plei* (Mollusca: Cephalopoda). *Journal of Morphology*, *273*, 248–278.

Mikkelsen, P. M., & Bieler, R. (2003). Systematic revision of the western Atlantic file clams, *Lima* and *Ctenoides* (Bivalvia: Limoida: Limidae). *Invertebrate Systematics*, *17*, 667.

Moir, A. J. G. (1977). Ultrastructural studies on the ciliated receptors of the long tentacles of the giant scallop, *Placopecten magellanicus* (Gmelin). *Cell and Tissue Research*, *184*, 367–380.

Morton, B. (1973). The biology and functional morphology of *Galeomma* (*Paralepida*) *takii* (Bivalvia: Leptonacea). *Journal of Zoology, 169*, 133–150.

Narchi, W. (1972). Comparative study of the functional morphology of *Anomalocardia brasiliana* (Gmelin, 1791) and *Tivela mactroides* (Born, 1778) (Bivalvia, Veneridae). *Bulletin of Marine Science*, *22*, 643–670.

Nielsen, C., & Riisgård, H. (1998). Tentacle structure and filter-feeding in *Crisia eburnea* and other cyclostomatous bryozoans, with a review of upstream-collecting mechanisms. *Marine Ecology Progress Series, 168*, 163–186.

Owen, G., & McCrae, J. M. (1979). Sensory cell/gland cell complexes associated with the pallial tentacles of the bivalve *Lima hians* (Gmelin), with a note on specialized cilia on the pallial curtains. *Philosophical Transactions of the Royal Society B: Biological Sciences, 287*, 45–62.

Passos, F. D., Domaneschi, O., & Sartori, A. F. (2005). Biology and functional morphology of the pallial organs of the Antarctic bivalve *Mysella charcoti* (Lamy, 1906) (Galeommatoidea: Lasaeidae). *Polar Biology, 28*, 372–380.

Passos, F. D., & Machado, F. M. (2014). A new species of *Cyamiocardium* Soot-Ryen, 1951 from shallow waters off Brazil, with a discussion on the anatomical characters of the cyamiidae (Bivalvia: Cyamioidea). *American Malacological Bulletin*, *32*, 122–131.

Pearse, A. G. E. (1985). *Histochemistry, theoretical and applied* (4th ed., Vol. 2). London: Churchill Livingstone.

Piffer, P. R., Arruda, E. P. de, & Passos, F. D. (2011). The biology and functional morphology of *Macoma biota* (Bivalvia: Tellinidae: Macominae). *Zoologia (Curitiba, Impresso), 28*, 321–333.

Pilger, J. F. (1982). Ultrastructure of the tentacles of *Themiste lageniformis* (Sipuncula). *Zoomorphology*, *100*, 143–156.

Prezant, R. S. (1990). Form, function and phylogeny of bivalve mucins. In *The Bivalvia—The Proceedings of a Memorial Symposium in Honour of Sir Charles Maurice Yonge* (pp. 83–95). Hong Kong: Hong Kong University Press.

Richardson, C. A., Runham, N. W., & Crisp, D. J. (1981). A histological and ultrastructural study of the cells of the mantle edge of a marine bivalve, *Cerastoderma edule*. *Tissue and Cell*, *13*, 715–730.

Rifkin, J. F. (1991). A study of the spirocytes from the Ceriantharia and Actiniaria (Cnidaria: Anthozoa). *Cell and Tissue Research*, *266*, 365–373.

Riisgård, H. U. (2002). Methods of ciliary filter feeding in adult *Phoronis muelleri* (phylum Phoronida) and in its free-swimming actinotroch larva. *Marine Biology*, *141*, 75–87.

Sartori, André F, & Domaneschi, O. (2005). The functional morphology of the antarctic bivalve *Thracia meridionalis* Smith, 1885 (Anomalodesmata: Thraciidae). *Journal of Molluscan Studies*, *71*, 199–210.

Sartori, André Fernando, Printrakoon, C., Mikkelsen, P. M., & Bieler, R. (2008). Siphonal structure in the Veneridae (Bivalvia: Heterodonta) with an assessment of its phylogenetic application and a review of venerids of the Gulf of Thailand. *The Raffles Bulletin of Zoology*, *18*, 103–125.

Schwaha, T. F., & Wanninger, A. (2015). The serotonin-lir nervous system of the Bryozoa (Lophotrochozoa): a general pattern in the Gymnolaemata and implications for lophophore evolution of the phylum. *BMC Evolutionary Biology, 15*. doi:10.1186/s12862-015-0508-9

Shimizu, H., & Namikawa, H. (2009). The body plan of the cnidarian medusa: distinct differences in positional origins of polyp tentacles and medusa tentacles. *Evolution & Development*, *11*, 619–621.

Sleigh, M. A. (1989). Adaptations of ciliary systems for the propulsion of water and mucus. *Comparative Biochemistry and Physiology Part A: Physiology*, *94*, 359–364.

Sleigh, M. A., Blake, J. R., & Liron, N. (1988). The propulsion of mucus by cilia. *American Review of Respiratory Disease*, *137*, 726–741.

Tamberg, Y., & Shunatova, N. (2016). Feeding behavior in freshwater bryozoans: function, form, and flow. *Invertebrate Biology*, *135*, 138–149.

Tamberg, Y., & Shunatova, N. (2017). Tentacle structure in freshwater bryozoans. *Journal of Morphology*, *278*, 718–733.

Tëmkin, I. (2006). Morphological perspective on the classification and evolution of Recent Pterioidea (Mollusca: Bivalvia). *Zoological Journal of the Linnean Society*, *148*, 253–312.

Thorington, G. U., & Hessinger, D. A. (1998). Efferent mechanisms of discharging cnidae: II. A nematocyst release response in the sea anemone tentacle. *The Biological Bulletin*, *195*, 145–155.

Vitonis, J. E. V. V., Zaniratto, C. P., Machado, F. M., & Passos, F. D. (2012). Comparative studies on the histology and ultrastructure of the siphons of two species of Tellinidae (Mollusca: Bivalvia) from Brazil. *Zoologia (Curitiba)*, *29*, 219–226.

von Byern, J., Wani, R., Schwaha, T., Grunwald, I., & Cyran, N. (2012). Old and sticky—adhesive mechanisms in the living fossil *Nautilus pompilius* (Mollusca, Cephalopoda). *Zoology*, *115*, 1–11.

Waller, T. R. (1975). The behavior and tentacle morphology of pteriomorphian bivalves: a motion-picture study. *Bulletin of the American Malacological Union*, 7–13.

Watson, G. M., & Mariscal, R. N. (1983). The development of a sea anemone tentacle specialized for aggression: morphogenesis and regression of the catch tentacle of *Haliplanella luciae* (Cnidaria, Anthozoa). *The Biological Bulletin*, *164*, 506–517.

Yonge, C. M. (1953). Form and Habit in *Pinna carnea* Gmelin. *Philosophical Transactions of the Royal Society B: Biological Sciences*, *237*, 335–374.

Yonge, C. M. (1983). Symmetries and the role of the mantle margins in the bivalve Mollusca. *Malacological Review*, *16*, 1–10.

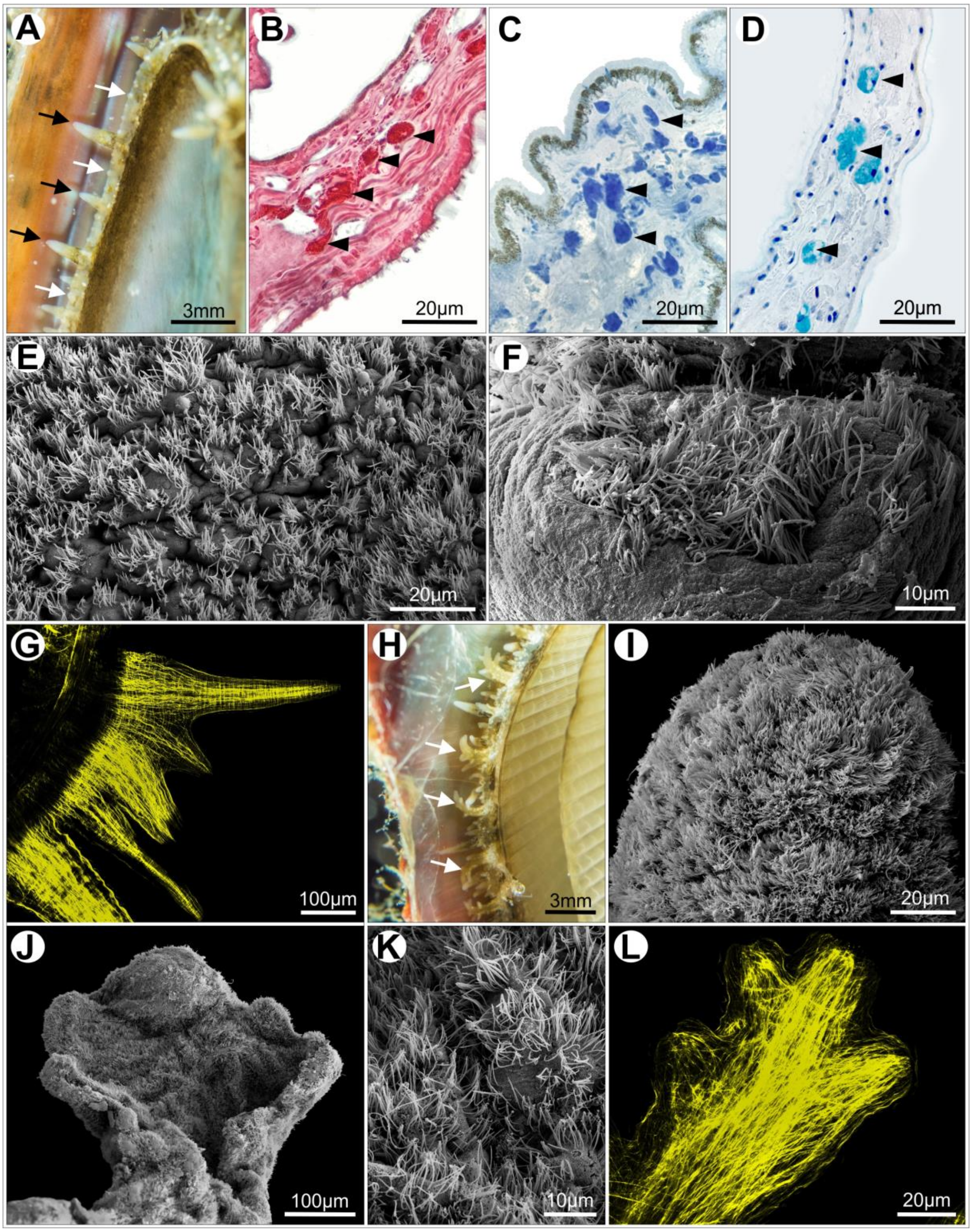

Figure 1. Mantle tentacles of *Pteria colymbus* (Pteriidae). Middle fold tentacles (MFT) in B-G and inner fold tentacles (IFT) in H-L. **A.** MFT (white arrows) and IFT (black arrows) in the posterodorsal region. **B.** Sagittal section of a tentacle showing subepithelial secretory cells with granular content (arrowheads); HE. **C.** Same as B, but stained with BB, evidencing protein aggregates (arrowheads). **D.** Same as B, but stained with AB, evidencing acidic mucosubstances. **E.** Ciliary tufts covering the tentacle surface at its base; scanning electron micrograph (SEM). **F.** Cilia cluster at the tip of the tentacle; SEM. **G.** Tentacle musculature with abundant longitudinal fibers; confocal micrograph (CLSM). **H.** Tentacles on the inner fold; some of them are branched (white arrows), ventral view. **I.** Dense cilia distribution on short, not-branched tentacles; SEM. **J.** Branched tentacle with typical flattened shape; SEM. **K.** Detail from the previous image, showing cilia distribution; SEM. **L.** Musculature in a branched tentacle, including branching fibers; CLSM.

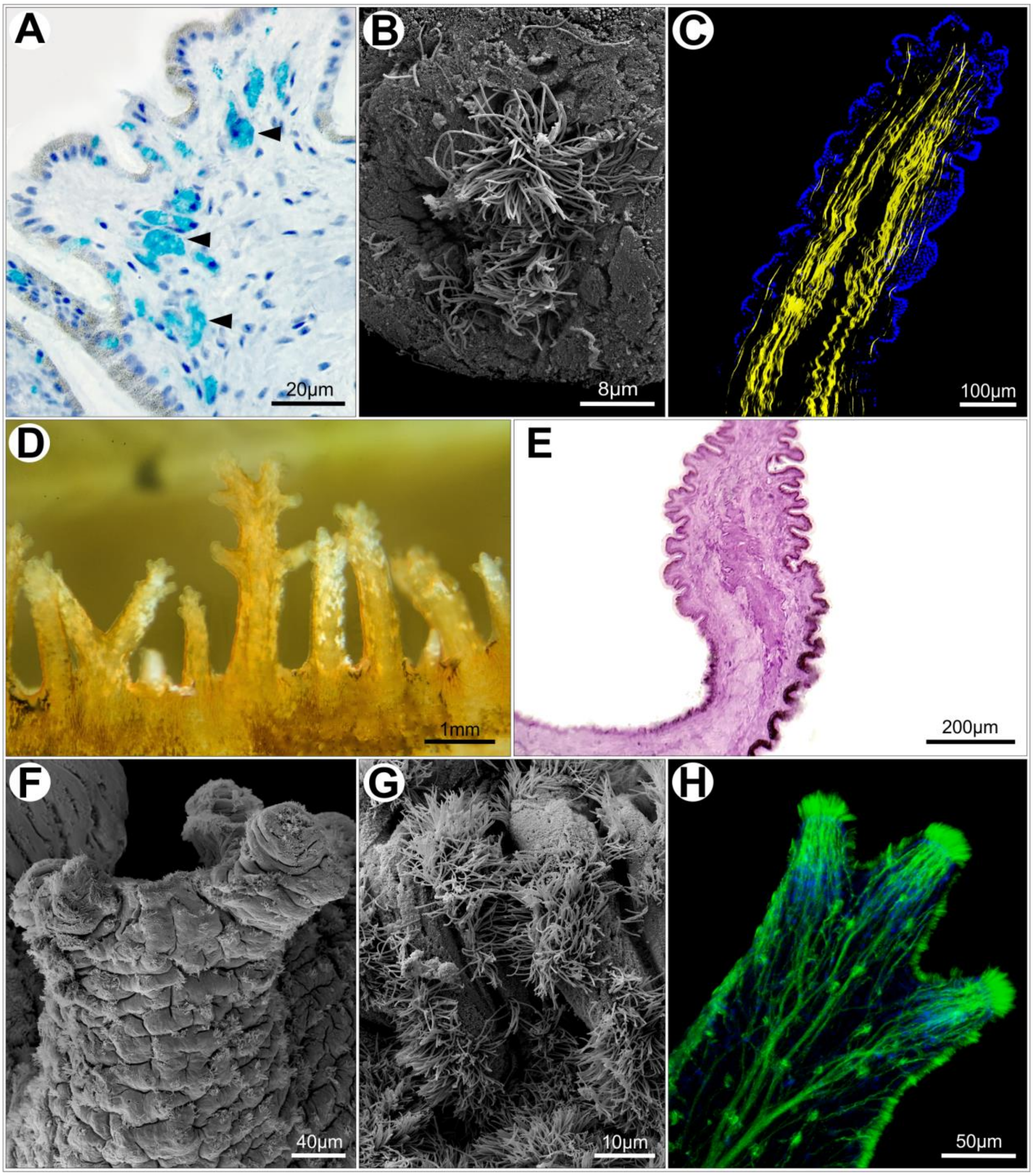

Figure 2. Mantle tentacles of *Pinctada imbricata* (Pteriidae). Middle fold tentacles in A-C and inner fold tentacles in D-H. **A.** Sagittal section showing subepithelial gland cells with acidic mucosubstances (arrowheads); AB. **B.** Cilia cluster at the tip of the tentacle; scanning electron micrograph (SEM). **C**. Muscle fibers (yellow) along the tentacle, nuclei in blue; confocal micrograph (CLSM). **D.** Branched tentacles on the ventral region. **E.** Sagittal section of the tentacle, showing the absence of secretory content; PAS. **F.** Branched tentacle with sparse tufts of cilia; SEM. **G.** Detail of the previous image; SEM. **H.** Branched tentacle innervation (in green) with branching nerves reaching the ciliary rootlets at the tip of the branches; nuclei in blue; CLSM.

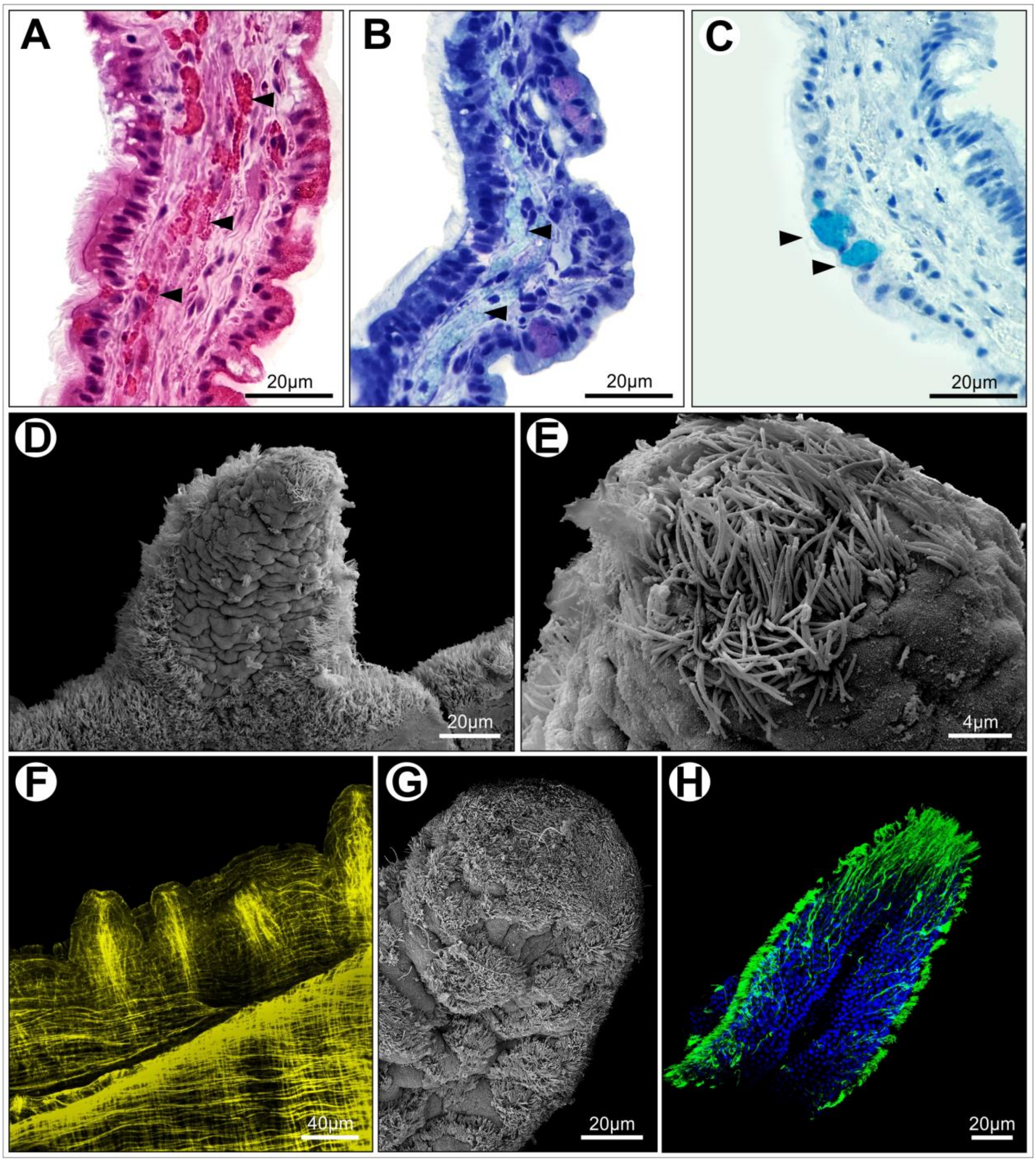

Figure 3. Mantle tentacles of *Isognomon bicolor* (Pteriidae). Middle fold tentacles in A-F and inner fold tentacles in G-H. **A.** Sagittal section showing subepithelial secretory cells with granular content (arrowheads); HE. **B.** Same as A, but showing subepithelial secretory cells with granular content stained in light blue (arrowhead), and epithelial secretory cells stained in pink (arrows); TF. **C.** Sagittal section showing epithelial or part subepithelial secretory cells with acidic mucosubstances (arrowheads); AB. **D.** Cilia distribution on the tentacle; scanning electron micrograph (SEM). Ciliary tufts are largely scarce on the inner surface. **E.** Detail of the cilia cluster at the tip of the tentacle; SEM. **F.** Tentacle musculature with prominent longitudinal fibers; confocal micrograph (CLSM). **G.** Cilia distribution on tentacle surface; SEM. **H.** Cilia distribution (in green), including long rootlets possibly related to innervation; nuclei in blue; CLSM.

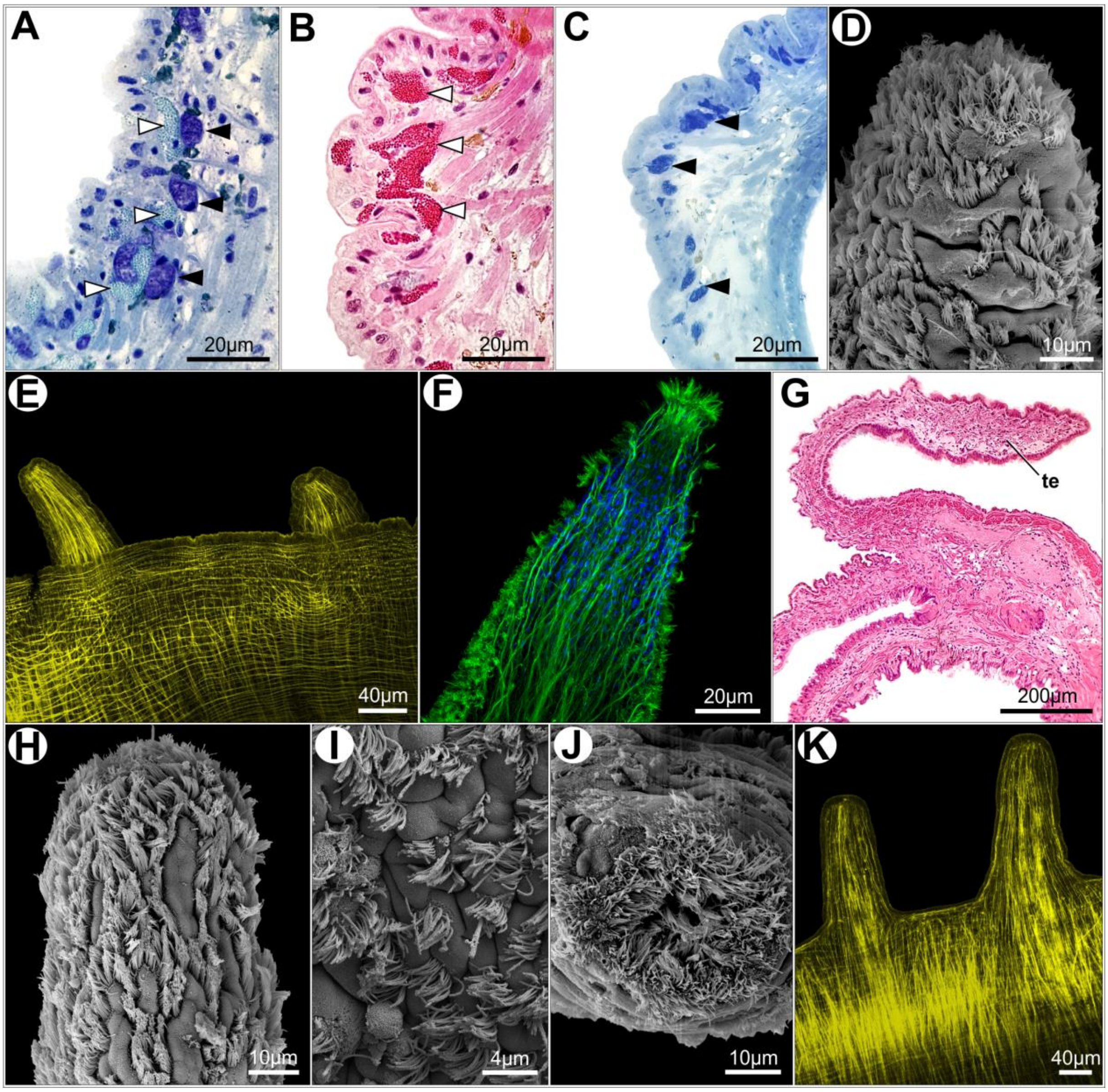

Figure 4. Mantle tentacles of *Ostrea equestris* (Ostreidae). Middle fold tentacles in A-F and inner fold tentacles in G-K. **A.** Sagittal? section showing two types of subepithelial secretory cells, which either have more densely (white arrowheads) or more sparsely distributed granules (black arrowheads); TF. **B.** Same as A, but stained with HE, showing the eosinophilic nature of the secretory cells with more densely distributed granules (white arrowheads). **C.** Same as A, but stained with BB, evidencing the proteinaceous content of the secretory cell type with sparsely distributed granules (black arrowheads). **D.** Cilia distribution on the distal portion of the tentacle; scanning electron micrograph (SEM). **E.** Mantle and tentacle musculature; confocal micrograph (CLSM). **F.** Branching nerves (in green) reaching the ciliary rootlets from the cilia cluster at the tip of the tentacle; nuclei in blue; CLSM. **G.** Inner fold tentacle (te) in sagittal section showing an enlarged, marginal structure with no evidence of secretion; HE. **H.** Cilia distribution on the distal portion of the tentacle; SEM. **I.** Detail of H, showing ciliary tufts; SEM. **J.** Detail of the cilia cluster at the tip; SEM. **K.** Tentacle musculature; CLSM.

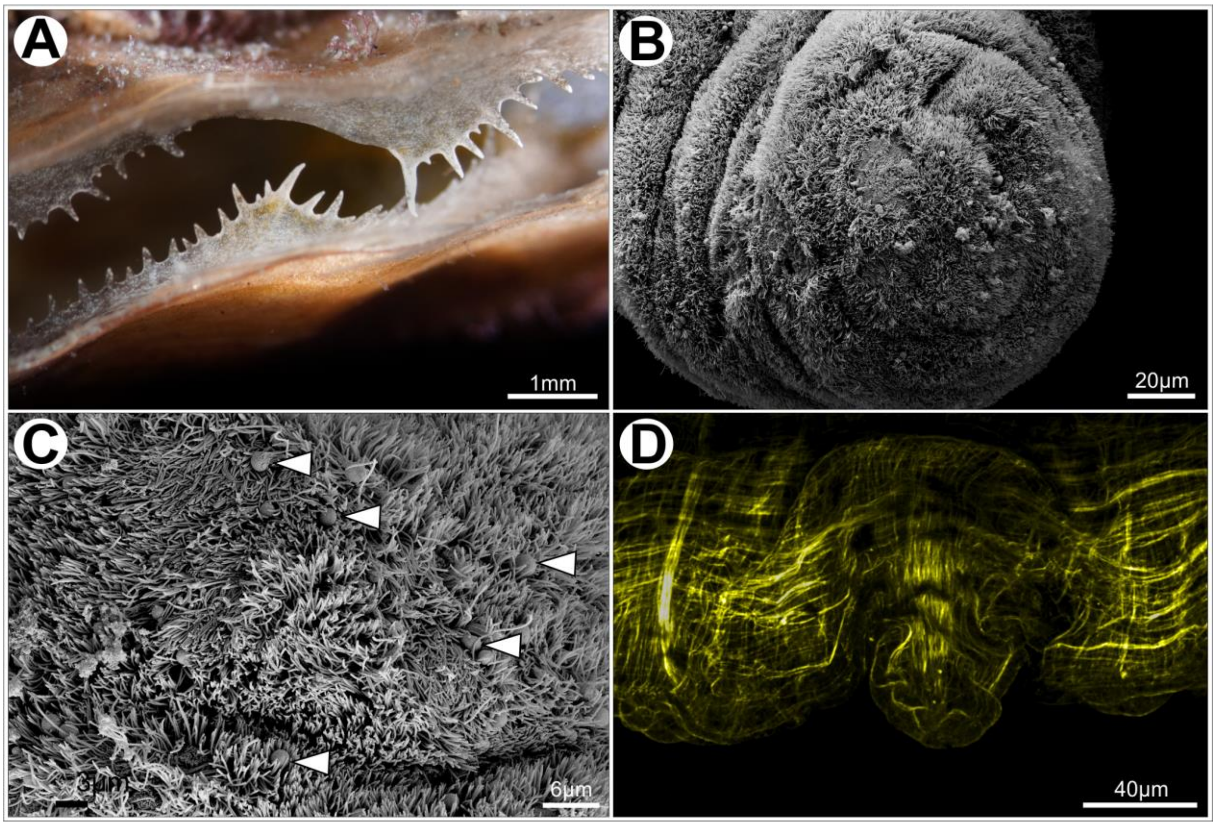

Figure 5. Inner fold tentacles of *Pinna carnea* (Pinnidae). A. Posterior view of the tentacles located on the margin of the inner mantle fold at the inhalant region. **B.** Uniform cilia distribution on the tentacle; scanning electron micrograph (SEM). **C.** Detail of cilia and droplets of possible mucosubstances (arrowheads); SEM. **D.** Tentacle musculature with longitudinal fibers greatly contracted; confocal micrograph.

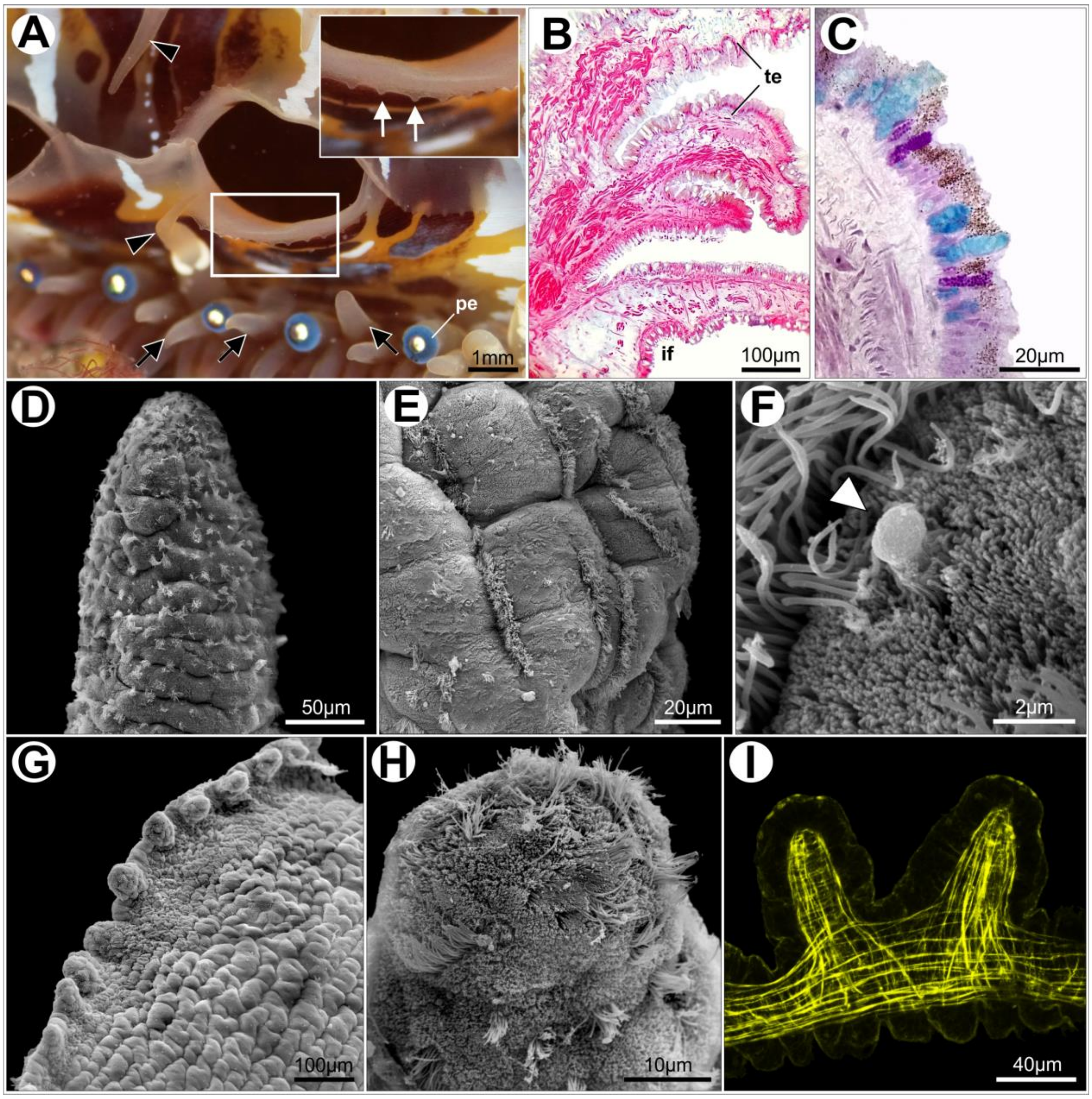

Figure 6. Mantle tentacles of *Spondylus ictericus* (Spondylidae). Middle fold tentacles (MFT) in B-F and inner fold tentacles (IFT) in G-I. Scanning electron micrographs in D-H. **A.** Tentacle types on the mantle margin: MFT (black arrows), including very long tentacles (arrowhead), and very small IFT (white arrows; inset). **B.** Sagittal section of the mantle margin, showing tentacles formed on the inner surface of the middle fold; HE. **C.** Different types of epithelial gland cells distinguished by neutral (magenta) and acidic (blue) mucosubstances; AB and PAS combined method. **D.** Sparse tufts of cilia on the distal portion of a long tentacle. **E.** Cilia organized in longitudinal rows on the surface of ordinary tentacles. **F.** Detail from E, showing a droplet (arrowhead) released close to the cilia row, indicating possible secretion of mucosubstances. **G.** Small tentacles on the margin of the inner fold. **H.** Ciliary tufts sparsely distributed on the tentacle surface. **I.** Muscle fibers forming a small tentacle; confocal micrograph. Abbreviations: if, inner mantle fold; pe, pallial eye; te, tentacles.

Table 1. Selected features of the inner (IFT) and middle fold tentacles (MFT) in the studied pteriomorphian species. Tentacle morphology includes: (1) similar size, (2) size variation, and (3) branched tentacles. In the ventral region, tentacles can be: (1) larger and more abundant in comparison to the anterior and posterior regions or (2) similar to the other regions. Absence of a trait is indicated by "–", affinity to stain is indicated by "+", and unavailable information is indicated by "?". For more anatomical information, please see the results described in the main text.

Species	**MFT**						
	Position on the fold	Morphology	Ventral distribution	Secretory cells	Cluster of cilia at the tip	Musculature	Innervation
Pteria colymbus	marginal	2	1	eosin+, BB+, PAS+, AB+	present	longitudinal and transverse muscles	branching nerves
Pinctada imbricata	marginal	1	1	eosin+, PAS+, AB+	present	longitudinal muscles	branching nerves
Isognomon bicolor	marginal	1	1	eosin+, TF+, AB+	present	longitudinal and transverse muscles	?
Ostrea equestris	submarginal	2	1	eosin+, TF+, AB+	present	longitudinal and transverse muscles	branching nerves
Pinna carnea	–	–	–	–	–	–	–
Spondylus ictericus	submarginal	2	2	PAS+, AB+, AF+	–	longitudinal and transverse muscles	central nerve
	IFT						
Pteria colymbus	marginal	2, 3	1	–	–	longitudinal and transverse muscles	branching nerves
Pinctada imbricata	marginal	2, 3	1	–	present	longitudinal and transverse muscles	branching nerves
Isognomon bicolor	marginal	1	1	–	present	longitudinal and transverse muscles	branching nerves
Ostrea equestris	marginal	1	1	–	present	longitudinal muscles	branching nerves
Pinna carnea	marginal	1	–	–	–	longitudinal and transverse muscles	?
Spondylus ictericus	marginal	1	2	–	–	longitudinal and transverse muscles	?

CHAPTER 4

The evolution of tentacles untangled: revealing tentacle homology and convergence in epifaunal bivalves

CHAPTER 4

The evolution of tentacles untangled: revealing tentacle homology and convergence in epifaunal bivalves

Abstract

Molluscan tentacular organs have always fascinated scientists focused on organismal biology. In bivalves, for instance, mantle tentacles are diverse, performing protective and sensory roles in taxa displaying varied lifestyles. Such diversity is particularly accentuated in Pteriomorphia, a clade comprising scallops, oysters, file clams, and relatives. However, little is known about the evolution of these organs and their role in bivalve radiation. To test hypotheses of homology and gain insights into morphological and ecological associations, we investigated tentacle presence and position in Pteriomorphia based on comparative morphology of 121 species from 13 families in combination with comparative phylogenetic methods. Inner fold tentacles (IFT) had likely four independent origins within Pteriomorphia, while middle fold tentacles (MFT) were acquired twice. Tentacle size and location on the fold are also discussed, revealing broad morphological patterns and expanding the knowledge of less studied bivalve taxa. In addition, evolution of MFT shows the same history of the transition in the sagittal plane orientation relative to the substrate, *i.e.*, from perpendicular to parallel. Such shift in the epifaunal position is related to significant ecological changes, such as increase of mantle exposure, suggesting that MFT were a putative innovation during bivalve radiation. Altogether, our results support the repeated evolution of tentacles across different taxonomic levels, providing new evidence to explore phenotypic evolution and macroecology in bivalves.

Keywords: innovation, Mollusca, morphology, phylogeny, sensory

Introduction

Tentacles are common structures in Mollusca, representing a variety of non-homologous organs with similar morphological features and functions. In general, tentacles are soft, elongated appendages, usually organized as repeated units (Brusca, Moore, & Shuster, 2016). A classic example includes the gastropod buccal and cephalic tentacles involved in sensory tasks related to feeding and reproductive behaviors (Croll, 1983; Künz & Haszprunar, 2001). In cephalopods, muscular tentacular organs form an arm crown, acting in prey capture, mating behaviors, and sensory roles (Kier, 1982; von Byern *et al.*, 2012; Nödl *et al.*, 2016).

Mantle tentacles are known for many bivalve families, occurring either on the middle, inner, or on both middle and inner mantle folds (Yonge, 1983). In infaunal taxa, tentacles are commonly found at the tip of siphons or distributed on their inner walls, protecting the inhalant and exhalant apertures (Hodgson & Fielden, 1984; Fishelson, 2000; Sartori *et al.*, 2008; Vitonis *et al.*, 2012). Within Bivalvia, the largest diversity of tentacles is observed in the Pteriomorphia, which comprises the scallops, oysters, file clams, and relatives. Tentacular structures share morphological similarity across pteriomorphian lineages, performing sensory (photo-, mechano-, and chemoreception) and protective roles, such as preventing the entrance of large particles into the mantle cavity where the gills are located (Gilmour, 1967; Waller, 1975; Moir, 1977; Audino & Marian, 2016).

Even though tentacles share apparent external similarity, detailed anatomical investigation of selected representatives suggested that these structures may not be homologous within Pteriomorphia (Audino & Marian in prep.), possibly representing evolutionary convergences. Nevertheless, historical and comparative information are still required to test this hypothesis. In addition, lifestyle and habitat data are also critical to understand tentacle evolution, considering the hypothesis that they may be homoplastic structures that evolved in response to similar selective pressures (Audino & Marian in prep.). In this context, major progress has recently been achieved to understand macroevolutionary patterns in bivalve history by the integration of ecological and morphological data (Tsubaki, Kameda, & Kato, 2011; Lorion *et al.*, 2013; Morton, 2015; Li, Ó Foighil, & Strong, 2016; Serb *et al.*, 2017).

Bivalves exhibit a wide range of traits considered key innovations in their ecological diversification, including variation in adductor musculature, presence of siphons, and gill type (Yonge, 1962; Stanley, 1968, 1972; Giribet, 2008; Morton, 2015). Previous hypotheses suggested that body position relative to substrate also represented a critical condition influencing shell shape and lifestyle evolution (Kauffman, 1969; Stanley, 1972; Seilacher, 1984; Harper & Skelton, 1993; Sherratt *et al.*, 2016). For instance, the orientation of the sagittal plane (*i.e.*, which divides the body in left and right sides) defines the position for physical stabilization and which part of the body reclines on the substrate. In epifaunal bivalves like mussels, the byssal attachment is ventral, so the sagittal plane is perpendicular to the substrate, resulting in both valves supporting the body (Stanley, 1972). In contrast, only one valve supports the body in scallops, in which the sagittal plane is at a low angle (parallel) to the substrate (Stanley, 1972). In this latter condition, bivalves have typically rounded shell forms, which was regarded as an adaptive trait for enlarging the mantle margin area for repeated sensory receptors (Kauffman, 1969).

While the adoption of the epifaunal parallel position on the substrate is well documented for pteriomorphians, including paleontological data for shell shape and muscle scars (Kauffman, 1969; Stanley 1972), anatomical changes in body parts, such as the mantle, are more obscure because fossil information is unavailable and comparative data for extant groups is limited. Furthermore, such evolutionary association between lifestyle position and mantle organs lacks an explicit phylogenetic background. Considering that tentacles generally have sensory roles (Gilmour, 1963; Moir, 1977; Yonge, 1983; Audino *et al.*, 2015) and that Kauffman’s (1969) hypothesis explicitly defends an association between parallel orientation and development of sensory organs, such an association between body position and tentacle diversification may have been present in the radiation of Pteriomorphia. Accordingly, tentacles are expected to have evolved in lineages of Pteriomorphia that adopted a parallel position of the sagittal plane on the substrate. This clade is a suitable model to explore this hypothesis for including either tentacled or tentacle-less groups, as well as epifaunal lineages with the sagittal plane either perpendicular or parallel to the substrate.

Considering the functional and morphological diversity of tentacles in Pteriomorphia, theses organs show great potential to gain insights into phenotypic evolution and adaptations in bivalves. Therefore, the present study aimed at characterizing the diversity of tentacles across Pteriomorphia in combination with comparative phylogenetic methods to 1) test whether tentacles are homologous, 2) infer how many times they have evolved, and 3) investigate if their evolution was associated with body orientation relative to the substrate.

Material and methods

Taxa sampling

Mantle tentacles were investigated for location and general morphology in 121 species from 13 families of Pteriomorphia (Table 1). Representatives of Mytilida and Arcida were not investigated for morphology considering the absence of tentacles on their mantle margin, as previously reported in many morphological studies (e.g., Soot-Ryen, 1955; Morton & Peharda, 2008; Audino & Marian, 2018). Preserved specimens from museum collections were examined in ethanol under stereomicroscope and dissected when necessary. Catalog numbers are listed in Table 1 according to the following collections: Museum of Comparative Zoology (MCZ), Museum of Zoology “Prof. Adão José Cardoso” of the University of Campinas (ZUEC-BIV), Museum of Zoology of the University of São Paulo (MZSP), Smithsonian National Museum of Natural History (USNM), and Santa Barbara Museum of Natural History (SBMNH).

Character evolution

A recent phylogenetic study of Pteriomorphia with a broad taxonomic sampling (Audino *et al.* in prep.) was used to provide a phylogenetic background to study tentacle history. The original dataset and maximum likelihood tree were used to perform ancestral state reconstructions (ASR) in Mesquite (Maddison & Maddison, 2018). Tentacles traits were coded according to location in the mantle margin (inner mantle fold or middle mantle fold) and position on the mantle fold (marginal or submarginal). From the 121 species investigated for morphology, 100 of them correspond to sequenced species used in the phylogeny, while the remaining includes congeneric species used to assign character states to the remaining terminal taxa; additional genera were also surveyed to enlarge our comparative database. In addition, body position relative to the substrate was coded based on information from literature about the orientation of the sagittal plane, *i.e.*, perpendicular to the substrate or at a low angle (parallel) to the substrate (Table S1).

Analysis of ancestral state reconstruction were performed under maximum likelihood, adopting the MK1 model that assumes equal rates for any particular change. This one-parameter model (MK1) presented a better fit to the data according to the likelihood ratio test when compared to the two-parameter model (AsymmMK), which allows different transition rates (Mark Pagel, 1999; Maddison & Maddison, 2018). For data presentation, some clades were collapsed to evidence the results for tentacled pteriomorphian families.

Results

In pteriomorphian bivalves, tentacles are located either only on the middle mantle fold, only on the inner mantle fold, or on both folds (Table 1). They are named middle fold tentacles (MFT) and inner fold tentacles (IFT) depending on their location. MFT and IFT may originate at the margin of the fold (marginal tentacles; Figs. 1C, 4C) or close to the edge (submarginal tentacles; Figs. 1D, 4D). Tentacles are distributed along the free mantle margin, although differences in tentacle density and size along the antero-posterior or dorso-ventral axes do occur. Morphological details across the studied species are described below and listed in Table 1.

Inner fold tentacles

This type of tentacle was likely absent in the ancestor of Pteriomorphia, with four independent acquisitions: in Pectinidae, Plicatulidae, Spondylidae, and Ostreida (Fig. 1A). The Ostreida clade comprises the families Gryphaeidae, Malleidae, Ostreidae, Pinnidae, and Pteriidae, all of them exhibiting marginal IFT (Fig. 1C). Spondylids and plicatulids also have marginal IFT, whereas the pectinids (scallops) have submarginal IFT (Fig. 1D).

In the Ostreida, IFT are usually abundant and densely grouped. Tentacle size varies greatly, from small papillae to long filiform tentacles. In Pinnidae, IFT are present only posteriorly, varying in size and pigmentation across species (Fig. 2A, B). In Gryphaeidae, IFT are usually small in contrast to Ostreidae, in which tentacles are comparatively longer (Fig. 2C-G). In both families, tentacles are long, numerous, and pigmented in the posteroventral region, particularly close to the inhalant and exhalant regions. A similar pattern was observed in the IFT of Malleidae and Pteriidae (Fig. 2H-L), although unique branched tentacles occur in the ventral region of *Pinctada* and *Pteria* (Fig. 2L, Fig. S1).

In Spondylidae, small papillae are uniformly distributed along the middle fold margin (Fig. 3A, B). Small papillae are also present in *Plicatula gibbosa*, although greatly reduced due to preservation. In the Pectinidae, IFT are submarginal and located on the outer surface of the inner fold (Figs. 2D, 3C-L). Differently from other pteriomorphians, a great diversity of IFT is observed within Pectinidae regarding tentacle shape, number, pigmentation, and position (Fig. 3C-L). For instance, in representatives of *Amusium*, *Crassodoma*, *Euvola*, *Palliolum*, *Pecten*, *Pedum*, and *Placopecten*, the IFT are organized in a single row with uniform tentacles (Fig. 3C-F). In contrast, tentacle position is varied in *Argopecten*, *Chlamys*, *Gloripallium*, and *Lindapecten*, being usually organized in two rows, a proximal one with smaller tentacles and distal one with longer tentacles (Fig. 3G-I). A third condition includes small tentacles distributed over a large area of the fold's outer surface far from the margin. This condition was observed in *Adamussium colbecki*, *Delectopecten vitreus,* and *Zygochlamys patagonica* (Fig. 3J-L).

Middle fold tentacles

Ancestral state reconstruction indicates two distinct origins for MFT, *i.e.*, in the Pectinida and in the clade Ostreoidea + Pterioidea, which comprises Gryphaeidae, Malleidae, Ostreidae, and Pteriidae (Fig. 4A). Whereas MFT are marginal in Malleidae and Pteriidae (Fig. 4C), they are submarginal in the remaining groups (Fig. 4D).

In Ostreida, MFT are abundant, particularly in the ventral region, and are usually less pigmented than the IFT (Fig. 5). Both tentacles types are frequently similar in shape and size. In Ostreidae (Fig. 5A-D) and Gryphaeidae (Fig. E-F), longer MFT are located proximally, while smaller MFT are located in a distal position, adjacent to the fold's margin. In Malleidae (Fig. 5G) and Pteriidae (Fig. 5H-L), MFT are marginal, uniform, and densely distributed along the ventral region.

In the Pectinida, MFT are submarginal, occupying proximal to distal positions on the inner surface of the middle fold (Fig. 6). In *Dimya argentea* (Dimyidae), MFT are small and sparsely distributed apparently in a single row (Fig. 6A). In *Plicatula gibbosa* (Plicatulidae), tentacles are more abundant, including small (distal) and large (proximal) tentacles in two apparent rows (Fig. 6B). In the Anomiidae, MFT are abundant and distributed along three apparent rows, including larger tentacles towards the proximal region (Fig. 6C-E). In the Limidae, tentacles can be greatly enlarged, forming long organs densely distributed in up to five rows on the middle fold (Fig. 6F-J). A longitudinal groove is present along the tentacles of *Ctenoides* (Fig. 6I), *Limaria* (Fig. 6J), and *Limatula* (Fig. 6F). An annulate (septate) pattern is typical for MFT of *Limaria* (Fig. 6J) and *Limatula* (Fig. 6F). In Pectinoidea (*i.e.*, Spondylidae, Propeamussiidae, and Pectinidae), MFT are similarly organized in multiple rows, including abundant, short tentacles more distally located, and much longer tentacles more proximally located (Fig. 6K-P).

Sagittal plane orientation relative to the substrate

Ancestral reconstructions suggest that the Pteriomorphia's ancestor was likely positioned with the sagittal plane perpendicular to the substrate (Fig. 7A). This epibyssate position can be observed in familiar bivalves such as mussels (Mytilidae) and ark clams

(Arcidae), in which the byssal attachment pulls the ventral body region towards the substrate (Fig. 7B). Consequently, the antero-ventral mantle margin also faces the substrate. Independent changes in epifaunal position were reconstructed for the ancestors of Pectinida and Ostreoidea + Pterioidea (Fig. 7A). In this case, the byssal attachment is anterior and orientation of the sagittal plane is at a low angle to the substrate, nearly parallel, with one valve supporting the body (Fig. 7C). As a consequence, the entire mantle margin is exposed to the surrounding environment. The independent acquisitions of MFT within Pteriomorphia exhibits the same history for the evolution of body position relative to the substrate (Fig. 7D).

Discussion

In pteriomorphian bivalves, detailed information on tentacle anatomy and function was obtained for representatives from selected families, *e.g.*, Limidae (Gilmour, 1963, 1967; Owen & McCrae, 1979), Ostreidae (Audino and Marian in prep), Pteriidae (Tëmkin, 2006), and Pectinidae (Moir, 1977; Audino *et al.*, 2015). In addition to the phylogenetic comparative results, our morphological survey represents a contribution to the knowledge of soft parts in less studied bivalve genera and families, particularly those related to Anomiidae, Dimyidae, Gryphaeidae, Limidae, Malleidae, Plicatulidae, and Propeamussiidae (Table 1).

Inner fold tentacles

Tentacles on the inner mantle fold evolved at least four times independently according to our analysis. In the Ostreida (*i.e.*, Pinnoidea, Ostreoidea, and Pterioidea), tentacles are marginal and distributed along the mantle margin, being frequently longer and more numerous in the posteroventral region. In a phylogenetic study of Pterioidea, tentacles were investigated for location and morphology (simple or branched), suggesting great similarity to Ostreoidea (Tëmkin, 2006). Consistent with our results, anatomical details, such as a ciliary tuft at the tentacle tip, supports the homology of IFT for Ostreoidea and Pterioidea (Audino and Marian in prep.). In addition, branched tentacles were described for *Pinctada* and *Pteria* (Morton, 1995; Tëmkin, 2006; Audino and Marian in prep.), indicating this morphology is restricted to Pteriidae. Our results complement these observations, suggesting convergent gains of lateral branches in the genera (Fig. S1).

For oysters and relatives (Ostreoidea), comparative studies with *Crassostrea* species revealed uniform tentacular morphology on the inner fold with tendency to size increase towards the ventral region (Amaral & Simone, 2014). We also observed this pattern in other

Ostreidae genera, as well as in Gryphaeidae representatives. In the Pinnidae, tentacle anatomy was described for *Pinna carnea*, revealing tentacle distribution restricted to the posterior region (inhalant and exhalant apertures) and marginal tentacles regularly spaced (Yonge, 1953; Audino and Marian in prep.).

Tentacles on the inner fold have also evolved in the ancestor of Spondylidae, which bear numerous small papillae along the margin. The anatomy of these structures was previously described for *Spondylus ictericus*, including muscular organization and cilia distribution (Audino and Marian in prep.). Similarly, very small papillae, greatly reduced due to contraction, are present in Plicatulidae, previously noted in *Plicatula gibbosa* (Yonge, 1973) and *Plicatulostrea onca* (Simone & Amaral, 2008). In Pectinidae, IFT were reported for *Argopecten irradians* (Gutsell, 1931), *Nodipecten nodosus* (Audino *et al.*, 2015), and *Placopecten magellanicus* (Moir, 1977) as a row of tentacles occurring close to the edge. However, our survey has demonstrated a surprisingly diversity of IFT in Pectinidae, which should stimulate further investigations focused on comparative and functional anatomy. Tentacle distribution includes different sizes according to the proximal-distal position over the fold, as well as small tentacles occurring throughout the fold's surface.

In contrast to the other families of Pectinida, IFT were not observed in any studied species of Anomiidae, Dimyidae, Limidae, and Propeamussiidae. The absence of tentacles on this fold was also reported for *Propeamussium lulcidum* (Morton & Thurston, 1989) and many limid species (Morton, 1979; Mikkelsen & Bieler, 2003).

While IFT are marginal in Ostreida, Spondylidae, and Plicatulidae, submarginal tentacles are present only in Pectinidae. This morphological pattern argues against the homology of these organs for Pteriomorphia. In addition, our study provides evidence for multiple convergent acquisitions of IFT, demonstrating high plasticity of the bivalve mantle. In this sense, morphological convergences may be more pervasive than expected, as already demonstrated for ark clams (Arcida) (Oliver & Holmes, 2006; Audino *et al.* 2019) and scallops (Sherratt *et al.*, 2016; Serb *et al.*, 2017).

The evolutionary origin and maintenance of inner fold tentacles can be associated with protection of the mantle cavity, as well as with sensory roles (Yonge, 1983; Sartori & Domaneschi, 2005). When valves are opened and the mantle aperture is exposed, tentacles from right and left lobes remain interlocked, creating a physical barrier that prevents the entrance of large particles into the mantle cavity (Yonge, 1968). Water turbulence and suspended debris may have acted as selective forces, resulting in mantle tentacles as selected protective responses in numerous bivalve lineages. For instance, in bivalves living buried in the sediment, an analogous condition is observed in simple and branched tentacles that help to protect the inhalant aperture from larger particles (Owen, 1961; Narchi, 1972; Fishelson, 2000; Sartori & Domaneschi, 2005; Sartori *et al.*, 2008; Piffer, Arruda, & Passos, 2011; Vitonis *et al.*, 2012).

Middle fold tentacles

MFT likely had two distinct origins (Pectinida and Ostreoidea + Pterioidea). Within Ostreida, tentacles are submarginal only in Ostreidae and Gryphaeidae. In both families, the middle fold bears small and long tentacles in two rows, as also noted for *Hyotissa mcgintyi* and some *Crassostrea* and *Saccostrea* species (Dinamani, 1971; Tëmkin, 2006; Amaral & Simone, 2014; Simone, Mikkelsen, & Bieler, 2015). Detailed information on tentacle innervation, ciliary receptors at the tip of MFT, and tentacle distribution, supports the homology of MFT for Ostreoidea and Pterioidea (Audino and Marian in prep.). In addition to previously described MFT in Pterioidea (Yonge, 1968; Morton, 1995; Tëmkin, 2006), our results expand the morphological knowledge for more representatives of Malleidae and Pteriidae, in which tentacles are marginal and more developed ventrally.

In all taxa from Pectinida, the mantle margin bears submarginal MFT distributed along the entire mantle margin. Tentacles are described as small papillae in Plicatulidae and Dimyidae (Yonge, 1973, 1975; Simone & Amaral, 2008), occurring in two rows. In the Anomiidae, tentacle information was previously restricted to two species of *Pododesmus* (Holmes, 2017). Our observations indicate long and abundant tentacles forming three rows in this genus, in accordance with previous observations, and comparatively longer organs in *Anomia simplex* and *Heteranomia squamula.*

In scallops, very long tentacles were observed in *Nodipecten nodosus* (Audino *et al.*, 2015), *Pecten maximus* (Dakin, 1909), and *Argopecten irradians* (Wilkens, 2006). Sensory roles have been attributed to the MFT of these animals, based on different lines of anatomical, behavioral, and physiological evidence for mechano- and chemoreception (Gutsell, 1931; Thomas & Gruffydd, 1971; Wilkens, 2006; Audino *et al.*, 2015). In Limidae, multiple rows of tentacles of different sizes are also a constant pattern, as noted in previous studies (Morton, 1979; Mikkelsen & Bieler, 2003). Anatomical details are restricted to *Limaria hians*, including the inner organization of annulate tentacles, morphology of sensory cilia, and characterization of mucus secretion (Gilmour, 1963, 1967; Owen & McCrae, 1979). Very enlarged tentacles in *Ctenoides*, *Lima*, and *Limaria* are thought to support the body, facilitate swimming movements, and act as defensive structures against predators (Gilmour, 1967; Morton, 1979).

Lifestyle associations

The position of the bivalve body relative to the substrate is regarded as a key feature in the diversification of bivalve lifestyles (Yonge, 1962; Stanley, 1970, 1972; Seilacher, 1984). In pteriomorphian bivalves, two positions are related to physical stabilization in the epifaunal habit, *i.e.*, sagittal plane of the body perpendicular or at low angle (parallel) to the substrate (Stanley, 1972). Fossil evidence for different extinct groups (e.g., related to the ancestors of recent Pectinidae, Limidae, Malleidae, Pinnidae, and Pteriidae) supports the transition from perpendicular orientation of the sagittal plane to forms that came to rest upon one valve (Stanley, 1972). In this case, transitions to a parallel position seem associated with major morphological changes, such as anterior byssal attachment, rounded shells, and reduced (or event absent) anterior adductor muscle (Stanley, 1972; Seilacher, 1984; Oliver & Holmes, 2006; Owada, 2007). Based on extant diversity and paleontological data, the adoption of a parallel position relative to the substrate was hypothesized to be associated with the evolution of rounded shells, which may have contributed to physical stabilization above one valve (Kauffman, 1969). In combination with a rounded shell, the parallel position on the substrate could have resulted in exposure of the entire mantle margin to the surrounding environment, therefore, providing more area to development of multiple sensory organs (Kauffman, 1969).

Our results suggest that the independent transitions from perpendicular to parallel position occurred in the ancestors of two pteriomorphian clades that also gained MFT independently (Fig. 7). We are aware that the observed pattern of codistribution should be interpreted cautiously, because it does not provide evidence for dependent evolution between traits (Maddison & FitzJohn, 2015). However, it suggests an ancient evolutionary scenario where the previous hypothesis (Kauffman, 1969) seems plausible. Reclining upon one valve may have freed the entire mantle margin for interaction with the environment, increasing the area for mantle sensory organs, such as tentacles.

In conclusion, our data indicate that MFT and IFT are not homologous within Pteriomorphia, representing convergent acquisitions in separate clades, and supporting repeated evolution of tentacles in bivalves across different taxonomic levels. These results reinforce the plasticity of the molluscan body (Wanninger *et al.*, 2008) and the relevance of evolutionary convergences in the radiation of the class (Distel, 2000; Oliver & Holmes, 2006; Alejandrino, Puslednik, & Serb, 2011; Lorion *et al.*, 2013; Li *et al.*, 2016; Serb *et al.*, 2017)

(Audino et al. 2019). We also found support for tentacle evolution in association with parallel orientation of the sagittal plane, a putative innovation during bivalve diversification. In addition to muscle organization, byssal apparatus morphology, and shell shape, our tentacle data for extant pteriomorphians highlight another anatomical evidence that sheds light on bivalve evolutionary radiation.

Acknowledgements

The authors acknowledge the grants 2015/09519-4 and 2017/01365-3, São Paulo Research Foundation (FAPESP). This study was financed in part by the Coordenação de Aperfeiçoamento de Pessoal de Nível Superior - Brasil (CAPES) - Finance Code 001. This study is part of the first author’s Doctorate’s thesis through the Graduate Program in Zoology of the Institute of Biosciences (University of São Paulo). The authors thank the following institutions that provided materials for the development of this study: Museum of Comparative Zoology (MCZ), Museum of Zoology “Prof. Adão José Cardoso” of the University of Campinas (ZUEC), Museum of Zoology of the University of São Paulo (MZSP), Santa Barbara Museum of Natural History (SBMNH), and Smithsonian National Museum of Natural History (USNM). This is a contribution of NP-BioMar (Research Center for Marine Biodiversity – USP).

References

Alejandrino A, Puslednik L, Serb JM. 2011. Convergent and parallel evolution in life habit of the scallops (Bivalvia: Pectinidae). *BMC Evolutionary Biology* 11.

Amaral VSD, Simone LRL. 2014. Revision of genus *Crassostrea* (Bivalvia: Ostreidae) of Brazil. *Journal of the Marine Biological Association of the United Kingdom* 94: 811–836.

Audino JA, Marian JEAR. 2016. On the evolutionary significance of the mantle margin in pteriomorphian bivalves. *American Malacological Bulletin* 34: 148–159.

Audino, Marian JEAR. 2018. Comparative and functional anatomy of the mantle margin in ark clams and their relatives (Bivalvia: Arcoidea) supports association between morphology and life habits. *Journal of Zoology* 305: 149–162.

Audino, Marian JEAR, Wanninger A, Lopes SGBC. 2015. Anatomy of the pallial tentacular organs of the scallop *Nodipecten nodosus* (Linnaeus, 1758) (Bivalvia: Pectinidae). *Zoologischer Anzeiger - A Journal of Comparative Zoology* 258: 39–46.

Brusca RC, Moore W, Shuster RM. 2016. *Invertebrates*. Sunderland, MA: Sinauer Associates.

von Byern J, Wani R, Schwaha T, Grunwald I, Cyran N. 2012. Old and sticky—adhesive mechanisms in the living fossil *Nautilus pompilius* (Mollusca, Cephalopoda). *Zoology* 115: 1–11.

Croll RP. 1983. Gastropod chemoreception. *Biological Reviews* 58: 293–319.

Dakin WJ. 1909. *Pecten*. *Proceedings of the Liverpool Biological Society* 23: 332–468.

Dinamani P. 1971. Occurrence of the Japanese oyster, *Crassostrea Gigas* (thunberg), in northland, New Zealand. *New Zealand Journal of Marine and Freshwater Research* 5: 352–357.

Distel DL. 2000. Phylogenetic relationships among Mytilidae (Bivalvia): 18S rRNA data suggest convergence in mytilid body plans. *Molecular Phylogenetics and Evolution* 15: 25–33.

Fishelson L. 2000. Comparative morphology and cytology of siphons and siphonal sensory organs in selected bivalve molluscs. *Marine Biology* 137: 497–509.

Gilmour THJ. 1963. A note on the tentacles of *Lima hians* (Gmelin)(Bivalvia). *Journal of Molluscan Studies* 35: 82–85.

Gilmour THJ. 1967. The defensive adaptations of *Lima hians* (Mollusca, Bivalvia). *Journal of the Marine Biological Association of the United Kingdom* 47: 209–221.

Giribet G. 2008. Bivalvia. *Phylogeny and Evolution of the Mollusca*. Berkeley: University of California Press, 105–141.

Gutsell JS. 1931. Natural history of the bay scallop. *Bulletin of the Bureau of Fisheries (United States Bureau of Fisheries)* 46: 569–632.

Harper EM, Skelton PW. 1993. The Mesozoic marine revolution and epifaunal bivalves. *Scripta Geologica, Special Issue* 2: 127–153.

Hodgson AN, Fielden LJ. 1984. The structure and distribution of peripheral ciliated receptors in the bivalve molluscs *Donax serra* and *D. sordidus*. *Journal of Molluscan Studies* 50: 104–112.

Holmes AM. 2017. Phylogenetics of British saddle oysters (Bivalvia: Anomiidae)—A review of the shell morphology, internal anatomy and genetics of *Pododesmus* in British waters. *Journal of Conchology* 42: 317–325.

Kauffman EG. 1969. Form, function, and evolution. *Treatise on Invertebrate Paleontology, Vol. N. Mollusca 6. Bivalvia*. Kansas: Geological Society of America and University of Kansas.

Kier WM. 1982. The functional morphology of the musculature of squid (Loliginidae) arms and tentacles. *Journal of Morphology* 172: 179–192.

Künz E, Haszprunar G. 2001. Comparative ultrastructure of gastropod cephalic tentacles: Patellogastropoda, Neritaemorphi and Vetigastropoda. *Zoologischer Anzeiger - A Journal of Comparative Zoology* 240: 137–165.

Li J, Ó Foighil D, Strong EE. 2016. Commensal associations and benthic habitats shape macroevolution of the bivalve clade Galeommatoidea. *Proceedings of the Royal Society B: Biological Sciences* 283: 20161006.

Lorion J, Kiel S, Faure B, Kawato M, Ho SYW, Marshall B, Tsuchida S, Miyazaki JI, Fujiwara Y. 2013. Adaptive radiation of chemosymbiotic deep-sea mussels. *Proceedings of the Royal Society B: Biological Sciences* 280: 20131243–20131243.

Maddison WP, FitzJohn RG. 2015. The unsolved challenge to phylogenetic correlation tests for categorical characters. *Systematic Biology* 64: 127–136.

Maddison WP, Maddison DR. 2018. Mesquite: a modular system for evolutionary analysis. Version 3.51 http://www.mesquiteproject.org.

Mark Pagel. 1999. The maximum likelihood approach to reconstructing ancestral character states of discrete characters on phylogenies. *Systematic Biology* 48: 612–622.

Mikkelsen PM, Bieler R. 2003. Systematic revision of the western Atlantic file clams, *Lima* and *Ctenoides* (Bivalvia: Limoida: Limidae). *Invertebrate Systematics* 17: 667.

Moir AJG. 1977. Ultrastructural studies on the ciliated receptors of the long tentacles of the giant scallop, *Placopecten magellanicus* (Gmelin). *Cell and Tissue Research* 184: 367–380.

Morton B. 1979. A comparison of lip structure and function correlated with other aspects of the functional morphology of *Lima lima*, *Limaria* (*Platilimaria*) *fragilis*, and *Limaria* (*Platilimaria*) *hongkongensis* sp.nov. (Bivalvia: Limacea). *Canadian Journal of Zoology* 57: 728–742.

Morton B. 1995. The biology and functional morphology of *Pteria brevialata* (Bivalvia: Pterioidea), epizoic on gorgonians in Hong Kong. *Journal of Zoology* 236: 223–241.

Morton B. 2015. Evolution and adaptive radiation in the Mytiloidea (Bivalvia): clues from the pericardial–posterior byssal retractor musculature complex. *Molluscan Research* 35: 227–245.

Morton B, Peharda M. 2008. The biology and functional morphology of *Arca noae* (Bivalvia: Arcidae) from the Adriatic Sea, Croatia, with a discussion on the evolution of the bivalve mantle margin. *Acta Zoologica* 89: 19–28.

Morton B, Thurston MH. 1989. The functional morphology of *Propeamussium lucidum* (Bivalvia: Pectinacea), a deep-sea predatory scallop. *Journal of Zoology* 218: 471–496.

Narchi W. 1972. Comparative study of the functional morphology of *Anomalocardia brasiliana* (Gmelin, 1791) and Tivela mactroides (Born, 1778) (Bivalvia, Veneridae). *Bulletin of Marine Science* 22: 643–670.

Nödl MT, Kerbl A, Walzl MG, Müller GB, de Couet HG. 2016. The cephalopod arm crown: appendage formation and differentiation in the Hawaiian bobtail squid *Euprymna scolopes*. *Frontiers in Zoology* 13.

Oliver PG, Holmes AM. 2006. The Arcoidea (Mollusca: Bivalvia): a review of the current phenetic-based systematics. *Zoological Journal of the Linnean Society* 148: 237–251.

Owen G. 1961. A note on the habits and nutrition of *Solemya parkinsoni* (Protobranchia: Bivalvia). *Journal of Cell Science* 3: 15–21.

Owen G, McCrae JM. 1979. Sensory cell/gland cell complexes associated with the pallial tentacles of the bivalve *Lima hians* (Gmelin), with a note on specialized cilia on the pallial curtains. *Philosophical Transactions of the Royal Society B: Biological Sciences* 287: 45–62.

Piffer PR, Arruda EP de, Passos FD. 2011. The biology and functional morphology of *Macoma biota* (Bivalvia: Tellinidae: Macominae). *Zoologia (Curitiba, Impresso)* 28: 321–333.

Sartori AF, Domaneschi O. 2005. The functional morphology of the antarctic bivalve *Thracia meridionalis* Smith, 1885 (Anomalodesmata: Thraciidae). *Journal of Molluscan Studies* 71: 199–210.

Sartori AF, Printrakoon C, Mikkelsen PM, Bieler R. 2008. Siphonal structure in the Veneridae (Bivalvia: Heterodonta) with an assessment of its phylogenetic application and a review of venerids of the Gulf of Thailand. *The Raffles Bulletin of Zoology* 18: 103–125.

Seilacher A. 1984. Constructional morphology of bivalves: evolutionary pathways in primary versus secondary soft-bottom dwellers. *Palaeontology* 27: 207–237.

Serb JM, Sherratt E, Alejandrino A, Adams DC. 2017. Phylogenetic convergence and multiple shell shape optima for gliding scallops (Bivalvia: Pectinidae). *Journal of Evolutionary Biology* 30: 1736–1747.

Sherratt E, Alejandrino A, Kraemer AC, Serb JM, Adams DC. 2016. Trends in the sand: Directional evolution in the shell shape of recessing scallops (Bivalvia: Pectinidae). *Evolution* 70: 2061–2073.

Simone LRL, Amaral VS do. 2008. *Plicatulostrea*, a new genus of Plicatulidae (Bivalvia: Pectinoidea) from Thailand. *The Raffles Bulletin of Zoology* 18: 127–135.

Simone LRL, Mikkelsen PM, Bieler R. 2015. Comparative anatomy of selected marine bivalves from the Florida Keys, with notes on Brazilian congeners (Mollusca: Bivalvia). *Malacologia* 58: 1–127.

Soot-Ryen T. 1955. A report on the family Mytilidae (Pelecypoda). *Allan Hancock Pacific Expeditions* 20: 1–175.

Stanley SM. 1968. Post-Paleozoic adaptive radiation of infaunal bivalve molluscs: A consequence of mantle fusion and siphon formation. *Journal of Paleontology* 42: 214–229.

Stanley SM. 1970. *Relation of shell form to life habits of the Bivalvia (Mollusca)*. Geological Society of America.

Stanley SM. 1972. Functional morphology and evolution of byssally attached bivalve mollusks. *Journal of Paleontology* 46: 165–212.

Tëmkin I. 2006. Morphological perspective on the classification and evolution of Recent Pterioidea (Mollusca: Bivalvia). *Zoological Journal of the Linnean Society* 148: 253–312.

Thomas GE, Gruffydd LD. 1971. The types of escape reactions elicited in the scallop *Pecten maximus* by selected sea-star species. *Marine Biology* 10: 87–93.

Tsubaki R, Kameda Y, Kato M. 2011. Pattern and process of diversification in an ecologically diverse epifaunal bivalve group Pterioidea (Pteriomorphia, Bivalvia). *Molecular Phylogenetics and Evolution* 58: 97–104.

Vitonis JEVV, Zaniratto CP, Machado FM, Passos FD. 2012. Comparative studies on the histology and ultrastructure of the siphons of two species of Tellinidae (Mollusca: Bivalvia) from Brazil. *Zoologia (Curitiba)* 29: 219–226.

Waller TR. 1975. The behavior and tentacle morphology of pteriomorphian bivalves: a motion-picture study. *Bulletin of the American Malacological Union*: 7–13.

Wanninger A, Koop D, Moshel-Lynch S, Degnan BM. 2008. Molluscan evolutionary development. *Phylogeny and Evolution of the Mollusca* 16.

Wilkens LA. 2006. Neurobiology and behaviour of the scallop. In: Shumway SE,, In: Parsons GJ, eds. *Scallops: Biology, Ecology and Aquaculture*. *Developments in Aquaculture and Fisheries Science*. Elsevier, 317–356.

Yonge CM. 1953. Form and Habit in *Pinna carnea* Gmelin. *Philosophical Transactions of the Royal Society B: Biological Sciences* 237: 335–374.

Yonge CM. 1962. On the primitive significance of the byssus in the Bivalvia and its effects in evolution. *Journal of the Marine Biological Association of the United Kingdom* 42: 113–125.

Yonge CM. 1968. Form and habit in species of *Malleus* (including the" hammer oysters") with comparative observations on *Isognomon isognomon*. *The Biological Bulletin* 135: 378–405.

Yonge M. 1973. Functional morphology with particular reference to hinge and ligament in *Spondylus* and *Plicatula* and a discussion on relations within the superfamily Pectinacea (Mollusca: Bivalvia). *Philosophical Transactions of the Royal Society B: Biological Sciences* 267: 173–208.

Yonge CM. 1975. The status of the Plicatulidae and the Dimyidae in relation to the superfamily Pectinacea (Mollusca: Bivalvia). *Journal of Zoology* 176: 545–553.

Yonge CM. 1983. Symmetries and the role of the mantle margins in the bivalve Mollusca. *Malacological Review* 16: 1–10.

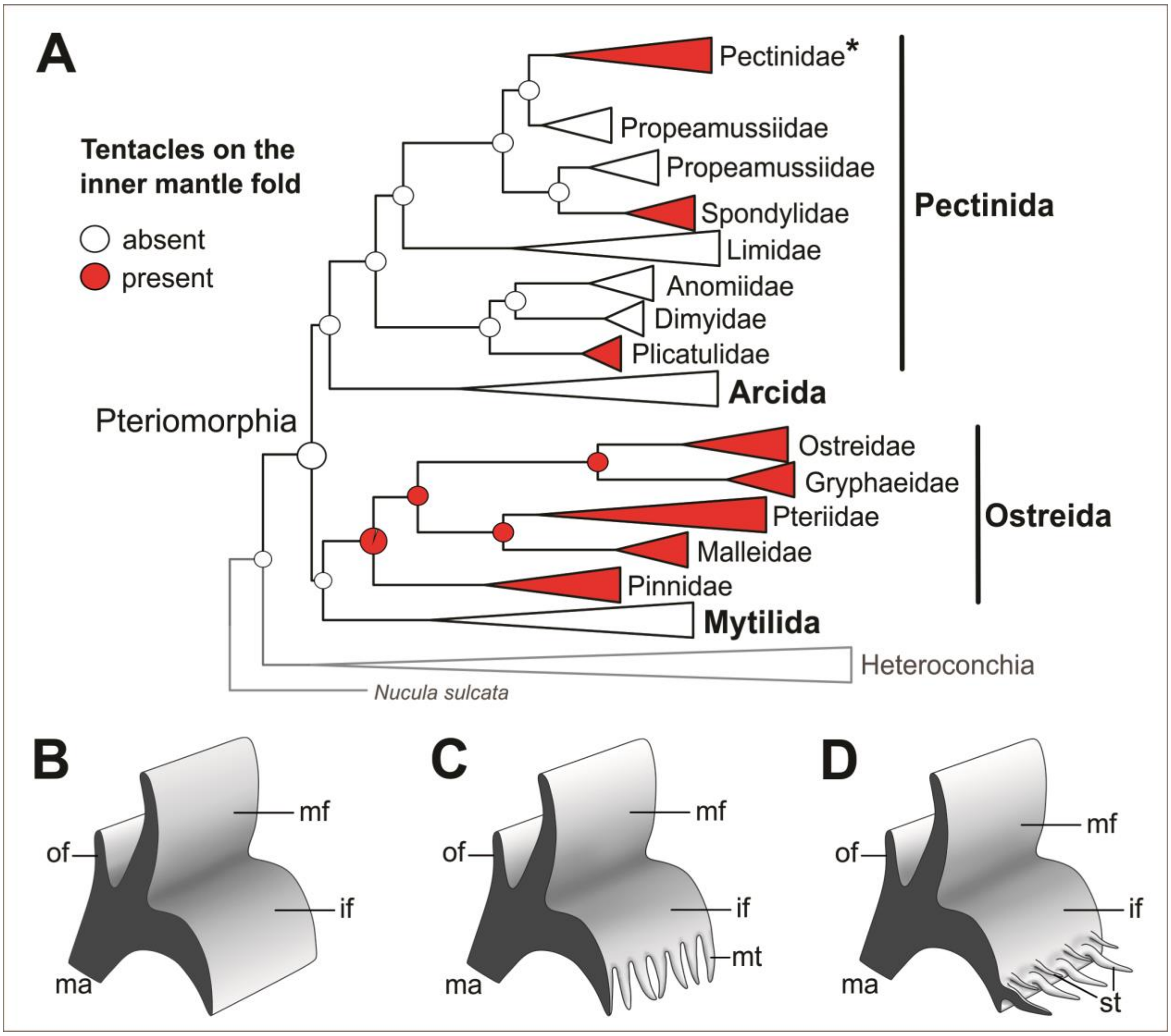

Figure 1. Evolution of inner fold tentacles in Pteriomorphia. A. Maximum likelihood reconstruction of inner fold tentacles (IFT) indicates four independent gains: in the ancestor of Pectinidae, in the ancestor of Spondylidae, in the ancestor of Plicatulidae, and in the ancestor of Ostreida. Likelihood proportions for ancestral states are indicated in pie charts. Tentacles can either be marginal (C) or submarginal (asterisk, D). **B-D.** Schematic representation of the mantle margin; middle fold tentacles are not represented. **B.** Mantle margin devoid of IFT. **C.** Marginal IFT. **D.** Submarginal IFT. Abbreviations: if, inner mantle fold; ma, mantle; mf, middle mantle fold; mt, marginal tentacles; of, outer mantle fold; st, submarginal tentacles.

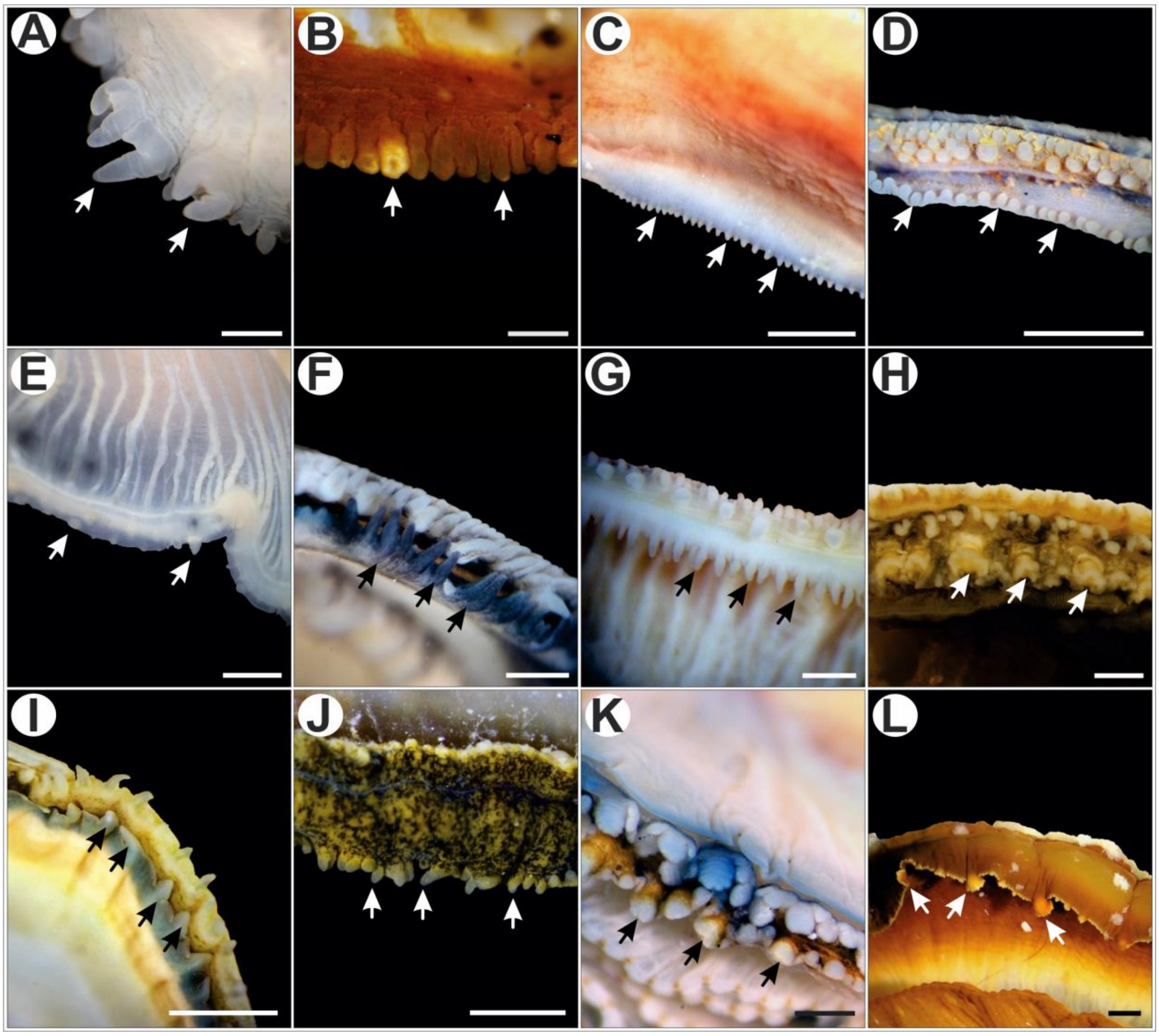

Figure 2. Tentacles on the inner mantle fold of Ostreida (arrows). Pinnidae (A-B), Gryphaeidae (C-D), Ostreidae (E-G), Pteriidae (H-L). Scale bars=1mm. **A.** *Atrina rigida* (USNM847971). **B.** *Pinna rudis* (MZSP114038). **C.** *Neopycnodonte cochlear* (MCZ379076). **D.** *Hyotissa mcgintyi* (USNM804282). **E.** *Lopha cristagalli* (USNM793723). **F.** *Striostrea prismatica* (SBMNH211884). **G.** *Ostrea permollis* (USNM850800). **H.** *Pteria heteroptera* (MZSP55575). **I.** *Isognomon ephippium* (USNM701010). **J.** *Isognomon isognomum* (MZSP54988). **K.** *Pinctada imbricata* (ZUEC-BIV2383). **L.** *Pinctada margaritifera* (USNM836493).

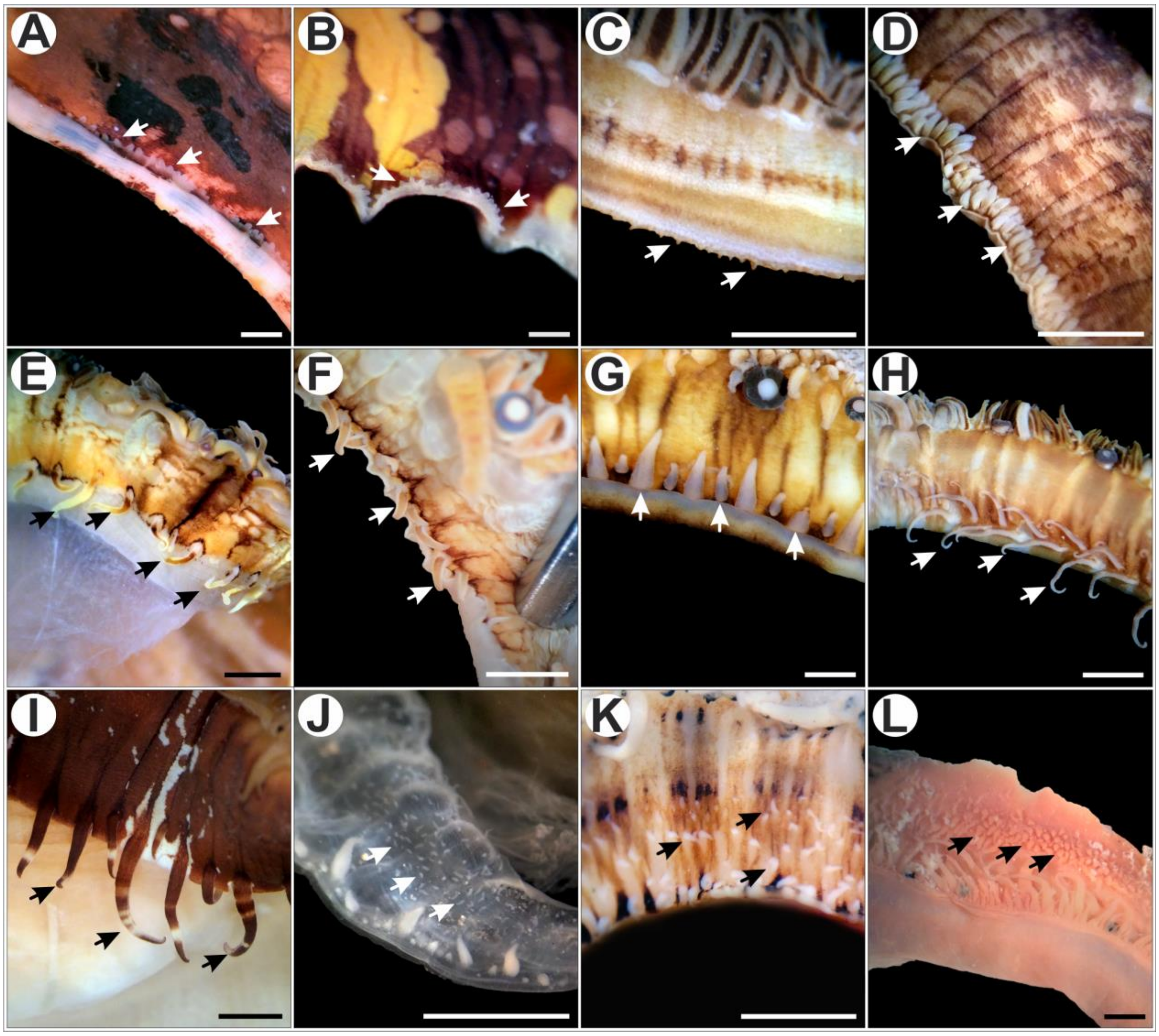

Figure 3. Tentacles on the inner mantle fold of Pectinidae (arrows). Spondylidae (A-B), Pectinidae (C-L). Scale bars=1mm. **A.** *Spondylus squamosus* (USNM793728). **B.** *Spondylus americanus* (USNM833744). **C.** *Pedum spondyloideum* (USNM793736). **D.** *Crassodoma gigantea* (SBMNH466682). **E.** *Euvola raveneli* (USNM801009). **F.** *Amusium sp.* (USNM804083). **G.** *Argopecten irradians* (MCZ278251). **H.** *Lindapecten muscosus* (USNM855448). **I.** *Gloripallium pallium* (USNM701201). **J.** *Delectopecten vitreus* (USNM757159). **K.** *Zygochlamys patagonica* (USNM886527). **L.** *Adamussium colbecki* (USNM886965).

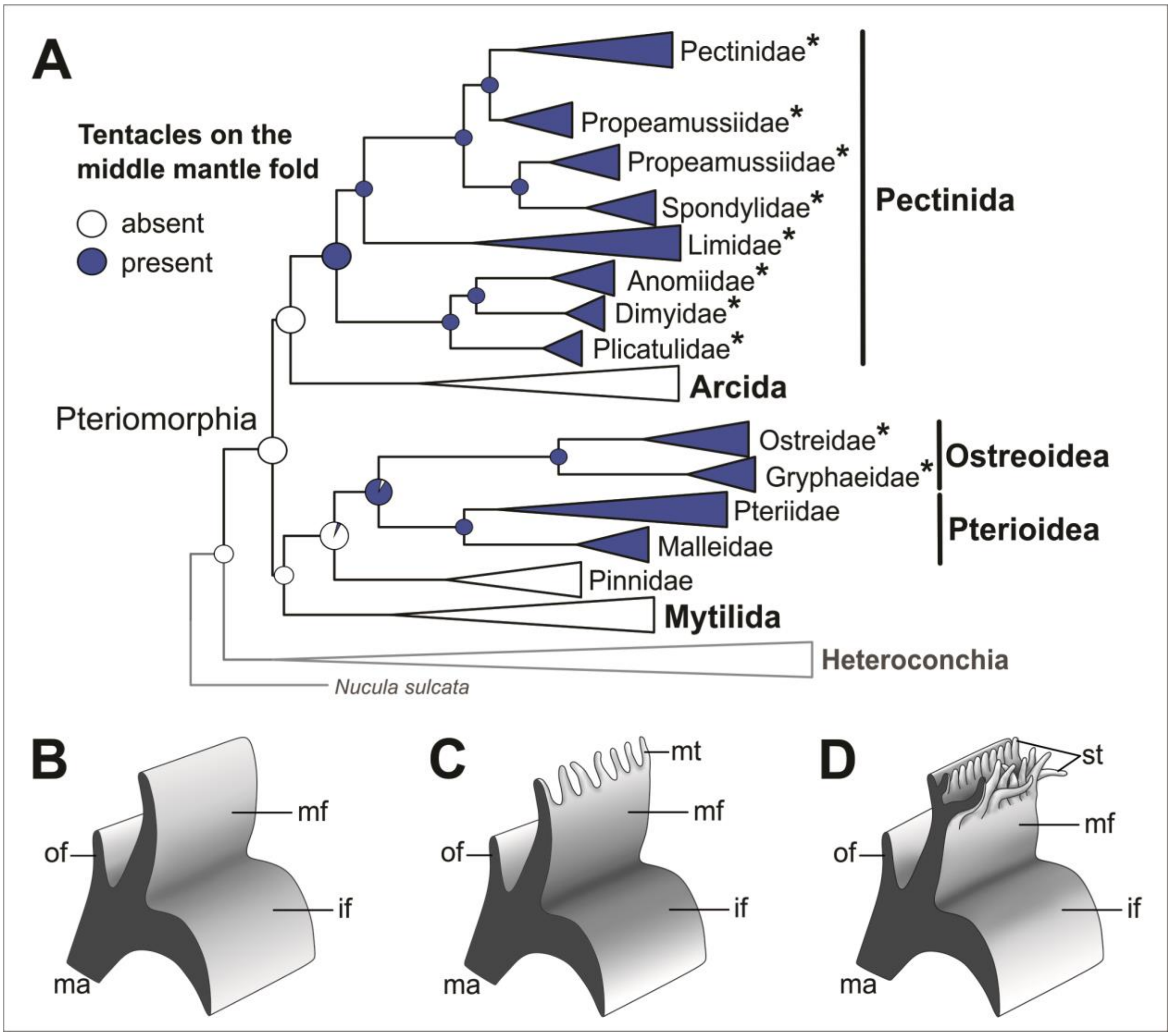

Figure 4. Evolution of middle fold tentacles in Pteriomorphia. A. Maximum likelihood reconstruction of middle fold tentacles (MFT) indicates two independent gains: in the ancestor of Pectinida and in the ancestor of the clade Ostreoidea+Pterioidea. Likelihood proportions for ancestral states are indicated in pie charts. Tentacles can either be marginal (C) or submarginal (asterisks, D). **B-D.** Schematic representation of the mantle margin; inner fold tentacles are not represented. **B.** Mantle margin devoid of MFT. **C.** Marginal MFT. **D.** Submarginal MFT. Abbreviations: if, inner mantle fold; ma, mantle; mf, middle mantle fold; mt, marginal tentacles; of, outer mantle fold; st, submarginal tentacles.

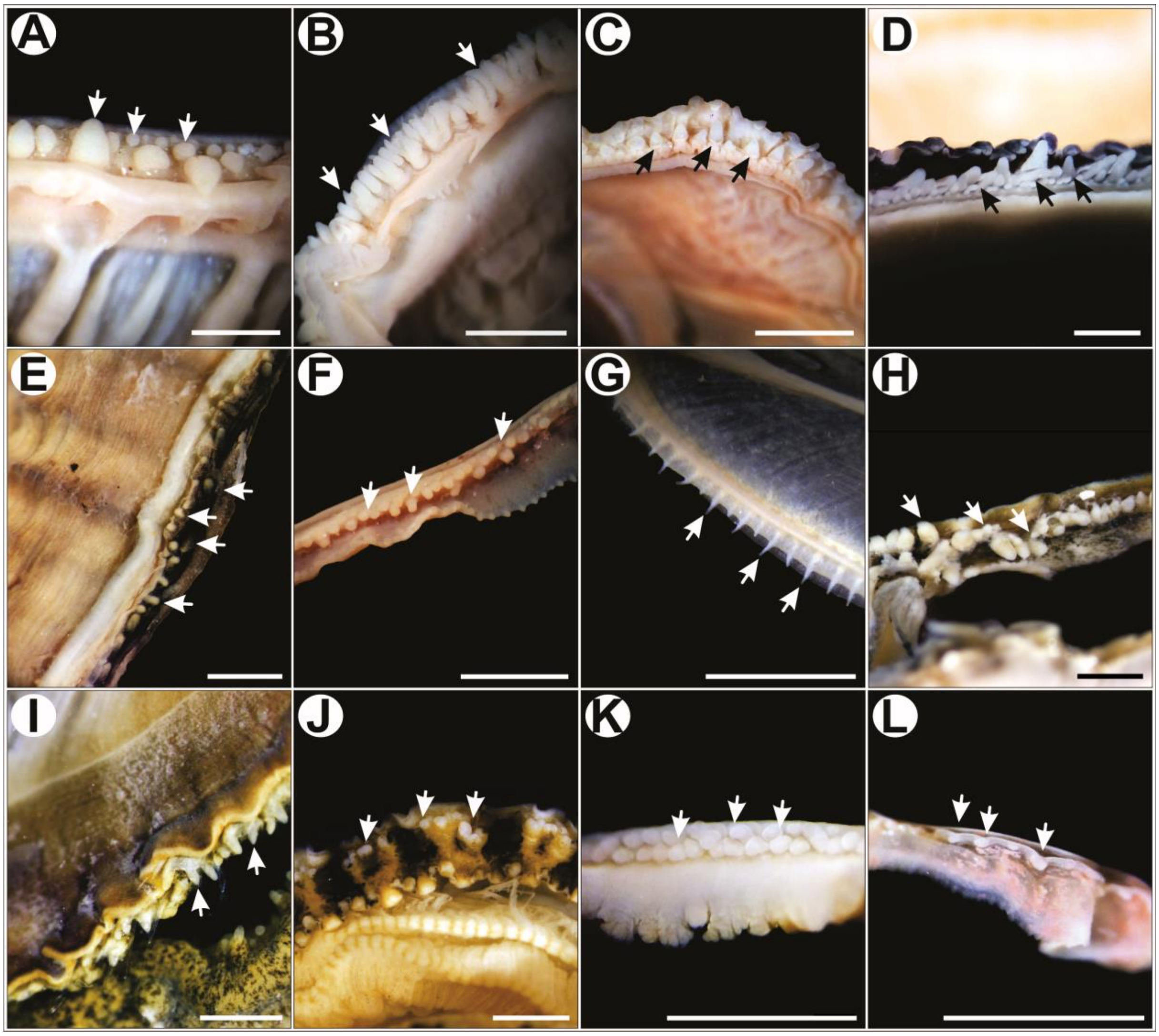

Figure 5. Tentacles on the middle mantle fold of Ostreida (arrows). Ostreidae (A-D), Gryphaeidae (E-F), Malleidae (G), Pteriidae (H-L). Scale bars=1mm. **A.** *Ostrea edulis* (USNM836256). **B.** *Crassostrea virginica* (USNM804279). **C.** *Dendostrea folium* (USNM802346). **D.** *Striostrea prismatica* (SBMNH211884). **E.** *Hyotissa hyotis* (MCZ378999). **F.** *Neopycnodonte cochlear* (MCZ379076). **G.** *Malleus candeanus* (MCZ340681). **H.** *Pteria hirundo* (ZUEC-BIV1401). **I.** *Isognomon isognomum* (MZSP54988). **J.** *Pinctada imbricata* (MZSP106549). **K.** *Vulsella minor* (USNM896263). **L.** *Electroma alacorvi* (USNM801689).

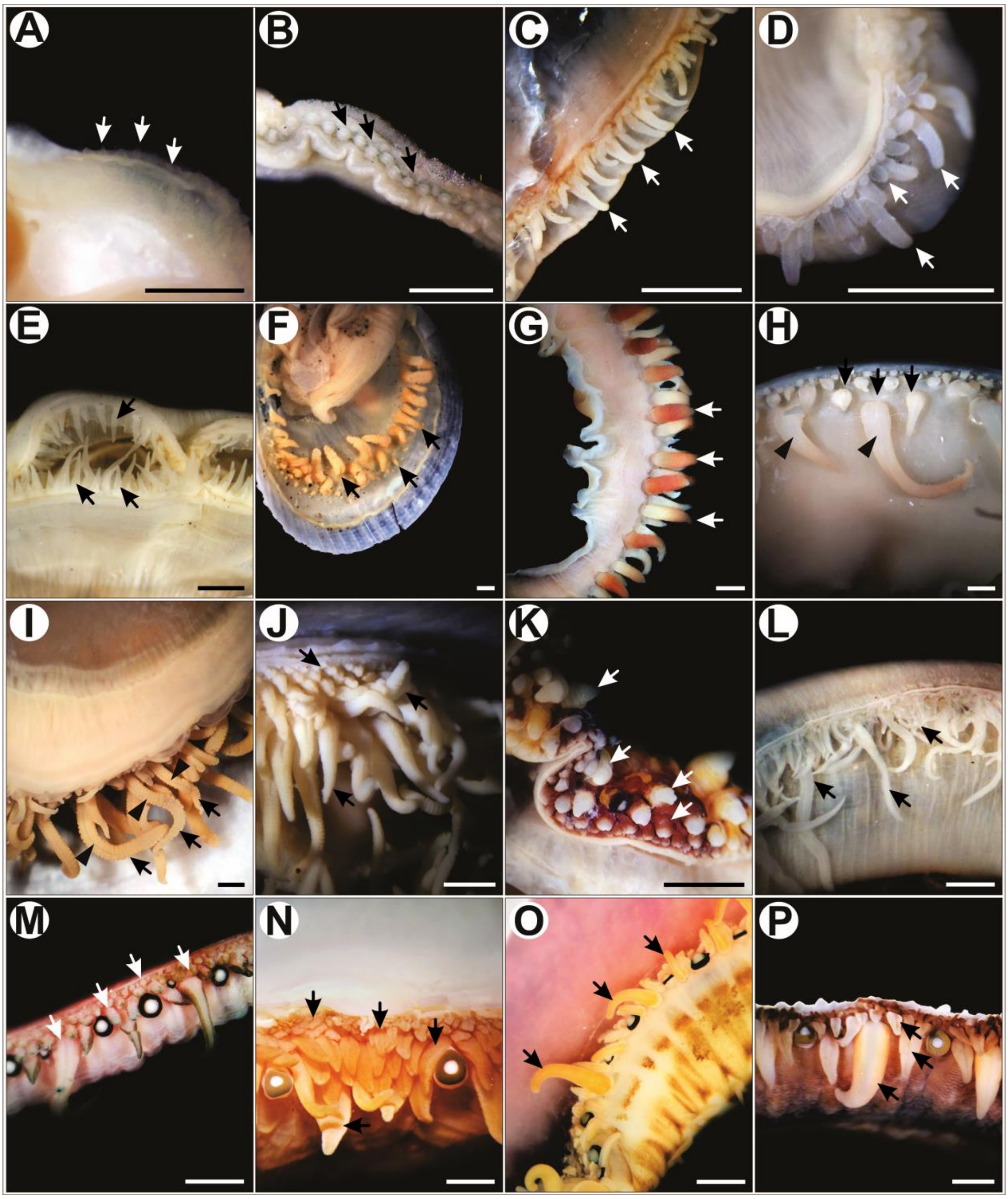

Figure 6. Tentacles on the middle fold of Pectinida (arrows). Dimyidae (A), Plicatulidae (B), Anomiidae (C-E), Limidae (F-J), Spondylidae (K), Propeamussiidae (L), Pectinidae (M-P). Longitudinal grooves are indicated by arrowheads. Scale bars=1mm. **A.** *Dimya argentea* (USNM855224). **B.** *Plicatula gibbosa* (USNM801022). **C.** *Pododesmus macrochisma* (SBMNH361457). **D.** *Pododesmus rudis* (USNM850821). **E.** *Anomia simplex* (ZUEC-BIV1423). **F.** *Limatula hodgsoni* (USNM882395). **G.** *Lima lima* USNM754383. **H.** *Acesta oophaga* (USNM1263635). **I.** *Ctenoides scaber* (USNM833716). **J.** *Limaria orbignyi* (SBMNH19892). **K.** *Spondylus senegalensis* (USNM1086035). **L.** *Propeamussium dalli* (USNM856943). **M.** *Placopecten magellanicus* (USNM829091). **N.** *Crassodoma gigantea* (SBMNH466682). **O.** *Palliolum tigerinum* (MCZ376695). **P.** *Chlamys hastata* (USNM739716).

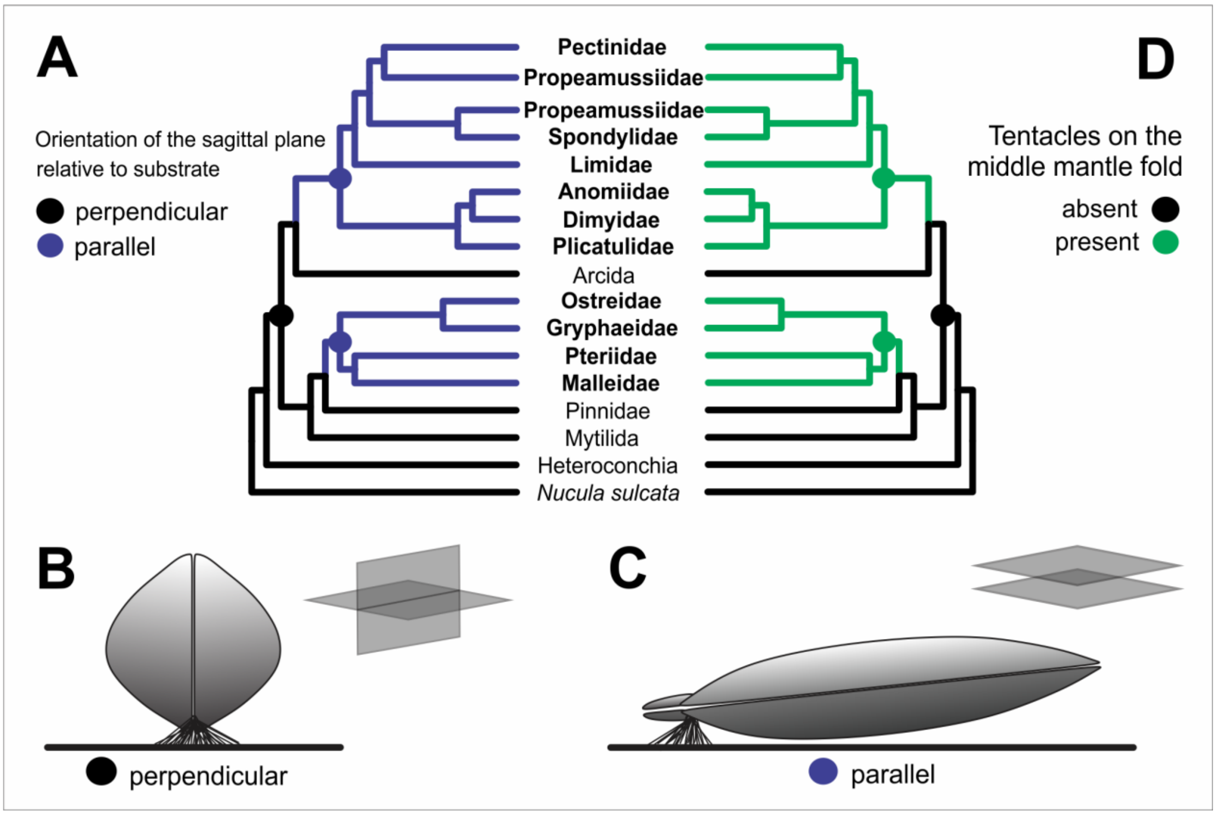

Figure 7. Evolution of tentacles and body position in Pteriomorphia. A. Reconstruction of sagittal plane orientation on the substrate (body position). The sagittal plane defines the left and right sides of the bivalve body. The ancestor of Pteriomorphia likely had the sagittal plane perpendicular to the substrate (**B**), making the ventral mantle region face the surface. This is the typical position adopted by many epifaunal bivalves, such as mussels and ark clams. In two independent events, the sagittal plane orientation was shifted to parallel (**C**). In scallops, oysters, file clams, and other representatives from the clades coded in blue, the body is supported by one valve only, leaving the entire mantle margin exposed above the substrate. **D.** Same reconstruction indicated in Figure 4 for middle fold tentacles evolution.

Table 1. Pteriomorphian taxa investigated, respective catalog numbers and collections, and summary of the survey on tentacle presence and position. Abbreviations: IFT, inner fold tentacles; MCZ; Museum of Comparative Zoology; MFT, middle fold tentacles; MZSP; Museum of Zoology of the University of São Paulo; SBMNH, Santa Barbara Museum of Natural History; USNM, Smithsonian National Museum of Natural History; ZUEC-BIV, Museum of Zoology “Prof. Adão José Cardoso” of the University of Campinas. Tentacle absence is indicated by “–”.

Taxa	**Catalog number**	**IFT**	**MFT**
Plicatulidae			
Plicatula gibbosa	USNM801020, USNM801022	marginal	submarginal
Dimyidae			
Dimya argentea	USNM855224	–	submarginal
Anomiidae			
Anomia simplex	ZUECBIV1423, USNM804291 USNM804325, MCZ280425	–	submarginal
Heteranomia squamula	USNM871362, MCZ300656	–	submarginal
Pododesmus macrochisma	SBMNH361457	–	submarginal
Pododesmus rudis	USNM850821, USNM847837	–	submarginal
Limidae			
Acesta mori	MCZ384449	–	submarginal
Acesta oophaga	USNM1263635	–	submarginal
Acesta sphoni	SBMNH424265	–	submarginal
Ctenoides mitis	USNM664306, MCZ378941	–	submarginal
Ctenoides scaber	USNM833716, MCZ376728	–	submarginal
Lima lima	USNM754383	–	submarginal
Limaria fragilis	USNM700291, USNM78784	–	submarginal
Limaria hians	MCZ371725	–	submarginal
Limaria orbignyi	SBMNH19892	–	submarginal
Limaria pelucida	ZUECBIV2130, USNM850805	–	submarginal
Limatula celtica	MCZ357556	–	submarginal
Limatula hodgsoni	USNM882395	–	submarginal
Limatula pygmaea	ZUECBIV2207	–	submarginal
Limatula setifera	USNM850807	–	submarginal
Limatula subovata	ZUECBIV5733, MCZ357577	–	submarginal
Pectinidae			
Adamussium colbecki	USNM886965	submarginal	submarginal
Aequipecten glyptus	USNM803317	submarginal	submarginal

Aequipecten opercularis	MCZ371755	submarginal	submarginal
Argopecten gibbus	USNM801015, MCZ319455	submarginal	submarginal
Argopecten irradians	MCZ278251	submarginal	submarginal
Chlamys hastata	USNM739716	submarginal	submarginal
Chlamys islandica	MCZ319213	submarginal	submarginal
Crassadoma gigantea	SBMNH466682	submarginal	submarginal
Delectopecten vitreus	USNM757159	submarginal	submarginal
Euvola raveneli	USNM801009	submarginal	submarginal
Euvola ziczac	USNM833726	submarginal	submarginal
Flexopecten glaber	MCZ371469	submarginal	submarginal
Gloripallium pallium	USNM701201	submarginal	submarginal
Lindapecten muscosus	USNM855448	submarginal	submarginal
Mimachlamys munda	USNM855527, USNM855529	submarginal	submarginal
Mimachlamys varia	MCZ378918	submarginal	submarginal
Mirapecten mirificus	USNM886347	submarginal	submarginal
Palliolum tigerinum	MCZ376695	submarginal	submarginal
Pecten jacobaeus	USNM1086023	submarginal	submarginal
Pedum spondyloideum	USNM793736	submarginal	submarginal
Placopecten magellanicus	USNM829091, MCZ319444	submarginal	submarginal
Spathochlamys benedicti	USNM804647	submarginal	submarginal
Zygochlamys patagonica	USNM886527	submarginal	submarginal
Propeamussiidae			
Catillopecten eucymatus	MCZ361432	–	submarginal
Cyclopecten subimbrifer	ZUECBIV5702	–	submarginal
Parvamussium cancellatum	USNM803323, USNM856966	–	submarginal
Parvamussium pourtalesianum	ZUECBIV2265, USNM856965	–	submarginal
Propeamussium dalli	USNM803326, USNM856943	–	submarginal
Propeamussium lucidum	MCZ361413	–	submarginal
Propeamussium meridionale	USNM897961	–	submarginal
Propeamussium sp	USNM803320, USNM856941	–	submarginal
Similipecten nanus	ZUECBIV2269, USNM803327	–	submarginal
Spondylidae			
Spondylus americanus	USNM833744, USNM804280	marginal	submarginal
Spondylus senegalensis	USNM1086035	marginal	submarginal
Spondylus squamosus	USNM793728	marginal	submarginal
Pinnidae			

Atrina inflata	MZSP55029	marginal	–
Atrina maura	USNM828614	marginal	–
Atrina rigida	USNM847971	marginal	–
Atrina seminuda	ZUECBIV2135	marginal	–
Atrina serrata	USNM801651	marginal	–
Atrina vexillum	USNM793718	marginal	–
Pinna carnea	MZSP29040, USNM804284	marginal	–
Pinna muricata	USNM836526, MCZ238056	marginal	–
Pinna rudis	MZSP114038	marginal	–
Pinna saccata	USNM793744, USNM780031	marginal	–
Gryphaeidae			
Hyotissa hyotis	MCZ378999	marginal	submarginal
Hyotissa mcgintyi	MZSP118279, USNM804282	marginal	submarginal
Hyotissa numisma	USNM803328	marginal	submarginal
Hyotissa sinensis	SBMNH141713	marginal	submarginal
Neopicnodonte cochlear	MCZ379076	marginal	submarginal
Ostreidae			
Crassostrea gigas	USNM836263	marginal	submarginal
Crassostrea virginica	USNM804279	marginal	submarginal
Dendostrea folium	USNM802346	marginal	submarginal
Dendostrea frons	USNM804288, MCZ378951	marginal	submarginal
Lopha cristagalli	USNM793723	marginal	submarginal
Ostrea edulis	USNM836256, MCZ379114	marginal	submarginal
Ostrea equestris	USNM801030	marginal	submarginal
Ostrea permolis	USNM850800	marginal	submarginal
Pustulostrea australis	USNM787959	marginal	submarginal
Saccostrea cucullata	SBMNH345722	marginal	submarginal
Saccostrea palmula	USNM796192	marginal	submarginal
Striostrea prismatica	SBMNH212884	marginal	submarginal
Malleidae			
Malleus albus	MZSP55595	marginal	marginal
Malleus candeanus	USNM847920, MCZ340681	marginal	marginal
Malleus malleus	USNM802338	marginal	marginal
Malleus regula	MCZ379030	marginal	marginal
Pteriidae			
Electroma alacorvi	USNM700050, USNM801689	marginal	marginal

Electroma papilionacea	USNM616482	marginal	marginal
Isognomon alatus	MZSP89628, USNM836243	marginal	marginal
Isognomon bicolor	ZUECBIV2123	marginal	marginal
Isognomon ephippium	USNM701010	marginal	marginal
Isognomon isognomum	MZSP54988	marginal	marginal
Isognomon perna	MZSP71186, MZSP11583	marginal	marginal
Isognomon radiatus	USNM803357	marginal	marginal
Pinctada albina	USNM755664	marginal	marginal
Pinctada imbricata	ZUECBIV2383	marginal	marginal
Pinctada maculata	USNM801689	marginal	marginal
Pinctada margaritifera	USNM836493	marginal	marginal
Pinctada mazatlantica	SBMNH42703	marginal	marginal
Pinctada radiata	MZSP106549	marginal	marginal
Pteria brevialata	MZSP55575, USNM836352	marginal	marginal
Pteria colymbus	USNM801027	marginal	marginal
Pteria hirundo	MZSP10885, ZUECBIV1401	marginal	marginal
Pteria penguim	USNM801027	marginal	marginal
Vulsella minor	USNM896263	marginal	marginal
Vulsella vulsella	MZSP896263	marginal	marginal

Supplementary material

Table S1. Orientation of the sagittal plane relative to the substrate in pteriomorphian taxa included in the phylogenetic inference.

Taxa	**Orientation**
Anomiidae	
Anomia ephippium	parallel
Monia patelliformis	parallel
Pododesmus caelata	parallel
Arcidae	
Acar dominguensis	perpendicular
Acar plicata	perpendicular
Anadara antiquata	perpendicular
Anadara broughtonii	perpendicular
Anadara cornea	perpendicular
Anadara crebricostata	perpendicular
Anadara globosa	perpendicular
Anadara gubernaculum	perpendicular
Anadara inaequivalvis	perpendicular
Anadara notabilis	perpendicular
Anadara pilula	perpendicular
Anadara subcrenata	perpendicular
Anadara trapezia	perpendicular
Anadara vellicata	perpendicular
Arca imbricata	perpendicular
Arca navicularis	perpendicular
Arca noae	perpendicular
Arca patriarchalis	perpendicular
Arca ventricosa	perpendicular
Arca zebra	perpendicular
Barbatia barbata	perpendicular
Barbatia cancellaria	perpendicular
Barbatia candida	perpendicular
Barbatia fusca	perpendicular
Barbatia lacerata	perpendicular
Barbatia lima	perpendicular
Barbatia virescens	perpendicular
Bathyarca glomerula	perpendicular
Lunarca ovalis	perpendicular
Tegillarca granosa	perpendicular
Tegillarca nodifera	perpendicular
Trisidos kiyonoi	perpendicular
Trisidos tortuosa	perpendicular
Cucullaeidae	
Cucullaea labiata	perpendicular
Dimyidae	
Dimya lima	parallel
Glycymerididae	
Glycymeris gigantea	perpendicular
Glycymeris glycymeris	perpendicular
Glycymeris holoserica	perpendicular
Glycymeris nummaria	perpendicular
Glycymeris septentrionalis	perpendicular
Glycymeris tenuicostata	perpendicular
Tucetona pectinata	perpendicular
Gryphaeidae	
Hyotissa hyotis	parallel
Hyotissa imbricata	parallel
Hyotissa mcgintyi	parallel
Hyotissa numisma	parallel
Neopicnodonte cochlear	parallel
Limidae	
Acesta excavata	parallel
Ctenoides annulatus	parallel
Ctenoides mitis	parallel
Ctenoides scaber	parallel
Lima lima	parallel
Limaria hians	parallel
Limopsidae	
Limopsis cumingi	perpendicular

Limopsis enderbyensis	perpendicular
Limopsis marionensi	perpendicular
Limopsis sp.	perpendicular
Malleidae	
Malleus albus	parallel
Malleus candeanus	parallel
Malleus malleus	parallel
Malleus regula	parallel
Mytilidae	
Bathymodiolus mauritanicus	perpendicular
Bathymodiolus thermophilus	perpendicular
Benthomodiolus lignocola	perpendicular
Benthomodiolus geikotsucola	perpendicular
Brachidontes darwinianus	perpendicular
Brachidontes exustus	perpendicular
Brachidontes rodriguezii	perpendicular
Dacrydium sp.	perpendicular
Geukensia demissa	perpendicular
Gregariella coarctata	perpendicular
Idas washingtonia	perpendicular
Ischadium recurvum	perpendicular
Leiosolenus curtus	perpendicular
Lithophaga antillarum	perpendicular
Lithophaga lithophaga	perpendicular
Lithophaga nigra	perpendicular
Modiolus auriculatus	perpendicular
Modiolus modiolus	perpendicular
Modiolus philippinarum	perpendicular
Modiolus rumphii	perpendicular
Musculista senhousia	perpendicular
Musculus discors	perpendicular
Musculus niger	perpendicular
Mytilus californianus	perpendicular
Mytilus edulis	perpendicular
Mytilus galloprovincialis	perpendicular
Mytilus trossulus	perpendicular
Perna perna	perpendicular
Perna viridis	perpendicular
Perumytilus purpuratus	perpendicular
Septifer bifurcatus	perpendicular
Septifer virgatus	perpendicular
Xenostrobus securis	perpendicular
Noetiidae	
Arcopsis adamsi	perpendicular
Didimacar tenebrica	perpendicular
Eontia ponderosa	perpendicular
Striarca lactea	perpendicular
Ostreidae	
Crassostrea gigas	parallel
Crassostrea virginica	parallel
Dendostrea frons	parallel
Lopha cristagalli	parallel
Ostrea edulis	parallel
Saccostrea cucullata	parallel
Pectinidae	
Adamussium colbecki	parallel
Aequipecten opercularis	parallel
Amusium balloti	parallel
Argopecten gibbus	parallel
Argopecten irradians	parallel
Chlamys hastata	parallel
Chlamys islandica	parallel
Crassadoma gigantea	parallel
Euvola ziczac	parallel
Excellichlamys spectabilis	parallel
Flexopecten glaber	parallel
Mimachlamys varia	parallel
Mizuhopecten yessoensis	parallel
Palliolum tigerinum	parallel

Pecten jacobaeus	parallel
Pecten maximus	parallel
Placopecten magellanicus	parallel
Pinnidae	
Atrina assimilis	perpendicular
Atrina chautardi	perpendicular
Atrina exusta	perpendicular
Atrina fragilis	perpendicular
Atrina pectinata	perpendicular
Atrina rigida	perpendicular
Atrina seminuda	perpendicular
Atrina vexillum	perpendicular
Pinna atropurpurea	perpendicular
Pinna bicolor	perpendicular
Pinna carnea	perpendicular
Pinna dolabrata	perpendicular
Pinna muricata	perpendicular
Pinna nobilis	perpendicular
Pinna rudis	perpendicular
Pinna saccata	perpendicular
Pinna trigonalis	perpendicular
Philobryidae	
Adacnarca nitens	perpendicular
Lissarca notorcardensis	perpendicular
Neocardia sp.	perpendicular
Philobrya magellanica	perpendicular
Philobrya sublaevis	perpendicular
Plicatulidae	
Plicatula australis	parallel
Plicatula plicata	parallel
Propeamussiidae	
Parvamussium pourtalesianum	parallel
Propeamussium dalli	parallel
Propeamussium sibogai	parallel
Propeamussium sp	parallel

Pteriidae	
Crenatula avicularis	parallel
Electroma alacorvi	parallel
Electroma papilionacea	parallel
Isognomon alatus	parallel
Isognomon bicolor	parallel
Isognomon californicum	parallel
Isognomon ephippium	parallel
Isognomon isognomum	parallel
Isognomon legumen	parallel
Isognomon perna	parallel
Isognomon radiatus	parallel
Pinctada albina	parallel
Pinctada capensis	parallel
Pinctada fucata	parallel
Pinctada imbricata	parallel
Pinctada longisquamosa	parallel
Pinctada maculata	parallel
Pinctada margaritifera	parallel
Pinctada maxima	parallel
Pinctada mazatlantica	parallel
Pinctada nigra	parallel
Pinctada radiata	parallel
Pteria avicular	parallel
Pteria brevialata	parallel
Pteria colymbus	parallel
Pteria hirundo	parallel
Pteria howensis	parallel
Pteria loveni	parallel
Pteria penguim	parallel
Vulsella vulsella	parallel
Spondylidae	
Spondylus ambiguus	parallel
Spondylus crassisquamatus	parallel
Spondylus hystrix	parallel
Spondylus ictericus	parallel

Spondylus sinensis	parallel
Outgrup	
Chione elevata	perpendicular
Donax trunculus	perpendicular
Hiatella arctica	perpendicular
Macoma balthica	perpendicular
Margaritifera margaritifera	perpendicular
Mya arenaria	perpendicular
Neotrigonia lamarckii	perpendicular
Nucula sulcuta	perpendicular
Nuculana minuta	perpendicular
Solemya velum	perpendicular
Yoldia limatula	perpendicular
Antalis entalis	perpendicular
Chaetopleura apiculata	perpendicular
Haliotis tuberculata	perpendicular
Laevipilina hyalina	perpendicular

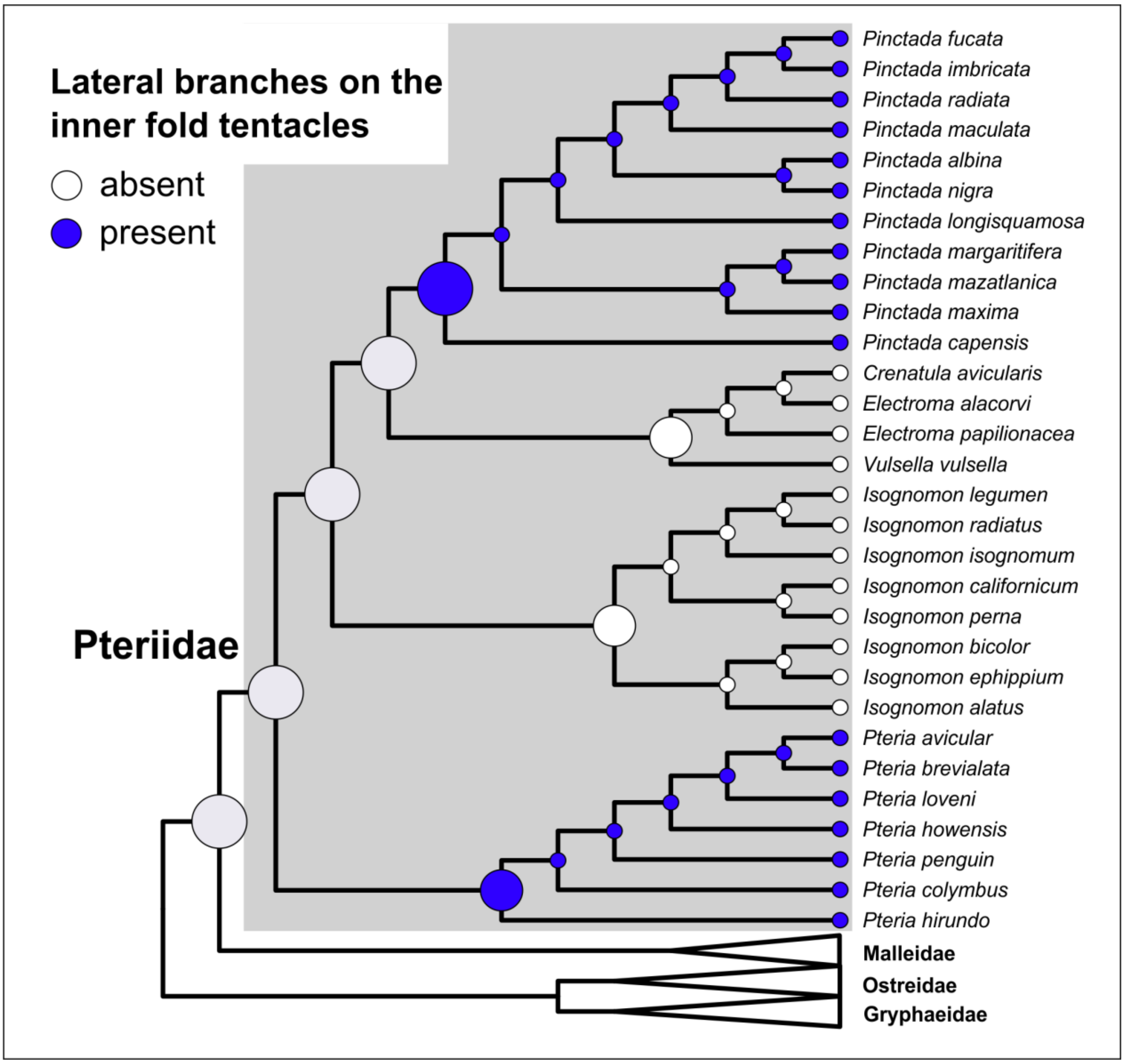

Figure S1. Evolution of branched tentacles on the inner fold. Tentacles with lateral branches were acquired twice in the genera *Pinctada* and *Pteria*. Likelihood proportions for ancestral states are indicated in pie charts. The grey box comprises the family Pteriidae.

CHAPTER 5

Comparative and functional anatomy of the mantle margin in ark clams and their relatives (Bivalvia: Arcoidea) supports association between morphology and life habits

CHAPTER 5

Comparative and functional anatomy of the mantle margin in ark clams and relatives (Bivalvia: Arcoidea) supports association between morphology and life habits

---

Abstract

Evaluating the association between ecology and the evolution of morphological traits is a central question of macroevolutionary studies. The Arcoidea comprises several lineages of epibyssate (epifaunal) and endobyssate (semi-infaunal or infaunal) bivalves, which makes them a suitable model for analyzing the implications of similar life habits on phenotype. Also, the families current assigned to the clade (Arcidae, Cucullaeidae, Glycymerididae, and Noetiidae) exhibit great variation in the mantle margin, a region responsible for interacting with the surrounding environment and provided with sensory structures (e.g., photoreceptor organs). Consequently, this anatomical region includes traits relevant for testing hypotheses of morphological attributes associated with lifestyles. For this purpose, we investigated the detailed anatomy of the mantle margin of three arcoidean species (i.e., *Arca imbricata*, *Barbatia candida,* and *Arcopsis adamsi*) applying integrative microscopy, and complemented the study with basic morphological analysis of 27 species obtained in museum collections. Secretory cells, muscle fibers and sensory organs are described in detail, including sensory ciliated cells of the inner mantle fold, reported for the first time. Our results corroborate a very reduced to absent middle fold in arcoideans, with transfer of sensory functions to the first outer and inner folds. Moreover, our data indicates association of some pallial characters with life habits, i.e., presence of pallial pigmentation and photoreceptor organs in epibyssates, and development of an enlarged pallial curtain in endobyssates, which should stimulate further investigations on these potentially adaptive morphological features.

Keywords: bivalve, epibyssate, endobyssate, lifestyle, pallial fold, sensory

This is the accepted version of the following article: *Comparative and functional anatomy of the mantle margin in ark clams and relatives (Bivalvia: Arcoidea) supports association between morphology and life habits*, which has been published in final form at *Journal of Zoology* 305(3): 149-162 (2018), https://doi.org/10.1111/jzo.12544

Introduction

Unrelated lineages may evolve similar features when transitioning to a similar environment (Losos, 2011). Given that convergences are potentially adaptive (i.e., the result of similar selective pressures), the study of convergent evolution in similar contexts (e.g., habitats, climate, life habits) may provide new insights into the factors that influence the evolution and diversification of life (Agrawal, 2017). Also, convergent phenotypes may hinder the understanding of the phylogeny of a taxon, leading to considerable confusion in the taxonomy of many animal groups (e.g., Daniels et al., 2006; Jörger et al., 2010). Therefore, a thorough comprehension of convergences may lead not only to a more complete understanding of the evolution of a particular group, but also provide insights into exciting questions in macroecology. Studies using marine invertebrates to test hypotheses on convergent evolution have been, however, scarce (Lindgren et al., 2010; Serb et al., 2011).

In this context, the evolution of arcoidean bivalves (order Arcida, superfamily Arcoidea) shows well-defined patterns of morphological variation and ecological diversity. Trends into epibyssate and endobyssate forms are strongly correlated with the adoption of different modes of life, i.e., epifaunal on hard substrate and semi-infaunal/infaunal in soft-sediment, respectively (Stanley, 1972). The evolutionary and ecological radiations of Arcoidea suggest the presence of numerous homoplasies possibly associated with transitions between modes of life (Oliver & Holmes, 2006), making this group an excellent model for evolutionary studies on adaptation and macroecology.

The family Arcidae represents the most diverse arcoidean group and is organized in two subfamilies, i.e., Arcinae and Anadarinae. Most Arcinae are epibyssate bivalves living attached on rocks or corals. Anadarinae comprises endobyssate forms, and their phylogeny suggests a transition from semi-infaunal to completely infaunal habits (Oliver & Holmes, 2006). The remaining arcoidean families display a variety of morphological patterns and modes of life. The Glycymerididae include abyssate shallow burrowers (Thomas, 1975) while epibyssate and endobyssate forms occur in the Noetiidae (MacNeil, 1938; Stanley, 1972). The Cucullaeidae have a very rich fossil record (Nicol, 1954), although they are currently represented by a single shallow burrowing species (Morton, 1981).

The bivalve mantle margin is a complex organ deeply associated with the animal's mode of life (Yonge, 1983). Therefore, a wide range of mantle margin structures represent presumed adaptive traits relevant for phylogenetic, macroecological, and anatomical studies (Audino & Marian, 2016), and Arcoidea is probably no exception. Given that some morphological attributes (i.e., rectangular shell, well-developed foot/byssus musculature) are typical of distinct lineages of epibyssate arcoideans (Stanley, 1972; Oliver & Holmes, 2006), it is reasonable to expect similar associations between mantle margin organization and life habits. For example, previous studies consistently describe the presence of pallial photoreceptor organs in epifaunal arcoideans, including pigmented eyespots and large compound eyes (Waller, 1980; Nilsson, 1994; Morton & Peharda, 2008; Morton & Puljas, 2015). In the endobyssate *Anadara notabilis*, however, only a few pigmented cups might be present in the anterodorsal region, suggesting reduction of photoreception organs in burrowing species (Nilsson, 1994). However, the knowledge of the mantle margin of arcoideans is still fragmented, data for Anadarinae, Noetiidae and other lineages being still necessary to carefully evaluate pallial evolution in the group.

Thus, in a first attempt to infer functional implications of pallial organization in the group, and shed light on possible morphological patterns associated with distinct life habits, we have applied integrative microscopy techniques to investigate in detail the mantle margin of three arcoidean species, i.e., *Arca imbricata* (Arcidae), *Barbatia candida* (Arcidae), and *Arcopsis adamsi* (Noetiidae), and complemented the study with basic morphological analysis of 27 species obtained from archived specimens (including Arcidae, Noetiidae, and Glycymerididae).

Material and Methods

Sample collection and fixation

Specimens of *Arca imbricata*, *Barbatia candida*, and *Arcopsis adamsi* were collected in rocky shores during low tide in Araçá Bay (São Sebastião, State of São Paulo, Brazil). The animals were attached by the byssus to the surface or crevices of hard substrata (mainly rocks; Fig. 1A), and individuals of *B. candida* were also found attached to fragments of dead coral. All individuals were anesthetized in a 7.5% solution of $MgCl_2$ mixed with seawater for 3 h prior fixation. For histology and scanning electron microscopy (SEM), fragments of the mantle margin were dissected and fixed for 3 h at 4 °C in a modified Karnovsky solution and stored in cacodylate buffer (Marian, 2012). For confocal laser scanning microscopy (CLSM), samples were fixed in 4% paraformaldehyde in 0.1 M phosphate buffered (PB) for 2 h, followed by three rinses with buffer solution.

Mantle margin morphology was also examined in other 27 arcoidean species from the collections of Museum of Zoology “Prof. Adão José Cardoso” of the University of Campinas

(ZUEC), Museum of Zoology of the University of São Paulo (MZSP), and Santa Barbara Museum of Natural History (SBMNH) (Table 1). When necessary, samples from the mantle margin were removed and prepared for histology to clarify the anatomical organization (see Table 1). Morphological data on *Cucullaea* was obtained from literature (Waller 1980), as well as life habits data for most species considered herein (e.g., Valentich-Scott 2003, Oliver & Holmes 2006).

Histological procedures

Samples were dehydrated in graded ethanol series and then embedded in glycol-methacrylate resin (Leica Historesin Kit, Germany). Serial sections of 3 μm were obtained on a Leica RM2255 microtome (Leica, Germany). Staining methods included hematoxylin and eosin (HE) and toluidine blue and basic fuchsin (TB-BF). To evidence mucosubstances in secretory cells, simple histochemical methods were applied using periodic acid-Schiff stain (PAS) and alcian blue (AB) for glycoconjugates having neutral or acidic carbohydrates, respectively (Bancroft & Stevens, 1982).

Scanning Electron Microscopy

Post-fixation, dehydration, preparation of samples in stubs, and analysis were performed as described in Audino et al. (2015a).

Confocal Laser Scanning Microscopy

Samples were permeabilized and incubated in Alexa Fluor 488 phalloidin (Molecular Probes, USA; for F-actin staining) according to Audino et al. (2015a). Then, samples were washed three times in PBS for about 15 min prior mounting in ProLong Diamond Antifade Mountant with DAPI (Molecular Probes, USA) on standard microscope slides. Analysis and image acquisition were performed on a ZEISS LSM 880 confocal laser scanning microscope (Zeiss, Germany). Confocal image stacks were recorded with 2 μm step size along the z-axis and digitally merged as maximum intensity projections in the software ZEN lite 2.3 (Zeiss, Germany). Samples of *A. imbricata* were revealed to be unsuitable for CLSM because of the intense pallial pigmentation, preventing CLSM data acquisition for this species.

Results

To avoid redundancy, we first describe all relevant features observed in the mantle margin of *Arcopsis adamsi*. Then, for the remaining species, we only describe major differences and variations. A summary of the mantle margin structure of all studied taxa is presented in Table 2.

Mantle margin anatomy in Noetiidae

The mantle margin of the epibyssate *Arcopsis adamsi* is uniform throughout its extension, not pigmented, and slightly longer posteriorly (Fig. 1B). Four folds are present in the margin, i.e., first and second outer folds, middle and inner folds (Fig. 1C: of-1, mf, if,), the second outer fold being very thin and projecting from the mantle near the attachment of the pallial muscles to the shell. Small, dark eyespots, covered by the periostracum, are present at the anterior dorsal region of the first outer fold of each pallial lobe. The middle fold is short compared to the longer, undulate inner fold (Fig. 1C, D: mf, if). Both structures are densely covered by short cilia (Fig. 1E). A second type of cilia is also present on the inner fold. In this case, the cilium is more than twice longer than ordinary cilia (Fig. 1F, G). These long-cilium bearing cells are irregularly distributed, and occur mainly on the outer surface of the inner fold at the posterior region. Musculature of the mantle margin is mostly composed of radial and commarginal fibers in the inner fold (Fig. 1H, I), resulting in a very muscular and flexible organ, as observed in living specimens. Commarginal muscles fibers are parallel to the mantle margin; radial muscles extend radially to the mantle margin, but some fibers deviate from the general straight pattern and are not parallel to the regular radial fibers (Fig. 1H, I). Pallial nerves were not identified in cross-sections. Few epithelial gland cells were found, while subepithelial secretory cells with eosinophilic and PAS-positive granular content are abundant in the mantle and mantle folds, except the outer ones (Fig. 1J). Staining affinities of the secretory contents of the mantle margin gland cells are summarized in Table 3.

Mantle margin in Noetiidae can vary significantly. In the endobyssates *Noetia ponderosa* and *Sheldonella bisulcata* (Fig. 2A), the first outer fold bears no photosensitive structures and the margin is uniformly unpigmented. In these species, the middle fold is lacking, and the inner fold is an enlarged muscular organ (Fig. 2B: if), forming an undulate pallial curtain posteriorly. In contrast, the unpigmented mantle margin in the epibyssate *Striarca symmetrica* comprises four pallial folds (Fig. 2C, D), with the middle and inner folds, and the whole inner pallial epithelium densely ciliated (as observed under light microscopy). Differently from *A. adamsi*, the mantle folds in *S. symmetrica* are similar in length and the first fold bears compound eyes (Fig. 2D: ce). Pallial margin of the epibyssate *Didimacar tenebrica* closely resembles *A. adamsi*, with unpigmented margin and dark eyespots in the anterodorsal region.

Mantle margin anatomy in Glycymerididae

In contrast to the variable morphology observed in the mantle margin of other arcoidean families, the Glycymerididae display a uniform pallial organization (Table 2). In *Glycymeris decussata*, *G. longior* (Fig. 2E, F), *G. undata*, and *Tucetona pectinata* (Fig. 2G, H), the mantle margin is pigmented posteriorly and has two outer folds and an inner fold. Folds are short, similar in length, and no elongated pallial curtain is formed (Fig. 2E-H). The first outer fold bears compound eyes distributed on both sides of the posteroventral region (Fig. 2F, H: ce). In *G. longior*, PAS-positive gland cells are present in the inner and outer folds, and AB-positive content was detected in subepithelial cells of the inner fold (Table 3).

Mantle margin anatomy in Arcidae

Pallial morphology in Arcidae is remarkably diverse, varying in number and relative size of folds, and sensory structures (Table 2). In the epifaunal *Barbatia candida*, the mantle margin is slightly pigmented posteriorly and no compound eyes are present (Fig. 3A). The margin is progressively more developed toward the posterior region where the inner fold is longer and undulate (Fig. 3B). Four pallial folds are present (Fig. 3C). At the most dorsal region, the first outer fold bears pigmented eyespots (Fig. 3I), which are simple photosensitive structures, with an amorphous, secreted lens. The middle fold is the shortest while the inner fold is much longer than the other folds, exhibiting a curtain-like morphology (Fig. 3C, D: if). Short cilia cover the surface of the middle and inner folds (Fig. 3E, F). Long, isolate cilia (Fig. 3G, H), similar to those observed in *A. adamsi*, occur on the inner fold, being irregularly distributed on the outer surface of the posterior region. Musculature is more developed in the inner fold (Fig. 3J). Radial fibers are more parallel between each other than in *A. adamsi*, resulting in a perpendicular pattern with the commarginal muscles. A section of a pallial nerve was identified in a proximal position, distant from the mantle margin (Fig. 3K: pn). Secretory cells were identified in the pallial folds, most of them distributed beneath pallial epithelia (Fig. 3K, L). The glandular content is strongly positive to PAS and AB on the outer pallial epithelium (Fig. 3L; Table 3), while gland cells of the middle and inner folds and those of the inner pallial epithelium show reactivity to eosin, TB-BF (pink; Fig. 3K), and PAS.

In the epibyssate *Arca imbricata*, the mantle margin is highly pigmented with two outer folds and an inner fold. The first outer fold and the inner fold have similar lengths (Fig. 4A: of-1, if). The first outer fold bears small eyespots (pigmented cups) along the anteroventral edge, and large compound eyes posteriorly (Fig. 4A, B: ce). The photosensitive cells that form the compound eyes are covered by microvilli (Fig. 4C) and surrounded by pigmented cells (Fig. 4D: ph, pi). The inner fold is densely covered by cilia (Fig. 4E), and numerous small droplets were observed on its surface (Fig. 4F, G), suggesting intense secretion in this region. Accordingly, abundant epithelial and subepithelial gland cells were observed in both inner and first outer folds. Glands from the latter are strongly eosinophilic (Fig. 4A), PAS-positive (Fig. 4H), with granular content (Table 3). Subepithelial glands of the inner fold, in turn, show intense reaction to HE (Fig. 4A), being positive to both PAS and AB (Fig. 4H, I; Table 3).

In other epifaunal arcoideans, compound eyes are also restricted to the ventro-posterior region (Fig. 5A-G: ce), and always formed in the first outer fold (Table 2). In *Acar plicata* (Fig. 5A, B), *Acar dominguensis* (Fig. 5C, D), *Arca patriarchalis*, *Arca ventricosa*, *Arca zebra* (Fig. 5E, F), *Barbatia amygdalumtostum* and *Barbatia cancellaria* (Fig. 5G, H), the compound eyes are very similar in structure, as described above for *A. imbricata*. In these species, the mantle margin is strongly pigmented posteriorly, except for *A. plicata* (Fig. 5A), and pigmented eyespots are present at the anteroventral region (e.g., Fig. 5H: pc). The *Arca* group lacks the middle fold (Fig. 5F), while both middle and inner folds are present in *Acar* (Fig. 5B, D: mf) and *Barbatia* (Fig. 5H: mf). In these cases, the middle fold is shorter than the first outer fold, while the inner fold is longer than the remaining folds, forming a pallial curtain (Table 2, Fig. 5B, D, H).

Pallial morphology in endobyssate arcids, which includes the genera *Anadara*, *Bathyarca*, *Trisidos*, and *Tegillarca* is remarkably different from the general condition described for epibyssate forms (Table 2). All species, but *Anadara ovalis* (Fig. 5K), display a uniform mantle margin, almost unpigmented (Fig. 5I, M, O). Photoreceptor organs are absent, except for anterodorsal eyespots, as observed in *Anadara notabilis* and *A. ferruginea*. Four pallial folds are usually present, as observed in *A. inaequivalvis* (Fig. 5P), *A. notabilis* (Fig. 5J), and *Tegillarca granosa* (Fig. M, N). However, all endobyssate species show a strong reduction of the middle fold, with its maximum length being half of the length of the first outer fold (e.g., Fig. 5J, N, P: mf, of-1; Table 2). In the case of *A. ovalis*, the middle fold is lacking (Fig. 5L). The inner fold of *Anadara*, *Bathyarca* and *Tegillarca* is greatly enlarged posteriorly, forming a long pallial curtain (e.g., Fig. 5I-P: if; Table 2). PAS- and AB-positive content was detected in subepithelial and epithelial cells of both inner and outer folds of *A. ovalis* (Table 3). In contrast, strong eosinophilic gland cells, also stained with TB-BF (pink), were present only in the inner fold (Table 3).

Discussion

Comparative anatomy

The presence of a second outer fold is regarded as an exclusive feature of arcoideans (Waller, 1980; Morton & Peharda, 2008). The first outer fold is also present in all Arcoidea, being a thick projection in *Arca* and *Glycymeris*. This fold is commonly pigmented in epifaunal species, mainly posteriorly, as described herein and for other *Barbatia* species (Simone & Chichvarkhin, 2004). Conversely, the first outer fold in endobyssate species is weakly pigmented or even unpigmented. Such is the case of most *Anadara*, *Bathyarca*, *Noetia*, and *Trisidos* species (e.g., Fig. 5). In Arcoidea, photosensory organs are generally located on the first outer fold (Morton, 2008; present study), always covered by transparent layers of periostracum.

Pigmented spots are simple ocelli spread on the outer fold of many genera, including *Acar*, *Anadara*, *Arca*, *Arcopsis*, *Barbatia,* and *Didimacar* (Nilsson, 1994; present study). In *Barbatia virescens*, this structure is a cluster of pigmented cup cells with an extracellular secretion, i.e., lens (Morton, 1987). The same morphological pattern was observed in the pigmented cup of *Barbatia candida* (present study, Fig. 3I) and *Anadara notabilis* (Nilsson, 1994). Compound eyes are unique photosensory structures of Arcoidea, and when present only occur posteriorly in the first outer fold. The surface and organization of the compound eyes were previously demonstrated for *Arca noae*, *Arca zebra*, *Barbatia cancellaria*, and glycymeridids (Waller, 1980; Nilsson, 1994; Morton & Peharda, 2008; Morton & Puljas, 2015). Our results show that *Acar dominguensis*, *Arca imbricata*, and *Striarca symmetrica* share a similar organization (Fig. 4B, D, 5B, D, F). The eyes are triggered by visual motion, likely working as burglar alarms for detecting predators rather than imaging eyes (Nilsson, 1994).

Middle and inner folds are usually present in the bivalve mantle margin (Yonge, 1983). Nevertheless, some arcoideans apparently lack the middle fold (e.g., *Arca*, *Glycymeris*, and *Sheldonella*). The reduction of the middle fold in *Anadara*, a trend also shared by several other species (see Table 2), suggests that this is the missing fold in some lineages. In *Arca* and *Glycymeris,* in which the mantle margin is devoid of a middle fold, the inner and the first outer fold act together as pallial curtains (Waller, 1980). Alternatively, in *Anadara, Barbatia, Bathyarca,* and *Trisidos,* the inner fold alone is a greatly enlarged pallial curtain. This is more accentuated in endobyssate forms, where the enlarged pallial curtain might act as a functional siphon (Oliver & Allen, 1980; Morton, 1982a, b).

As revealed by this study with *Barbatia candida* and *Arcopsis adamsi*, the inner fold is a muscular organ capable of great mobility. Radial and commarginal muscles were also observed in *Anadara trapezia* (Sullivan, 1961), but data on muscle arrangement is lacking for most taxa and would certainly improve the understanding of the functional morphology of this region. In Arcidae, mantle innervation comprises branches from the cerebral and visceral ganglia, which form a plexus that extends over the mantle (Heath, 1941). Nevertheless, it is not clear if a ganglionic circumpallial nerve is present. A simple nerve was observed in a cross-section of the mantle margin of *Barbatia virescens* (Morton, 1987). Our histological data does not provide evidence for a circumpallial nerve running close to the mantle folds. This seems to be a striking difference from other pteriomorphians, which clearly exhibit a circumpallial nerve (e.g., Jabbour-Zahab et al., 1992; Audino et al., 2015b).

Functional anatomy of pallial folds

Several secretory roles are attributed to the bivalve mantle, including mucus for mucociliary activities, shell secretion, particle adhesion, and chemical boring (Morton & Scott, 1980; Beninger & St-Jean, 1997; Beninger et al., 1999; Sartori et al., 2006). Mucins are a combination of glycoconjugates, i.e., mucosubstances containing distinct polysaccharides and proteins (Prezant, 1990). Mucin-producing cells are commonly observed in the bivalve mantle (e.g., Richardson et al., 1981; Jabbour-Zahab et al., 1992), their type and location being indicators of specialization (Beninger et al., 1999).

In the Arcidae, pallial mucin-producing cells were described only for a few species, i.e., *Anadara trapezia*, *Anadara broughtonii*, and *Bathyarca pectunculoides* (Sullivan, 1961; Morton, 1982a; Lee, 2002), and we observed a similar condition of abundant PAS-positive granular content in the pallial subepithelial glands of *Anadara ovalis*. In general, our histochemical results for the arcoidean species revealed high abundance and diversity of secretory cells, including neutral and acidic mucosubstances, in all folds but the second outer fold, and in the inner and outer pallial epithelia. In these animals, massive production of mucous mainly by the inner fold may be involved with cleaning of the pallial apertures by agglutinating suspended material and removing waste sediments (Prezant 1990, Lee 2002).

Cilia type and distribution are deeply related to mantle mucous secretion when there is mucociliary transport of particles or propulsion of a mucus raft (Sleigh, 1989; Beninger et al., 1999). In all arcoidean species studied herein, the inner fold is densely covered by short cilia and droplets of mucosubstances (e.g., Fig. 4E-G). Previous studies have demonstrated how mucus is propelled by the tips of short, densely distributed cilia (Sleigh, 1989). This seems to be the case of the ciliary cells on the middle and inner folds of arcoideans, which possibly promote cleansing and lubrication of the marginal surface.

Mantle ciliated cells may also perform sensory functions, although ciliated chemo- and mechanoreceptors can hardly be distinguished by morphological criteria alone (Owen & McCrae, 1979). The cilia organized in tufts on the pallial tentacles of scallops (Pectinidae) and file clams (Limidae) are regarded as sensory receptors (Moir 1977, Owen & McCrae, 1979; Audino et al., 2015a), as well as those at the tip of the siphons of several bivalves (e.g., Vitonis et al., 2012). In *Arcopsis adamsi* and *Barbatia candida*, we found long cilium-bearing cells sparsely distributed on the inner mantle fold at the region of the inhalant aperture (Fig. 1F, G, 3G, H). These long, solitary cilia do not attend the physical conditions for mucociliary transport (Sleigh, 1989). Alternatively, these ciliated cells might perform sensory functions. Sensory cells with a single or few cilia were described for other mollusks as well, such as the mechanoreceptor cells in the statocyst of *Nautilus pompilius* (Neumeister & Budelmann, 1997).

Morphological patterns and modes of life

Considering the latest published phylogenies of the order Arcida (Combosch & Giribet, 2016), epibyssate and endobyssate habits would not be restricted to single origins (Fig. 6). This pattern suggests multiple life habit transitions during the evolution and diversification of Arcoidea, as previously suggested by Oliver & Holmes (2006). The transition to similar habits and/or habitats may lead to convergent or parallel evolution of particular phenotypes, an apparently common phenomenon in Mollusca. For example, a small, worm-like, shell-less body has evolved several times independently in euthyneuran gastropods, often in association with the meiofaunal habit, sufficiently enough to blur the phylogenetic signal (Jörger et al. 2010; Schrödl & Neusser, 2010). Similarly, in cephalopods, the evolution of autogenic photophores and the development of a cornea have been correlated with transitions to the pelagic and benthic habitats, respectively, indicating the repeated evolution of similar features conferring crypsis in the open ocean, and eye protection from the sediment in the benthos (Lindgren et al. 2012). In scallops, independent evolution of long-distance swimming behavior was accompanied by a convergent “gliding” shell morphotype (Serb et al., 2017).

Our results on the mantle margin morphology of arcoidean species, combined with previous data from literature, suggest general patterns of pallial morphology associated with life habits. Figure 7 summarizes the most important differences and variations observed in the arcoidean mantle margin, i.e., presence of photoreceptor organs, pigmentation, and relative development of middle and inner folds. Epibyssate species generally display anteroposterior differentiation of the mantle margin, i.e., they show gradual increase in pigmentation, number and size of photoreceptor organs, and inner fold length towards the posterior region (Fig. 7). Differently, endobyssate species generally exhibit unpigmented mantle margin, a very enlarged posterior inner fold, and eyespots, when present, are restricted to the anterodorsal region (Fig. 7).

The gain in complexity and number of eyes is a notorious characteristic of epifaunal species that inhabit shallow waters, as demonstrated by numerous compound eyes in some lineages of different arcoidean families (Fig. 6, 7). Eyes might have been lost in endobyssate groups since light seems to impose less or no influence in this mode of life. That would be the case of *Anadarinae*, *Trisidos*, the deep-water *Bathyarca* (Oliver & Allen, 1980; Waller, 1980; Morton, 1982a, b), and the endobyssate noetiids, such as *Noetia ponderosa* and *Sheldonella bisulcata*. In addition, fossil and phylogenetic evidence indicate that infaunal and semi-infaunal habits have arisen secondarily in the group, supporting this view (Stanley, 1972; Oliver & Holmes, 2006; Combosch & Giribet, 2016; see also Fig. 6). In this context, photoreceptor organs (as well as pallial pigmentation) may represent putative adaptive features in the early evolution of arcoidean epibyssate lineages.

Another interesting pattern in the mantle margin of arcoideans is the great reduction of the middle fold, or even its absence, in several representatives (Fig. 7, Table 3). Previous investigations have already hypothesized how typical sensory roles played by the middle fold, such as photoreception, could have been transferred to the outer fold (Morton, 1982a; Morton & Peharda, 2008). Our results support the transference of sensory functions of the middle fold also to the inner fold. Long cilium-bearing cells, supposedly sensory receptors, are present only in the inner fold in *Barbatia candida* and *Arcopsis adamsi*, reinforcing the sensory function of the pallial curtain.

The absence of the middle fold in some arcoideans, combined with the presence of a second outer fold and unique shell features, were previously interpreted as plesiomorphic conditions by some authors (Morton & Peharda, 2008), or as secondarily derived traits by others (Waller, 1980). In recent phylogenetic analyses, the Arcida group was not recovered as an early branch of Pteriomorphia (Bieler et al., 2014; Combosch & Giribet, 2016), so mantle character evolution should be discussed cautiously. For example, the absence of the middle fold in adults may represent a fold not differentiated into middle and inner folds. Such an ontogenetic differentiation has been confirmed for some bivalves (Waller, 1981; Audino et al., 2015b), so in arcoideans the non-differentiation of the middle fold may represent the retention of a larval feature. Neoteny has already been evocated to explain the retention of byssus in adult bivalves (Yonge, 1962), and may be responsible for the variations in arcoidean mantle folds. Furthermore, our comparative results suggest that the middle fold was repeatedly lost in some lineages, thus indicating secondary losses rather than a plesiomorphic condition.

In conclusion, through a comprehensive morphological analysis of the mantle margin in Arcoidea, this study supports association between pallial morphology and life habits. Future studies should focus on integrating improved phylogenies of the clade with comparative methods (e.g., Martins 2000). Testing the hypothesis that the life habit may influence convergent evolution of particular pallial phenotypes (e.g., inner fold development in infaunal and compound eyes in epifaunal lineages) would not only help us better understand the phylogeny of Arcoidea and resolve taxonomical conflicts, but also shed light on the selective pressures of each environmental context (epifaunal vs. infaunal).

Acknowledgements

The authors acknowledge funding provided by FAPESP (São Paulo Research Foundation; 2015/09519-4). This study is part of the first author's Doctorate's thesis through the Graduate Program in Zoology of the Institute of Biosciences (University of São Paulo). The authors thank the Malacological Society of London for the research grant provided for the fluorescent dyes used in confocal microscopy. The authors thank also the following institutions, which provided the necessary facilities or materials for the development of this study: Center for Marine Biology (CEBIMar), Museum of Zoology "Prof. Adão José Cardoso" of the University of Campinas (ZUEC), Museum of Zoology of the University of São Paulo (MZSP), and Santa Barbara Museum of Natural History (SBMNH). Dr. Alvaro E. Migotto provided assistance during *in vivo* studies, and Dr. Daniel J. G. Lahr provided equipment to capture images from histological slides. The authors also acknowledge two anonymous reviewers for their comments and suggestions.

References

Agrawal, A.A. (2017). Toward a predictive framework for convergent evolution: Integrating natural history, genetic mechanisms, and consequences for the diversity of life. *Am. Nat.* **190**, S1–S12.

Audino, J.A. & Marian, J.E.A.R. (2016). On the evolutionary significance of the mantle margin in pteriomorphian bivalves. *Am. Malacol. Bull.* **34**, 148–159.

Audino, J.A., Marian, J.E.A.R., Wanninger, A. & Lopes, S.G.B.C. (2015a). Anatomy of the pallial tentacular organs of the scallop *Nodipecten nodosus* (Linnaeus, 1758) (Bivalvia: Pectinidae). *Zool. Anz.* **258**, 39–46.

Audino, J.A., Marian, J.E.A.R., Wanninger, A. & Lopes, S.G.B.C. (2015b). Mantle margin morphogenesis in *Nodipecten nodosus* (Mollusca: Bivalvia): New insights into the development and the roles of bivalve pallial folds. *BMC Dev. Biol.* **15**, 22.

Bancroft, J.D., Stevens A. (1982). Theory and practice of histological techniques, 2nd ed. London: Churchill Livingstone. p 662.

Beninger, P.G. & St-Jean, S.D. (1997). The role of mucus in particle processing by suspension-feeding marine bivalves: Unifying principles. *Mar. Biol.* **129**, 389–397.

Beninger, P.G., Veniot, A. & Poussart, Y. (1999). Principles of pseudofeces rejection on the bivalve mantle: Integration in particle processing. *Mar. Ecol. Prog. Ser.* **178**, 259–269.

Bieler, R., Carter, J.G. & Coan, E.V. (2010). Classification of bivalve families. *Malacologia* **52**, 113–133.

Bieler, R., Mikkelsen, P.M., Collins, T.M., Glover, E.A., González, V.L., Graf, D.L., … & Giribet, G. (2014). Investigating the Bivalve Tree of Life - An exemplar-based approach combining molecular and novel morphological characters. *Invertebr. Syst.* **28**, 32–115.

Carter, J.G., Altaba, C.R., Anderson, L.C., Araujo, R., Biakov, A.S., Bogan, A.E., … & Yancey, T. (2011). A synoptical classification of the Bivalvia (Mollusca). *Paleontol. Contrib.* **4**, 1–47.

Combosch, D.J. & Giribet, G. (2016). Clarifying phylogenetic relationships and the evolutionary history of the bivalve order Arcida (Mollusca: Bivalvia: Pteriomorphia). *Mol. Phylogenet. Evol.* **94**, 298–312.

Daniels, S.R., Cumberlidge, N., Pérez-Losada, M., Marijnissen, S.A. & Crandall, K.A. (2006). Evolution of Afrotropical freshwater crab lineages obscured by morphological convergence. *Mol. Phylogenet. Evol.* **40(1)**, 227–235.

Feng, Y., Li, Q. & Kong, L. (2015). Molecular phylogeny of Arcoidea with emphasis on Arcidae species (Bivalvia: Pteriomorphia) along the coast of China: Challenges to current classification of arcoids. *Mol. Phylogenet. Evol.* **85**, 189–196.

Giribet, G. & Wheeler, W. (2002). On bivalve phylogeny: a high-level analysis of the Bivalvia (Mollusca) based on combined morphology and DNA sequence data. *Invertebr. Biol.* **121**, 271–324.

Heath, H. (1941). The anatomy of the pelecypod family Arcidae. *Trans. Am. Philos. Soc.* 287–319.

Jabbour-Zahab, R., Chagot, D., Blanc, F. & Grizel, H. (1992). Mantle histology, histochemistry and ultrastructure of the pearl oyster *Pinctada margaritifera* (L.). *Aquat. Living Resour.* **5**, 287–298.

Jörger, K.M., Stöger, I., Kano, Y., Fukuda, H., Knebelsberger, T. & Schrödl, M. (2010). On the origin of Acochlidia and other enigmatic euthyneuran gastropods, with implications for the systematics of Heterobranchia. *BMC Evol. Biol.* **10(1)**, 323.

Lindgren, A.R., Pankey, M.S., Hochberg, F.G. & Oakley, T.H. (2012). A multi-gene phylogeny of Cephalopoda supports convergent morphological evolution in association with multiple habitat shifts in the marine environment. *BMC Evol. Biol.* **12(1)**, 129.

Losos, J.B. (2011). Convergence, adaptation, and constraint. Evolution **65,** 1827–1840.

MacNeil, F.S. (1938). Species and genera of Tertiary Noetinae. *United States Geol. Surv. Prof. Pap.* **189**, 1–50.

Marian, J.E.A.R. (2012). Spermatophoric reaction reappraised: Novel insights into the functioning of the loliginid spermatophore based on *Doryteuthis plei* (Mollusca: Cephalopoda). *J. Morphol.* **273**, 248–278.

Martins, E.P. (2000). Adaptation and the comparative method. *Trends Ecol. Evol.* **15**, 296–299.

Moir, A.J.G. (1977). Ultrastructural studies on the ciliated receptors of the long tentacles of the giant scallop, *Placopecten magellanicus* (Gmelin). *Cell Tissue Res.* **184**, 367–380.

Morton, B. (1981). The mode of life and function of the shell buttress in *Cucullaea concamerata* (Martini)(Bivalvia: Arcacea). *J. Conchol.* **30**, 295.

Morton, B. (1982a). Functional morphology of *Bathyarca pectunculoides* (Bivalvia: Arcacea) from a deep Norwegian fjord with a discussion of the mantle margin in the Arcoida. *Sarsia* **67**, 269–282.

Morton, B. (1982b).The biology and functional morphology of the twisted ark *Trisidos semitorta* (Bivalvia: Arcacea) with a discussion on shell ‘torsion’ in the genus. Malacologia **23**, 375–396.

Morton, B. (1987). The pallial photophores of *Barbatia virescens* (Bivalvia: Arcacea). *J. Molluscan Stud.* **53**, 241–244.

Morton, B. (2008). The evolution of eyes in the Bivalvia: New insights. *Am. Malacol. Bull.* **26**, 35–45.

Morton, B. & Peharda, M. (2008). The biology and functional morphology of *Arca noae* (Bivalvia: Arcidae) from the Adriatic Sea, Croatia, with a discussion on the evolution of the bivalve mantle margin. *Acta Zool.* **89**, 19–28.

Morton, B. & Puljas, S. (2015). The ectopic compound ommatidium-like pallial eyes of three species of Mediterranean (Adriatic Sea) *Glycymeris* (Bivalvia: Arcoida). Decreasing visual acuity with increasing depth? *Acta Zool.* **474**, 464–474.

Morton, B. & Scott, P.J.B. (1980). Morphological and functional specializations of the shell, musculature and pallial glands in the Lithophaginae (Mollusca: Bivalvia). *J. Zool.* **192**, 179–203.

Neumeister, H. & Budelmann, B.U. (1997). Structure and function of the *Nautilus* statocyst. *Philos. Trans. R. Soc. B Biol. Sci.* **352**, 1565–1588.

Nicol, D. (1954). Nomenclatural review of genera and subgenera of Cucullaeidae. *J. Paleontol.* 96–101.

Nilsson, D.E. (1994). Eyes As optical alarm systems in fan worms and ark clams. *Philos. Trans. R. Soc. London Ser. B Biol. Sci.* **346**, 195–212.

Oliver, P.G. & Allen, J.A. (1980). The functional and adaptive morphology of the deep-sea species of the Arcacea (Mollusca: Bivalvia) from the Atlantic. *Philos. Trans. R. Soc. London Ser. B Biol. Sci.* **291**, 45–76.

Oliver, P.G. & Holmes, A.M. (2006). The Arcoidea (Mollusca: Bivalvia): A review of the current phenetic-based systematics. *Zool. J. Linn. Soc.* **148**, 237–251.

Owen, G. & McCrae, J.M. (1979). Sensory cell/gland cell complexes associated with the pallial tentacles of the bivalve *Lima hians* (Gmelin), with a note on specialized cilia on the pallial curtains. *Philos. Trans. R. Soc. B Biol. Sci.* **287**, 45–62.

Prezant, R.S. (1990). Form, function and phylogeny of bivalve mucins. In: Bivalvia - Proc. a Meml. Symp. Honour Sir Charles Maurice Yonge. Morton, B. ed., pp. 83–95. Hong Kong : Hong Kong University Press.

Richardson, C.A., Runham, N.W. & Crisp, D.J. (1981). A histological and ultrastructural study of the cells of the mantle edge of a marine bivalve, *Cerastoderma edule*. *Tissue Cell* **13**, 715–730.

Sartori, A.F., Passos, F.D. & Domaneschi, O. (2006). Arenophilic mantle glands in the Laternulidae (Bivalvia: Anomalodesmata) and their evolutionary significance. *Acta Zool.* **87**, 265–272.

Schrödl, M., Neusser, T.P. (2010). Towards a phylogeny and evolution of Acochlidia (Mollusca: Gastropoda: Opisthobranchia). *Zool J Linn Soc.***158,** 124–154.

Serb, J.M., Alejandrino, A., Otarola-Castillo, E. & Adams, D.C. (2011). Morphological convergence of shell shape in distantly related scallop species (Mollusca: Pectinidae). *Zool. J. Linn. Soc.* **163(2)**, 571–584.

Serb, J.M., Sherratt, E., Alejandrino, A. & Adams, D.C. (2017). Phylogenetic convergence and multiple shell shape optima for gliding scallops (Bivalvia: Pectinidae). *J Evol Biol.* DOI 10.1111/jeb.13137

Simone, L.R.L. & Chichvarkhin, A.Y. (2004). Comparative morphological study of four species of *Barbatia* occurring on the southern Florida coast (Arcoidea, Arcidae). *Malacologia* **46**, 355–379.

Sleigh, M.A. (1989). Adaptations of ciliary systems for the propulsion of water and mucus. Comp. Biochem. *Physiol. Part A Physiol.* **94**, 359–364.

Stanley, S.M. (1972). Functional morphology and evolution of byssally attached bivalve mollusks. *J. Paleontol.* **46**,165–212.

Valentich-Scott, P. (2003). A taxonomic, distributional and bibliographic checklist of Hong Kong marine bivalve molluscs and research published on them from 1971-2000. In: Perspectives on marine environmental change in Hong Kong and southern China, 1977-2001: Proceedings of an international workshop reunion conference, Hong Kong, 21-26 October 2001. Hong Kong: Hong Kong University Press.

Steiner, G. & Hammer, S. (2000). Molecular phylogeny of the Bivalvia inferred from 18S rDNA sequences with particular reference to the Pteriomorphia. *Geol. Soc. London, Spec. Publ.* **177**, 11–29.

Sullivan, G.E. (1961). Functional morphology, micro-anatomy, and histology of the “Sydney Cockle” *Anadara trapezia* (Deshayes) (Lamellibranchia: Arcidae). *Aust. J. Zool.* **9**, 219–257.

Thomas, R.D.K. (1975). Functional morphology, ecology and evolutionary conservatism in the Glycymerididae (Bivalvia). *Palaeontology* **18**, 217–254.

Vitonis, J.E.V.V., Zaniratto, C.P., Machado, F.M. & Passos, F.D. (2012). Comparative studies on the histology and ultrastructure of the siphons of two species of Tellinidae

(Mollusca: Bivalvia) from Brazil. *Zool.* **29**, 219–226.

Waller, T.R. (1980). Scanning electron microscopy of shell and mantle in the order Arcoida. *Smithson. Contrib. to Zool.* **313**, 1–58.

Waller, T.R. (1981). Functional morphology and development of veliger larvae of the European Oyster, *Ostrea edulis* Linne. *Smithson. Contrib. to Zool.* **328**, 1–70.

Yonge, C.M. (1962). On the primitive significance of the byssus in the Bivalvia and its effects in evolution. *J. Mar. Biol. Assoc. United Kingdom* **42**, 113–125.

Yonge, C.M. (1983). Symmetries and the role of the mantle margins in the bivalve Mollusca. *Natl. Widl.* **16**, 1–10.

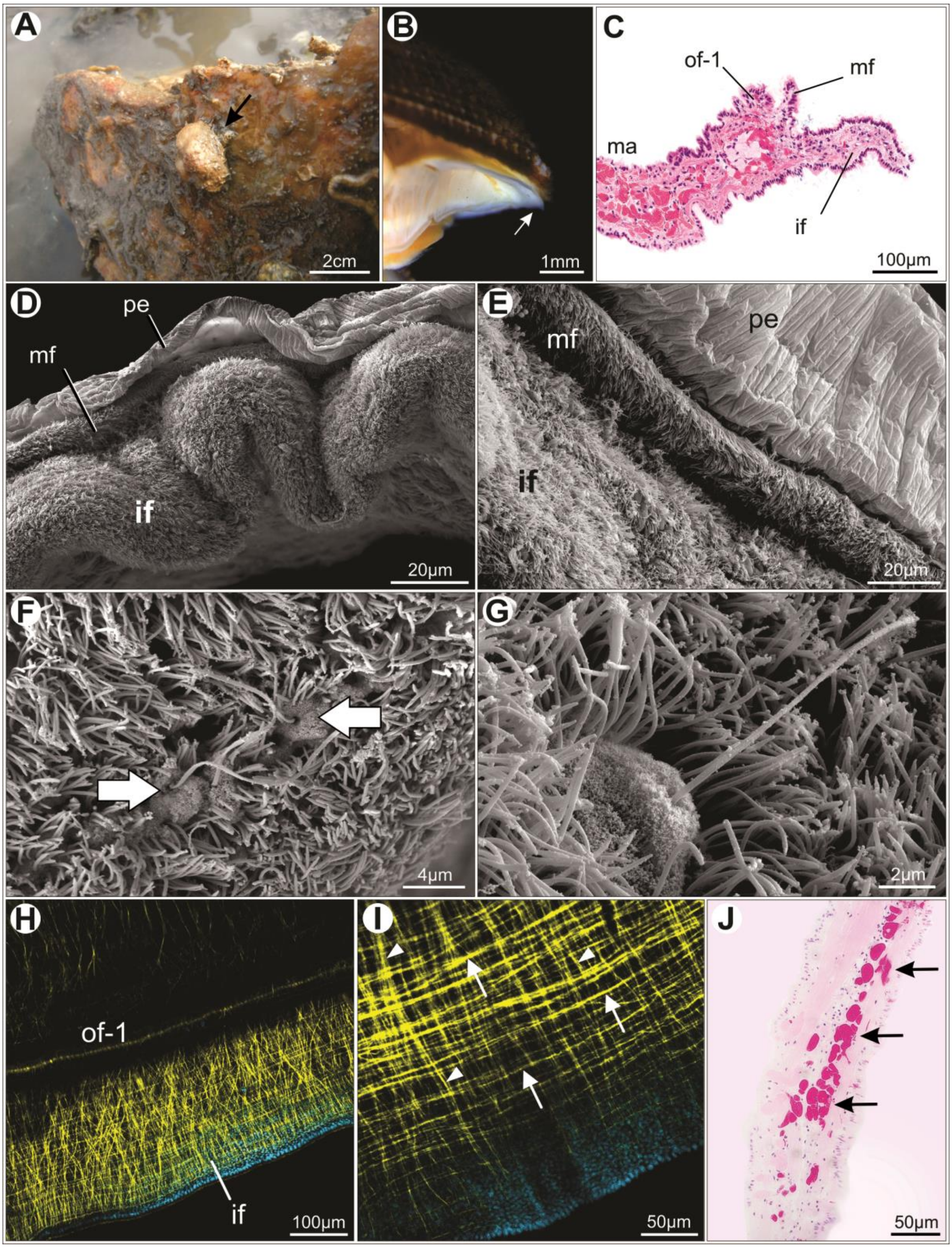

Figure 1. Mantle margin anatomy of the noetiid *Arcopsis adamsi*. Anatomical details as observed by histological sections (C, J), scanning electron microscopy (D-G), and confocal microscopy (H, I). **A.** Specimen attached to rock by byssus. **B.** Mantle margin with the inner fold more prominent (arrow); posterior to the right. **C.** Cross-section of the mantle margin showing the first outer fold, middle fold, and inner fold (second outer fold not visible in this region); distal portion to the right. HE. **D.** Inner fold (covered by cilia) much longer than the middle fold; frontal view. **E.** Surfaces of the middle and inner folds, showing dense distribution of short cilia. **F.** Long cilium-bearing cells (arrows) observed among ordinary cilia. **G.** Long cilium in detail. **H.** Mantle margin musculature (yellow); distal region to the bottom and nuclei in blue. **I.** Detail of H, showing commarginal (arrow) and radial muscle fibers (arrowhead) in the inner fold. **J.** Cross-section of the mantle showing subepithelial gland cells stained by PAS. Abbreviations: *if*, inner fold; *ma*, mantle; *mf*, middle fold; *of-1*, first outer fold; *pe*, periostracum.

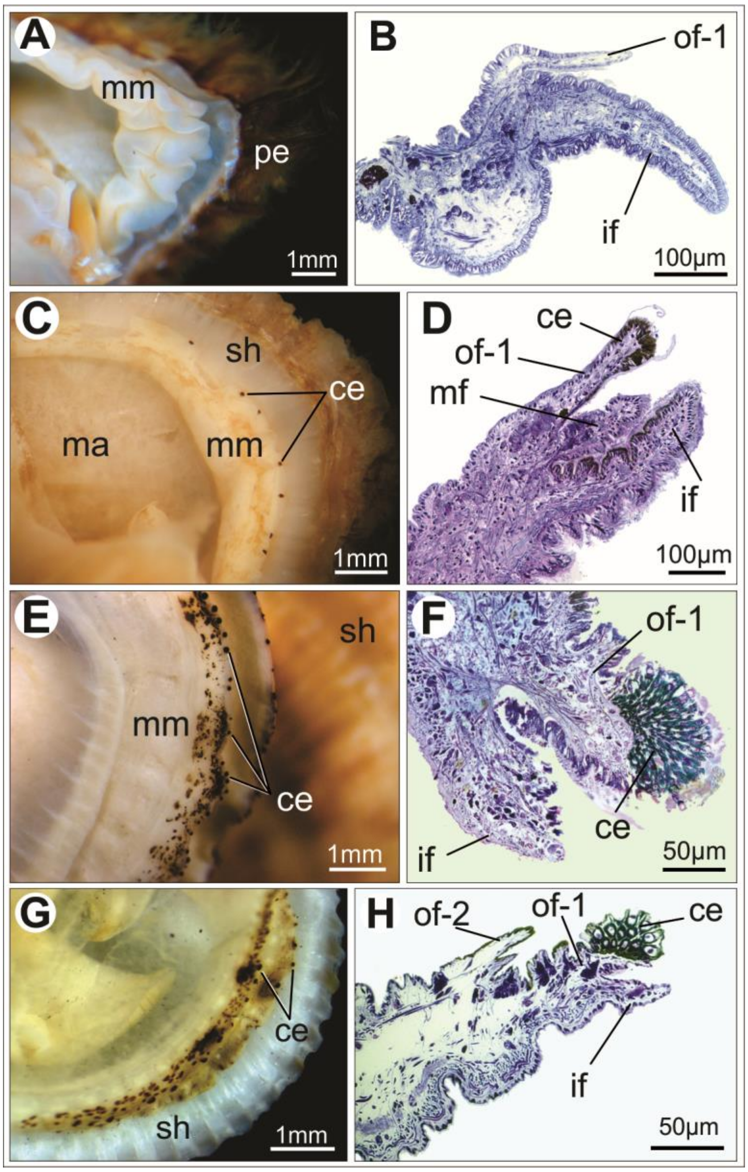

Figure 2. Mantle margin in representatives of Noetiidae and Glycymerididae, as observed in preserved specimens from collections. Posterior to right and dorsal on top in A, C, E, G. Distal portion of the mantle margin to the right in histological sections (B, D, F, H). **A.** *Sheldonella bisulcata* (same in B), showing the large, undulate inner fold. **B.** Detail of outer and inner folds. TB-BF. **C.** *Striarca symmetrica* (same in D), with dark compound eyes in the posterior region. **D.** Detail of the mantle margin; the first outer fold bears a compound eye. TB-BF. **E.** *Glycymeris longior* (same in F), showing pigmentation and numerous compound eyes posteriorly. **F.** Cross-section of the mantle margin. TB-BF. **G.** *Tucetona pectinata* (same in H), with posterior mantle margin pigmented and bearing compound eyes. **H.** Cross-section of the mantle margin showing the second outer fold, first outer fold with compound eye, and inner fold. TB. Abbreviations: *ce*, compound eye; *if*, inner fold; *ma*, mantle; *mf*, middle fold; *mm*, mantle margin; *of-1*, first outer fold; *of-2*, second outer fold; *pe*, periostracum; *sh*, shell.

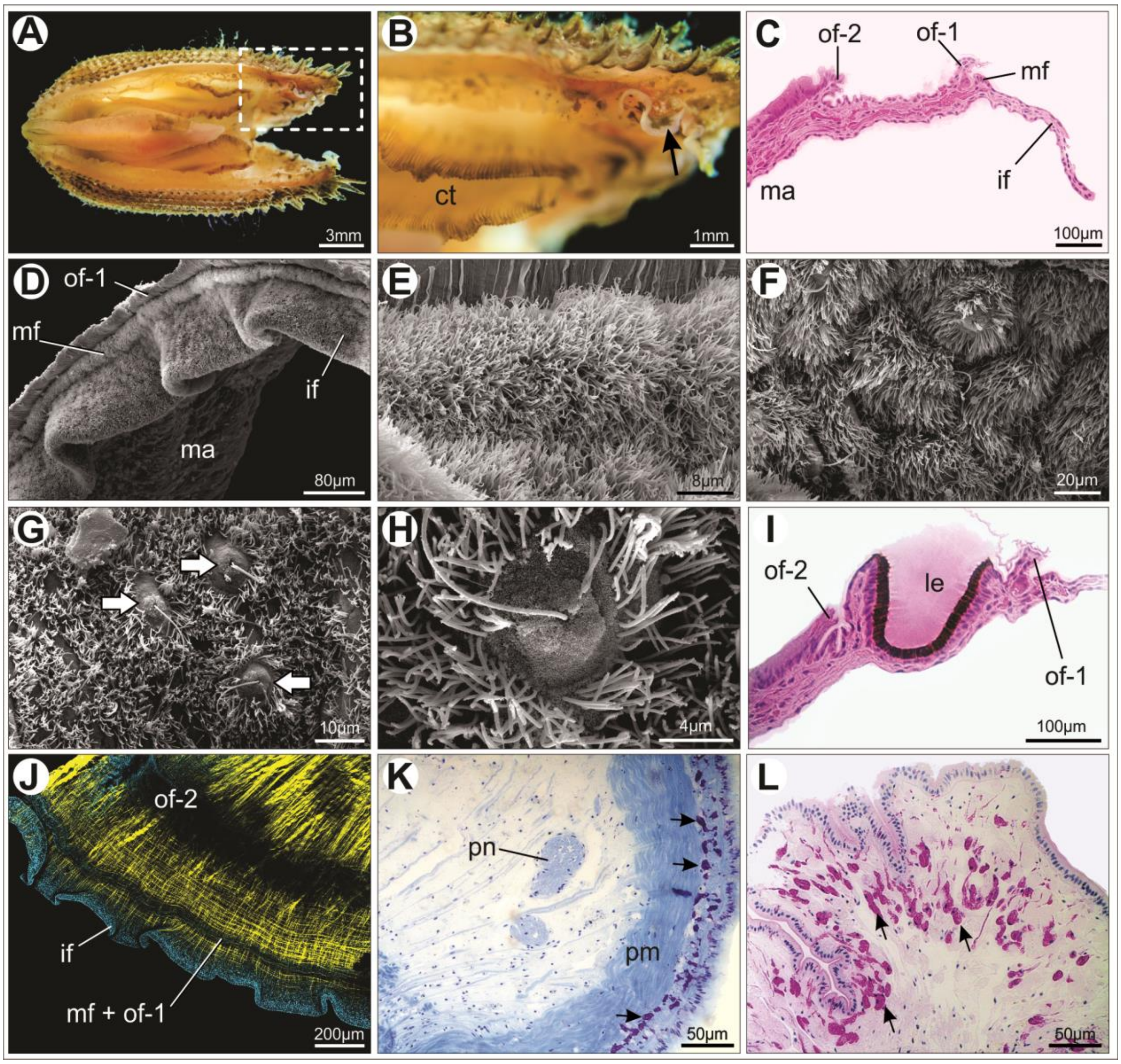

Figure 3. Mantle margin anatomy of *Barbatia candida*. Anatomical details as observed by histological sections (C, I, K, L), scanning electron microscopy (D-H), and confocal microscopy (J). **A.** Ventral view of a relaxed specimen with the pallial cavity exposed, posterior to the right. **B.** Detail of the inset in A, showing the undulate inner fold with curtain-like morphology (arrow). **C.** Cross-section of the mantle margin; the inner fold is much longer than the other folds. Distal region to the right. HE. **D.** Ciliated surface of middle and inner folds. **E.** Detail of dense cilia distribution on the middle fold. **F.** Detail of dense cilia distribution on the inner fold. **G.** Long cilium-bearing cells on the inner fold. **H.** Detail of the long cilium surrounded by short, ordinary cilia. **I.** Cross-section of the mantle margin with a pigmented cup filled by a secreted lens. HE. **J.** Musculature of the mantle margin in yellow, nuclei in blue; commarginal and radial fibers are visible. **K.** Subepithelial gland cells (arrows) in the inner fold, and apparently a pallial nerve in section. TB-BF. **L.** Subepithelial gland cells (arrows) on the outer mantle surface stained by PAS. Abbreviations: *ct*, ctenidium; *if*, inner fold; *le*, lens; *ma*, mantle; *mf*, middle fold; *of-1*, first outer fold; *of-2*, second outer fold; *pm*, pallial muscles; *pn*, pallial nerve.

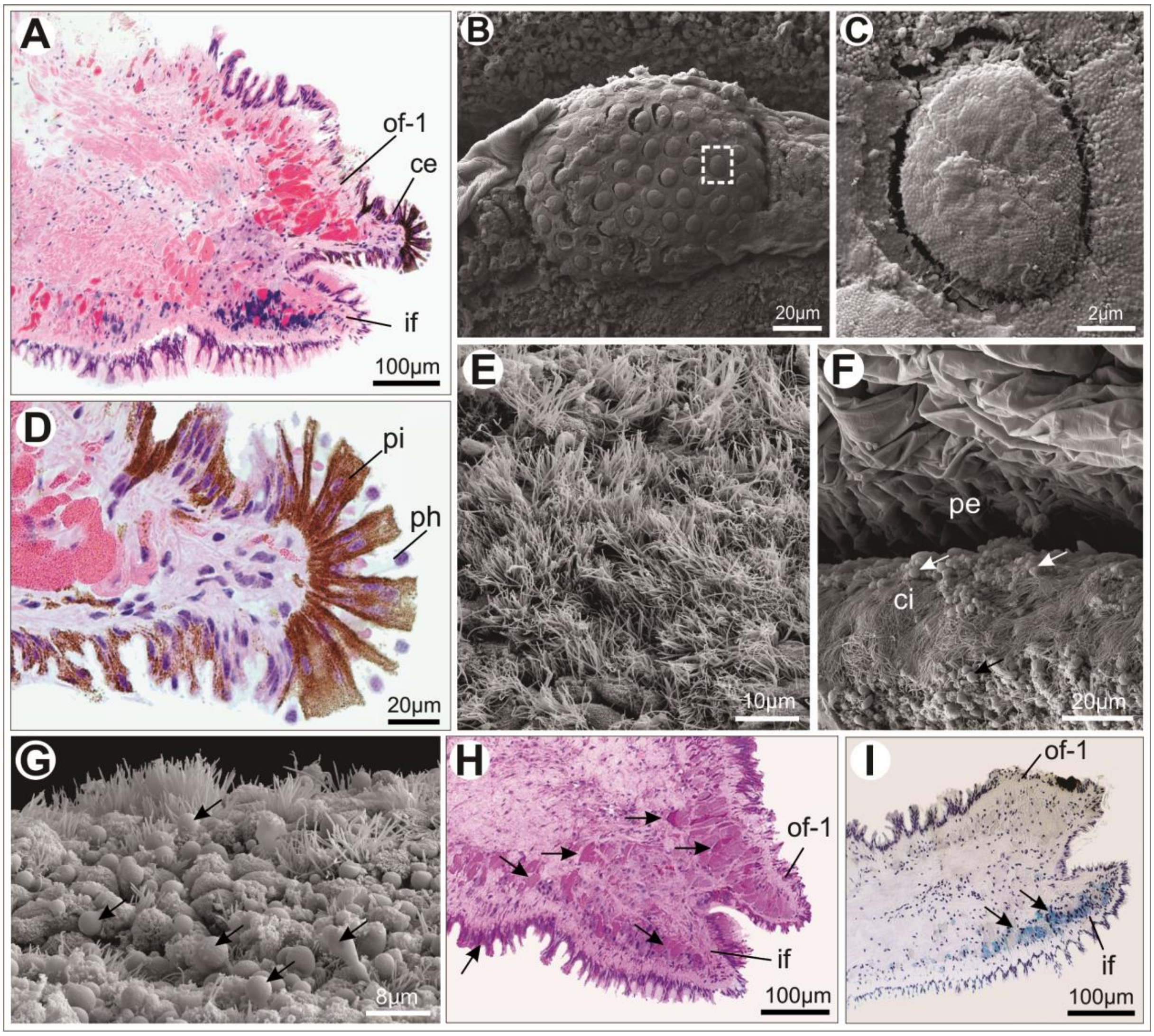

Figure 4. Mantle margin anatomy of *Arca imbricata*. Anatomical details as observed by histological sections (A, D, H, I; distal region to the right) and scanning electron microscopy (B, C, E-G). **A.** Cross-section of the mantle margin showing the compound eye on the first outer fold, as well as varied secretory cells in both pallial folds. HE. **B.** Surface of a compound eye, with ommatidium-like organization in facets. **C.** Detail of the inset in B, showing the surface of a photoreceptor cell covered by microvilli. **D.** Cross-section of the compound eye showing the organization of photoreceptor and pigmented cells. HE. **E.** Ciliated surface of the inner fold. **F.** Detail of the periostracal groove, showing the ciliated surface of the inner mantle fold and droplets of secretion (arrows). **G.** Droplets of secretion (arrows) emerging among the short cilia on the inner mantle fold. **H.** Gland cells stained by PAS (arrows) in both pallial folds. **I.** Subepithelial gland cells of the inner mantle fold stained by AB (arrows). Abbreviations: *ce*, compound eye; *ci*, cilia; *if*, inner fold; *of-1*, first outer fold; *pe*, periostracum; *ph*, photoreceptor cell; *pi*, pigmented cell.

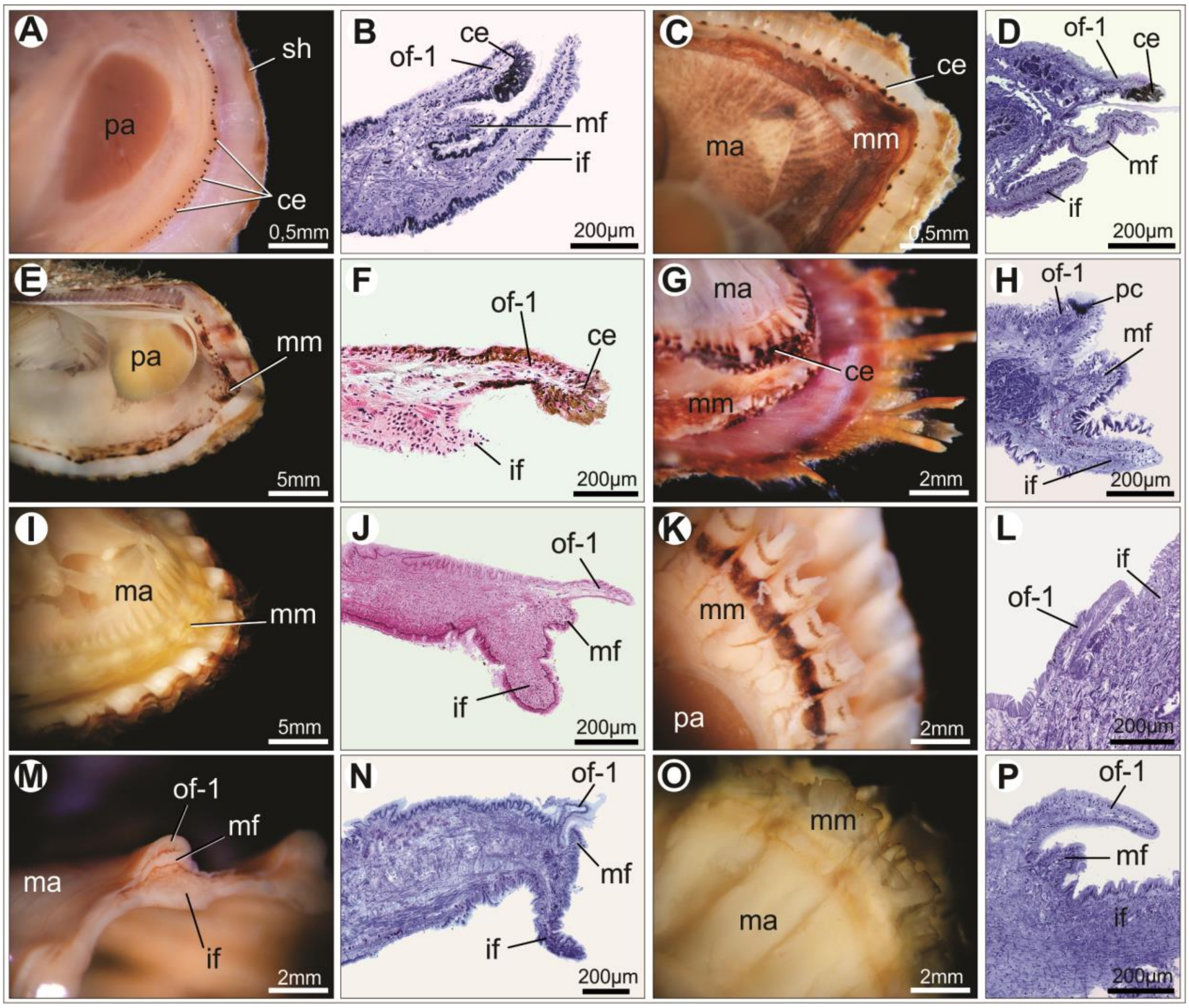

Figure 5. Mantle margin morphology in representatives of Arcidae, as observed in preserved specimens from collections. Posterior to right and dorsal on top in A, C, E, G, I, K, M, O. In histological sections (B, D, F, H, J, L, N, P), distal portion of the mantle margin is to the right. **A.** *Acar plicata* (same in B), posterior margin with numerous dark compound eyes. **B.** Cross-section of the mantle margin. TB-BF. **C.** *Acar dominguensis* (same in D), pigmented posterior margin with large compound eyes. **D.** Cross-section of the mantle margin. TB. **E.** *Arca zebra* (same in F), posterior pallial margin pigmented. **F.** Cross-section of the mantle margin. HE. **G.** *Barbatia cancellaria* (same in H), pigmented margin with large compound eyes. **H.** Cross-section of the mantle margin. TB. **I.** *Anadara notabilis* (same in J), unpigmented mantle margin. **J.** Cross-section of the mantle margin. HE. **K.** *Anadara ovalis* (same in L), posterior pigmented bands. **L.** Cross-section of the mantle margin. TB. **M.** *Tegillarca granosa* (same in N), unpigmented margin. **N.** Cross-section of the mantle margin. TB. **O.** *Anadara inaequivalvis* (same in P), unpigmented margin with a long inner fold. **P.** Cross-section of the mantle margin. TB. Abbreviations: *ce*, compound eye; *if*, inner fold; *ma*, mantle; *mf*, middle fold; *mm*, mantle margin; *of-1*, first outer fold; *pa*, posterior adductor muscle; *pc*; pigmented cup; *sh*, shell.

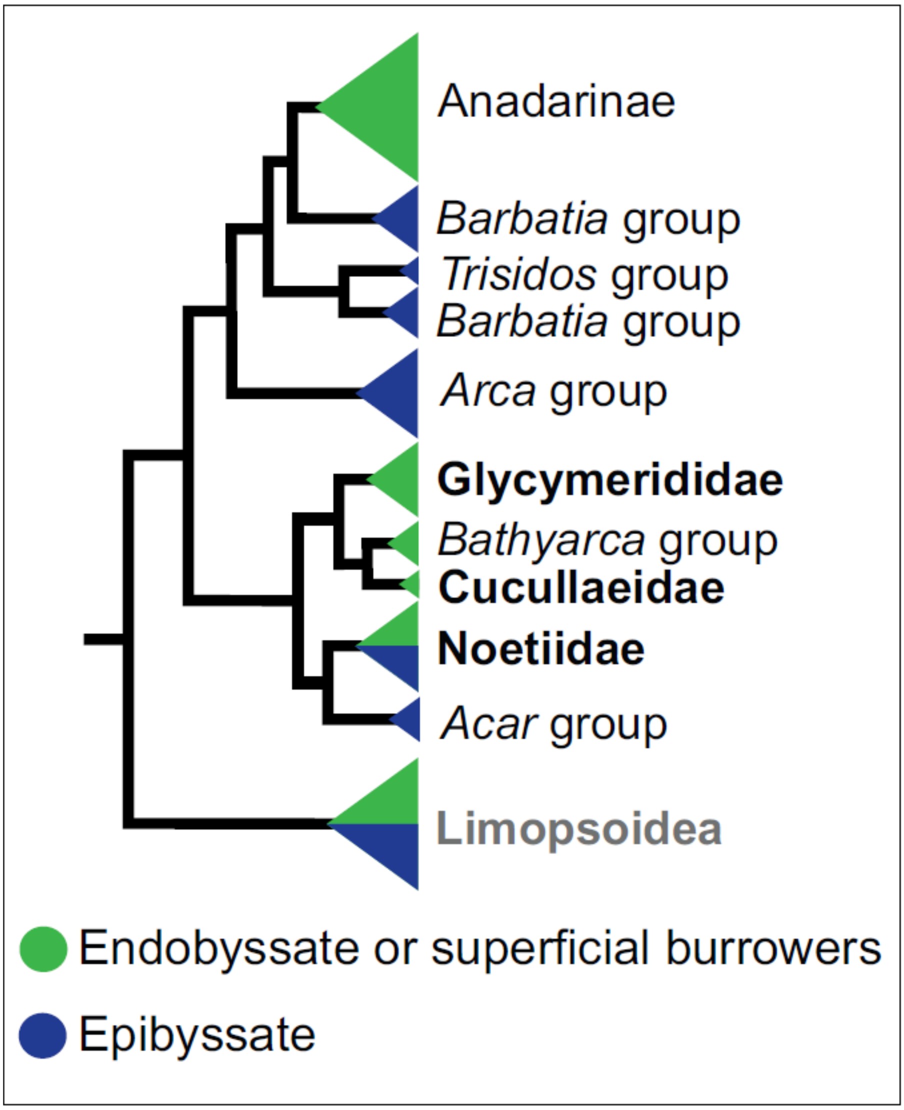

Figure 6. Phylogenetic relationships of Arcoidea and life habit variation within the group. Life habits are color coded and divided into epibyssate (epifaunal) and endobyssate or superficial burrowers (semi-infaunal/infaunal). The Arcoidea are indicated in black font, with familial names in bold, except for Arcidae, which is not monophyletic. The remaining Arcida, i.e., Limopsoidea, is indicated in grey. When both habits are indicated in the same terminal, it means the clade contains epibyssate and endobyssate lineages. Triangle size refers to a rough estimate of the relative diversity of each terminal. The present phylogenetic hypothesis illustrates how these habits are spread in the clade, possibly as consequence of multiple shifts. Phylogeny redrawn after Combosh & Giribet (2016).

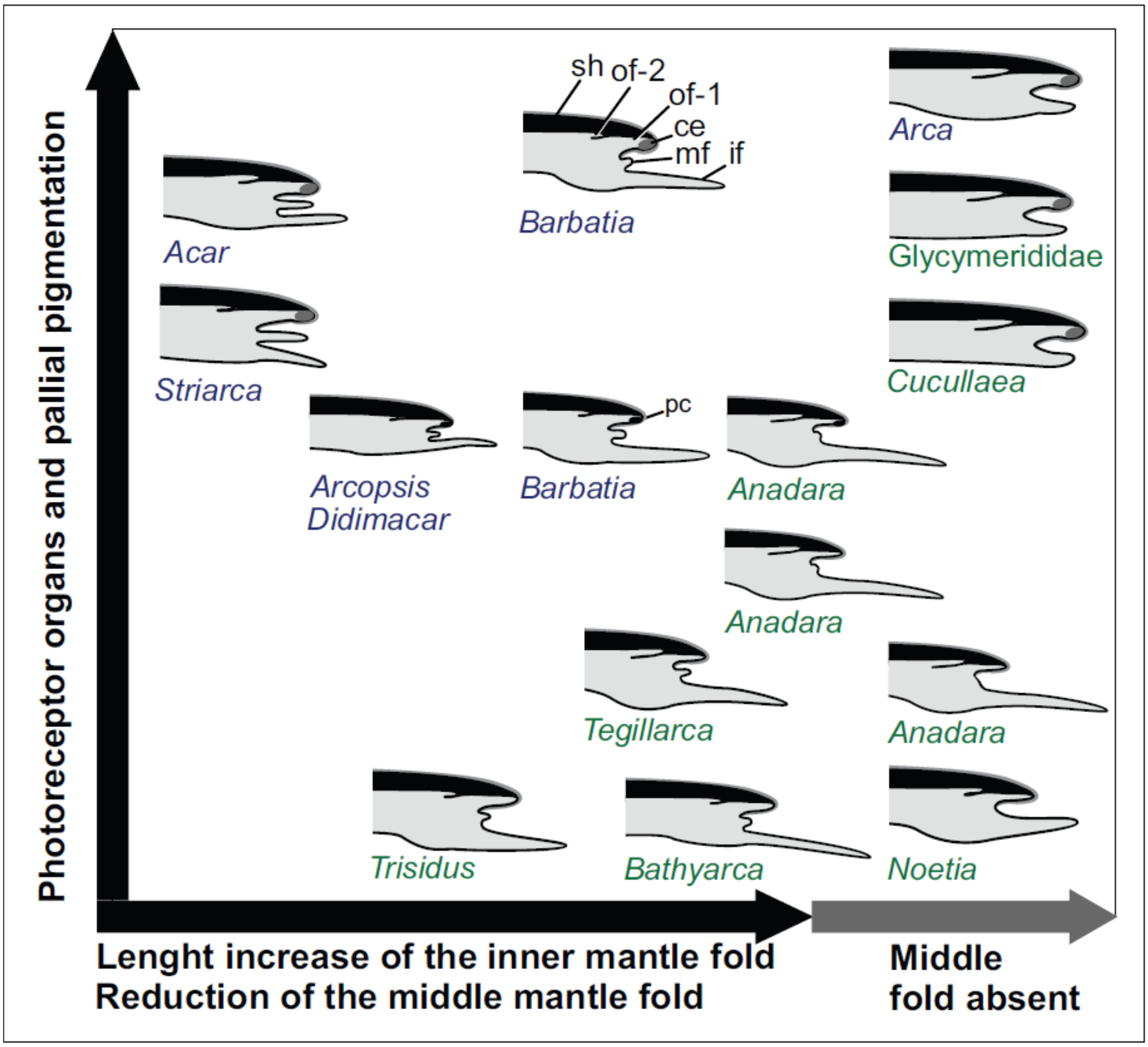

Figure 7. General morphological patterns in the mantle margin of Arcoidea. Schematic representation of the mantle margin (cross-section) in different arcoideans, showing a general comparison based on the presence of photoreceptor organs (pigmented eyespots and compound eyes), presence of pallial pigmentation, relative development of the middle fold, and relative development of the inner fold. Epibyssate and endobyssate species are indicated in blue and green, respectively. In epifaunal species, intense pallial pigmentation and photoreceptor organs are common. In endobyssates, the mantle margin is mostly unpigmented and devoid of photoreceptor organs, except in Glycymerididae and some *Anadara* and *Cucullaea* species. All arcoideans share the reduction of the middle fold (absent in several species). In most endobyssate animals, middle fold reduction is accompanied by length increase of the inner fold, forming enlarged pallial curtains. Abbreviations: *ce*, compound eye; *if*, inner fold; *mf*, middle fold; *of-1*, first outer fold; *of-2*, second outer fold; *pg*, pigmented cup; *sh*, shell.

Tables

Table 1. Arcoidean taxa included in the present morphological investigation. Taxa in bold were collected and investigated in detail by means of integrative microscopy techniques. Taxa not in bold were obtained in museum collections. When necessary, samples from their mantle margin were removed and prepared for histology to clarify the anatomical organization (*). Abbreviations: Museum of Zoology "Prof. Adão José Cardoso" of the University of Campinas (ZUEC), Museum of Zoology of the University of São Paulo (MZSP), and Santa Barbara Museum of Natural History (SBMNH).

Taxa	Author and date	Family	Collection
*Acar dominguensis**	(Lamarck, 1819)	Arcidae	MZSP118292
*Acar plicata**	(Dillwyn, 1817)	Arcidae	MZSP115322
*Anadara brasiliana**	(Lamarck, 1819)	Arcidae	ZUEC-BIV253
Anadara chemnitzii	(Philippi, 1851)	Arcidae	MZSP43259
Anadara ferruginea	(Reeve, 1844)	Arcidae	SBMNH81002
*Anadara inaequivalvis**	(Bruguière, 1789)	Arcidae	MZSP55060
*Anadara notabilis**	(Röding, 1798)	Arcidae	MZSP84987
Anadara ovalis	(Bruguière, 1789)	Arcidae	MZSP33964
Anadara trapezia	(Deshayes, 1839)	Arcidae	SBMNH10187
Arca imbricata*	Bruguière, 1789	Arcidae	-
Arca patriarchalis	Röding, 1798	Arcidae	MZSP99765
Arca ventricosa	Lamarck, 1819	Arcidae	MZSP55027
*Arca zebra**	(Swainson, 1833)	Arcidae	MZSP101688
Barbatia amygdalumtostum	(Röding, 1798)	Arcidae	SBMNH71477
*Barbatia cancellaria**	(Lamarck, 1819)	Arcidae	MZSP32336
Barbatia candida*	(Helbling, 1779)	Arcidae	-
Barbatia lima	(Reeve, 1844)	Arcidae	MZSP71135
*Barbatia virescences**	(Reeve, 1844)	Arcidae	MZSP71367
Bathyarca corpulenta	(E. A. Smith, 1885)	Arcidae	SBMNH349320
*Tegillarca ventricosa**	(Linnaeus, 1758)	Arcidae	MZSP55596
Trisidos kiyonoi	(Makiyama, 1931)	Arcidae	SBMNH97422
Arcopsis adamsi*	(Dall, 1886)	Noetiidae	-
Didimacar tenebrica	(Reeve, 1844)	Noetiidae	SBMNH80722
Noetia ponderosa	(Say, 1822)	Noetiidae	SBMNH235066
*Sheldonella bisulcata**	(Lamarck, 1819)	Noetiidae	MZSP26911
*Striarca symmetrica**	(Reevi, 1844)	Noetiidae	MZSP55574
Glycymeris decussata	(Linnaeus, 1758)	Glycymerididae	MZSP91966
*Glycymeris longior**	(G. B. Sowerby I, 1833)	Glycymerididae	ZUEC-BIV78
Glycymeris undata	(Linnaeus, 1758)	Glycymerididae	MZSP91983
*Tucetona pectinata**	(Gmelin, 1791)	Glycymerididae	ZUEC-BIV2198

Table 2. Comparative morphology of the mantle margin in arcoidean species analyzed in this study. Habits of life, i.e., epifaunal (*EP*) and semi-infaunal/infaunal (*IN*), are indicated. An asterisk (*) indicates when the inner mantle fold is much longer posteriorly than the other folds. Abbreviation: *OF1*, first outer fold.

Taxa	**Pigmentation (OF1)**	**Compound eyes on OF1**	**Pigmented eyespot on OF1**	**Middle mantle fold length**	**Inner mantle fold length**	**Habit of life**
Acar dominguensis	pigmented	present	present	< OF1	= OF1	EP
Acar plicata	unpigmented	present	present	< OF1	= OF1	EP
Anadara brasiliana	unpigmented	absent	absent	< OF1	> OF1*	IN
Anadara chemnitzii	unpigmented	absent	absent	< OF1	> OF1*	IN
Anadara ferruginea	unpigmented	absent	present	absent	> OF1*	IN
Anadara inaequivalvis	unpigmented	absent	absent	< OF1	> OF1*	IN
Anadara notabilis	unpigmented	absent	present	< OF1	> OF1*	IN
Anadara ovalis	pigmented	absent	present	absent	> OF1*	IN
Anadara trapezia	unpigmented	absent	present	absent	> OF1*	IN
Arca imbricata	pigmented	present	present	absent	= OF1	EP
Arca patriarchalis	pigmented	present	present	absent	= OF1	EP
Arca ventricosa	pigmented	present	present	absent	= OF1	EP
Arca zebra	pigmented	present	present	absent	= OF1	EP
Barbatia amygdalumtostum	pigmented	present	present	< OF1	> OF1	EP
Barbatia cancellaria	pigmented	present	present	< OF1	> OF1	EP
Barbatia candida	pigmented	absent	present	< OF1	> OF1	EP
Barbatia lima	pigmented	absent	absent	< OF1	> OF1	EP
Barbatia virescences	pigmented	absent	present	< OF1	> OF1*	EP
Bathyarca corpulenta	unpigmented	absent	absent	< OF1	> OF1*	IN
Tegillarca ventricosa	unpigmented	absent	absent	< OF1	> OF1*	IN
Trisidos kiyonoi	unpigmented	absent	absent	< OF1	> OF1*	IN
Arcopsis adamsi	unpigmented	absent	present	< OF1	> OF1	EP
Didimacar tenebrica	unpigmented	absent	present	< OF1	> OF1	EP
Noetia ponderosa	pigmented	absent	absent	absent	> OF1	IN
Sheldonella bisulcata	pigmented	absent	absent	absent	> OF1	IN
Striarca symmetrica	pigmented	present	absent	= OF1	= OF1	EP
Glycymeris decussata	pigmented	present	absent	absent	= OF1	IN
Glycymeris longior	pigmented	present	absent	absent	= OF1	IN
Glycymeris undata	pigmented	present	absent	absent	= OF1	IN
Tucetona pectinata	pigmented	present	absent	absent	= OF1	IN

Table 3. Staining reactions of the secretory cells from the mantle margin of arcoideans. Positive reaction (+), strong positive reaction (++), weak/no reaction (–). Abbreviation: *AB*, alcian blue; *B*, stained in blue by TB-BF method; *E*, eosin; *H*, hematoxylin; *IF*, inner mantle fold and inner pallial epithelium; *MF*, middle mantle fold; *OF*, first outer fold and outer pallial epithelium; *P*, stained in pink by TB-BF method; *PAS*, periodic-Schiff method; *TB-BF*, toluidine blue and basic fuchsin.

Species	**Staining method**				
	H	**E**	**TB-BF**	**PAS**	**AB**
Anadara ovalis					
OF	–	–	–	+	+
IF	–	+	+(P)	+	+
Arca imbricata					
OF	–	++	–	+	–
IF	++	+	++(P)	+	++
Barbatia candida					
OF	–	+	+(P)	++	++
MF	–	+	++(P)	+	+
IF	–	+	++(P)	+	+
Arcopsis adamsi					
OF	–	++	+ (B)	+	–
MF	–	++	+ (B)	+	–
IF	–	++	+ (B)	+	–
Glycymeris longior					
OF	+	+	+ (B&P)	+	+
IF	+	+	+ (B&P)	+	–

CHAPTER 6

Ark clams and relatives (Bivalvia: Arcida) show convergent morphological evolution associated with lifestyle transitions in the marine benthos

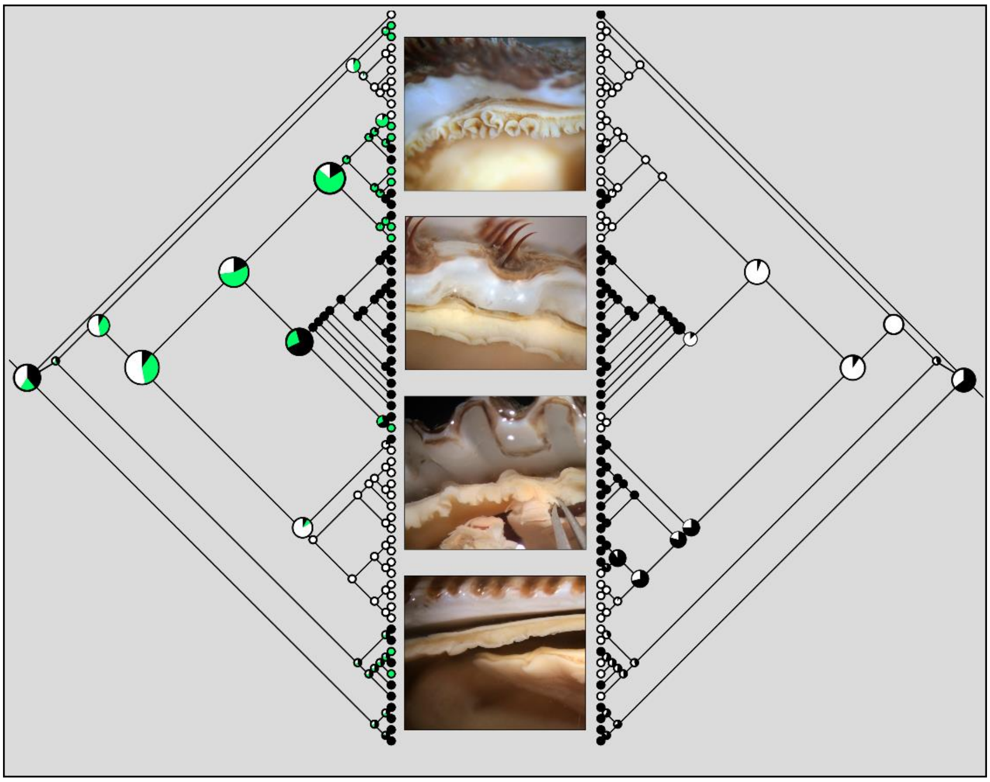

CHAPTER 6

Ark clams and relatives (Bivalvia: Arcida) show convergent morphological evolution associated with lifestyle transitions in the marine benthos

---

Abstract

One of the most intriguing questions in macroevolutionary studies is to understand how distantly related taxa can evolve towards similar phenotype in response to similar ecological conditions. Ark clams and their relatives (Arcida) display two main ecologies represented by epifaunal and infaunal lifestyles. Their mantle margin includes features, such as photosensory and muscular organs, that may coincide with each habit, making these bivalves a suitable model to explore evolutionary convergence in the marine benthos. To test for the evolutionary association between lifestyles and morphology, we gathered data on the mantle margin for 64 species across all six extant arcidan families. A molecular phylogeny of Arcida was inferred based on four gene sequences from 54 species and used to study trait evolution. Our results support that photoreceptor organs had a single origin and that infaunal lineages lost these structures in independent events, suggesting a correlated pattern of evolution. In addition, the enlargement of the posterior inner fold, which acts as a functional siphon, favored the occurrence of convergent transitions to infaunal habits during the Mesozoic. We provide evidence of ecomorphological associations and putative adaptations in a bivalve clade that sheds light into the underlying factors driving evolution of the marine benthos.

Keywords: adaptation – correlation – lifestyle – mantle – phenotype – phylogeny

This is the accepted version of the following article: *Ark clams and relatives (Bivalvia: Arcida) show convergent morphological evolution associated with lifestyle transitions in the marine benthos*, which has been published in final form at *Biological Journal of the Linnean Society*, 126(4): 866–884 (2019), https://doi.org/10.1093/biolinnean/blz017

Introduction

Macroevolutionary questions compose the core of evolutionary biology and focus on the association of phenotypical diversity with adaptive landscapes (Simpson, 1953; Schluter, 2000). Understanding whether and how similar ecological factors can drive independent taxa towards the same phenotype may help us better understand factors that drive evolution (Losos, 2011; Serb *et al.*, 2017). In this context, the repeated evolution of traits across independent lineages, i.e., evolutionary convergence (Agrawal, 2017), in association with similar environmental factors suggests putative adaptations and predictable responses to similar selective regimes (Harvey & Pagel, 1991; Losos, 2011; Mahler *et al.*, 2017). Whereas numerous vertebrate taxa are used as models for studies on evolutionary processes and convergence (Losos & Mahler, 2010), invertebrates are proportionally less studied, and supposed ecomorphological patterns in invertebrate taxa remain largely obscure.

Ark clams and their relatives (Bivalvia, Arcida) are marine pteriomorphian bivalves and are a suitable model to gain insights into convergent evolution due to their morphological and ecological diversity. Two main lifestyles are observed in the group (Oliver & Holmes, 2006). Epifaunal animals are attached to hard substrate (e.g., rocks and coral fragments) by a strong byssus (i.e., filaments secreted to attach the animal to solid surfaces). Alternatively, infaunal and semi-infaunal animals bury into soft sediment with the posterior region exposed above the surface. Previous anatomical studies have identified apparent associations between both modes of life with putative adaptations of shell shape, muscle organization, and photoreceptor organs (Stanley, 1972; Oliver & Holmes, 2006; Audino & Marian, 2018); however, these hypotheses were not directly tested using comparative methods.

The Arcida Gray, 1854 have a comprehensive fossil record dating back to the lower Ordovician (~450 Ma, million years ago) (Morton *et al.*, 1998; Cope, 2000). The Order currently encompasses the superfamilies Arcoidea and Limopsoidea, with an estimated diversity of more than 300 extant species (Oliver & Holmes, 2006; Carter *et al.*, 2011). The Arcoidea traditionally includes the families Arcidae, Cucullaeidae, Noetiidae, and Glycymerididae, while Limopsidae and Philobryidae are assigned to Limopsoidea (Oliver & Holmes, 2006; Carter *et al.*, 2011). Nevertheless, taxonomic classifications are controversial, with numerous morphological features likely representing homoplasies in response to similar ecologies (Oliver & Holmes, 2006).

One of these features is the mantle margin, a narrow region of soft tissues organized as lobe-like extensions lining the shell margin (Fig. 1A, B). This region is expected to evolve in response to shifts in lifestyle given that the mantle margin plays primary roles of interaction with the surrounding environment, including sensory, protective, and muscular functions (Yonge, 1983; Audino & Marian, 2016). The siphons are a classical example of a key morphological innovation in infaunal bivalves as a result of enlargement and fusion of the mantle folds. Siphons create channels for water circulation through the mantle cavity – where the gills are located – in animals that live constantly buried within the sediment (Yonge, 1983; Stanley, 1968). Other mantle structures, such as eyes and tentacles, have also been linked to ecological transitions. For instance, in scallops, depth was suggested to be an important driving force in the evolution of mantle eye components associated with light sensitivity (Malkowsky & Götze, 2014). Light-guided behaviors, e.g., related to predator detection and posture control (Nilsson, 1994), could also be associated with transitions to the epifaunal habit, *i.e.,* when the animal lives on top of the substrate. Consequently, the mantle margin in Arcida represents a promising source of information to identify convergent traits and test correlated evolution. Phenotypic diversity in number and length of mantle folds, and presence and complexity of photoreceptor organs are among key traits of this region (Waller, 1980; Morton, 1982; Morton & Peharda, 2008; Audino & Marian, 2018). Nevertheless, the structure of the mantle margin in the ancestor of ark clams and its subsequent morphological diversification have never been inferred, rendering several interesting questions. For example, did photoreceptor organs of the mantle margin evolve as adaptive traits in epifaunal groups? Are changes in mantle morphology related to shifts to the infaunal lifestyle? For instance, the enlarged posterior mantle fold of infaunal lineages may act as a functional siphon (*e.g.*, Morton, 1982) – did this attribute evolve convergently as an adaptation (or exaptation, Gould & Vrba, 1982) to the infaunal lifestyle?

A phylogenetic framework is crucial to provide initial steps towards these answers and elucidate the number of ecological transitions in the clade. Although the Arcida has been recovered monophyletic in many analyses (Steiner & Hammer, 2000; Giribet & Wheeler, 2002; Matsumoto, 2003; Bieler *et al.*, 2014), relationships among families and superfamilies remain under debate (Oliver & Holmes, 2006; Bieler *et al.*, 2014; Feng *et al.*, 2015; Combosch & Giribet, 2016). The placement of some groups, such as the Glycymerididae and the Limopsoidea, are particularly challenging (Combosch & Giribet, 2016). Consequently, a more robust phylogeny is needed to enable further evolutionary studies on the radiation of the group.

The present study provides a the most comprehensive phylogenetic analysis of Arcida to investigate morphological evolution in the clade and cast light on presumed adaptive features. Particularly, mantle margin morphology and lifestyles were studied in 64 species under a phylogenetic framework to test for correlation between lifestyle and morphology. The inferred molecular phylogenies, combined to the extensive morphological survey, provided a robust basis to discuss evolutionary patterns in the clade.

Material and Methods

Taxa sampling

Nucleotide sequences for four genes (18S rRNA, 28S rRNA, COI mtDNA, and histone H3) were obtained on GenBank for 54 species of Arcida, covering both superfamilies, all six families, and 20 genera (Table 1). The outgroup comprises seven species from other pteriomorphian orders and five species from the remaining major bivalve clades (Protobranchia and Heteroconchia) (Table 1). Missing data corresponded to 12% of the dataset for nucleotide sequences (Table 1). When possible, sampling effort was proportional to the diversity of each family, *i.e.*, relatively more samples were analyzed in groups comparatively more diverse (Table 1).

Morphological investigation of the mantle margin includes data from 64 species obtained from preserved specimens of the following collections: Museum of Comparative Zoology (MCZ), Museum of Zoology “Prof. Adão José Cardoso” of the University of Campinas (ZUECBIV), Museum of Zoology of the University of São Paulo (MZSP), Smithsonian National Museum of Natural History (USNM), and Santa Barbara Museum of Natural History (SBMNH). Respective catalog numbers are listed in Table 1. From the 64 species studied for morphology, 38 species have available sequences used for phylogenetic inference, while 26 species either belong to genera that include the remaining sequenced species or correspond to taxa included to complement the observations (Table 1). One to five specimens per species were dissected depending on the availability of preserved material.

Phylogenetic analysis and divergence times

Sequence alignments were generated with MAFFT v7.311 under the L-INS-i option (accurate strategy) (Katoh & Standley, 2013). ModelFinder (Kalyaanamoorthy *et al.*, 2017) was used to obtain the best-fit model of sequence evolution under the corrected Akaike information criterion (AICc), returning GTR + I + G for the concatenated dataset, which was applied in subsequent analyses. Maximum likelihood (ML) analysis was conducted in IQ-TREE (Nguyen *et al.*, 2014) and node support was estimated by standard nonparametric bootstrap (100 replicates) (Felsenstein, 1985). Divergence times of clades were estimated by Bayesian Inference (BI) in RevBayes v.1.0.9 under the fossilized birth-death model (Heath, Huelsenbeck,

& Stadler, 2014; Höhna *et al.*, 2016). This model imposes a time structure on the tree by marginalizing over all possible attachment points for the fossils on the extant tree. In addition, instead of treating the calibration density as an additional prior distribution on the tree, the model treats it as the likelihood of the fossil data given the tree parameter (Heath *et al.*, 2014).

Following Bieler *et al.* (2014), the root age for Bivalvia was constrained applying a uniform distribution prior between 520.5 and 530 Ma based on the fossil *Fordilla troyensis* (Pojeta *et al.*, 1973). Four additional fossils were used to calibrate internal node ages, three of them previously adopted elsewhere (Combosch & Giribet, 2016). The age of Arcida was constrained around 478.6 ± 5 Ma, based on *Glyptarca serrata* (Cope, 1997). Glycymerididae was constrained around 167.7 ± 5 Ma, based on *Trigonarca tumida* (Imlay, 1962). The fossil of *Anadara ferruginea* was used to constrain the age of the subfamily Anadarinae around 138.3 ± 5 Ma (Huber, 2010). Finally, the age of Philobryidae was constrained around 45 ± 11 Ma based on the oldest fossil records for the family (Moore & Teichert, 1969). All priors for fossil ages were drawn from uniform distributions. An uncorrelated exponential model on molecular branch rates was assumed for the relaxed molecular clock. Posterior probabilities were sampled using the MCMC (Markov Chain Monte Carlo) method with four independent chains running for 500,000 iterations, each one containing 534 moves (changes of values in stochastic parameters). Convergence of the posteriors were observed in Tracer version 1.6 (Rambaut *et al.*, 2018). Fossil taxa were then pruned from trees because they were solely used to calibrate node ages, rather than to infer phylogenetic placements. Subsequently, phylogenetic trees were summarized as a maximum clade credibility tree with a burn-in of 10% removed. A lineages-through-time plot was generated in IcyTree (https://icytree.org/).

Character evolution

Mantle margin evolution in Arcida was studied based on morphological data for 64 species from museum collections (Table 1). Specimens were dissected in ethanol and observed under the stereomicroscope for anatomical investigation. Characters were coded and states were assigned to terminals based on observations of the corresponding species. In the absence of data from literature, unobserved species had their states assigned as equivalent to closest relatives (i.e., congeneric species) obtained from collections (supplementary material, Table S1, S2). Characters are related to number and relative size of mantle folds, pigmentation, presence and type of photoreceptor organs, and presence of the mantle nerve (supplementary material, Table S1). Because ethanol often shrinks/distorts tissues during preservation, mantle fold length is a character defined by the relative length of a fold in comparison to another fold, rather than absolute length. Some multistate characters were also coded as binary (see supplementary material, Table S1), as required by the correlation test (Pagel, 1994).

Information on habits of life was compiled from literature for all species included in the phylogenetic analysis (supplementary material, Table S3). Modes of life include: epifaunal (above the substrate, frequently attached to the surface), semi-infaunal (partially buried in soft sediment), and infaunal (buried in soft sediment), with respective modes of byssal attachment, i.e., epibyssate, endobyssate, and abyssate. Additional information was also recovered, such as type of substrate and occurrence relative to depth, varying from shallow (<200 m) to deep waters (>200 m). Subsequently, lifestyles were coded (supplementary material, Table S1, S2) and studied for character evolution as detailed below.

Ancestral state reconstructions (ASR) were conducted under maximum likelihood in Mesquite (Maddison & Maddison, 2018). Two possible models for trait evolution were applied, *i.e.*, the Markov k-state one parameter model (MK1) that assumes equal transition rates and the asymmetrical Markov k-state two parameter model (AsymmMK), in which transition rates can be different. In contrast to the MK1 model, the AsymmMK model allow different rates for "forward" ($0 \rightarrow 1$) and "backward" ($1 \rightarrow 0$) transitions. A likelihood ratio (LR) test was used to verify which model fits the data better (Pagel, 1999, Maddison & Maddison, 2018). Because the two models are nested, the likelihood ratio test follows a chi-square distribution with df=1 (because the AsymmMK model has only one additional parameter than the MK1 model). The reconstructions presented herein follow the statistical decision to reject the null hypothesis (MK1 model) whenever $LR > 3.84$ (critical value for $\alpha = 0.05$, df=1). To evaluate the possible effects of branch supports and alternative topologies in the reconstruction, bootstrap trees were also investigated to inspect the consistency of the reconstructed evolutionary patterns (see Maddison & Maddison, 2018).

Pagel's correlation test was applied in Mesquite (Pagel, 1994; Maddison & Maddison, 2018) to compare the evolution of modes of life and morphological traits, such as photoreceptor organs, mantle folds, and pigmentation. Even though the method has some shortcomings (Maddison & Fitzjohn, 2015), it provides a helpful approach to statistically analyse the evolution of traits by incorporating phylogenetic information. Additionally, tests were conducted considering models representing evolutionary dependence among traits, *i.e.*, when the shift of state in one character likely depends on the state of the second character. Searches were carried out (iterations; n=10) with the p value being estimated from 10,000 repeated simulations. Hypotheses of character correlations were accepted whenever a model with eight-parameters (correlated hypothesis) presented a better fit ($p<0.05$) than a model of evolution with four parameters (uncorrelated hypothesis) (Pagel, 1994; Maddison & Fitzjohn, 2015).

Results

Mantle margin diversity in Arcida

Mantle margin in arcids may comprise four marginal extensions, named mantle folds, identified according to the position relative to the periostracal groove (Fig. 1A, B). They are named, from the outside to the inside: second outer fold (2OF), first outer fold (1OF), middle fold (MF), and inner fold (IF) (Fig. 1B). The second outer fold is a short and delicate projection in a proximal position, present in most Arcida representatives. This structure is usually unpigmented and located close to the region where the pallial muscles are attached to the valve. While this fold is apparent in ark clams and blood cockles, like *Anadara* and *Tegillarca* (Fig. 1L), it seems to be extremely reduced or even absent in smaller species. This is the case of some Philobryidae species (e.g., *Adacnarca*, *Lissarca*, and *Neocardia*) in which the second outer fold was not observed.

The first outer fold is usually well developed in most species, being frequently pigmented and bearing photoreceptor organs. Strong pigmentation is common in epifaunal species, such as *Arca* (Fig. 1D), although pigmentation is also present in some semi-infaunal (e.g., Glycymerididae; Fig. 2E, F) and infaunal species (e.g., some *Anadara* spp.). Photoreceptor organs vary from small eyespots to large compound eyes (Fig. 1, 2). Pigmented eyespots are present in epifaunal Noetiidae, such as *Arcopsis* (Fig. 2B), *Didimacar*, and *Stryarca*, most Arcidae taxa (Fig. 1H), except *Trisidos* (infaunal) and *Bathyarca* (infaunal; deep-sea), and some Philobryidae, including *Lissarca notorcardensis* and *Neocardia* sp. (Fig. 2K). These eyespots are frequently restricted to the anterodorsal region. Compound eyes are larger, multifaceted structures, occurring on the posterior region of *Acar*, *Arca*, *Cucullaea* (Fig. 1C, D, F), Glycymerididae (Fig. 2E, F), and some *Barbatia* species (Fig. 1E, G).

The middle mantle fold, when present, represents a reduced projection, shorter than the first outer fold (Fig. 1E). No photoreceptor or tentacular structures are associated with this projection. The middle fold is absent in the genera *Arca*, *Cucullaea*, and *Trisidos* (Fig. 1C, D, F, N). The mantle margin also lacks a middle fold in Glycymerididae, Philobryidae, and infaunal Noetiidae (e.g., *Eontia* and *Noetia*) (Fig. 2).

The inner mantle fold is an enlarged, muscular projection in most arcid taxa, usually longer and robust posteriorly. In the Cucullaeidae, Glycymerididae, Limopsidae, Philobryidae, and the genus *Arca*, the inner mantle fold is about the length of the first outer fold or slightly longer (Figs. 1D, 2G-M). In contrast, the inner fold is about twice the length of the first outer fold in Noetiidae, *Barbatia*, and *Acar* (Figs. 1E, G). A massive enlargement of the inner fold is observed in some *Barbatia* species and in numerous infaunal species, such as *Trisidos*, *Anadara*, *Tegillarca*, *Eontia*, and *Noetia* (Figs. 1I-N). A posterior flap, formed by the inner fold, is a long projection found in *Bathyarca* species (Fig. 1M).

The mantle margin in arcids exhibits different levels of variation among taxa. For example, fold number and relative lengths are very uniform within the Anadarinae (Fig. 1J-L), but highly variable within *Barbatia* (Fig. 1E, G-I). Within Noetiidae, mantle organization is also variable (Fig. 2A-D), while in Glycymerididae it is more uniform (Fig. 2E, F). In contrast, the Limopsidae (Fig. 2G-I) and Philobryidae (Fig. 2J-M) have a less complex and miniaturized mantle margin, usually devoid of photoreceptor organs, pigmentation or enlarged folds.

Phylogenetic hypotheses

The maximum likelihood tree of the Arcida corroborates the monophyly of the clade, as well as the monophyly of all families, except for Arcidae, which is split into five branches (Fig. 3). Although some internal nodes show low bootstrap values, higher support was obtained for some relationships among families and genera (e.g., *Arca*, Anadarinae, Glycymerididae, Limopsidae). The remaining Pteriomorphia were recovered as the sister-group of Arcida.

Arcidae is polyphyletic in our analysis, with *Arca* and *Acar* descending from an early branch of the order. All Anadarinae species are nested together, being sister-group to a pair of *Barbatia* species (*B. candida* and *B. lacerata*). Interestingly, *Barbatia* species are scattered across the phylogeny, suggesting separate lineages taxonomically included under the same name. Noetiidae is a monophyletic family, although *Adacnarca nitens*, formally a philobryid, seems to also be included in this clade. A close relationship between Limopsidae and Philobryidae was recovered, with Glycymerididae as the sister-group. The three former families were recovered as the sister-group of (*Cucullaea* + *Bathyarca*).

A similar topology was recovered for the time-calibrated phylogeny (Fig. 4). Diversification times were estimated for the major lineages with the 95% highest posterior density interval (HPD): Arcida, 341.3 Ma (95% HPD 261.2–424.1 Ma); Glycymerididae, 194.6 Ma (95% HPD 112.1–278.3 Ma); Anadarinae, 190.5 Ma (95% HPD 124–256.7 Ma); Limopsoidea, 187.7 Ma (95% HPD 113.4–259.3 Ma); Noetiidae, 175.5 Ma (95% HPD 96.6–248.1 Ma); Philobryidae, 143 Ma (95% HPD 77.1–215.9 Ma); and Limopsidae, 110.4 Ma (95%

HPD 37.8–195.1 Ma). A lineage-through-time plot also shows a major diversification of Arcida lineages during the Mesozoic (Fig. 4).

Mantle margin evolution

The history of changes in the mantle margin was reconstructed based on key traits. A second outer fold has arisen in the origin of the Arcida clade, and likely lost in Limopsidae and Philobryidae lineages (data not shown). Intense mantle pigmentation was acquired multiple times, *i.e.* in the origin of Glycymerididae, *Arca* + *Acar*, *Barbatia barbata* + *B. cancellaria* + *B. fusca*, and some lineages within Anadarinae (supplementary material, Fig. S1). The ancestor of Arcida had a reduced middle fold, i.e., shorter than the first outer fold (Fig. 5), which is a striking contrast to the remaining Pteriomorphia, in which the middle fold is long and usually bears tentacles and photoreceptor organs. While most arcids share a reduced middle fold, the complete loss of this projection occurred at least ten times (Fig. 5). Photoreceptor organs were reconstructed to be present in the mantle margin of the Arcida's ancestor. More specifically, the presence of pigmented eyespots represents a plesiomorphy for all arcid taxa, with secondary losses for many infaunal lineages, such as *Eontia*, *Limopsis*, and *Trisidos* (Fig. 6A). Similarly, compound eyes were likely present in the Arcida's ancestor, which were subsequently lost in four separate lineages: Limopsoidea, *Bathyarca*, Anadarinae+(*Barbatia candida*+*B. lacerata*), and a clade formed by Noetiidae with some *Barbatia* and *Trisidus* species (supplementary material, Fig. S2).

The inner fold is commonly longer than the other mantle folds in most bivalves, but in Arcida this trait displays significant variation. The inner fold is reconstructed to be about the length of the first outer fold, or only slightly longer, in the origin of the order (Fig. 7A). The enlargement of this fold, forming a long projection about twice the length of the first outer fold, occurred in the *Acar*'s ancestor and in the ancestor of a large clade including Noetiidae, Anadarinae, and *Barbatia* species (Fig. 7A). Another change in state is represented by a very enlarged inner fold, much longer than first outer fold, forming extensible curtains and flaps. This transition occurred in different clades, e.g., *Trisidos*, *Eontia*, *Bathyarca*, and Anadarinae + *Barbatia*, most of them including infaunal bivalves (Fig. 7B).

Association between mantle margin morphology and lifestyles

The reconstruction of modes of life suggests that the ancestor of Arcida was likely an epifaunal bivalve, possibly attached to rocks and hard substrate by byssus (Fig. 6B, supplementary Table S3). Soft sediments, such as mud and sand, were later independently occupied by different groups. The semi-infaunal/infaunal lifestyle was secondarily adopted four times during Arcida evolution during the Mesozoic (Fig.4, 6B), by lineages originating Anadarinae, *Trisidos*, *Eontia* (infaunal noetiids), and the ancestor of all Limopsoidea + Glycymerididae + (*Bathyarca* + Cucullaeidae). Among infaunal lineages, a shift to epifaunal lifestyle has occurred in the origin of Philobryidae (Fig. 6B), animals that are frequently byssate on other organisms, such as algae.

Correlation tests were applied when mantle traits seemed to be associated with particular lifestyles. For instance, pigmentation on the first outer fold is common in epifaunal bivalves. Tested hypotheses of evolutionary correlation are shown in Table 2. Pigmentation, which is typical for epifaunal bivalves, is not statistically correlated to lifestyle (Table 2). Pigmented eyespots, however, had a statistically significant correlation to lifestyle (Table 2). Ancestral state reconstructions of eyespots and lifestyles suggest that this correlation is associated with the adoption of infaunal habits and loss of pigmented eyespots (Fig. 6). Inner fold enlargement is also correlated to mode of life, the results suggesting that the evolutionary shift to infaunal habit was more likely when the inner fold became much longer than the first outer fold (Table 2).

Discussion

Phylogenetic relationships and divergence times

Arcida is a well-supported, monophyletic group (see also Bieler *et al.*, 2014; Feng *et al.*, 2015; Combosch & Giribet, 2016). All families were recovered monophyletic, with the exceptions of a polyphyletic Arcidae and the placement of the philobryid *Adacnarca nitens* within Noetiidae. While a previous analysis found support to separate Arcoidea from Limopsoidea (Combosch & Giribet, 2016), our results indicate Arcoidea as non-monophyletic. This is consequence of an early branch giving rise to *Acar* and *Arca*, while Limopsoidea is nested within the remaining Arcoidea. Therefore, the Limopsoidea would have an origin from within the Arcoidea, a hypothesis not supported by previous topologies (Combosch & Giribet, 2016), but already suggested elsewhere (Jackson *et al.*, 2015). Our topology is consistent with the view that Limopsidae and Philobryidae share an exclusive, common history based on similar development of hinge and alivincular ligament type (Malchus & Warén, 2005; Oliver & Holmes, 2006).

The taxonomic position of Glycymerididae has always been controversial and our data supports this family within Arcoidea, as also suggested by Combosch & Giribet (2016). In contrast to their results, however, the Glycymerididae is the sister group of Limopsoidea in our analysis, forming a clade closely related to *Cucullaea* and *Bathyarca*. The Glycymerididae was previously thought to have originated from the Cucullaeidae based on the duplivincular ligament and other shell characters observed in fossil species (Nicol, 1950). Our results do not corroborate this view, but their morphological similarity is supported by the close relationship between these families.

Arcidae is not monophyletic in our analyses, which is consistent with previous studies (Marko, 2002; Matsumoto, 2003; Feng *et al.*, 2015; Combosch & Giribet, 2016). For instance, the genus *Barbatia* is polyphyletic, and thus in great need of taxonomic revisions. Similarly to previous findings (Combosch & Giribet, 2016), some *Barbatia* species, such as *B. candida* and *B. lacerata*, form the sister group of Anadarinae, while others, such as *B. virescens*, are close to *Trisidos* and Noetiidae.

The oldest fossils of Arcida, i.e. *Glyptarca serrata*, date back to the Ordovician (~480 Ma) (Cope, 1997). According to our analysis, the arcid divergence occurred in late Cambrian (~488 Ma) and the crown group of Arcida had a Carboniferous origin, around 341 Ma. Our time-calibrated phylogeny agrees with the fossil record (Thomas, 1978a; Oliver & Holmes, 2006), suggesting most diversification of Arcida occurred during the Mesozoic, including the origin of most modern families, i.e., Cucullaeidae, Glycymerididae, Limopsidae, and Philobryidae. The convergent transitions to semi-infaunal or infaunal habits by different lineages, such as noetiids, Anadarinae, Cucullaeidae, Glycymerididae, and Limopsidae, may have contributed to the diversification of Arcida, which is consistent with the Cretaceous fossil record (Thomas, 1978b; Thomas *et al.*, 2000; Oliver & Holmes, 2006; Combosch & Giribet, 2016). The adoption of an infaunal lifestyle in bivalves is regarded as one of the most important strategies to avoid predation by a diversity of duraphagous predators during the long-lasting ecological arms race of the so-called Mesozoic Marine Revolution (Stanley, 1968; Vermeij, 1977). Our results provide, therefore, further evidence for the Mesozoic infaunalization of bivalves.

Evolution of mantle traits and lifestyle

The second outer mantle fold is an exclusive feature of Arcida, shared by most of its descendants (see also Waller, 1980). Photoreceptor organs on the first outer fold are also distinctive traits of Arcida, and they are present mainly in epifaunal species inhabiting shallow waters (Waller, 1980; Morton & Peharda, 2008; Morton & Puljas, 2015; Audino & Marian, 2018; present study). Our data support the correlated evolution of photoreceptor organs and mode of life, as previously suggested based on morphological studies alone (Audino & Marian, 2018).

The Arcida's ancestor had pigmented eyespots and posterior compound eyes that were lost in numerous lineages (Fig. 6, S2). These findings suggest an important role of light-guided behaviors in ancestral ark clams living on the substrate, possibly related to predator detection and posture control (Nilsson, 1994). A single origin of compound eyes is in accordance with the anatomical similarity of these organs in the distinct arcidan lineages that were studied so far, such as Glycymerididae, the genera *Arca* and *Acar*, and some *Barbatia* species (Waller, 1980; Morton & Puljas, 2015, Audino & Marian, 2018). Additionally, the loss of photoreceptor organs also provides important insights into the evolution of ark clams. Infaunal lineages frequently lost photoreceptor organs present in their epifaunal ancestor (Fig. 6, S2), which can be explained either by a condition of relaxed selection under the infaunal condition or a positive selective pressure for eye reduction.

Relaxed selection can be defined as the elimination or reduction, by means of environmental changes, of a selective force that was important for the maintenance of a particular trait (Lahti *et al.*, 2009). This is an evolutionary process frequently evoked to explain eye and pigment reduction in several groups, including numerous lineages of cave animals (Porter & Crandall, 2003; Wilkens, 2010). Alternatively, other processes can also produce similar patterns. For example, variability in eye size and pigmentation in cave fishes occurs through multiple mechanisms, suggesting different evolutionary forces synergistically driving eye regression via pleiotropy (Protas *et al.*, 2008). Studies of both vertebrate and invertebrate cave lineages have also demonstrated the high energetic costs of maintaining sensory systems, such as eyes, even in dark conditions (Niven 2007; Niven & Laughlin 2008). For example, eye loss in cavefishes may have been driven by selection for regression of neural tissue, which is associated with high metabolic costs (Moran *et al.*, 2015). In cave crabs, eye reduction seems to be most likely driven by strong directional selective regimes in the subterranean environment (Klaus *et al.*, 2013). In the marine infaunal context, our results provide the initial steps to understand the evolutionary trajectory of photoreceptor organs in ark clams. Similar to many intriguing cave lineages' cases (Niven, 2007), further studies are still necessary to clarify if eye loss in infaunal bivalves is produced by selective pressure or by genetic drift when selective pressures for eye maintenance are absent.

The middle fold is a mantle margin projection usually well-developed in most bivalves, frequently bearing associated structures and playing sensorial roles (Yonge, 1983). An opposite condition was observed in most specimens studied herein, in which the middle fold is shorter than the outer and inner folds, corresponding to only a slight projection, when present. A shorter middle fold was also noted in *Limopsis cristata* (Morton, 2013) and *Barbatia* species (Simone & Chichvarkhin, 2004). Our results suggest that this fold was already reduced in the ancestor of Arcida, which is a remarkable difference from other pteriomorphians, which frequently display a long and complex projection (Audino & Marian, 2016). The reduction of the middle fold seems to have been a common phenomenon during Arcida diversification, resulting in the complete loss of this structure in several lineages (Fig. 5). Such evolutionary pattern is unique among bivalves and leaves many unsolved functional questions. One possible explanation was provided by Morton (1982), who suggested that sensorial roles, such as photoreception, were transferred to the first outer fold. In addition, recent anatomical evidence from different arcid species also corroborated this view, indicating that chemo-/mechano-sensorial roles were possibly transferred to the enlarged inner fold (Audino & Marian, 2018).

The hypertrophy of the inner fold in a very extensible organ is observed in many lineages of Arcida (Fig. 7). For example, most semi-infaunal or infaunal arcids, such as some Noetiidae, Anadarinae, *Trisidos,* and *Bathyarca*, have very long inner folds (see also Morton, 1982; Audino & Marian, 2018). In infaunal bivalves of other clades (e.g., Heterodonta), siphons (i.e., long, fused inner folds) are present and allow them to inhabit soft sediments and maintain water circulation through the pallial cavity (Yonge, 1983). In the case of the infaunal *Bathyarca pectunculoides,* the posterior flaps formed by the inner fold are thought to act as functional siphons (Morton, 1982). Accordingly, our phylogenetic and morphological data strongly support the evolution of the inner fold as a functional siphon in arcid lineages, which has possibly facilitated the transition to infaunal lifestyles.

Evolutionary convergence and macroevolution

Ecological shifts shaping morphological evolution are known for many vertebrate groups (e.g., lizards, Mahler *et al.*, 2013; fishes, Davis & Betancur-R, 2017; snakes, Esquerré & Scott Keogh, 2016). While marine invertebrates still lack detailed information about ecomorphological evolution, recent progress has been achieved using different clades as models. In cephalopods, for example, several morphological traits represent evolutionary convergences and possible adaptive features associated with benthic or pelagic environments (Lindgren *et al.,* 2012). While bivalves have traditionally being considered classic examples of convergent evolution associated with life-habits in the marine benthos (e.g., Stanley, 1972), even in Invertebrate Zoology textbooks (e.g., Ruppert *et al.*, 2004), these adaptive hypotheses have rarely been tested under an explicit phylogenetic approach. In this context, important progresses were recently obtained for Pectinidae (Alejandrino *et al.*, 2011; Serb *et al.*, 2017) and Galeommatoidea (Li *et al.*, 2016).

The Arcida have been consistently regarded as an example of adaptive radiation, with their homoplastic shell characters adapted to infaunal and epifaunal modes of life (Stanley, 1968, 1972; Thomas, 1976, 1978a). Our study provides, for the first time, phylogenetic-based evidence for correlated evolution between morphology of soft parts and lifestyle transitions in arcids. In addition, evolutionary convergence seems a recurrent pattern, including independent losses of eyespots, compound eyes, pigmentation and middle fold, as well as independent enlargements of the inner fold. Our results suggest that predation pressure was important in the evolution of Arcida, mainly during the Mesozoic. Pigmented eyespots and compound eyes may aid in predator recognition in epifaunal bivalves (Nilsson, 1994), while the infaunal habit itself, facilitated by enlarged mantle curtains, may have been a response to predation pressure (Bush & Bambach, 2011). The dramatic increase of infaunal lineages in the marine benthos suggests a successful trend to survive the intensification of predation during the Mesozoic Marine Revolution (Stanely, 1968, 1972; Vermeij, 1977). In addition to the extensive fossil information for hard parts, we were able to contribute to this hypothesis based on the soft parts of extant lineages of arcids in an integrative approach. Altogether, our results demonstrate evolutionary associations between ecology and morphology during the diversification of bivalve lineages across different benthic lifestyles.

Acknowledgments

The authors acknowledge the grants 2015/09519-4 and 2017/01365-3, São Paulo Research Foundation (FAPESP). This study was financed in part by the Coordenação de Aperfeiçoamento de Pessoal de Nível Superior - Brasil (CAPES) - Finance Code 001. This study is part of the first author’s Doctorate’s thesis through the Graduate Program in Zoology of the Institute of Biosciences (University of São Paulo). The authors thank the following institutions that provided materials for the development of this study: Museum of Comparative Zoology (MCZ), Museum of Zoology “Prof. Adão José Cardoso” of the University of Campinas (ZUEC), Museum of Zoology of the University of São Paulo (MZSP), Santa Barbara Museum of Natural History (SBMNH), and Smithsonian National Museum of Natural History (USNM). We also thank two anonymous reviewers for their helpful comments. This is a contribution of NP-BioMar (Research Center for Marine Biodiversity – USP).

References

Alejandrino A, Puslednik L, Serb JM. 2011. Convergent and parallel evolution in life habit of the scallops (Bivalvia: Pectinidae). *BMC Evolutionary Biology* 11: 164.

Audino JA, Marian JEAR. 2016. On the evolutionary significance of the mantle margin in pteriomorphian bivalves. *American Malacological Bulletin* 34: 148–159.

Audino JA, Marian JEAR. 2018. Comparative and functional anatomy of the mantle margin in ark clams and their relatives (Bivalvia: Arcoidea) supports association between morphology and life habits. *Journal of Zoology* 305(3): 149–162.

Bieler R, Mikkelsen PM, Collins TM, Glover EA, González VL, Graf DL, Harper EM, Healy J, Kawauchi GY, Sharma PP, Staubach S, Strong EE, Taylor JD, Tëmkin I, Zardus JD, Clark S, Gusmán A, McIntyre E, Sharp P, Giribet G. 2014. Investigating the Bivalve Tree of Life - An exemplar-based approach combining molecular and novel morphological characters. *Invertebrate Systematics* 28: 32–115.

Bush AM, Bambach RK. 2011. Paleoecologic megatrends in marine metazoa. *Annual Review of Earth and Planetary Sciences* 39: 241–269.

Carter JG, Altaba CR, Anderson LC, Araujo R, Biakov AS, Bogan AE, Campbell DC, Campbell M, Jin-hua C, Cope JCW, Dijkstra HH, Zong-jie F, Gardner RN, Gavrilova VA, Goncharova IA, Harries PJ, Hartman JH, Hautmann M, Hoeh WR, Hylleberg J, Johnston P, Kirkendale L, Kleemann K, Koppka J, Machado D, Malchus N, Márquez-aliaga A, Masse J pierre, Mcroberts CA, Peter U, Mitchell S, Nevesskaja LA, Özer S, Jr JP, Polubotko I V, Pons M, Popov S, Sánchez T, Sartori AF, Scott RW, Sey II, Javier H, Silantiev V V, Skelton PW, Steuber T, Waterhouse JB, Lynn G, Yancey T, Carter JG, Altaba CR, Anderson LC, Araujo R, Biakov AS, Bogan AE, Campbell DC, Campbell M, Jin-hua C, Cope JCW, Delvene G, Dijkstra HH, Gardner RN, Gavrilova VA, Goncharova IA, Harries PJ, Hartman JH, Hoeh WR, Hylleberg J, Bao-yu J, Johnston P, Kirkendale L, Kleemann K, Middelfart PU, Mitchell S, Nevesskaja LA, Özer S, Pojeta J, Polubotko I V, Silantiev V V, Skelton PW, Steuber T, Waterhouse JB, Wingard GL, Yancey T, Harries PJ, Skelton P. 2011. A synoptical classification of the Bivalvia (Mollusca). *Paleontological Contributions* 4: 1–47.

Combosch DJ, Giribet G. 2016. Clarifying phylogenetic relationships and the evolutionary history of the bivalve order Arcida (Mollusca: Bivalvia: Pteriomorphia). *Molecular Phylogenetics and Evolution* 94: 298–312.

Cope JCW. 1997. The early phylogeny of the class Bivalvia. *Palaeontology* 40: 713–746.

Cope JCW. 2000. A new look at early bivalve phylogeny. *Geological Society, London, Special Publications* 177: 81–95.

Davis AM, Betancur-R R. 2017. Widespread ecomorphological convergence in multiple fish families spanning the marine–freshwater interface. *Proceedings of the Royal Society B: Biological Sciences* 284: 20170565.

Esquerré D, Scott Keogh J. 2016. Parallel selective pressures drive convergent diversification of phenotypes in pythons and boas. *Ecology Letters* 19(7): 800–809.

Felsenstein J. 1985. Confidence limits on phylogenies: an approach using the bootstrap. *Evolution* 39: 783–791.

Feng Y, Li Q, Kong L. 2015. Molecular phylogeny of Arcoidea with emphasis on Arcidae species (Bivalvia: Pteriomorphia) along the coast of China: Challenges to current classification of arcoids. *Molecular Phylogenetics and Evolution* 85: 189–196.

Giribet G, Wheeler W. 2002. On bivalve phylogeny: a high-level analysis of the Bivalvia (Mollusca) based on combined morphology and DNA sequence data. *Invertebrate Biology* 121: 271–324.

Gould SJ, Vrba ES. 1982. Exaptation—a missing term in the science of form. *Paleobiology* 8(1): 4–15.

Harvey PH, Pagel MD. 1991. *The comparative method in evolutionary biology*. Oxford: Oxford University Press.

Heath TA, Huelsenbeck JP, Stadler T. 2014. The fossilized birth--death process for coherent calibration of divergence-time estimates. *Proceedings of the National Academy of Sciences* 111: E2957–E2966.

Höhna S, Landis MJ, Heath TA, Boussau B, Lartillot N, Moore BR, Huelsenbeck JP, Ronquist F. 2016. RevBayes: Bayesian phylogenetic inference using graphical models and an interactive model-specification language. *Systematic Biology* 65: 726–736.

Huber M. 2010. *Compendium of Bivalves*. Hackenheim: ConchBooks.

Imlay RW. 1962. *Jurassic (Bathonian or early Callovian) ammonites from Alaska and Montana*. US Government Printing Office.

Jackson JA, Linse K, Whittle R, Griffiths HJ. 2015. The evolutionary origins of the southern ocean philobryid bivalves: Hidden biodiversity, ancient persistence. *PLoS ONE* 10(4): e0121198.

Kalyaanamoorthy S, Minh BQ, Wong TKF, von Haeseler A, Jermiin LS. 2017. ModelFinder: fast model selection for accurate phylogenetic estimates. *Nature Methods* 14: 587.

Katoh K, Standley DM. 2013. MAFFT multiple sequence alignment software version 7: improvements in performance and usability. *Molecular Biology and Evolution* 30: 772–780.

Klaus S, Mendoza JCE, Liew JH, Plath M, Meier R, Yeo DCJ. 2013. Rapid evolution of troglomorphic characters suggests selection rather than neutral mutation as a driver of eye reduction in cave crabs. *Biology Letters* 9(2): 20121098.

Lahti DC, Johnson NA, Ajie BC, Otto SP, Hendry AP, Blumstein DT, Coss RG, Donohue K, Foster SA. 2009. Relaxed selection in the wild. *Trends in Ecology and Evolution* 24: 487–496.

Li J, Ó Foighil D, Strong EE. 2016. Commensal associations and benthic habitats shape macroevolution of the bivalve clade Galeommatoidea. *Proceedings of the Royal Society B: Biological Sciences* 283: 20161006.

Lindgren AR, Pankey MS, Hochberg FG, Oakley TH. 2012. A multi-gene phylogeny of Cephalopoda supports convergent morphological evolution in association with multiple habitat shifts in the marine environment. *BMC Evolutionary Biology* 12: 129.

Losos JB. 2011. Convergence, adaptation, and constraint. *Evolution* 65: 1827–1840.

Losos JB, Mahler DL. 2010. Adaptive radiation: The interaction of ecological opportunity, adaptation, and speciation. In: Bell MA, Futuyma DJ, Eanes WF, Levinton JS, eds. *Evolution since Darwin: the first 150 years*. Sanderland: Sinauer Associates, 381–420.

Maddison WPM, Fitzjohn RG. 2015. The unsolved challenge to phylogenetic correlation tests for categorical characters. *Systematic Biology* 64: 127–136.

Maddison WP, Maddison DR. 2018. Mesquite: a modular system for evolutionary analysis. Version 3.51 http://www.mesquiteproject.org

Mahler DL, Ingram T, Revell LJ, Losos JB. 2013. Exceptional convergence on the macroevolutionary landscape in island lizard radiations. *Science* 341(6143): 292–295.

Mahler DL, Weber MG, Wagner CE, Ingram T. 2017. Pattern and process in the comparative study of convergent evolution. *The American Naturalist* 190: S13–S28.

Malchus N, Warén A. 2005. Shell and hinge morphology of juvenile *Limopsis* (Bivalvia: Arcoida) - Implications for limopsid evolution. *Marine Biology Research* 1(5): 350–364.

Malkowsky Y, Götze MC. 2014. Impact of habitat and life trait on character evolution of pallial eyes in Pectinidae (Mollusca: Bivalvia). *Organisms Diversity & Evolution* 14(2): 173–185.

Marko PB. 2002. Fossil calibration of molecular clocks and the divergence times of geminate species pairs separated by the Isthmus of Panama. *Molecular Biology and Evolution* 19: 2005–2021.

Matsumoto M. 2003. Phylogenetic analysis of the subclass Pteriomorphia (Bivalvia) from mtDNA COI sequences. *Molecular Phylogenetics and Evolution* 27: 429–440.

Moore RC, Teichert C. 1969. *Treatise on Invertebrate Paleontology: Pt. N Mollusca 6, Bivalvia*. Geological Society of America.

Morton B. 1982. Functional morphology of *Bathyarca pectunculoides* (Bivalvia: Arcacea) from a deep Norwegian fjord with a discussion of the mantle margin in the Arcoida. *Sarsia* 67: 269–282.

Morton B. 2013. The functional morphology of the abyssal *Limopsis cristata* (Arcoida: Limopsidae) with a discussion on the evolution of the more advanced bivalve foot. *Acta Zoologica* 94: 74–85.

Morton B, Peharda M. 2008. The biology and functional morphology of *Arca noae* (Bivalvia: Arcidae) from the Adriatic Sea, Croatia, with a discussion on the evolution of the bivalve mantle margin. *Acta Zoologica* 89: 19–28.

Morton B, Prezant RS, Wilson B. 1998. Class Bivalvia. In: Beesley PL, Ross GJB, Wells A, eds. *Mollusca: The southern synthesis. Fauna of Australia. Vol. 5*. Melbourne: CSIRO Publishing, 195–234.

Morton B, Puljas S. 2015. The ectopic compound ommatidium-like pallial eyes of three species of Mediterranean (Adriatic Sea) *Glycymeris* (Bivalvia: Arcoida). Decreasing visual acuity with increasing depth? *Acta Zoologica* 474: 464–474.

Nguyen LT, Schmidt HA, von Haeseler A, Minh BQ. 2014. IQ-TREE: a fast and effective stochastic algorithm for estimating maximum-likelihood phylogenies. *Molecular Biology and Evolution* 32: 268–274.

Nicol D. 1950. Origin of the pelecypod family Glycymeridae. *Journal of Paleontology* 24: 89–98.

Nilsson DE. 1994. Eyes as optical alarm systems in fan worms and ark clams. *Philosophical Transactions of the Royal Society B: Biological Sciences* 346(1316): 195–212.

Oliver PG, Holmes AM. 2006. The Arcoidea (Mollusca: Bivalvia): A review of the current phenetic-based systematics. *Zoological Journal of the Linnean Society* 148: 237–251.

Pagel M. 1994. Detecting correlated evolution on phylogenies: a general method for the comparative analysis of discrete characters. *Proceedings of the Royal Society B-Biological*

Sciences 255: 37–45.

Pagel M. 1999. The maximum likelihood approach to reconstructing ancestral character states of discrete characters on phylogenies. *Systematic Biology* 48(3): 612–622.

Pojeta J, Runnegar B, Kriz J. 1973. *Fordilla troyensis* Barrande: the oldest known pelecypod. *Science* 180: 866–868.

Porter ML, Crandall KA. 2003. Lost along the way: The significance of evolution in reverse. *Trends in Ecology and Evolution* 18: 541–547.

Protas M, Tabansky I, Conrad M, Gross JB, Vidal O, Tabin CJ, Borowsky R. 2008. Multi-trait evolution in a cave fish, *Astyanax mexicanus*. *Evolution & Development* 10: 196–209.

Rambaut A, Drummond AJ, Xie D, Baele G, Suchard MA. 2018. Posterior summarisation in Bayesian phylogenetics using Tracer 1.7. *Systematic Biology* syy032

Schluter D. 2000. *The ecology of adaptive radiation*. Oxford: Oxford University Press.

Serb JM, Sherratt E, Alejandrino A, Adams DC. 2017. Phylogenetic convergence and multiple shell shape optima for gliding scallops (Bivalvia: Pectinidae). *Journal of Evolutionary Biology* 30: 1736–1747.

Simone LRL, Chichvarkhin AY. 2004. Comparative morphological study of four species of *Barbatia* occurring on the southern Florida coast (Arcoidea, Arcidae). *Malacologia* 46: 355–379.

Simpson GG. 1953. *The major features of evolution*. New York: Columbia University Press.

Stanley SM. 1968. Post-Paleozoic adaptive radiation of infaunal bivalve molluscs: A consequence of mantle fusion and siphon formation. *Journal of Paleontology* 42: 214–229.

Stanley SM. 1972. Functional morphology and evolution of byssally attached bivalve mollusks. *Journal of Paleontology* 46: 165–212.

Steiner G, Hammer S. 2000. Molecular phylogeny of the Bivalvia inferred from 18S rDNA sequences with particular reference to the Pteriomorphia. *Geological Society, London, Special Publications* 177: 11–29.

Thomas RDK. 1976. Constraints of ligament growth, form and function on evolution in the Arcoida (Mollusca: Bivalvia). *Paleobiology* 2: 64–83.

Thomas RDK. 1978a. Shell form and the ecological range of living and extinct Arcoida. *Paleobiology* 4: 181–194.

Thomas RDK. 1978b. Limits to opportunism in the evolution of the Arcoida (Bivalvia). *Philosophical Transactions of the Royal Society B: Biological Sciences* 284: 335–344.

Thomas RDK, Madzvamuse A, Maini PK, Wathen AJ. 2000. Growth patterns of noetiid ligaments: implications of developmental models for the origin of an evolutionary novelty among arcoid bivalves. *Geological Society, London, Special Publications* 177: 279–289.

Vermeij GJ. 1977. The Mesozoic Marine Revolution: Evidence from snails, predators and grazers. *Journal of Paleontology* 3: 245–25.

Waller TR. 1980. Scanning electron microscopyof shell and mantle in the order Arcoida. *Smithsonian Contributions to Zoology* 313: 1–58.

Wilkens H. 2010. Genes, modules and the evolution of cave fish. *Heredity* 105: 413.

Yonge CM. 1983. Symmetries and the role of the mantle margins in the bivalve Mollusca. *National Wildlife* 16: 1–10.

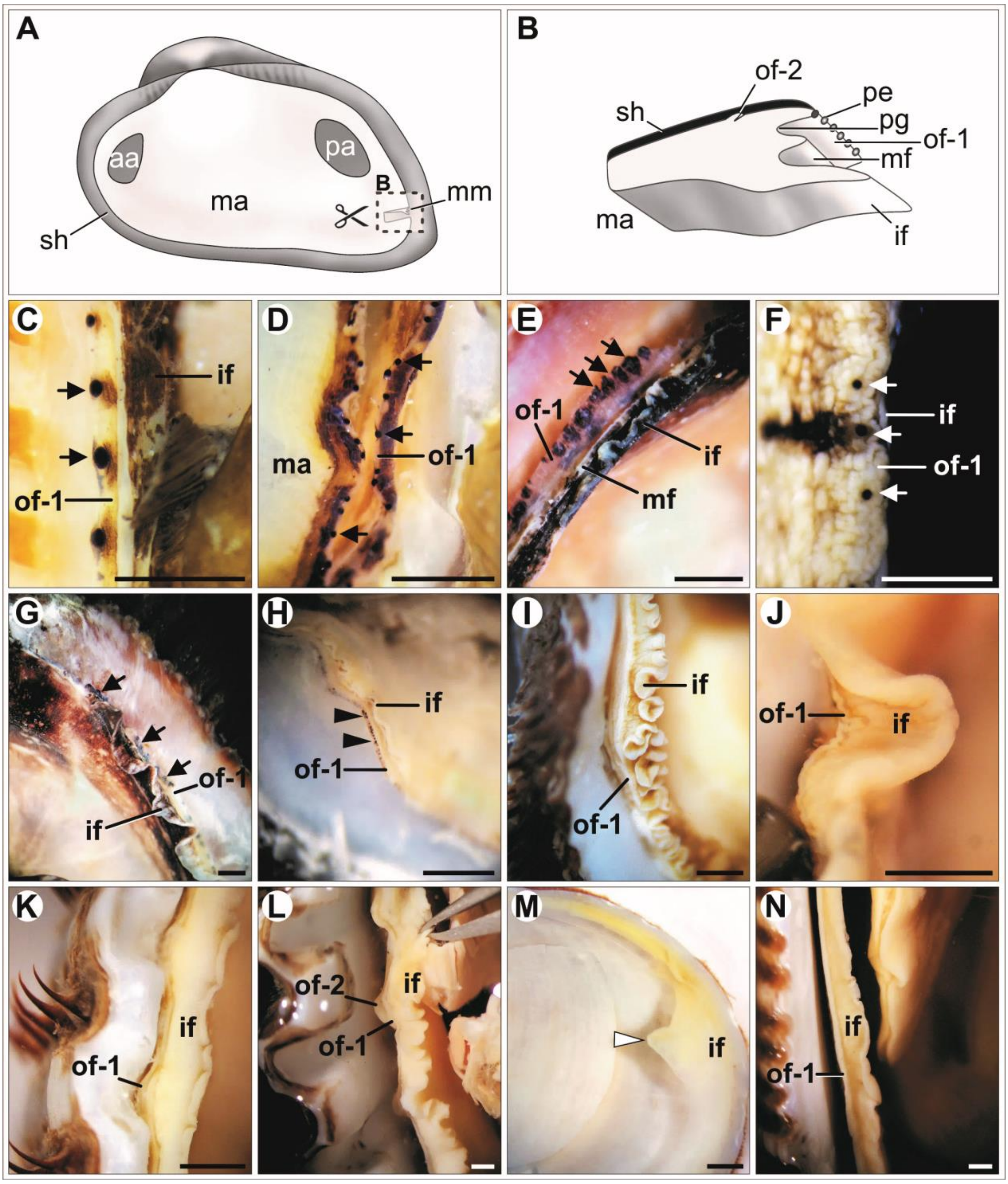

Figure 1. General organization of the mantle (**A**) and mantle margin (**B**) in Arcida represented by simplified schemes. Mantle margin morphology in Arcidae (C-E, G-N) and Cucullaeidae (F). Posterior mantle region, ventral view. Scale bars = 1mm. The first outer fold can be pigmented (C-G), bearing multiple compound eyes (arrows) and pigmented eyespots (arrowheads). The middle fold is reduced (E) or absent (J). The inner fold is much longer than the other folds, forming a large curtain (I-N) or a posterior flap (M). **C.** *Acar plicata* (USNM 886349). **D.** *Arca noae* (USNM 1086014). **E.** *Barbatia fusca* (SBMNH 349329). **F.** *Cucullaea labiata* (USNM 746883). **G.** *Barbatia barbata* (MCZ 378867). **H.** *Barbatia virescens* (MCZ 378874). **I.** *Barbatia candida* (MZSP 105572). **J.** *Anadara broughtonii* (USNM 802331). **K.** *Anadara ferruginea* (SBMNH 81002). **L.** *Tegillarca granosa* (MCZ 378820). **M.** *Bathyarca corpulenta* (SBMNH 349320). **N.** *Trisidos kiyonoi* (SBMNH 97422). Abbreviations: aa, anterior adductor; if, inner fold; ma, mantle; mf, middle fold; mm, mantle margin; of, outer fold; of-1, first outer fold; of-2, second outer fold; pa, posterior adductor; pe, pigmented eyespots; pg, periostracal groove; sh, shell.

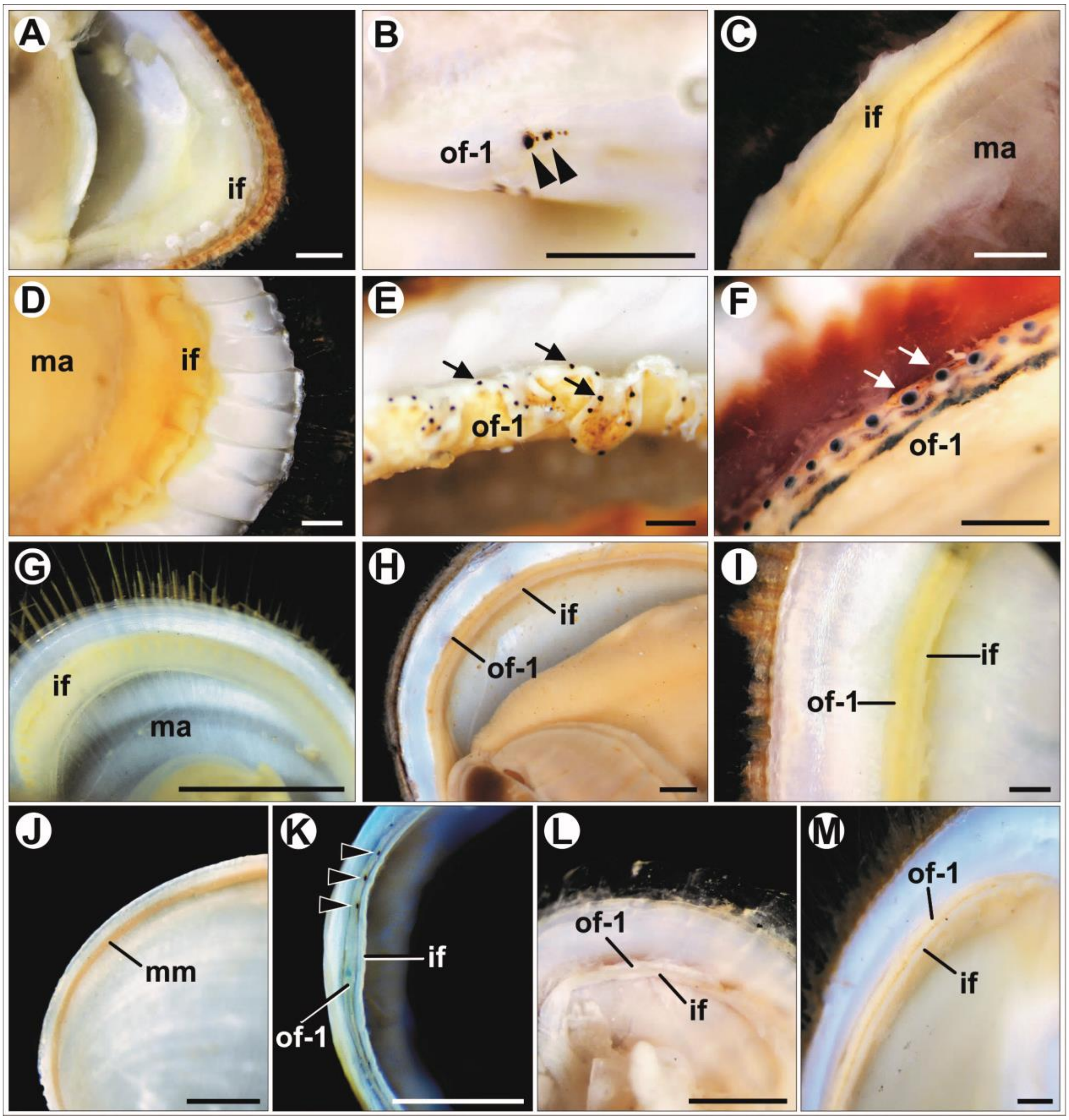

Figure 2. Mantle margin morphology in Noetiidae (A-D), Glycymerididae (E, F), Limopsidae (G-I), and Philobryidae (J-M). Posterior mantle region. Scale bars = 1mm. The first outer fold can bear compound eyes (arrows) and pigmented eyespots (arrowheads). **A.** *Striarca lactea* (USNM 857645). **B.** *Arcopsis solida* (USNM 733218). **C.** *Didimacar tenebrica* (SBMNH 80722). **D.** *Noetia ponderosa* (USNM 803530). **E.** *Tucetona pectinata* (MZSP 91971). **F.** *Glycymeris tenuicostata* (378982). **G.** *Limopsis aurita* (ZUEC-BIV 2248). **H.** *Limopsis lilliei* (MZSP 90647). **I.** *Limopsis marionensis* (USNM 760835). **J.** *Adacnarca nitens* (USNM 886551). **K.** *Lissarca notorcadensis* (MZSP 87826). **L.** *Neocardia sp.* (MCZ 378927). **M.** *Philobrya sublaevis* (MZSP 90645). Abbreviations: if, inner fold; ma, mantle; mm, mantle margin; of-1, first outer fold.

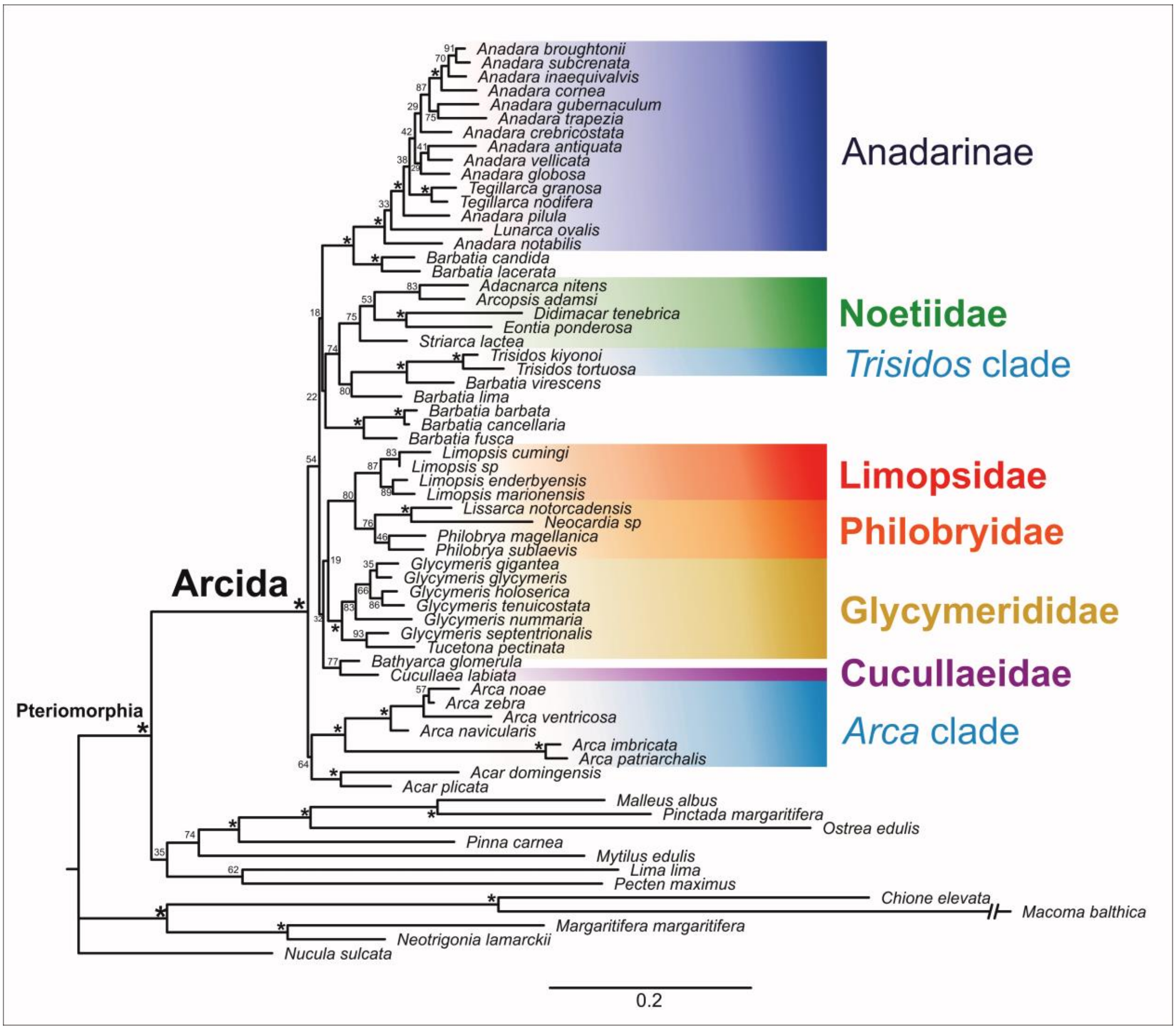

Figure 3. Phylogenetic relationships within Arcida based on maximum likelihood analysis of four genes (18S rRNA, 28S rRNA, COI mtDNA, and H3). Asterisks on nodes indicate bootstrap values > 95%. Selected clades are indicated by color groups. Arcidae is the only non-monophyletic family.

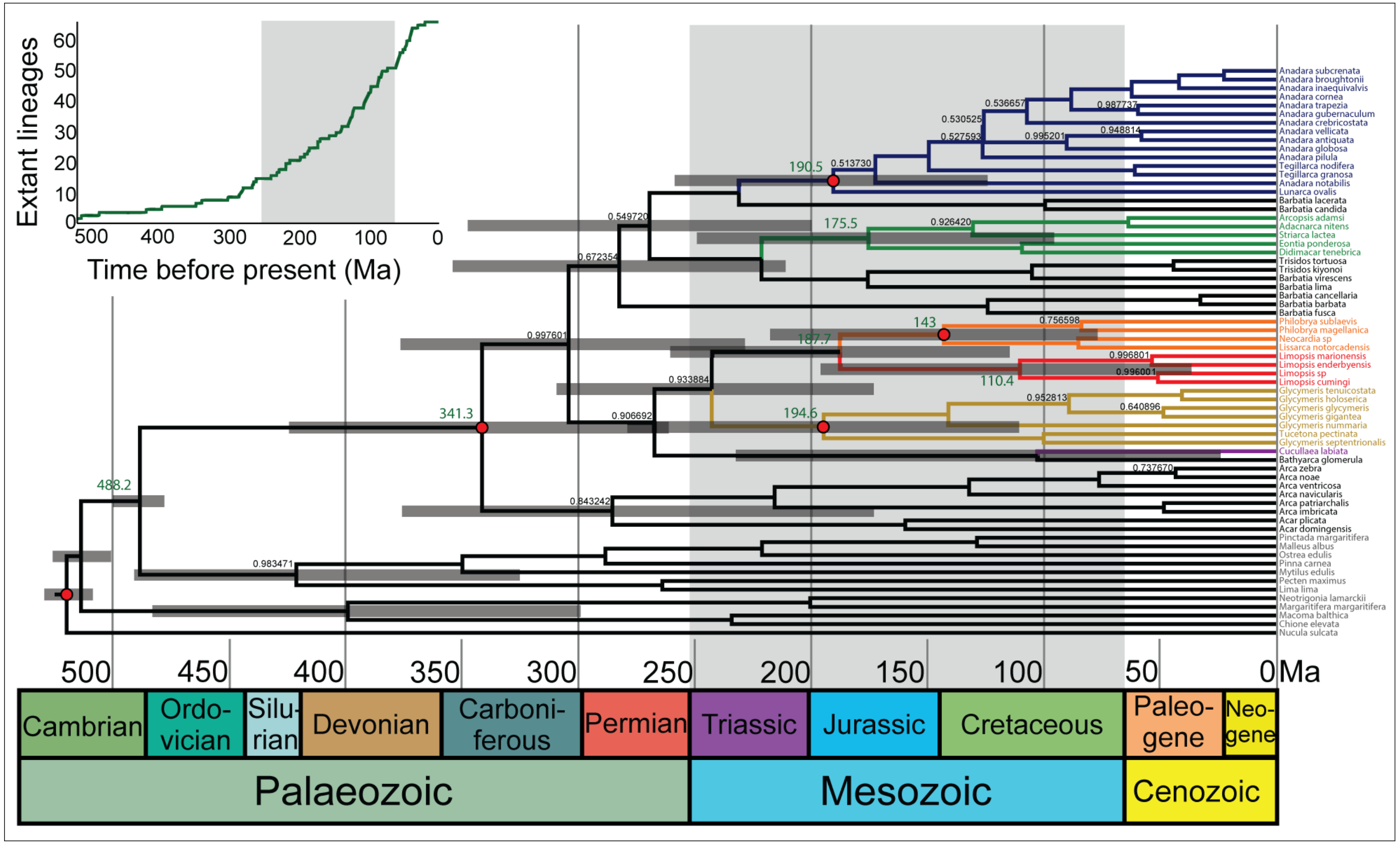

Figure 4. Time-calibrated phylogeny of Arcida under Bayesian inference based on four genes (18S rRNA, 28S rRNA, COI mtDNA, and H3) and five fossils used to calibrate internal nodes (red circles). Green values indicate median ages on selected nodes. Grey bars indicate 95% highest posterior density intervals (HPD) for nodes of interest. Posterior probabilities different than 1.0 are indicated on nodes. Color code for clades and taxa is the same used in Figure 3. A lineages-through-time plot is shown at the upper left. After a Cambrian divergence, the crown group of Arcida had an origin around 341 Ma (Carboniferous) and a major diversification during the Mesozoic.

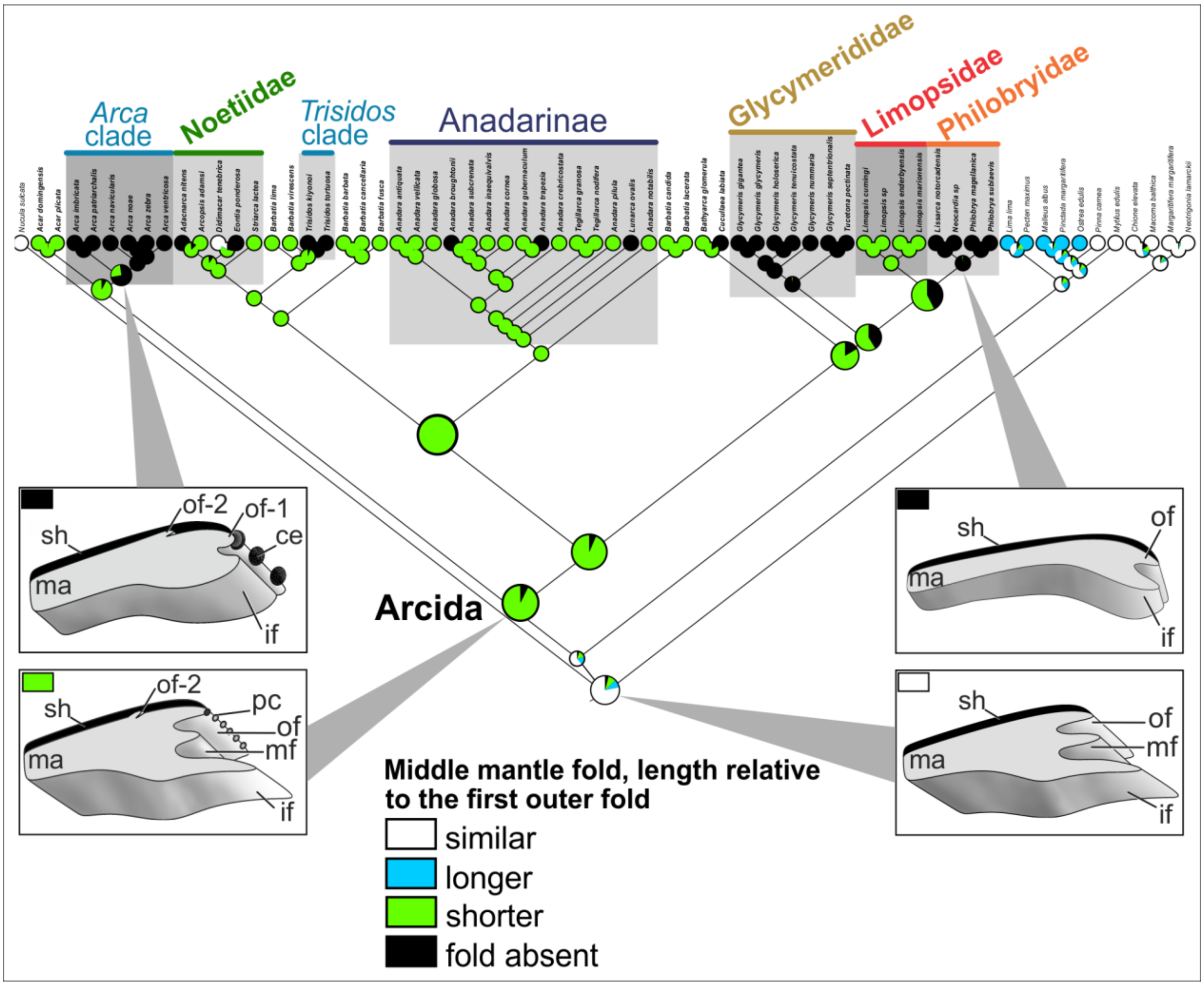

Figure 5. Ancestral state reconstruction of the middle mantle fold in Arcida under maximum likelihood, assuming a single rate for all possible transitions (MK1 model). Pie charts represent the likelihood proportions of reconstructed states; nodes of interest have their charts enlarged. Mantle margin schemes indicate mantle morphology as reconstructed by the analysis. Abbreviations: ce, compound eyes; if, inner fold; ma, mantle; mf, middle fold; of, outer fold; of-1, first outer fold; of-2, second outer fold; pc, pigmented eyespots; sh, shell.

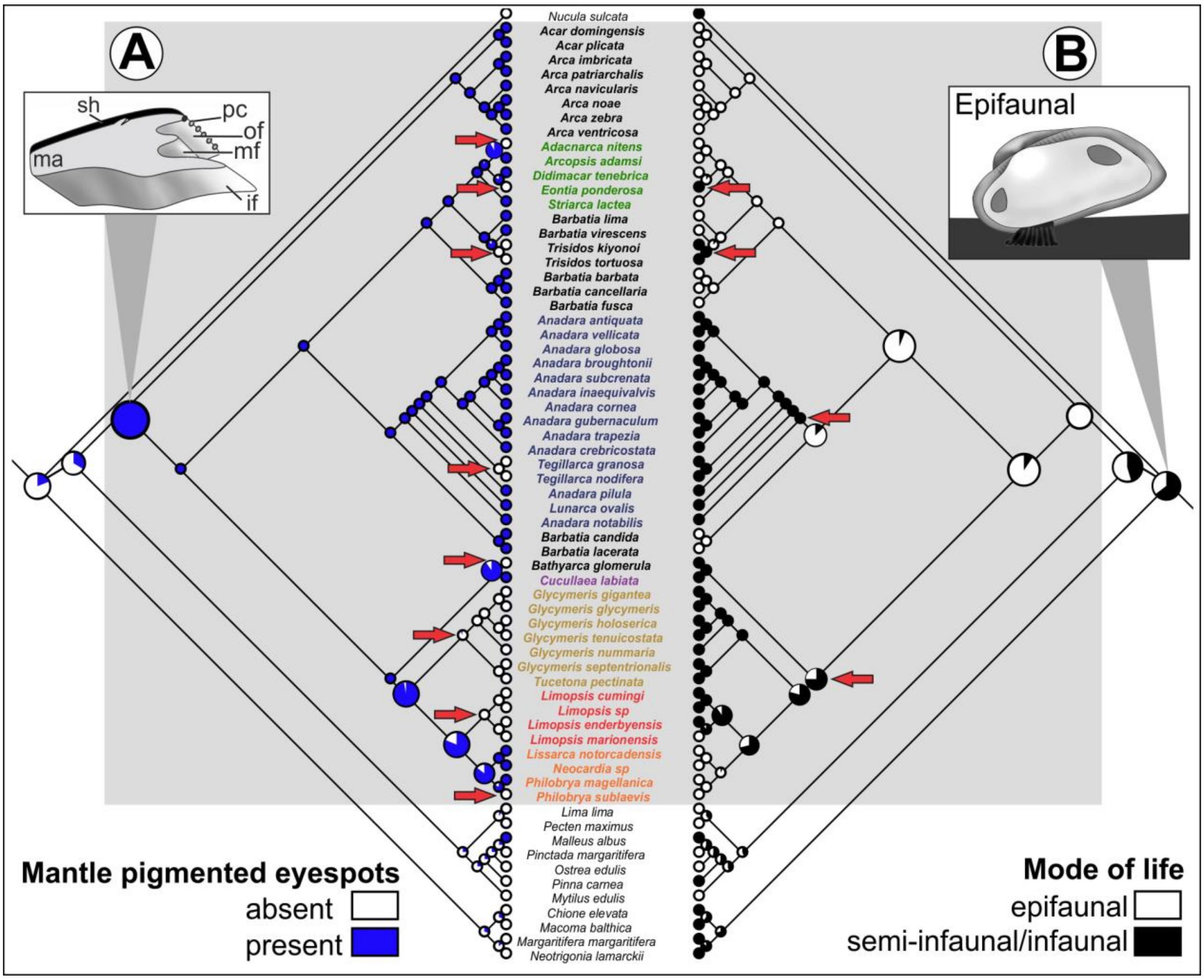

Figure 6. Ancestral state reconstruction of mantle photoreceptor organs (left, AsymmMK model) and mode of life (right, MK1 model) in Arcida under maximum likelihood. Ingroup is indicated by the grey boxes. Pie charts represent the likelihood proportions of reconstructed states; nodes of interest have their charts enlarged. The Arcida's ancestor is recovered as an epifaunal animal with simple eyespots on the mantle. Most subsequent losses of eyespots (red left arrows) are apparently associated with transitions to semi-infaunal/infaunal habits (red right arrows). Abbreviations: if, inner fold; ma, mantle; mf, middle fold; of, outer fold; of-1, first outer fold; pc, pigmented eyespots; sh, shell.

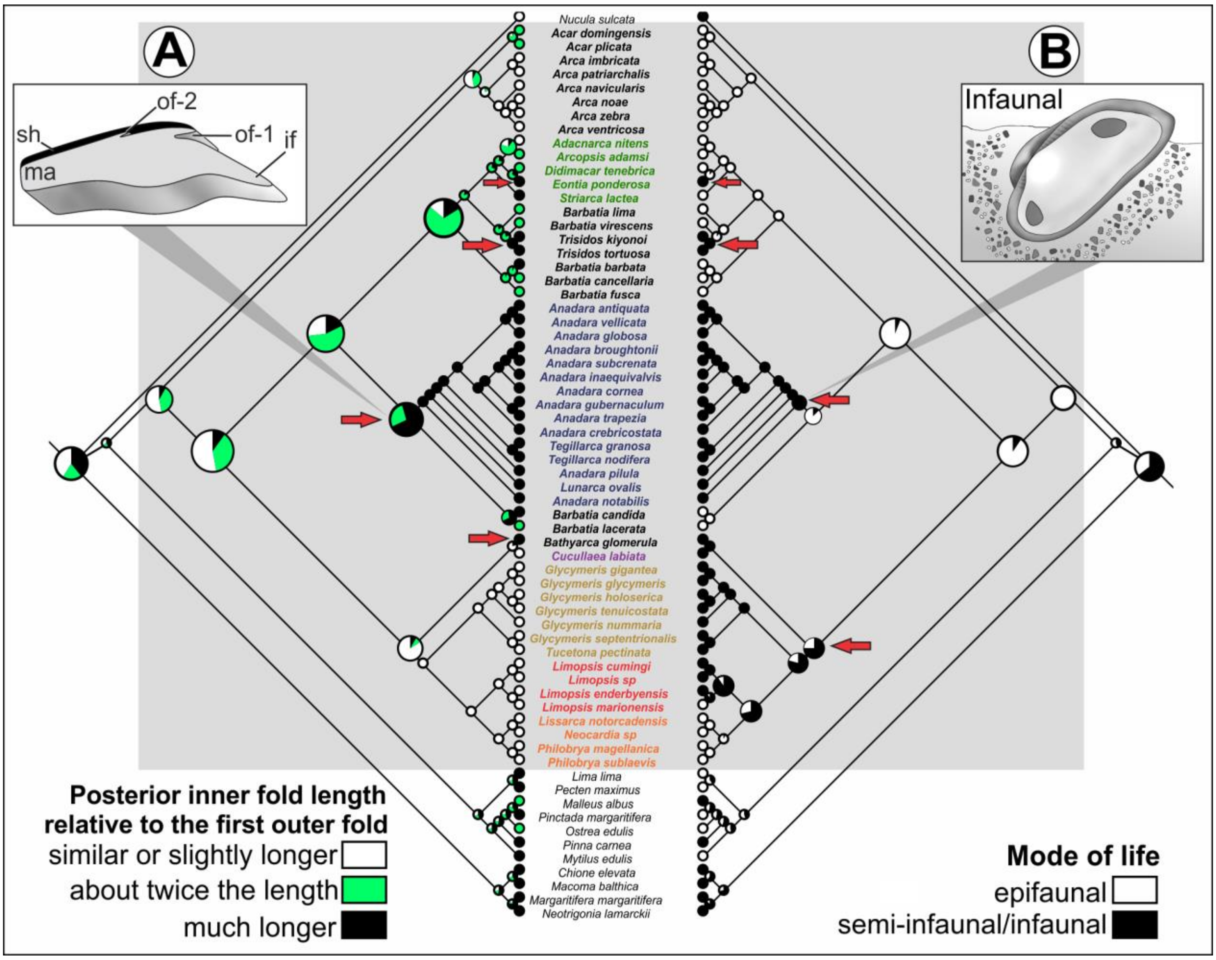

Figure 7. Ancestral state reconstruction of inner fold length (left) and mode of life (right) in Arcida under maximum likelihood, assuming a single rate for all possible transitions (MK1 model). Ingroup is indicated by the grey boxes. Pie charts represent the likelihood proportions of reconstructed states; nodes of interest have their charts enlarged. The inner mantle fold becomes much longer than the others in numerous lineages (left arrows), which is apparently associated with transitions to semi-infaunal/infaunal habits (right arrows). Abbreviations: if, inner fold; ma, mantle; of-1, first outer fold; of-2, second outer fold; sh, shell.

Table 1. Taxa included in the phylogenetic and morphological analyses. Nucleotide sequences were obtained in *GenBank* database; accession numbers are listed. Morphological investigation was conducted with taxa included in the phylogenetic study (when possible) and additional species; catalogue numbers are indicated. Abbreviations: Museum of Comparative Zoology (MCZ), Museum of Zoology "Prof. Adão José Cardoso" of the University of Campinas (ZUECBIV), Museum of Zoology of the University of São Paulo (MZSP), Smithsonian National Museum of Natural History (USNM), Santa Barbara Museum of Natural History (SBMNH).

Taxa	Reference	18S rRNA	28S rRNA	COI mtDNA	Histone H3	Collections
Arcidae						
Acar dominguensis	(Lamarck, 1819)			FJ480593	KT757861	MZSP118292
Acar gradata	(Broderip & Sowerby I, 1829)					USNM796185
Acar plicata	(Dillwyn, 1817)	AJ389630	AJ307533	FJ480453	AF416856	MZSP115322
Anadara antiquata	(Linnaeus, 1758)	JN974491	JN974542	HQ258850	JN974592	MZSP99848
Anadara baughmani	Hertlein, 1951					USNM803522
Anadara broughtonii	(Schrenck, 1867)	JN974489	JN974541	HQ258847	JN974590	USNM802331
Anadara chemnitzii	(Philippi, 1851)					MZSP43259, ZUECBIV4870
Anadara cornea	(Reeve, 1844)	JN974499	DQ343860	HQ258856	JN974600	
Anadara crebricostata	(Reeve, 1844)	JN974495	JN974547	HQ258859	JN974596	
Anadara ferruginea	(Reeve, 1944)					SBMNH81002
Anadara floridana	(Conrad, 1869)					USNM847847
Anadara globosa	(Reeve, 1844)	JN974484	JN974535	HQ258861	JN974584	
Anadara grandis	(Broderip & Sowerby I, 1829)					USNM803487
Anadara gubernaculum	(Reeve, 1844)	JN974493	JN974544	HQ258857	JN974594	
Anadara inaequivalvis	(Bruguiere, 1789)	JN974497	JN974548	AB076937	JN974598	MZSP55060
Anadara notabilis	(Röding, 1798)	KT757768	KT757816	AF416828	KT757863	MZSP84987, MZSP84886
Anadara obesa	(G. B. Sowerby I, 1833)					MCZ337676

Taxa	**Reference**	**18S rRNA**	**28S rRNA**	**COI mtDNA**	**Histone H3**	**Collections**
Anadara pilula	(Reeve, 1843)	JN974507	JN974558	HQ258862	JN974608	
Anadara subcrenata	(Lischle, 1869)	JN974501	DQ343861	HQ258851	JN974602	
Anadara transversa	(Say, 1822)					USNM801135, MCZ359001
Anadara trapezia	(Deshayes, 1839)	KT757770	KT757817	KX713443	KT757865	SBMNH10187
Anadara vellicata	(Reeve, 1844)	JN974487	JN974539	HQ258848	JN974588	
Arca imbricata	Bruguière, 1789	AY654986	KT757820	AF253494	AY654989	MZSP95208, MZSP109869
Arca navicularis	Bruguière, 1789	JN974517	KT757821	HQ258822	JN974618	USNM719071, MCZ378833
Arca noae	Linnaeus, 1758	KC429325	KT757822	KC429090	KC429160	USNM1086014
Arca patriarchalis	Röding, 1798	JN974527	JN974576		JN974627	MZSP99765
Arca ventricosa	(Lamarck, 1819)			AB076935	AF416854	MZSP55027
Arca zebra	(Swainson, 1833)	KT757776	KT757824		AF416864	MZSP101688
Barbatia amygdalumtostum	(Röding, 1798)	JN974526	JN974575		JN974626	SBMNH349329, USNM847011
Barbatia barbata	(Linnaeus, 1758)	KC429326	KT757825	KC429091	KC429161	MCZ378867
Barbatia cancellaria	(Lamarck, 1819)	KT757779	KT757827			MZSP32336, MZSP48857
Barbatia candida	(Helbling, 1779)	KT757784	KT757831	AF253487	AF416849	MZSP105572, ZUECBIV1407
Barbatia lacerata	(Bruguière, 1789)	JN974509	JN974560	HQ258826	JN974610	
Barbatia lima	(Reeve, 1844)	JN974511	JN974563	HQ258837	JN974612	MZSP71135
Barbatia virescens	(Reeve, 1844)	JN974524	KT757835	HQ258840	JN974624	MZSP71367, MCZ378874
Bathyarca corpulenta	(E A Smith, 1885)					SBMNH349320
Bathyarca glomerula	(Dall, 1881)	KT757790	KT757837		KT757880	
Bathyarca pectunculoides	(Scacchi, 1835)					MCZ348402
Bentharca asperula	(Dall, 1881)					MCZ348399
Lunarca ovalis	(Bruguière, 1789)			GQ166571	AF416844	MZSP84823, USNM803532

Taxa	**Reference**	**18S rRNA**	**28S rRNA**	**COI mtDNA**	**Histone H3**	**Collections**
Tegillarca granosa	(Linnaeus, 1758)	JN974505	KT757857	HQ258867	JN974606	MZSP55596, MCZ378820
Tegillarca nodifera	(Martens, 1860)	JN974503	JN974554	HQ258869	JN974604	
Trisidos kiyonoi	(Makiyama, 1931)	JN974522	JN974571	HQ258846	JN974622	SBMNH97422, SBMNH97423
Trisidos tortuosa	(Linnaeus, 1758)	KT757811	KT757858		KT757899	
Cucullaeidae						
Cucullaea labiata	(Lightfoot, 1786)	JN974513	JN974565	KJ774477	JN974614	USNM746883
Noetiidae						
Arcopsis adamsi	(Dall, 1886)	KC429327	KC429419	KC429092	KC429162	MZSP19724, ZUECBIV1153
Didimacar tenebrica	(Reeve, 1844)	JN974515	JN974566	HQ258870	JN974616	SBMNH80722
Eontia ponderosa	(Say, 1822)	KT757793	KT757840	AF416834	AF416860	SBMNH235066, USNM803530
Sheldonella bisulcata	(Lamarck, 1819)					MZSP26911
Striarca lactea	(Linnaeus, 1758)	AF120531	KT757855	AF120646		USNM857645, MCZ379156
Striarca symmetrica	(Reeve, 1844)					MZSP55574
Glycymerididae						
Glycymeris decussata	(Linnaeus, 1758)					MZSP91966
Glycymeris gigantea	(Reeve, 1843)	KT757794	KT757841		KT757883	MCZ 378989
Glycymeris glycymeris	(Linnaeus, 1758)	KC429328	KC429421	KC429093	KC429163	USNM794960
Glycymeris holoserica	(Reeve, 1843)	KT757796	KT757843		KT757885	MCZ378984
Glycymeris longior	(G B Sowerby, 1833)					MZSP91201, ZUECBIV78
Glycymeris nummaria	(Linnaeus, 1758)	KT757798	KT757845	KX785178	KT757887	MCZ378985
Glycymeris septentrionalis	(Middendorff, 1849)	KT757799	KT757846	KF643645	KT757888	
Glycymeris tenuicostata	(Reeve, 1843)	KT757800	KT757847		KT757889	MCZ378982
Glycymeris undata	(Linnaeus, 1758)					MZSP91983

Taxa	**Reference**	**18S rRNA**	**28S rRNA**	**COI mtDNA**	**Histone H3**	**Collections**
Tucetona pectinata	(Gmelin, 1791)	KT757812	KT757859	KX713507	KT757900	MZSP91971, ZUECBIV2198
Limopsidae						
Limopsis aurita	(Brocchi, 1814)					ZUECBIV2248, MCZ348438
Limopsis cristata	Jeffreys, 1876					MZSP104154, MCZ348410
Limopsis cumingi	Adams, 1863	KT757802		AB076930		
Limopsis enderbyensis	Powell, 1958	AJ422057	AY321301			
Limopsis galatheae	Knudsen, 1970					MCZ348437
Limopsis lilliei	E A Smith, 1915					MZSP90647, USNM904585
Limopsis marionensis	E A Smith, 1885	AJ422058	AY321303			USNM760835, USNM886526
Limopsis sp.	Sassi, 1827	KC429329	KC429422		KC429164	
Limopsis sulcata	Verrill & Bush, 1898					USNM832925
Limopsis tenella	Jeffreys, 1876					USNM807040
Philobryidae						
Adacnarca nitens	Pelseneer, 1903	KP340836	KT757815		KT757862	MZSP90616, USNM886551
Lissarca notorcardensis	Melvill & Standen, 1907		EF192520	KF612434		MZSP87826, USNM899485
Neocardia sp.	G B Sowerby III, 1892	KT757804	KT757850	KX713486	KT757891	USNM881121, MCZ378927
Philobrya magellanica	(Stempell, 1899)	KP340845	KT757853		KT757895	
Philobrya sublaevis	Pelseneer, 1903	KP340835	KP340812			MZSP90645, USNM882353
Outgroup–Pteriomorphia						
Lima lima	(Linnaeus, 1758)	KC429339	KC429434	KC429101	KC429174	USNM 754383
Malleus albus	Lamarck, 1819	KC429334	HQ329464	KC429097	KC429169	MZSP55595
Mytilus edulis	Linnaeus, 1758	KC429331	KC429424	KF644190	KC429166	MZSP120321
Ostrea edulis	Linnaeus, 1758	L49052	AF137047	AF120651	AY070151	USNM836256

Taxa	**Reference**	**18S rRNA**	**28S rRNA**	**COI mtDNA**	**Histone H3**	**Collections**
Pecten maximus	(Linnaeus, 1758)	L49053	HM630545	KC429102	EU379508	
Pinctada margaritifera	(Linnaeus, 1758)	AB214451	AB214466	AB259166	HQ329296	USNM836493
Pinna carnea	Gmelin, 1791	HQ329375	KJ366067	KJ366325	KC429172	MZSP29040
Outgroup–Bivalvia						
Chione elevata	(Say, 1822)	KC429387	KC429495	KC429136	KC429219	
Macoma balthica	(Linnaeus, 1758)	KC429393	KC429501	KC429141	KC429224	
Margaritifera margaritifera	(Linnaeus, 1758)	AF229612	KC429443	AF303316	KC429185	
Neotrigonia lamarckii	(Gray, 1838)	KC429345	KC429443	KC429105	KC429182	
Nucula sulcuta	Bronn, 1831	AF207642	KC984815	KC984746	KC984777	

Table 2. Evolutionary correlation tests between mantle margin traits and lifestyles in Arcida. The test compares the four-parameter model (independent evolution; h_0) and the eight-parameter models (correlated evolution; h_1, h_2, h_3) between two binary traits, returning the differences in log-likelihood (–logL) with *p* values calculated by 10,000 simulations. Significant differences, *i.e.*, *p* value < α=0.05, indicate a better fit to the model of correlated evolution. Characters and respective states: *first outer fold pigmentation*, absent (0) or present (1); *compound eyes*, absent (0) or present (1); *pigmented eyespots*, absent (0) or present (1); *inner mantle fold development*, up to twice the length (0) or much longer (1) than the first outer fold; *mode of life*, epifaunal (0) or semi-infaunal/infaunal (1).

Morphological traits (y) and hypotheses (h)	**Mode of life – epifaunal vs. infaunal (x)**		
	Difference in –logL *between models*	p *value*	*Conclusion*
First outer fold pigmentation			
h_1 correlation	2.8321	0.138	independent traits
Compound eyes			
h_1 correlation	0.9473	0.268	independent traits
Pigmented eyespots			
h_1 correlation	5.12	0.0223	correlated traits
h_2 x depends on y	0.4789	0.3884	x does not depend on y
h_3 y depends on x	2.0402	0.13	y does not depend on x
Inner mantle fold development			
h_1 correlation	6.4797	0.002	correlated traits
h_2 x depends on y	2.3043	0.0112	x depends on y
h_3 y depends on x	3.1362	0.0569	y does not depend on x

Table S1. Characters and states used to study mantle margin traits and lifestyles in Arcida. Abbreviations: IF, inner mantle fold; MF, middle mantle fold; OF, outer mantle fold.

Characters	**State 0**	**State 1**	**State 2**	**State 3**	**State 4**
1. Mantle margin, number of folds	3 (1OF, 1MF, 1IF)	3(2OF, 1IF)	4 (2OF, 1MF, 1IF)	2 (1OF, 1IF)	4 (1OF, 1MF, 2IF)
2. Mantle margin, middle mantle fold	present	absent			
3. Mantle margin, circumpallial nerve	absent	present			
4. Mantle margin, pigmentation	absent	uniform	intense posteriorly		
5. Mantle margin, proximal second outer mantle fold	absent	present			
6. Mantle margin, pallial photoreceptor organs	absent	present			
7. Mantle margin, antero-posterior differentiation in relative length and thickness	absent	present			
8. First outer mantle fold, compound eyes	absent	present			
9. First outer mantle fold, pigmented eyespots	absent	present			
10. First outer mantle fold, pigmented pit eyespots	absent	present			
11. First outer mantle fold, pigmented cup eyespots	absent	present			
12. First outer mantle fold, pigmentation	absent	present			
13. Middle mantle fold, length relative to the first outer fold	similar	longer	shorter	fold absent	
14. Middle mantle fold, length relative to the first outer fold (binary)	similar or longer	shorter or absent			
15. Inner mantle fold, posterior length relative to the first outer fold	similar or slightly longer	about twice the length	much longer		
16. Inner mantle fold, posterior length relative to the first outer fold (binary)	up to twice the length	much longer			
17. Mode of life, occurrence relative to depth	shallow waters (<200m)	shallow and deep waters	deep waters (>200m)		
18. Mode of life, position relative to substrate	epifaunal	semi-infaunal	infaunal		
19. Mode of life, position relative to substrate (binary)	epifaunal	semi-infaunal/infaunal			
20. Mode of life, type of substrate (binary)	hard substrate	soft substrate			
21. Mode of life, type of substrate	sandy and muddy	rocks and corals	living organisms		
22. Mode of life, use of byssus at adult stage	abyssate	endobyssate	epibyssate		

Table S2. Species-character matrix.

Taxa	**1**	**2**	**3**	**4**	**5**	**6**	**7**	**8**	**9**	**10**	**11**	**12**	**13**	**14**	**15**	**16**	**17**	**18**	**19**	**20**	**21**	**22**
Acar domingensis	2	0	0	1	1	1	1	1	1	1	0	1	2	1	1	0	0	0	0	0	1	2
Acar plicata	2	0	0	1	1	1	1	1	1	1	0	1	2	1	1	0	0	0	0	0	1	2
Adacnarca nitens	3	1	0	0	0	0	0	0	0	0	0	0	3	1	0	0	1	0	0	0	2	2
Anadara antiquata	2	0	0	2	1	1	1	0	1	1	0	1	2	1	2	1	0	2	1	1	0	1
Anadara broughtonii	1	1	0	0	1	1	1	0	1	1	0	0	3	1	2	1	0	2	1	1	0	1
Anadara cornea	2	0	0	0	1	1	1	0	1	1	0	0	2	1	2	1	0	2	1	1	0	1
Anadara crebricostata	2	0	0	0	1	1	1	0	1	1	0	0	2	1	2	1	0	2	1	1	0	1
Anadara globosa	2	0	0	0	1	1	1	0	1	1	0	0	2	1	2	1	0	2	1	1	0	1
Anadara gubernaculum	2	0	0	0	1	1	1	0	1	1	0	0	2	1	2	1	0	2	1	1	0	1
Anadara inaequivalvis	2	0	0	0	1	1	1	0	1	1	0	0	2	1	2	1	0	2	1	1	0	1
Anadara notabilis	2	0	0	0	1	1	1	0	1	1	0	0	2	1	2	1	0	2	1	1	0	1
Anadara pilula	2	0	0	0	1	1	1	0	1	1	0	0	2	1	2	1	0	2	1	1	0	1
Anadara subcrenata	2	0	0	0	1	1	1	0	1	1	0	0	2	1	2	1	0	2	1	1	0	1
Anadara trapezia	1	1	0	0	1	1	1	0	1	1	0	0	3	1	2	1	0	2	1	1	0	1
Anadara vellicata	2	0	0	0	1	1	1	0	1	1	0	0	2	1	2	1	0	2	1	1	0	1
Arca imbricata	1	1	0	2	1	1	1	1	1	1	0	1	3	1	0	0	0	0	0	0	1	2
Arca navicularis	1	1	0	2	1	1	1	1	1	1	0	1	3	1	0	0	0	0	0	0	1	2
Arca noae	1	1	0	2	1	1	1	1	1	1	0	1	3	1	0	0	0	0	0	0	1	2
Arca patriarchalis	1	1	0	2	1	1	1	1	1	1	0	1	3	1	0	0	0	0	0	0	1	2
Arca ventricosa	1	1	0	2	1	1	1	1	1	1	0	1	3	1	0	0	0	0	0	0	1	2
Arca zebra	1	1	0	2	1	1	1	1	1	1	0	1	3	1	0	0	0	0	0	0	1	2
Arcopsis adamsi	2	0	0	0	1	1	1	0	1	1	0	0	2	1	1	0	0	0	0	0	1	2
Barbatia barbata	2	0	0	2	1	1	1	1	1	1	0	1	2	1	2	1	0	0	0	0	1	2
Barbatia cancellaria	2	0	0	2	1	1	1	1	1	1	0	1	2	1	1	0	0	0	0	0	1	2
Barbatia candida	2	0	0	0	1	1	1	0	1	1	0	0	2	1	2	1	0	0	0	0	1	2
Barbatia fusca	2	0	0	2	1	1	1	1	1	1	0	1	2	1	1	0	0	0	0	0	1	2
Barbatia lacerata	2	0	0	0	1	1	1	0	1	1	0	0	2	1	1	0	0	0	0	0	1	2
Barbatia lima	2	0	0	0	1	1	1	0	1	1	0	0	2	1	1	0	0	0	0	0	1	2
Barbatia virescens	2	0	0	0	1	1	1	0	1	1	0	0	2	1	1	0	0	0	0	0	1	2

Taxa	**1**	**2**	**3**	**4**	**5**	**6**	**7**	**8**	**9**	**10**	**11**	**12**	**13**	**14**	**15**	**16**	**17**	**18**	**19**	**20**	**21**	**22**
Bathyarca glomerula	2	0	0	0	1	0	1	0	0	0	0	0	2	1	2	1	1	1	1	1	0	1
Chione elevata	4	0	0	0	0	0	1	0	0	0	0	0	0	0	2	1	0	2	1	1	0	0
Cucullaea labiata	1	1	0	0	1	1	1	1	1	1	0	0	3	1	0	0	0	1	1	1	0	1
Didimacar tenebrica	2	0	0	0	1	1	1	0	1	1	0	0	0	0	1	0	0	0	0	0	1	2
Eontia ponderosa	1	1	0	0	1	0	1	0	0	0	0	0	3	1	2	1	0	2	1	1	0	1
Glycymeris gigantea	1	1	0	2	1	1	1	1	0	0	0	1	3	1	0	0	0	1	1	1	0	0
Glycymeris glycymeris	1	1	0	2	1	1	1	1	0	0	0	1	3	1	0	0	0	1	1	1	0	0
Glycymeris holoserica	1	1	0	2	1	1	1	1	0	0	0	1	3	1	0	0	0	1	1	1	0	0
Glycymeris nummaria	1	1	0	2	1	1	1	1	0	0	0	1	3	1	0	0	0	1	1	1	0	0
Glycymeris septentrionalis	1	1	0	2	1	1	1	1	0	0	0	1	3	1	0	0	0	1	1	1	0	0
Glycymeris tenuicostata	1	1	0	2	1	1	1	1	0	0	0	1	3	1	0	0	0	1	1	1	0	0
Lima lima	0	0	1	1	0	1	0	0	0	0	0	0	1	0	2	1	0	0	0	0	1	2
Limopsis cumingi	0	0	0	0	0	0	0	0	0	0	0	0	2	1	0	0	1	1	1	1	0	1
Limopsis enderbyensis	0	0	0	0	0	0	0	0	0	0	0	0	2	1	0	0	1	1	1	1	0	1
Limopsis marionensis	0	0	0	0	0	0	0	0	0	0	0	0	2	1	0	0	1	0	0	0	1	2
Limopsis sp	0	0	0	0	0	0	0	0	0	0	0	0	2	1	0	0	1	1	1	1	0	1
Lissarca notorcadensis	3	1	0	0	0	1	0	0	1	0	1	0	3	1	0	0	0	0	0	0	2	2
Lunarca ovalis	1	1	0	2	1	1	1	0	1	1	0	1	3	1	2	1	0	2	1	1	0	1
Macoma balthica	0	0	0	0	0	0	1	0	0	0	0	0	0	0	2	1	0	2	1	1	0	0
Malleus albus	2	0	1	1	0	1	0	0	1	0	1	0	1	0	1	0	0	1	1	1	0	1
Margaritifera margaritifera	0	0	0	2	0	0	1	0	0	0	0	0	0	0	2	1	0	1	1	1	0	0
Mytilus edulis	0	0	1	2	0	0	1	0	0	0	0	0	0	0	2	1	0	0	0	0	1	2
Neocardia sp	3	1	0	0	0	1	0	0	1	0	1	0	3	1	0	0	0	0	0	0	2	2
Neotrigonia lamarckii	0	0	0	0	0	0	1	0	0	0	0	0	0	0	2	1	0	2	1	1	0	0
Nucula sulcata	0	0	0	0	0	0	0	0	0	0	0	0	0	0	0	0	1	2	1	1	0	0
Ostrea edulis	0	0	1	1	0	0	0	0	0	0	0	0	1	0	1	0	0	0	0	0	1	2
Pecten maximus	0	0	1	1	0	1	0	0	0	0	0	0	1	0	2	1	0	0	0	1	0	2
Philobrya magellanica	1	1	0	0	1	1	0	0	1	0	1	0	3	1	0	0	0	0	0	0	2	2
Philobrya sublaevis	1	1	0	0	1	0	0	0	0	0	0	0	3	1	0	0	0	0	0	0	2	2
Pinctada margaritifera	0	0	1	1	0	0	0	0	0	0	0	0	1	0	2	1	0	0	0	0	1	2
Pinna carnea	0	0	1	2	0	0	1	0	0	0	0	0	0	0	2	1	0	1	1	1	0	1

Taxa	**1**	**2**	**3**	**4**	**5**	**6**	**7**	**8**	**9**	**10**	**11**	**12**	**13**	**14**	**15**	**16**	**17**	**18**	**19**	**20**	**21**	**22**
Striarca lactea	2	0	0	0	1	1	1	0	1	1	0	0	2	1	2	1	0	0	0	0	1	2
Tegillarca granosa	2	0	0	0	1	0	1	0	0	0	0	0	2	1	2	1	0	2	1	1	0	1
Tegillarca nodifera	2	0	0	0	1	0	1	0	0	0	0	0	2	1	2	1	0	2	1	1	0	1
Trisidos kiyonoi	1	1	0	0	1	0	1	0	0	0	0	0	3	1	2	1	0	1	1	1	0	1
Trisidos tortuosa	1	1	0	0	1	0	1	0	0	0	0	0	3	1	2	1	0	1	1	1	0	1
Tucetona pectinata	1	1	0	2	1	1	1	1	0	0	0	1	3	1	0	0	0	1	1	1	0	0

Table S3. Lifestyle compilation of ark clams and relatives (Arcida) according to mode of life (position relative to the substrate & mode of attachment) and substrate.

Taxa	**Mode of life**		**Substrate**	**References**
Arcidae				
Acar domingensisi	Epifaunal	Epibyssate	Rocks	Simone and Chichverkrun 2004
Acar plicata	Epifaunal	Epibyssate	Mud, rubble, shell-hash, under corals	Kilburn 1983, Leung and Morton 2000
Anadara antiquata	Semi-infaunal	Endobyssate	Muddy sand, rock or coral fragments	Evseev and Lutaenko 1998, Broom 1985, Kilburn 1983
Anadara broughtonii	Infaunal	Endobyssate	Mud	Broom 1985, Oliver and Holmes 2006
Anadara cebricostata	Infaunal	Endobyssate		Oliver and Holmes 2006
Anadara cornea	Infaunal	Endobyssate	Mud and sand	Broom 1985, Tsi and Ma 1982, Li and Gao 1985, Morton 1986
Anadara globosa	Infaunal	Endobyssate		Oliver and Holmes 2006
Anadara gubernaculum	Infaunal	Endobyssate	Sand and silty sand	Evsee and Lutaenko 1998, Oliver and Holmes 2006
Anadara ferruginea	Infaunal	Endobyssate	Coarse sand, fine sand, and silty clay	Tsi and Ma 1982, Ong Che and Morton 1991, Scott 1994, Morton 1994, Leung and Morton 1997, 200, Nicholson and Morton 2000
Anadara inequivalvis	Infaunal	Endobyssate	Sand and muddy sand	Broom 1985, Tsi and Ma 1982, Scott 1994, Nicholson and Morton 2000
Anadara notabilis	Infaunal	Endobyssate	Sand	Rocha and Martins 1998, Oliver and Holmes 2006, Tugeon et al. 2009
Anadara ovalis	Infaunal	Endobyssate	Sand	Oliver and Holmes 2006, Alexander 2007, Turgeon et al. 2009

Taxa	**Mode of life**		**Substrate**	**References**
Anadara pilula	Infaunal	Endobyssate	Sand and silty sand	Evsee and Lutaenko 1998, Norte-Campos et al. 2005, Oliver and Holmes 2006
Anadara subcrenata	Infaunal	Endobyssate	Mud and muddy sand	Broom 1985, Oliver and Holmes 2006
Anadara trapezia	Infaunal	Endobyssate	Sandy mudflats	Sullivan 1960, Oliver and Holmes 2006
Anadara vellicata	Infaunal	Endobyssate	Silty sand	Evsee and Lutaenko 1998, Oliver and Holmes 2006
Arca imbricata	Epifaunal	Epibyssate	Rock crevices	Oliver and Holmes 2006, Pers. Obs., Turgeon et al. 2009
Arca navicularis	Epifaunal	Epibyssate	Rocks and coral fragments	Kilburn 1983
Arca noae	Epifaunal	Epibyssate	Rocks	Thomas 1996, Oliver and Holmes 2006, Morton and Peharda 2008
Arca patriarchalis	Epifaunal	Epibyssate	Coral fragments	Dudgeon and Morton 1982
Arca ventricosa	Epifaunal	Epibyssate	Coral fragments	Kilburn 1983, Oliver and Holmes 2006
Arca zebra	Epifaunal	Epibyssate	Rocks	Oliver and Holmes 2006, Turgeon et al. 2009
Barbatia barbata	Epifaunal	Epibyssate	Rocks	Thomas 1996, Oliver and Holmes 2006, Turgeon et al. 2009
Barbatia cancellaria	Epifaunal	Epibyssate	Rocks	Simone and Chichverkrun 2004
Barbatia candida	Epifaunal	Epibyssate	Rocks	Simone and Chichverkrun 2004, Turgeon et al. 2009, Pers.Obs.
Barbatia fusca	Epifaunal	Epibyssate	Coral fragments	Sanpanich 2011, Tsi and Ma 1982. Barbatia decussata. Oliver and Holmes 2006.

Taxa	**Mode of life**		**Substrate**	**References**
Barbatia lacerata	Epifaunal	Epibyssate	Corals, rubble, and rocks	Oliver et al. 2004
Barbatia lima	Epifaunal	Epibyssate	Rocks	Scott 1994, Leung and Morton 2000
Barbatia setigera	Epifaunal	Epibyssate	Coarse sand	Kilburn 1983
Barbatia virescens	Epifaunal	Epibyssate	Rocks, piers and boulders	Morton 1987, Britton 1990, Taylor and Morton 1996, Harper and Morton 1997
Bathyarca glomerula	Semi-infaunal	Endobyssate	Soft sediments	Oliver and Allen 1980, Turgeon et al. 2009
Cucullaea labiata	Semi-infaunal	Endobyssate	Sand and corals	Morton 1981, Oliver and Holmes 2006, Sanpanich 2011
Tegillarca granosa	Infaunal	Endobyssate	Muddy sand	Evsee and Lutaenko 1998, Broom 1985, Morton 1986
Tegillarca nodifera	Infaunal	Endobyssate	Mud, sand, and soft clay	Evsee and Lutaenko 1998
Trisidos kiyonoi	Semi-infaunal	Endobyssate	Gravelly sand and coarse sand	Scott 1994
Noetiidae				
Arcopsis adamsi	Epifaunal	Epibyssate	Rocks on sand	Oliver and Järnegren 2004, Pers. Obs.
Didimacar tenebrica	Epifaunal	Epibyssate	Rocks and boulders	Oliver 1990, Scott 1994, Harper and Morton 1997, Leung and Morton 2000
Noetia ponderosa	Infaunal	Endobyssate	Soft sediments	Oliver 1990
Striarca lactea	Epifaunal	Epibyssate	Rocks, boulders, and among gravel	Oliver and Holmes 2006, Turgeon et al. 2009

Taxa	Mode of life		Substrate	References
Glycymerididae				
Glycymeris gigantea	Semi-infaunal	Free living/ burrower	Coarse shell gravel, sand, and mud	Thomas 1995, 1996, Oliver and Holmes 2006
Glycymeris glycymeris	Semi-infaunal	Free living/ burrower	Coarse shell gravel, sand, and mud	Thomas 1995, 1996, Oliver and Holmes 2006
Glycymeris holoserica	Semi-infaunal	Free living/ burrower	Coarse shell gravel, sand, and mud	Thomas 1995, 1996, Oliver and Holmes 2006
Glycymeris nummaria	Semi-infaunal	Free living/ burrower	Coarse shell gravel, sand, and mud	Thomas 1995, 1996, Oliver and Holmes 2006
Glycymeris septentrionalis	Semi-infaunal	Free living/ burrower	Coarse shell gravel, sand, and mud	Thomas 1995, 1996, Oliver and Holmes 2006
Glycymeris tenuicostata	Semi-infaunal	Free living/ burrower	Coarse shell gravel, sand, and mud	Thomas 1995, 1996, Oliver and Holmes 2006
Tucetona pectinata	Semi-infaunal	Free living/ burrower	Coarse shell gravel, sand, and mud	Turgeon et al. 2009
Limopsidae				
Limospsis sp.	Semi-infaunal	Endobyssate	Soft sediments	Oliver and Allen 1980, Morton 2012, Linse 2014
Limopsis marionensis	Epifaunal	Epibyssate	Associated with sponges and rocks	Cattaneo-Vietti et al. 2000, Narchi et al. 2002, Pörtner et al. 1999
Philobryidae				
Adacnarca nitens	Epifaunal	Epibyssate, epibiotic	Sand, rocks, hydrozoans, bryozoans, sponges, ascidians, and gorgonians	Cattaneo-Vietti et al. 2000, Higgs et al. 2009, Pers. Obs.

Taxa	**Mode of life**		**Substrate**	**References**
Lissarca notorcardensis	Epifaunal	Epibyssate, epibiotic	Spines of cidaroid sea urchins	Brey et al. 1993, Linse et al. 2007
Neocardia sp.	Epifaunal	Epibyssate, epibiotic	Associated with phytals	Lasiak 1999
Philobrya sublaevis	Epifaunal	Epibyssate, epibiotic	Algae	Cattaneo-Vietti et al. 2000

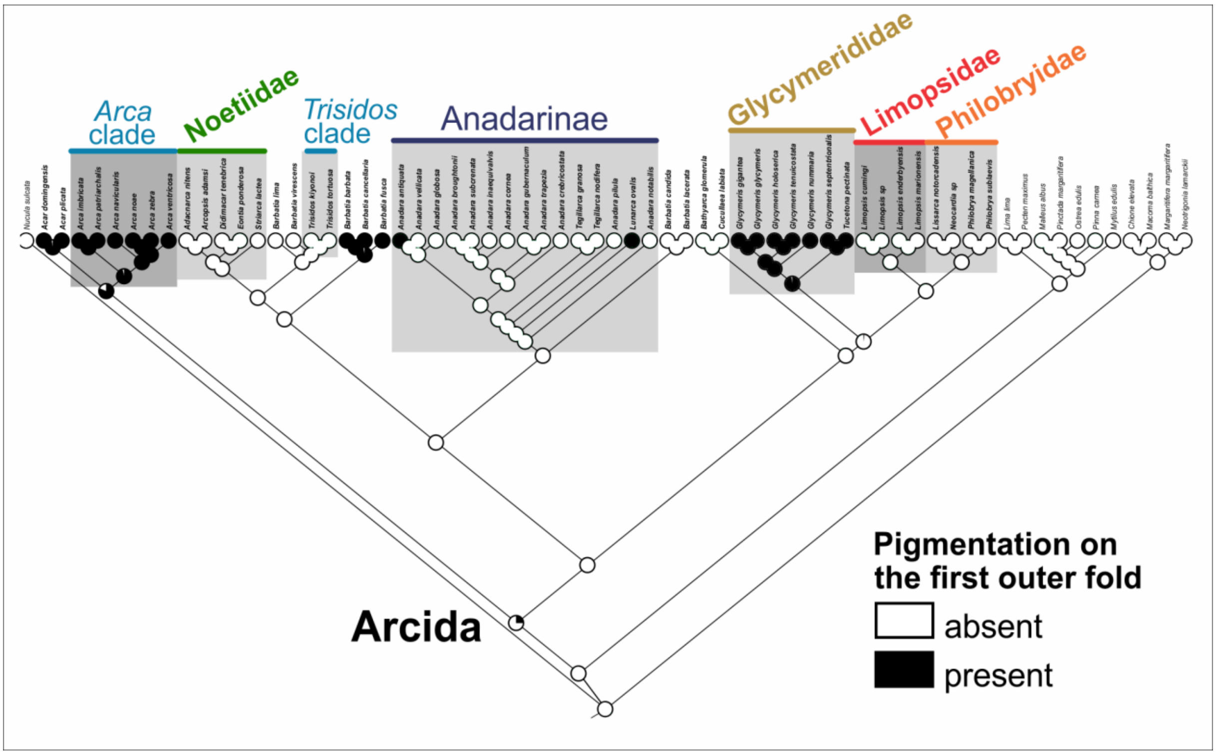

Figure S1. Ancestral state reconstruction of pigmentation on the first outer mantle fold in Arcida under maximum likelihood, assuming a single rate for all possible transitions (MK1 model). Pie charts represent the likelihood proportions of reconstructed states. Pigmentation has evolved multiple times in different lineages of epifaunal and infaunal arcids.

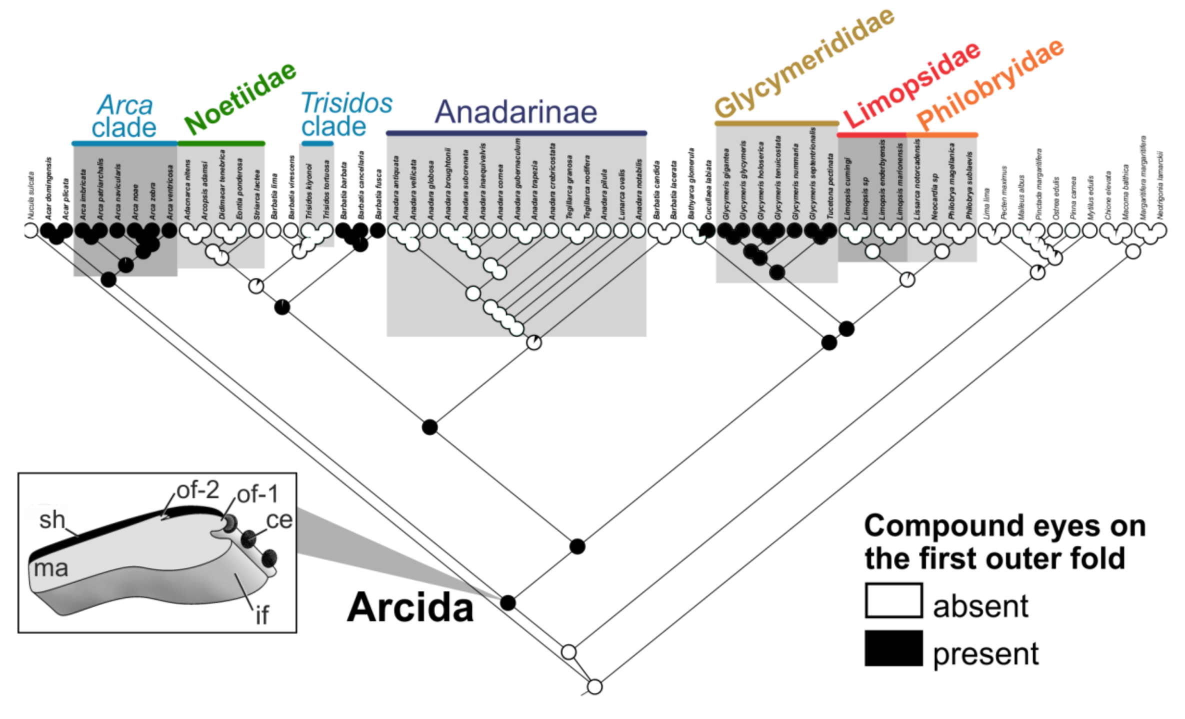

Figure S2. Ancestral state reconstruction of compound eyes on the first outer mantle fold in Arcida under maximum likelihood, allowing for a different rate for transitions (AsymmMK model). Pie charts represent the likelihood proportions of reconstructed states. Compound eyes have a single origin in the ancestor of Arcida with subsequent losses in at least four lineages. Abbreviations: ce, compound eyes; if, inner fold; ma, mantle; mf, middle fold; of-1, first outer fold; of-2, second outer fold; sh, shell.

CHAPTER 7

Phylogeny and anatomy of marine mussels (Mytilidae) reveal convergent evolution of siphon traits in association with similar ecology

CHAPTER 7

Phylogeny and anatomy of marine mussels (Mytilidae) reveal convergent evolution of siphon traits in association with similar ecology

---

Abstract

Marine mussels (Mytilidae) have long been studied for their ecology, morphology, and economic importance. Different lifestyles, habitat uses, and variable phenotypes also make them suitable models for evolutionary studies, including association between same ecological factors and evolution towards similar phenotypes. The mantle margin of mytilids comprises a diverse set of traits that can be used to test hypotheses of ecomorphological correlation and adaptation. The present study investigated the evolution of the mantle margin and lifestyles in Mytilidae to identify macroevolutionary patterns and test for convergent evolution. A phylogenetic hypothesis of Mytilidae was inferred based on five genes (16S rRNA, 18S rRNA, 28S rRNA, COI, and histone H3) for 33 species (19 genera), also including a time-calibrated phylogeny. The mantle margin was investigated in 43 preserved species (23 genera) from collections. Ancestral state reconstruction and correlation tests were performed to estimate trait evolution. In addition, to explore functional aspects of the mantle margin, four species were collected and investigated through detailed microscopy techniques. The inferred phylogeny recovered two main clades derived from an epifaunal ancestor. Subsequently, different lineages convergently shifted to other lifestyles, i.e., semi-infaunal and boring into hard substrate. Such transitions are correlated with development of long siphons in the posterior mantle region. Two origins with subsequent losses were reconstructed for the posterior lobules on the inner fold, which are associated with intense mucociliary transport, suggesting an important cleaning role in epifaunal mussels. Our results support multiple convergent morphological evolution in marine mussels associated with lifestyle transitions, shedding light on ecomorphological patterns in benthic invertebrates.

Keywords: adaptation, correlation, epifaunal, macroevolution, siphon

Introduction

Apart from their economic importance, mussels from the family Mytilidae Rafinesque, 1815 exhibit remarkable phenotypic and lifestyle diversity. These bivalves, also known as marine mussels, have an extensive fossil record, dating back to the Silurian (~427 million year ago, Mya) (Berry & Boucot, 1973; Kříž, 2008). From shallow to deep waters, marine mussels represent an important benthic component in many communities, playing key ecological roles, such as colonization, bioerosion, aggregation, and supporting associated fauna (Seed, Richardson, & Smith, 2000; Dinesen & Morton, 2014). Lifestyles are remarkably diverse, including epifaunal, infaunal, semi-infaunal, and boring into hard substrates (Morton, 2015). In addition, lineages of Mytilidae have proved to be suitable models for evolutionary studies, casting light on broader questions concerning adaptive radiation, diversification rates, and evolutionary novelties (Distel, 2000; Owada, 2007; Lorion *et al.*, 2013).

The literature on mytilid morphology offers compelling evidence for correlation between phenotype and environment (e.g., Stanley, 1972; Owada, 2007; Morton, 2015). A classic example is provided by borer species (e.g., *Adula*, *Botula*, *Leiosolenus*, *Lithophaga*), mostly living in calcareous substrates, which share similar patterns of body shape and boring methods (Yonge, 1955; Morton & Scott, 1980; Owada, 2007, 2015; Ockelmann & Dinesen, 2009). In addition, deep sea mussels living on vents, seeps or organic falls, were intensively studied, highlighting adaptive radiations based on symbiosis evolution and convergent transition to deep-sea environments (Distel *et al.*, 2000; Jones *et al.*, 2006; Samadi *et al.*, 2007; Duperron *et al.*, 2009; Lorion *et al.*, 2010, 2013; Fontanez & Cavanaugh, 2013). Variation in shell features and body plan also provided numerous insights into the evolution of Mytilidae, suggesting putative adaptations to epifaunal and infaunal lifestyles (Stanley, 1972; Morton & Dinesen, 2011; Dinesen & Morton, 2014; Morton, 2015).

In this context, the mantle margin also comprises a promising source of morphological characters, due to its putatively strong association with habitat use and lineage diversification (Yonge, 1983; Audino & Marian, 2016). In bivalves, this anatomical region is usually organized in three folds responsible for sensory, muscular, and secretory roles (Yonge, 1983) with great variation among bivalve groups. Anatomical data for the mytilid mantle margin are available for some species (e.g., Soot-Ryen, 1955; Morton & Scott, 1980; Narchi & Galvão-Bueno, 1983, 1997; Morton & Dinesen, 2010; Morton, 2012; Dinesen & Morton, 2014), but they are largely unknown for many representatives. Nevertheless, the observed plasticity in mantle margin morphology indicates that Mytilidae is a suitable model for testing hypotheses on trait evolution, correlation with lifestyles, and putative adaptations. Previous studies suggested that evolutionary convergences may have underlain morphological diversification of the family (Distel, 2000). Considering the mantle margin, for example, siphon development would be expected in distinct infaunal lineages as an adaptation to burrowing habits in soft sediments (Stanley, 1968).

Even though the Mytilidae exhibit very favorable features for evolutionary investigations, taxonomic issues and limited phylogenetic hypotheses represent current constraints. The family was recovered monophyletic in several analysis (Distel, 2000; Giribet & Wheeler, 2002; Matsumoto, 2003; Owada, 2007; Samadi *et al.*, 2007; Bieler *et al.*, 2014; Combosch & Giribet, 2016; Sun & Gao, 2017; Liu, Liu, & Zhang, 2018), always placed within the Pteriomorphia, along with oysters, scallops, and ark clams. The relationships of some internal groups are relatively well understood, such as the deep sea Bathymodiolinae (Jones *et al.*, 2006; Duperron *et al.*, 2009; Lorion *et al.*, 2010, 2013). Nevertheless, relationships among genera and subfamilies remain largely ambiguous. For example, the traditional "Lithophaginae" (comprised by hard-substrate borers) was suggested not to be monophyletic (Owada, 2007; Liu *et al.*, 2018).

The present study investigated the phylogenetic relationships within Mytilidae, including representatives of all but one subfamily (i.e., Crenellinae). The phylogenetic background was used to reconstruct the evolution of lifestyles and key mantle traits, based on extensive observations of archived specimens, and to test hypotheses of correlation. In addition, we thoroughly investigated the mantle margin of two epifaunal and two borer species to explore their detailed structure and associated functions.

Material and methods

Taxa sampling

Morphological investigation includes data for 43 species (23 genera) of Mytilidae from the following collections: Museum of Comparative Zoology (MCZ), Museum of Zoology "Prof. Adão José Cardoso" of the University of Campinas (ZUECBIV), Museum of Zoology of the University of São Paulo (MZSP), Smithsonian National Museum of Natural History (USNM), and Santa Barbara Museum of Natural History (SBMNH). Catalog numbers are listed in Table 1. Specimens were dissected in ethanol and observed under stereomicroscope. For phylogenetic inference, up to five genes (16S rRNA, 18S rRNA, 28S rRNA, COI, and histone H3) were obtained in GenBank for 33 species of Mytilidae, covering 18 genera (Table 1). Missing data corresponds to 21% of the dataset. From the 43 species studied for morphology, 21 have available sequences used for phylogenetic inference, and 22 species either belong to genera that include the remaining sequenced species or correspond to taxa used to complement the investigation on mantle variation in the family. The outgroup comprises eight species from other pteriomorphian groups and five other bivalve species (Table 1).

Taxonomic classification

A detailed history of taxonomic proposals for the family and subfamilies was summarized by Morton (2015). The classification adopted herein is in accordance with Huber (2010, 2015), also adopted by the World Register of Marine Species (WoRMS, http://www.marinespecies.org/aphia.php?p=taxdetails&id=211), including ten subfamilies.

Microscopy techniques

For detailed anatomical studies, four species were collected in São Sebastião's coast (São Paulo State, Brazil) during low tide. Specimens of *Perna perna* and *Brachidontes exustus* were collected on rocky shores and piers, while the borers *Leiosolenus aristatus* and *Leiosolenus bisulcatus* were removed from oyster aggregations and coral fragments. All individuals were anesthetized in an isotonic 7.5% solution of $MgCl_2$ for 2 h prior fixation. Fragments of the mantle margin were dissected and fixed for 3 h in a modified Karnovsky solution and stored in cacodylate buffer (Marian, 2012).

For scanning electron microscopy, samples were prepared and analyzed as described in Audino & Marian (2018). For histology, samples were completely dehydrated and embedded in resin (Leica Historesin Kit, Germany). Serial sections of 4 µm were stained by the following methods: hematoxylin and eosin (HE), toluidine blue and basic fuchsin (TF), Gomori trichrome stain (GO), mercury-bromophenol blue (BB), periodic acid-Schiff (PAS), and alcian blue (AB). To evidence secretory cells, PAS and AB methods were applied to identify mucosubstances while BB to stain protein aggregates (Pearse, 1985).

Phylogenetic analysis and divergence time estimation

Sequence alignments were generated with MAFFT v7.311 under the L-INS-i option (Katoh & Standley, 2013). Selection of the best-fit model of nucleotide evolution was performed in ModelFinder (Kalyaanamoorthy *et al.*, 2017) under the corrected Akaike information criterion (AICc). The best fit model for the concatenate dataset was GTR + I + G, which was applied in subsequent analyses, totalizing 5710 pb. Maximum likelihood (ML) searches were conducted in IQ-TREE (Nguyen *et al.*, 2014) and node support was estimated by bootstrap with 100 replicates (Felsenstein, 1985).

Divergence times were estimated by Bayesian Inference (BI) in RevBayes under the fossilized birth-death model (Heath, Huelsenbeck, & Stadler, 2014; Höhna *et al.*, 2016). A relaxed molecular clock was applied assuming an uncorrelated exponential model on molecular branch rates. Posterior probabilities were sampled using the Markov Chain Monte Carlo (MCMC) method in four independent chains for 500.000 iterations. Convergence of the posteriors were verified in Tracer (Rambaut *et al.*, 2018). Fossil taxa were pruned prior to summarize the phylogenetic trees as a maximum clade credibility tree, with a burn-in of 10%. In addition, a plot of lineages-through-time was produced in IcyTree (https://icytree.org/).

All priors for fossil ages were drawn from uniform distributions. The root age of Bivalvia was constrained between 520.5 and 530 Ma (million years ago), based on the fossil *Fordilla troyensis* (Pojeta, Runnegar, & Kriz, 1973). The age of Mytilidae was constrained around 423.3 ± 4.1 Ma, based on the fossils *Phthonia regularis* (427.4–425.6 Ma, Kříž, 2008) and *Mytilus* sp. (427.4–419.2 Ma) (Berry and Boucot, 1973), as also suggested by the Paleobiology Database (https://paleobiodb.org/). The fossil *Bathymodiolus heretaunga*, constrained around 301.1 ± 2.3 Ma (Saether *et al.*, 2010), was used to calibrate the Bathymodiolinae. The remaining fossil ages were constrained based on data recorded in the Paleobiology Database. The fossil *Lithophaga subelliptica*, constrained around 26.2 ± 1.1 Ma, was used to calibrate the Lithophaginae. For the Modiolinae, the fossil *Modiolus koneckii* was constrained around 292.8 ± 2.7 Ma. The fossil *Musculus somaliensis*, constrained around 164.8 ± 1.3 Ma, was used to calibrate the Musculinae. Finally, the Mytilinae was constrained based on the fossil *Mytilus nativus*, 244.6 ± 2.6 Ma.

Character evolution

Inhalant and exhalant apertures of mytilid mantle are traditionally treated as siphons, regardless of their level of development (Soot-Ryen, 1955). In this study, we considered short siphons those in which the aperture is wider than the length of the siphon, not forming a cylindrical structure. Alternatively, long siphons are formed by extended mantle projections, forming long conical structures. Mantle margin characters were coded (Table 2) and states were assigned to terminals based on observations of corresponding species or close relatives. Characters are related to the presence of posterior projections on the mantle margin and siphon length. Ecological data (i.e., lifestyle and substrate type) were compiled from the literature (supplemental material, Table S1). Lifestyles include epifaunal (above substrate), semi-infaunal (partially buried in the sediment), infaunal (buried in the sediment) and boring (into hard substrate such as wood or limestone) (Table 2).

Ancestral state reconstructions (ASR) were conducted under maximum likelihood in Mesquite (Maddison & Maddison, 2018). The MK1 model (one parameter model), which assumes the same rate for all possible transitions, and the AsymmMK model (two parameter moded), which allows different transition rates, were considered. Reconstructions for each character adopted the model that presented a better fit to the data when compared via a likelihood ratio test (Maddison & Maddison, 2018). When two characters with multiple transitions across the phylogeny seemed to be associated, a correlation test was applied to evaluate evolutionary dependence between traits (Pagel, 1994). Searches were carried out with 100 iterations and p value estimated from 10.000 simulations in Mesquite. Hypotheses of evolutionary correlation were accepted whenever the eight-parameters model presented a better fit ($p<0.05$) than the four parameters model (uncorrelated hypothesis) (Pagel, 1994; Maddison & FitzJohn, 2015).

Results

Mantle margin diversity

In mytilids, the mantle margin comprises three folds. The outer and middle mantle folds are located at the distal end of the margin (Fig. 1A). These folds are usually thin and homogenous along their extension with a thick periostracum formed between them (Fig. 1A, B). In contrast, the inner mantle fold is proximal, being much longer posteriorly (Fig. 1B). Despite this general pattern, the posterior mantle margin is highly variable regarding the type of associated structures, level of extension, and presence of pigmentation (Fig. 1).

Many epifaunal mussels bear posterior lobules on the inner surface of the inner fold along the inhalant aperture (Fig. 1B-E). They are usually large and folded, as observed in *Aulacomya atra* (Fig. 1B), *Mytella charruana* (Fig. 1C), all *Mytilu*s species (Fig. 1D), *Mytilisepta bifurcata*, *Xenostrubus pulex*, and *Perna perna* (Fig. 2A), but may be proportionally smaller, less numerous, and sparse, like in *Septifer bilocularis, Perumytilus purpuratus*, and all *Brachidontes* species examined (Table 2, Fig. 1E).

In the posterior region, there is a point where the inner folds of both mantle lobes become fused. Consequently, an exhalant siphon is formed in the posterior, dorsal region.

Conversely, the inhalant siphon does not form a delimited aperture, since the inner folds of each side do not fuse ventrally (Fig. 1B-L). Short siphons with wide apertures were observed in most genera, including *Mytella*, *Xenostrobus*, *Dacrydium* and those from Brachidontinae (except for *Geukensia demissa*), Bathymodiolinae, Modiolinae, and Mytilinae (Table 2). Long siphons were observed in the boring species *Adula diengensis*, *Gregariella coralliophaga* (Fig. 1H), *Leiosolenus*, and *Lithophaga* (Fig. 1K-L), and in the semi-infaunal/infaunal mussels *Arcuatula senhousia*, *Geukensia demissa* (Fig. 1I), and *Musculus discors* (Fig. 1J) (Table 2). Generally, long siphons were greatly contracted in preserved specimens, but still very extensible when pulled up.

Beneath the inhalant aperture, close to the fusing point, there is a mantle tissue connecting both mantle lobes at the base of the inner fold, also separating the exhalant and inhalant siphons. This membrane is named branchial septum and show great morphological diversity (Fig. 1M-P) in length, presence of a callus, presence of a median flap, and presence of papillae (Table 2). The septum is generally short in most species, forming a triangle immediately ventral to the mantle fusion point (Fig. 1M-N), as observed in *Brachidontes exustus* (Fig. 1E) and in the genera *Mytella*, *Mytilus* (Fig. 1D), and *Perna*. In other mytilids, such as *Lithophaga* and *Adula*, the septum is proportionally longer (Fig. 1O-P). In many species, for example from the genera *Brachidontes* (Fig. 1E), *Gregariella*, and *Leiosolenus*, the central margin of the septum can be thicker, forming a callus (Fig. 1N). In other mytilids, a median flap can present, corresponding to a long projection that extends between the ctenidia (Fig. 1O). This is the case of *Geukensia demissa* (Fig. 1I) and *Lithophaga*, for example. Papillae can be distributed along the septum margin, or on its outer surface, (Fig. 1P), as observed in *Bathymodiolus termophilus* (Fig. 1F) and most species of *Lithophaga* and *Leiosolenus*.

Functional anatomy

The mantle margin in *Perna perna* and *Brachidontes exustus* is very pigmented posteriorly, and lobules are present on the inner mantle fold along the inhalant aperture (Fig. 2A-D). The siphons are very short, forming only wide apertures. In detail, the posterior lobules are irregular structures intensely folded (Fig. 2A, B, D). They are covered by densely distributed, short cilia (Fig. 2C, E). The inner fold in *Perna perna* contains numerous secretory cells (Fig. 2F); their content is PAS-positive, but negative to Alcian blue, indicating neutral mucosubstances. Most secretory cells occupy an inner position within the fold, with extensions to the epithelium where they release their content (Fig. 2G). The lobules also have secretory cells, although they are much less numerous (Fig. 2H). Subepithelial gland cells are abundant at the base of the inner fold and on the inner mantle epithelium of *Perna perna*. These cells likely secrete a mixture of acid and neutral mucosubstances (Fig. 2I). In *Brachidontes exustus*, secretory activity was not observed in the lobules (Fig. 2J, K). Finally, both species have very short middle folds, distally located (Fig. 2J, L). In addition, the inner epithelium of the outer fold is taller than the epithelium of the other folds, and the periostracal gland is greatly developed (Fig. 2L).

The inner folds of *Leiosolenus aristatus* and *L. bisulcatus* are greatly enlarged, forming long siphons (Fig. 3A). The epithelium is covered by clusters of short cilia (Fig. 3B) and subepithelial secretory cells are distally located along the fold (Fig. 3C). In addition, an accessory fold is present in these species. This fold is located on the outer surface of the inner fold, forming a lateral ridge, which is longer posteriorly (Fig. 3D). The surface of the accessory fold is densely covered by cilia (Fig. 3E), but no evidence of secretory activity or musculature was found (Fig. 3F). The middle and outer folds are short, originating at a distal position (Fig. 3G). Ventrally, the mantle margin contains numerous subepithelial secretory cells positive for PAS (Fig. 3H). Intense secretory activity is present along the posterior mantle margin, close to the middle and outer folds, in a region named “posterior pallial gland”. The most abundant type of secretory cell of this gland forms clusters of cells containing large granules strongly positive for PAS (Fig. 3I) and for the Fast-Green stain of the Gomori method (Fig. 3J); they did not stain with eosin (Fig. 3K) and bromophenol blue (Fig. 3L). Interspersed with these large cells, another secretory cell type occurs; they are small cells containing granular content strongly stained by eosin (Fig. 3K), bromophenol blue (Fig. 3L), and by the acid fuchsin of the Gomori method (Fig. 3J); they are also PAS-negative (Fig. 3I).

Phylogenetic hypothesis and divergence time

Mytilidae is monophyletic in our ML analysis and splits into two main clades (Fig. 4). One of them includes mussels with a typical mytiliform shape. The small *Brachidontes* are closely related to *Geukensia demissa* and *Perumytilus purpuratus*, forming a clade sister to *Ischadium recurvum* and the Septiferinae. The boring *Gregariella coarctata* is recovered sister to *Mytilus*, while the semi-infaunal *Musculus* and *Arcuatula senhousia* form a clade close to the epifaunal *Perna*. In the other main clade, Modiolinae is monophyletic, as well as Bathymodiolinae, which groups the deep-sea genera. Interestingly, the boring species *Leiosolenus curtus* is not sister to *Lithophaga* despite their similar habit and cylindrical shape.

In our analysis, *Dacrydium sp*. is closely related to *Lithophaga*, while *Leiosolenus curtus* is sister to the modioliform clades.

The divergence time tree inferred by BI (Fig. 5) is mostly congruent with the ML topology, except for *Ischadium recurvum* and *Perumytilus purpuratus*, which change places. The family dates back to the Silurian, around 424.3 Ma, and the two main clades diverge in the Early and Late Devonian, around 395.7 Ma and 379.9 Ma, respectively (Fig. 5). The most recent common ancestor (MRCA) of distinguished clades dates back to the Late Triassic, including, for example, the genus *Lithophaga* (205 Ma), Modiolinae (225.1 Ma), Bathymodiolinae (211.5 Ma), Brachidontinae (222.7), and Musculinae (212.7 Ma). More recent divergences during the Mesozoic include the MRCA of *Mytilus* group (182.8 Ma, Early Jurassic), *Bathymodiolus* group (128.2 Ma, Early Cretaceous), and *Perna* group (125.2 Ma, Early Cretaceous).

Character evolution

Reconstructions indicate an epifaunal ancestor for all marine mussels (Fig. 6A). Transitions to the semi-infaunal habit occurred twice, within *Modiolus* and *Geukensia*. Similarly, transitions to complete infaunal habit were convergently achieved by *Dacrydium* and the ancestor of *Arcuatula* and *Musculus*. The habit of boring into hard substrate is convergent for *Gregariella*, *Leiosolenus*, and *Lithophaga*. In addition, siphon hypertrophy was investigated in combination with habits of life (Fig. 6B). According to ASR, short siphons (Fig. 6C) are plesiomorphic, and long siphons (Fig. 6D) have convergently evolved at least five times where lifestyle transition has occurred from epifaunal to either semi-infaunal, infaunal or boring (Fig. 6A, B). A correlation hypothesis was tested and returned a *p*-value of 0.03 ($p<0.05$), supporting evolutionary correlation between siphon enlargement and lifestyle transition.

The posterior lobules on the inner mantle fold have a single origin for the diverse clade including *Brachidontes*, *Perymytilus*, *Mytilus*, *Mytilispeta*, *Perna*, and *Septifer* (Fig. 7). In addition, similar structures were also gained in *Xenostrobus* (Fig. 7). Interestingly, posterior lobules were likely lost multiple times, including in some lineages in which lifestyle shifted from epifaunal to semi-infaunal/infaunal, such as *Arcuatula*+*Musculus*, *Geukensia*, and *Gregariella*.

Discussion

Mytilidae phylogeny

Even though our dataset (33 species, 19 genera) represents a restricted sample from the Mytilidae diversity, it does represent a significant improvement in mussel phylogenetics, along with other recent efforts (Liu et al., 2018). The family was recovered monophyletic, as indicated in previous analyses (Distel, 2000; Giribet & Wheeler, 2002; Matsumoto, 2003; Owada, 2007; Samadi *et al.*, 2007; Bieler *et al.*, 2014; Combosch *et al.*, 2017). Our results for the divergence time of Mytilidae is in accordance with the fossil record, assigning an ancient origin for the family in the Silurian. The division of Mytilidae into two main clades were also identified in a previous study with improved taxonomic sampling (Liu *et al.*, 2018). Considering all recent advancements in mytilid phylogenetics, internal relationships indicate that revisions are necessary to clarify taxonomic arrangements, as also urged by many authors.

The subfamily Mytilinae does not appear to be monophyletic, as previously suggested elsewhere (Distel, 2000), neither any other subfamily but Bathymodiolinae, Modiolinae, and Septiferinae. A close relationship between representatives of Musculinae and Mytilinae had already been reported previously (Owada, 2007; Liu *et al.*, 2018). The Arcuatulinae is another example of an unnatural taxonomic group that needs to be revised, considering, for example, *Arcuatula senhousia* and *Xenostrobus securis*, both classified within Arcuatulinae, but phylogenetically distant. In our ML analysis, the Brachidontinae clade includes all *Brachidontes* species, but also *Geukensia demissa* and *Perumytilus purpuratus*, corroborating previous phylogenetic proposals (Distel, 2000; Trovant *et al.*, 2013). Conversely, our data recovers *Ischadium recurvum* sister to the Septiferinae instead of nested among other *Brachidontes*.

Specialized bivalves boring calcareous substrate (Yonge, 1955; Kleemann, 1990; Morton, 1990) were traditionally classified within the Lithophaginae (Soot-Ryen, 1955; Morton & Scott, 1980; Morton, 2015). Nevertheless, our results indicate this subfamily is not monophyletic, because *Leiosolenos* and *Lithophaga* do not form a clade. These findings are in accordance with recent analyses (Liu *et al.*, 2018), arguing for convergent acquisition of the boring habit and the “lithophagiform” shape (Owada, 2007).

The Bathymodiolinae represents a clade that diverged from a modioliform ancestor in a single invasion of deep waters, including animals living in organic falls, vents, and seeps (Gustafson, 1998; Distel *et al.*, 2000; Fontanez & Cavanaugh, 2013). The evolutionary radiation of these deep-sea mussels has been thoroughly explored under the perspective of morphology, chemosymbioses, habits, and distribution (Jones *et al.*, 2006; Duperron *et al.*, 2009; Lorion *et al.*, 2010, 2013). While *Benthomodiolus* species seem to be sister to the remaining Bathymodiolinae, the genus *Bathymodiolus* is not monophyletic in our analysis for including *Idas washingtonia*. Accordingly, previous studies counting with an improved taxonomic sampling demonstrated the polyphyletic nature of many deep-sea mussel genera, such as the traditional *Bathymodiolus* (Cosel, 2002; Jones *et al.*, 2006; Lorion *et al.*, 2013).

Mantle margin diversity and functions

First described for *Mytilus edulis* (Kellogg, 1915), the branchial septum is quite diverse among Mytilidae. This structure, formed by fused projections from the inner folds, shows variable length and may exhibit papillae, a callus or a median flap. Nevertheless, few details are available and information about this region is often ignored in anatomical studies, maybe because of its difficult examination in preserved animals. Short triangular septa were previously described for the epifaunal *Brachidontes*, *Mytella*, and *Perna* (Narchi & Galvão-Bueno, 1983, 1997; Morton, 2012). In contrast, a long septum is common among the Bathymodiolinae. While some species have numerous, well-developed papillae, e.g., *Bathymodiolus heckerae*, *B. platifrons*, *B. thermophilus*, and *Benthomodiolus erebus* (Cosel, 2002; Oliver, 2015), others lack them entirely, e.g., *Bathymodiolus childressi* and *Idas argenteus* (Cosel, 2002; Ockelmann & Dinesen, 2011). A large septum is supposed to act as a valve, restricting the size of the inhalant aperture, and thus controlling the inflow of large particles into the mantle cavity (Morton, 1974). The presence of numerous papillae in *Lithophaga* and *Bathymodiolus*, for example, also suggests sensory roles, but further investigation is necessary to clarify possible functions. The present systematization of septum morphology for several species represents an important initial contribution to better understand this neglected structure and its diversity.

Posterior lobules are very enlarged in epifaunal mussels, e.g., *Mytella*, *Mytilus*, *Perna*, and *Xenostrobus* (Narchi & Galvão-Bueno, 1983, 1997) (present study). Small and sparse lobules are present in Brachidontinae and Septiferinae (Morton, 2012, present study). The character evolution analyses suggest a single origin of lobules, except for an independent acquisition in *Xenostrobus*. Secretory cells and cilia distribution in the inner mantle fold of *Perna perna* suggests intense secretion of mucous by this fold. Therefore, the lobules should provide mucociliary transport (Sleigh, 1989), cleaning the mantle and preventing the entrance and accumulation of undesirable, larger particles. Similarly, cilia type on the papillae of

Brachidontes exutus are likely related to transport of mucus rafts (Sleigh, 1989). In addition, lobules show contraction in response to disturbance (JAA, pers. obs.), suggesting simple sensory roles as well. Interestingly, the fact that they were independently lost in secondarily semi-infaunal/infaunal lineages suggests an adaptive role of the posterior lobes in epifaunal bivalves.

Glandular activity is abundant and highly specialized in species boring into calcareous substrates (Morton & Scott, 1980; Morton, 1990). Different types of glands have been described, including anterior and posterior-dorsal boring glands, posterior pallial glands, and siphonal glands (Yonge, 1955; Jaccarini, Bannister, & Micallef, 1968; Morton & Scott, 1980; Simone & Gonçalves, 2006). Our results on *Leiosolenus aristatus* and *L. bisulcatus* reveal a well-developed posterior pallial gland, not detected in previous studies on *Lithophaga* species (Morton & Scott, 1980; Morton, 1993). Located along the margin leading to the outer and middle folds, this gland discharges secretions containing either polysaccharides or eosinophilic, proteinaceous substances on the posterior mantle margin. This condition could correspond to the release of calcium-binding mucoproteins described for boring mechanisms in related species (Jaccarini *et al.*, 1968). According to previous assumptions, when the mantle is extended, this secretion is used to prevent calcification of the siphonal aperture, enlarging the borehole, and inhibiting skeleton formation in species boring live corals (Jaccarini *et al.*, 1968; Morton & Scott, 1980). The accessory fold observed on the outer surface of the inner fold in *Leiosolenus* and *Lithophaga* species may act as a canal, facilitating secretion distribution on the siphonal area by mucociliary transportation.

Mantle fusion in Mytilidae occurs in a single, posterior point, corresponding to the type A described by (Yonge, 1982). Consequently, the mantle aperture is divided in a delimited exhalant siphon and a ventrally opened inhalant siphon (Fig. 6C, D). Short siphons, usually forming a wide aperture, are present among most epibyssate mussels, as listed in Table 2. They were also reported for other epifaunal genera, such as *Benthomodiolus*, *Choromytilus*, *Limnoperna*, and *Semimytilus* (Soot-Ryen, 1955; Narchi & Galvão-Bueno, 1983, 1997; Cosel, 2002; Morton & Dinesen, 2010; Morton, 2012; Oliver, 2015). In contrast, long and extensible siphons were observed in borer species, such as *Gregariella*, *Leiosolenus*, and *Lithophaga*, as well as in the borers *Adula* and *Botula* (Soot-Ryen, 1955; Yonge, 1955; Morton & Scott, 1980; Valentich-Scott & Tongkerd, 2008; Ockelmann & Dinesen, 2009). Long siphons are also present in some semi-infaunal/infaunal species that display the byssal nest-building habit, like *Arcuatula*, *Geukensia*, and *Musculus* (Bertrand, 1971; Morton & Dinesen, 2011; Morton, 2015). Interestingly, siphons are short in the semi-infaunal

Dacrydium, *Crenatula*, and *Mytella*. The hypertrophy of the inner fold, forming long siphons, is observed in most infaunal groups of bivalves and is considered an adaptive trait to burrow in soft sediment (Stanley, 1968; Yonge, 1983; Audino et al., 2019). Similarly, boring species create channels or galleries within the hard substrate, with only the tip of the elongate siphons exposed through the borehole (Yonge, 1955).

Evolutionary convergences

Similar phenotypes can evolve independently, i.e., by convergence, when unrelated lineages experiment transitions to similar environments (Losos, 2011; Serb *et al.*, 2011). In addition, similar selective pressures can result in adaptive convergences, which represent crucial aspects to understand evolutionary radiations (Agrawal, 2017). Our results with marine mussels reveal new examples of convergent morphological evolution associated with lifestyle transitions.

The traditional view of mytilid evolution supports the semi-infaunal habit as the plesiomorphic condition based on endobyssate fossils with modioliform shapes (Stanley, 1972). In contrast, our results suggest that, from an epifaunal ancestor, multiple lineages of mytilids shifted to other lifestyles in association with changes in mantle morphology. For instance, transitions to semi-infaunal/infaunal and boring habits in association with posterior inner fold hypertrophy (i.e., siphon elongation) evidence acquisition of common adaptive phenotypes under similar ecological conditions. In addition, our results also support shifts to infaunal, semi-infaunal and boring habits in the Triassic, corroborating previous hypotheses of benthic diversification and infaunalization during the Mesozoic (Vermeij 1977). The Late Triassic is regarded as an epoch of development of an evolutionary arms race among marine groups, which characterizes the Mesozoic Marine Revolution, an era of taxonomic radiations and adaptations in response to diversification of predatory pressures (Vermeij 1977, Harper and Skelton 1993, Tackett and Bottjer 2012). A similar ecomorphological pattern was identified in ark clam lineages (Arcida) that evolved longer inner folds associated with epifaunal-infaunal transitions (Audino et al. 2019). These results highlight the plasticity of the mantle margin in bivalve evolution and point to trends in the radiation of marine benthic lineages.

In conclusion, this study provides a robust phylogenetic hypothesis for Mytilidae combined with increased knowledge on mantle structure and functional morphology. By characterizing the evolution of ecomorphological patterns in marine mussels, our results adds to the increasing body of evidence of ecological factors driving convergent phenotypical evolution in marine invertebrates (Distel 2000; Lindgren *et al.*, 2012; Li, Ó Foighil, & Strong, 2016; Sherratt *et al.*, 2016; Sherratt, Serb, & Adams, 2017; Serb *et al.*, 2017).

Acknowledgements

The authors acknowledge funding provided by FAPESP (São Paulo Research Foundation; 2015/09519-4, 2017/01365-3). This study was financed in part by the Coordenação de Aperfeiçoamento de Pessoal de Nível Superior – Brasil (CAPES), finance code 001. This study is part of the first author's Doctorate's thesis through the Graduate Program in Zoology of the Institute of Biosciences (University of São Paulo). The authors thank the following institutions that provided materials for the development of this study: Center for Marine Biology (CEBIMar), Museum of Comparative Zoology (MCZ), Museum of Zoology "Prof. Adão José Cardoso" of the University of Campinas (ZUEC), Museum of Zoology of the University of São Paulo (MZSP), Santa Barbara Museum of Natural History (SBMNH), and Smithsonian National Museum of Natural History (USNM). This is a contribution of NP-BioMar (Research Center for Marine Biodiversity – USP).

References

Agrawal AA. 2017. Toward a predictive framework for convergent evolution: Integrating natural history, genetic mechanisms, and consequences for the diversity of life. *The American Naturalist* 190: S1–S12.

Audino JA, Marian JEAR. 2016. On the evolutionary significance of the mantle margin in pteriomorphian bivalves. *American Malacological Bulletin* 34: 148–159.

Audino JA, Marian JEAR. 2018. Comparative and functional anatomy of the mantle margin in ark clams and their relatives (Bivalvia: Arcoidea) supports association between morphology and life habits. *Journal of Zoology* 305: 149–162.

Audino JA, Serb JM, Marian JEAR. 2019. Ark clams and relatives (Bivalvia: Arcida) show convergent morphological evolution associated with lifestyle transitions in the marine benthos. *Biological Journal of the Linnean Society* doi 10.1093/biolinnean/blz017

Berry WBN, Boucot AJ. 1973. Correlation of the African Silurian rocks. *Geological Society of America Special Papers* 127: 1–74.

Bertrand G. 1971. The ecology of the nest-building bivalve *Musculus lateralis* commensal with the ascidian *Molgula occidentalis*. *Veliger* 14: 23–29.

Bieler R, Mikkelsen PM, Collins TM, Glover EA, González VL, Graf DL, Harper EM, Healy J, Kawauchi GY, Sharma PP, Staubach S, Strong EE, Taylor JD, Tëmkin I, Zardus JD, Clark S, Guzmán A, McIntyre E, Sharp P, Giribet G. 2014. Investigating the Bivalve Tree of Life – an exemplar-based approach combining molecular and novel morphological characters. *Invertebrate Systematics* 28: 32.

Combosch DJ, Collins TM, Glover EA, Graf DL, Harper EM, Healy JM, Kawauchi GY, Lemer S, McIntyre E, Strong EE, Taylor JD, Zardus JD, Mikkelsen PM, Giribet G, Bieler R. 2017. A family-level Tree of Life for bivalves based on a Sanger-sequencing approach. *Molecular Phylogenetics and Evolution* 107: 191–208.

Combosch DJ, Giribet G. 2016. Clarifying phylogenetic relationships and the evolutionary history of the bivalve order Arcida (Mollusca: Bivalvia: Pteriomorphia). *Molecular Phylogenetics and Evolution* 94: 298–312.

Cosel R von. 2002. A new species of bathymodioline mussel (Mollusca, Bivalvia, Mytilidae) from Mauritania (West Africa), with comments on the genus *Bathymodiolus* Kenk & Wilson, 1985. *Zoosystema* 24: 259–271.

Dinesen GE, Morton B. 2014. Review of the functional morphology, biology and perturbation impacts on the boreal, habitat-forming horse mussel *Modiolus modiolus* (Bivalvia: Mytilidae: Modiolinae). *Marine Biology Research* 10: 845–870.

Distel DL. 2000. Phylogenetic relationships among Mytilidae (Bivalvia): 18S rRNA data suggest convergence in mytilid body plans. *Molecular Phylogenetics and Evolution* 15: 25–33.

Distel DL, Baco AR, Chuang E, Morrill W, Cavanaugh C, Smith CR. 2000. Do mussels take wooden steps to deep-sea vents? *Nature* 403: 725–726.

Duperron S, Lorion J, Samadi S, Gros O, Gaill F. 2009. Symbioses between deep-sea mussels (Mytilidae: Bathymodiolinae) and chemosynthetic bacteria: diversity, function and evolution. *Comptes Rendus Biologies* 332: 298–310.

Felsenstein J. 1985. Confidence limits on phylogenies: an approach using the bootstrap. *Evolution* 39: 783–791.

Fontanez K, Cavanaugh C. 2013. Phylogenetic relationships of hydrothermal vent mussels (Bathymodiolinae) and their symbionts. *Marine Ecology Progress Series* 474: 147–154.

Giribet G, Wheeler W. 2002. On bivalve phylogeny: a high-level analysis of the Bivalvia (Mollusca) based on combined morphology and DNA sequence data. *Invertebrate Biology* 121: 271–324.

Gustafson RG. 1998. A new genus and five new species of mussels (Bivalvia, Mytilidae) from deep-sea sulfide/hydrocarbon seeps in the Gulf of Mexico. *Malacologia* 40: 63–112.

Huber M. 2010. *Compendium of Bivalves. A Full-color Guide to 3,300 of the World's Marine Bivalves. A Status on Bivalvia after 250 Years of Research*. Hackenheim: ConchBooks.

Huber M. 2015. *Compendium of Bivalves 2. A Full-color Guide to the Remaining Seven Families. A Systematic Listing of 8,500 Bivalve Species and 10,500 Synonym*. Harxheim: ConchBooks.

Jaccarini V, Bannister W, Micallef H. 1968. The pallial glands and rock boring in *Lithophaga lithophaga* (Lamellibranchia, Mytilidae). *Journal of Zoology* 154: 397–401.

Jones WJ, Won YJ, Maas PAY, Smith PJ, Lutz RA, Vrijenhoek RC. 2006. Evolution of habitat use by deep-sea mussels. *Marine Biology* 148: 841–851.

Kalyaanamoorthy S, Minh BQ, Wong TK, von Haeseler A, Jermiin LS. 2017. ModelFinder: fast model selection for accurate phylogenetic estimates. *Nature Methods* 14: 587.

Katoh K, Standley DM. 2013. MAFFT multiple sequence alignment software version 7: improvements in performance and usability. *Molecular Biology and Evolution* 30: 772–780.

Kellogg JL. 1915. Ciliary mechanisms of lamellibranchs with descriptions of anatomy. *Journal of Morphology* 26: 625–701.

Kleemann K. 1990. Evolution of the chemically-boring Mytilidae (Bivalvia). *The Bivalvia — Proceedings of a Memorial Symposium in Honour of Sir Charles Maurice Yonge, Edinburgh, 1986*. Los Angeles: Hong Kong University Press, 111–124.

Kříž J. 2008. A new bivalve community from the Lower Ludlow of the Prague Basin (Perunica, Bohemia). *Bulletin of Geosciences*: 237–280.

Li J, Ó Foighil D, Strong EE. 2016. Commensal associations and benthic habitats shape macroevolution of the bivalve clade Galeommatoidea. *Proceedings of the Royal Society B: Biological Sciences* 283: 20161006.

Lindgren AR, Pankey MS, Hochberg FG, Oakley TH. 2012. A multi-gene phylogeny of Cephalopoda supports convergent morphological evolution in association with multiple habitat shifts in the marine environment. *BMC Evolutionary Biology* 12: 129.

Liu J, Liu H, Zhang H. 2018. Phylogeny and evolutionary radiation of the marine mussels (Bivalvia: Mytilidae) based on mitochondrial and nuclear genes. *Molecular Phylogenetics and Evolution* 126: 233–240.

Lorion J, Buge B, Cruaud C, Samadi S. 2010. New insights into diversity and evolution of deep-sea Mytilidae (Mollusca: Bivalvia). *Molecular Phylogenetics and Evolution* 57: 71–83.

Lorion J, Kiel S, Faure B, Kawato M, Ho SYW, Marshall B, Tsuchida S, Miyazaki JI, Fujiwara Y. 2013. Adaptive radiation of chemosymbiotic deep-sea mussels. *Proceedings of the Royal Society B: Biological Sciences* 280: 20131243–20131243.

Losos JB. 2011. Convergence, adaptation, and constraint. *Evolution* 65: 1827–1840.

Maddison WP, FitzJohn RG. 2015. The unsolved challenge to phylogenetic correlation tests for categorical characters. *Systematic Biology* 64: 127–136.

Maddison WP, Maddison DR. 2018. Mesquite: a modular system for evolutionary analysis. Version 3.51 http://www.mesquiteproject.org.

Marian JEAR. 2012. Spermatophoric reaction reappraised: Novel insights into the functioning of the loliginid spermatophore based on *Doryteuthis plei* (Mollusca: Cephalopoda). *Journal of Morphology* 273: 248–278.

Matsumoto M. 2003. Phylogenetic analysis of the subclass Pteriomorphia (Bivalvia) from mtDNA COI sequences. *Molecular Phylogenetics and Evolution* 27: 429–440.

Morton B. 1974. Some aspects of the biology, population dynamics, and functional morphology of *Musculista senhausia* Benson (Bivalvia, Mytilidae). *Pacific Science* 28: 19–33.

Morton B. 1990. Corals and their bivalve borers—the evolution of a symbiosis. *The Bivalvia—Proceedings of a Memorial Symposium in Honour of Sir Charles Maurice Yonge, Edinburgh, 1986*. Hong Kong: Hong Kong University Press, 11–46.

Morton B. 1993. How the ‘forceps’ of *Lithophaga aristata* (Bivalvia: Mytiloidea) are formed. *Journal of Zoology* 229: 609–621.

Morton B. 2012. A significant and unappreciated intertidal mytiloidean genus: the biology and functional morphology of *Brachidontes puniceus* (Bivalvia: Mytilidae) from the Cape Verde Islands. *African Journal of Marine Science* 34: 71–80.

Morton B. 2015. Evolution and adaptive radiation in the Mytiloidea (Bivalvia): clues from the pericardial–posterior byssal retractor musculature complex. *Molluscan Research* 35: 227–245.

Morton B, Dinesen GE. 2010. Colonization of Asian freshwaters by the Mytilidae (Bivalvia): a comparison of *Sinomytilus harmandi* from the Tonle-Sap River, Phnom Penh, Cambodia, with *Limnoperna fortunei*. *Molluscan Research* 30: 57.

Morton B, Dinesen GE. 2011. The biology and functional morphology of *Modiolarca subpicta* (Bivalvia: Mytilidae: Musculinae), epizoically symbiotic with *Ascidiella aspersa* (Urochordata: Ascidiacea), from the Kattegat, northern Jutland, Denmark. *Journal of the Marine Biological Association of the United Kingdom* 91: 1637–1649.

Morton B, Scott PJB. 1980. Morphological and functional specializations of the shell, musculature and pallial glands in the Lithophaginae (Mollusca: Bivalvia). *Journal of Zoology* 192: 179–203.

Narchi W, Galvão-Bueno MS. 1983. Anatomia funcional de *Mytella charruana* (D'Orbigny, 1846) (Bivalvia: Mytilidae). *Boletim de Zoologia* 6: 113–145.

Narchi W, Galvão-Bueno MS. 1997. Functional anatomy of *Perna perna* (Linné) (bivalvia, Mytilidae). *Revista Brasileira de Zoologia* 14: 135–168.

Nguyen LT, Schmidt HA, von Haeseler A, Minh BQ. 2014. IQ-TREE: a fast and effective stochastic algorithm for estimating maximum-likelihood phylogenies. *Molecular biology and evolution* 32: 268–274.

Ockelmann KW, Dinesen GE. 2009. Systematic relationship of the genus *Adula* and its descent from a *Mytilus*-like ancestor (Bivalvia, Mytilidae, Mytilinae). *Steenstrupia* 30: 141–152.

Ockelmann KW, Dinesen GE. 2011. Life on wood – the carnivorous deep-sea mussel *Idas argenteus* (Bathymodiolinae, Mytilidae, Bivalvia). *Marine Biology Research* 7: 71–84.

Oliver PG. 2015. Description and morphology of the "Juan de Fuca vent mussel", *Benthomodiolus erebus* sp. n. (Bivalvia, Mytilidae, Bathymodiolinae): "Phylogenetically basal but morphologically advanced". *Zoosystematics and Evolution* 91: 151–165.

Owada M. 2007. Functional morphology and phylogeny of the rock-boring bivalves *Leiosolenus* and *Lithophaga* (Bivalvia: Mytilidae): a third functional clade. *Marine Biology* 150: 853–860.

Owada M. 2015. Functional phenotypic plasticity of the endolithic mytilid *Leiosolenus curtus* (Lischke, 1874) (Bivalvia: Mytilidae). *Molluscan Research* 35: 188–195.

Pagel M. 1994. Detecting correlated evolution on phylogenies: a general method for the comparative analysis of discrete characters. *Proc. R. Soc. Lond. B* 255: 37–45.

Pearse AGE. 1985. Histochemistry, theoretical and applied. Vol. 2. Analytical technology, 4th ed. London: Churchill Livingstone.

Saether KP, Little CT, Campbell KA, Marshall BA, Collins M, Alfaro AC. 2010. New fossil mussels (Bivalvia: Mytilidae) from Miocene hydrocarbon seep deposits, North Island, New Zealand, with general remarks on vent and seep mussels. *Zootaxa* 2577: 1-45.

Samadi S, Quéméré E, Lorion J, Tillier A, von Cosel R, Lopez P, Cruaud C, Couloux A, Boisselier-Dubayle MC. 2007. Molecular phylogeny in mytilids supports the wooden steps to deep-sea vents hypothesis. *Comptes Rendus Biologies* 330: 446–456.

Seed R, Richardson CA, Smith K. 2000. Marine mussels, their evolutionary success, ecological significance and use as chronometers of environmental change. *Geological Society, London, Special Publications* 177: 465–478.

Serb JM, Alejandrino A, OtáRola-Castillo E, Adams DC. 2011. Morphological convergence of shell shape in distantly related scallop species (Mollusca: Pectinidae). *Zoological Journal of the Linnean Society* 163: 571–584.

Serb JM, Sherratt E, Alejandrino A, Adams DC. 2017. Phylogenetic convergence and multiple shell shape optima for gliding scallops (Bivalvia: Pectinidae). *Journal of Evolutionary Biology* 30: 1736–1747.

Sherratt E, Alejandrino A, Kraemer AC, Serb JM, Adams DC. 2016. Trends in the sand: Directional evolution in the shell shape of recessing scallops (Bivalvia: Pectinidae). *Evolution* 70: 2061–2073.

Sherratt E, Serb JM, Adams DC. 2017. Rates of morphological evolution, asymmetry and morphological integration of shell shape in scallops. *BMC Evolutionary Biology* 17.

Simone LRL, Gonçalves EP. 2006. Anatomical study on *Myoforceps aristatus*, an invasive boring bivalve in S.E. Brazilian coast (Mytilidae). *Papéis Avulsos de Zoologia (São Paulo)* 46: 57–65.

Sleigh MA. 1989. Adaptations of ciliary systems for the propulsion of water and mucus. *Comparative Biochemistry and Physiology Part A: Physiology* 94: 359–364.

Soot-Ryen T. 1955. A report on the family Mytilidae (Pelecypoda). *Allan Hancock Pacific Expeditions* 20: 1–175.

Stanley SM. 1968. Post-Paleozoic adaptive radiation of infaunal bivalve molluscs: A consequence of mantle fusion and siphon formation. *Journal of Paleontology* 42: 214–229.

Stanley SM. 1972. Functional morphology and evolution of byssally attached bivalve mollusks. *Journal of Paleontology* 46: 165–212.

Sun W, Gao L. 2017. Phylogeny and comparative genomic analysis of Pteriomorphia (Mollusca: Bivalvia) based on complete mitochondrial genomes. *Marine Biology Research* 13: 255–268.

Trovant B, Ruzzante DE, Basso NG, Orensanz JM (Lobo). 2013. Distinctness, phylogenetic relations and biogeography of intertidal mussels *(Brachidontes*, Mytilidae) from the south-western Atlantic. *Journal of the Marine Biological Association of the United Kingdom* 93: 1843–1855.

Valentich-Scott P, Tongkerd P. 2008. Coral-boring bivalve molluscs of southeastern Thailand, with the description of a new species. *Raffles Bulletin of Zoology, Suppl* 18: 191–216.

Yonge CM. 1955. Adaptation to rock boring in *Botula* and *Lithophaga* (Lamellibranchia, Mytilidae) with a discussion on the evolution of this habit. *Journal of Cell Science* 3: 383–410.

Yonge CM. 1982. Mantle margins with a revision of siphonal types in the Bivalvia. *Journal of Molluscan Studies* 48: 102–103.

Yonge CM. 1983. Symmetries and the role of the mantle margins in the bivalve Mollusca. *Malacological Review* 16: 1–10.

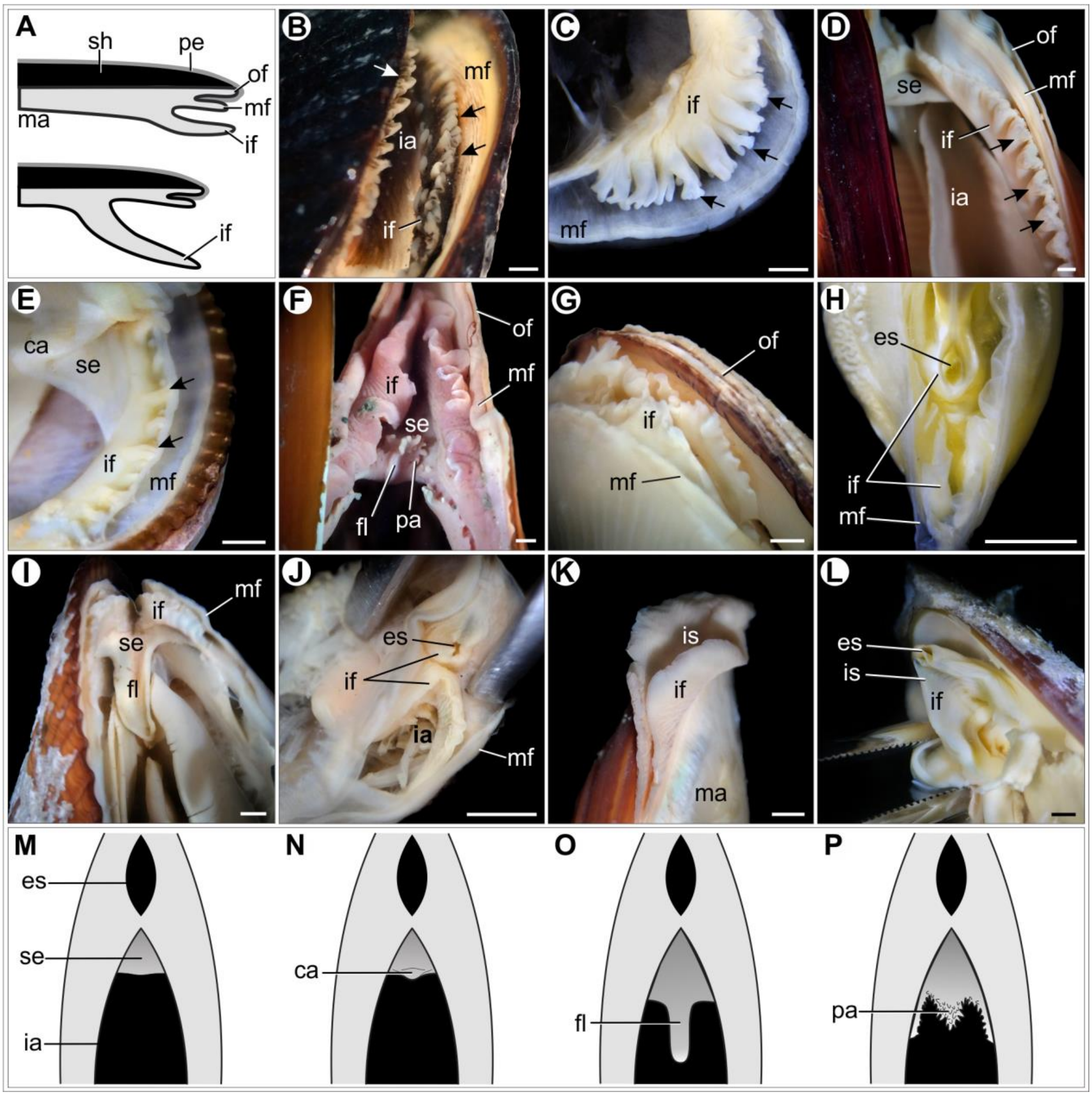

Figure 1. Mantle margin morphology and diversity in Mytilidae. Lateral view in C and E; ventro-posterior view in B, D, F-L. Posterior lobules on the inner fold are indicated by arrows. **A.** Schematic representation of the mantle margin in section; anterior region at top and posterior region at bottom. **B.** *Aulacomya atra* (MCZ288117). C**.** *Mytella charruana* (ZUECBIV2177). **D.** *Mytilus californianus* (USNM802552). **E.** *Brachidontes exustus* (USNM760843). **F.** *Bathymodiolus termophilus* (SBMNH350528). **G.** *Adula diegensis* (SBMNH83588). **H.** *Gregariella coralliophaga* (MZSP96956). **I.** *Geukensia demissa* (SBMNH95794). **J.** *Musculus discors* (USNM832507). **K.** *Lithophaga lithophaga* (MCZ271738). **L.** *Lithophaga nigra* (USNM833842). **M-P.** Schematic representations of the branchial septum morphology (posterior view). **M.** Short septum. **N.** Short septum with callus. **O.** Long septum with flap. **P.** Long septum with papillae. Abbreviations: ca, callus; es, exhalant siphon; fl, flap; ia, inhalant aperture; if, inner mantle fold; is, inhalant siphon; mf, middle mantle fold; of, outer mantle fold; pa, papillae; pe, periostracum; se, branchial septum; sh, shell.

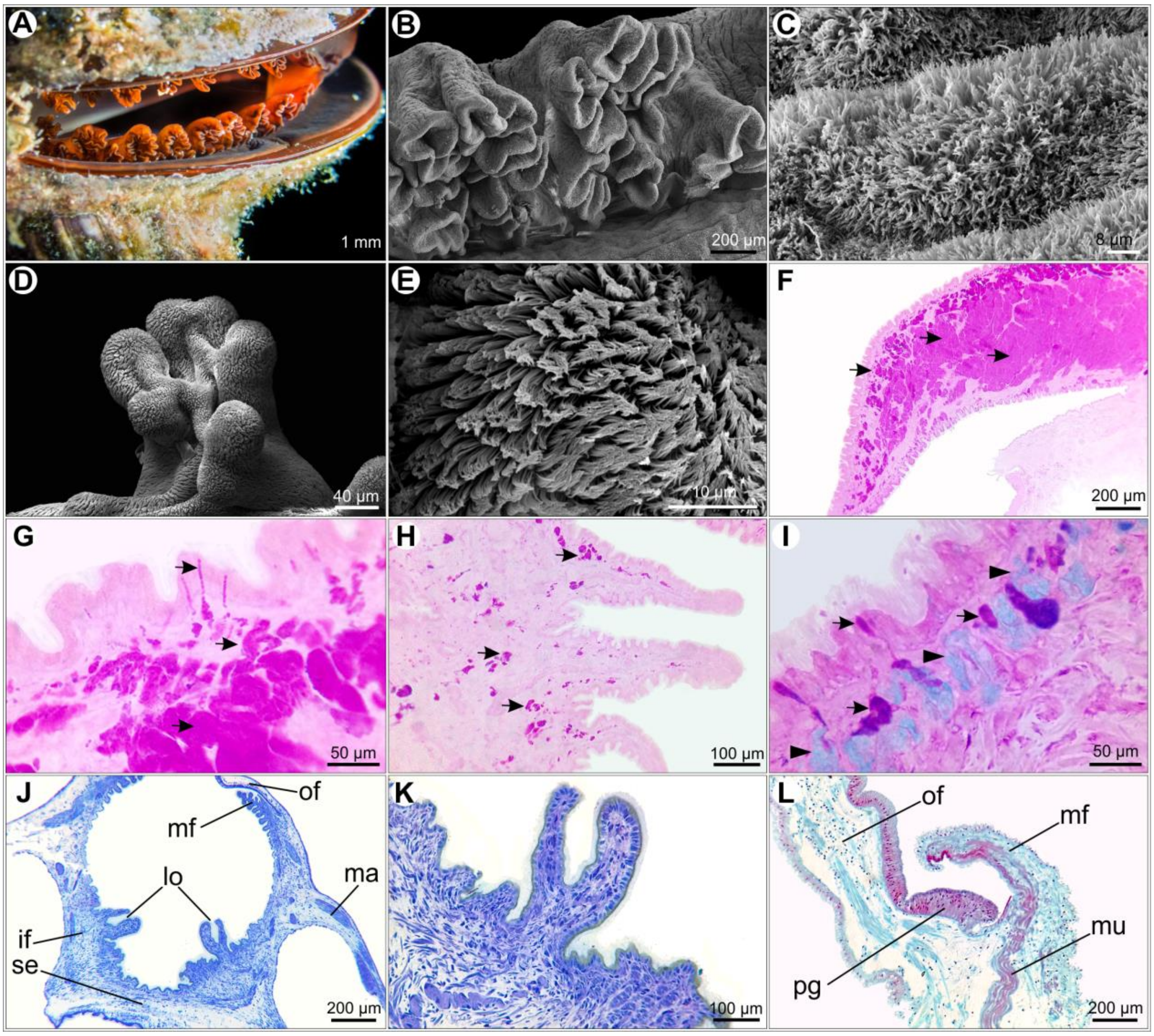

Figure 2. Mantle margin anatomy in the mussels *Perna perna* (A-C, F-I) and *Brachidontes exustus* (D, E, J-L). Scanning electron microscopy in B-E, and histological sections in F-L evidencing secretory cells (arrows and arrowheads). **A.** Inhalant aperture and posterior lobules on the inner fold, as observed in a living specimen (ventro-posterior view). **B.** Detail of lobules. **C.** Short cilia covering lobule's surface. **D.** Detail of a lobule. **E.** Cilia distributed on lobule's surface. **F.** Intense secretory content within the inner fold; PAS. **G.** Detail of secretory cells opening on the outer surface of the inner fold; PAS. **H.** Secretory cells in the lobules; PAS. **I.** Detail of two types of subepithelial secretory cells at the base of the inner fold and on the inner mantle epithelium; PAS (arrow) and AB (arrowhead). **J.** Section through the region where the inner folds are partially fused; TF. **K.** Detail of a small lobule on the inner fold; TF. **L.** Outer mantle fold and middle mantle fold with the periostracal gland located between them; GO. Abbreviations: if, inner mantle fold; lo, posterior lobules; ma, mantle; mf, middle mantle fold; mu, muscle bundles; of, outer mantle fold; pg, periostracal gland; se, branchial septum.

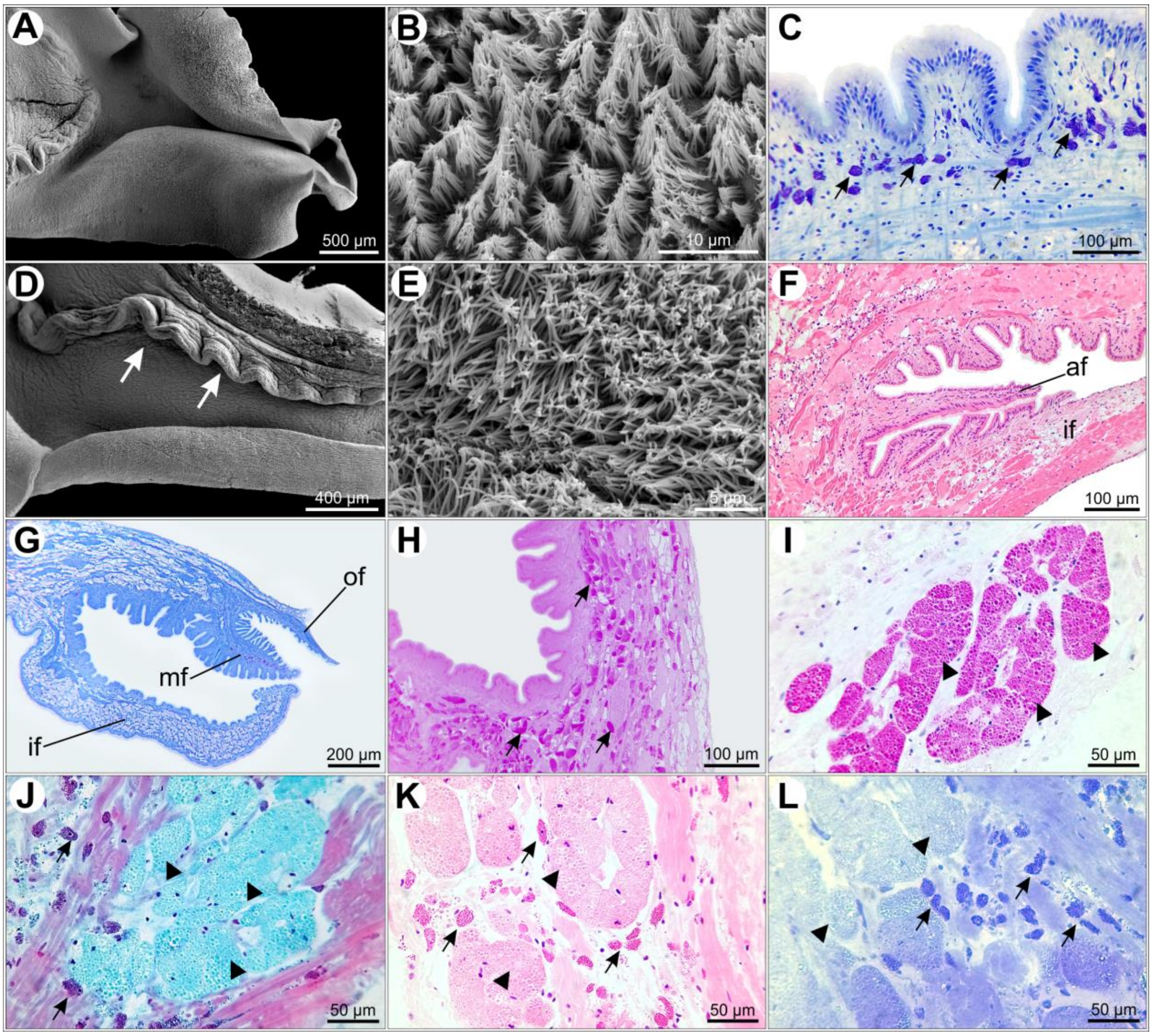

Figure 3. Mantle margin anatomy in the borers *Leiosolenus aristatus* (A-E, I-L) and *Leiosolenus bisulcatus* (F-H). Scanning electron microscopy in A, B, D, and E, and histological sections in C, F-L evidencing secretory cells. **A.** Inhalant siphon formed by long inner folds, ventral view. **B.** Detail of cilia covering the surface shown in A. **C.** Epithelium of the inhalant siphon with subepithelial secretory cells (arrows); TF. **D.** Short accessory fold (arrows) on the outer surface of the inner fold. **E.** Detail of cilia distributed on the accessory fold. **F.** Section through the accessory fold; HE. **G.** Mantle margin with longer inner fold; TF. **H.** Subepithelial secretory cells with mucopolysaccharide content within the mantle margin, ventral region; PAS. **I-L.** Posterior mantle glands composed of large granules (arrowheads) interspersed with small secretory cells (arrows) stained by several methods. **I.** PAS. **J.** GO. **K.** HE. **L.** BB. Abbreviations: af, accessory fold; if, inner mantle fold; mf, middle mantle fold; of, outer mantle fold.

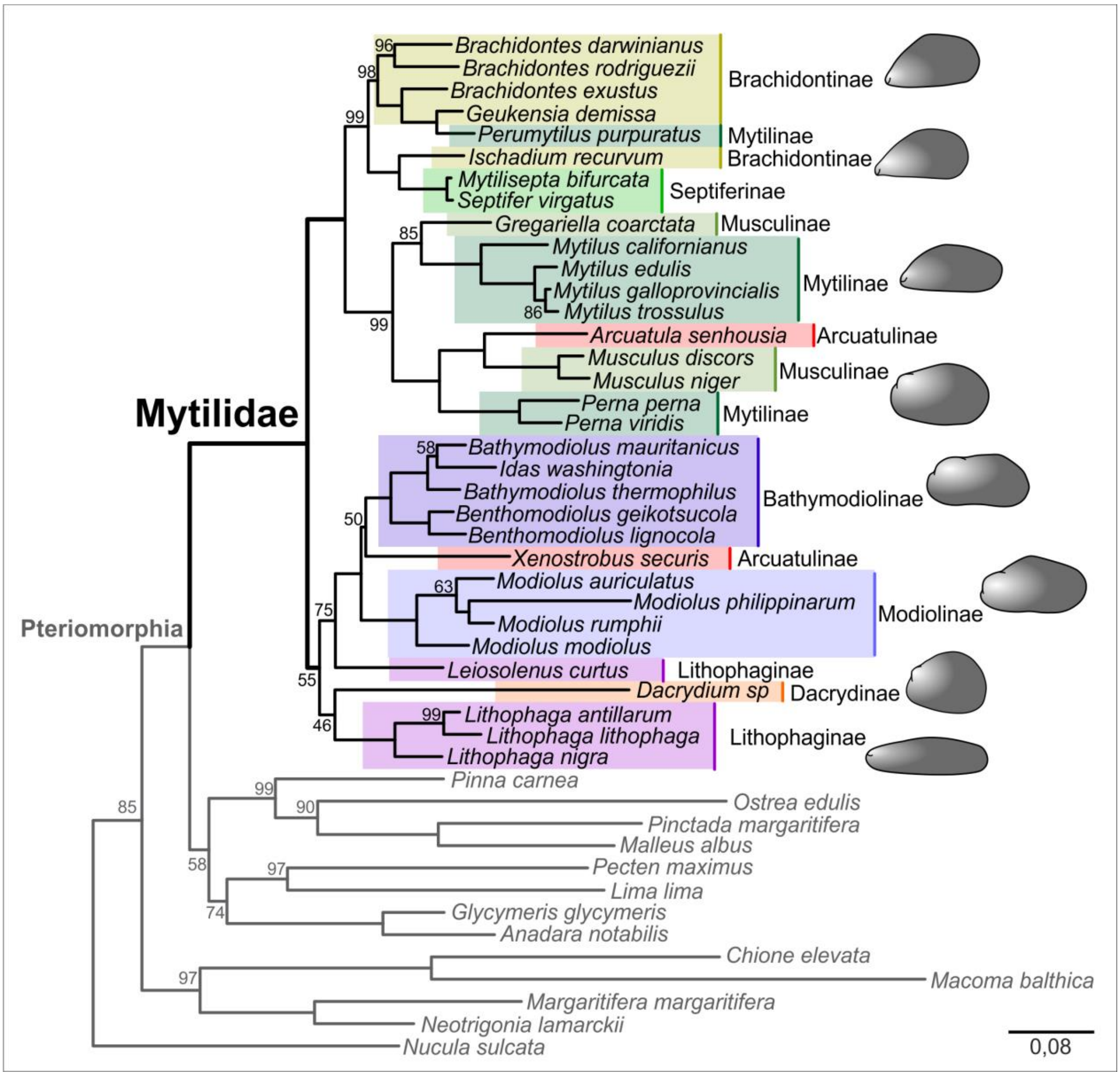

Figure 4. Phylogenetic relationships within Mytilidae. Maximum likelihood tree of Mytilidae based on five nucleotide sequences (16S rRNA, 18S rRNA, 28S rRNA, COI, and H3). Bootstrap values less than 100 are indicated in the internal nodes. Mytilidae encompasses two main clades. Remarkably, some subfamilies, such as Lithophaginae and Mytilinae, are not recovered monophyletic. Subfamily names, in accordance with classification proposed by Huber (2015), are indicated and color coded. Generalized shell silhouettes are depicted on the right.

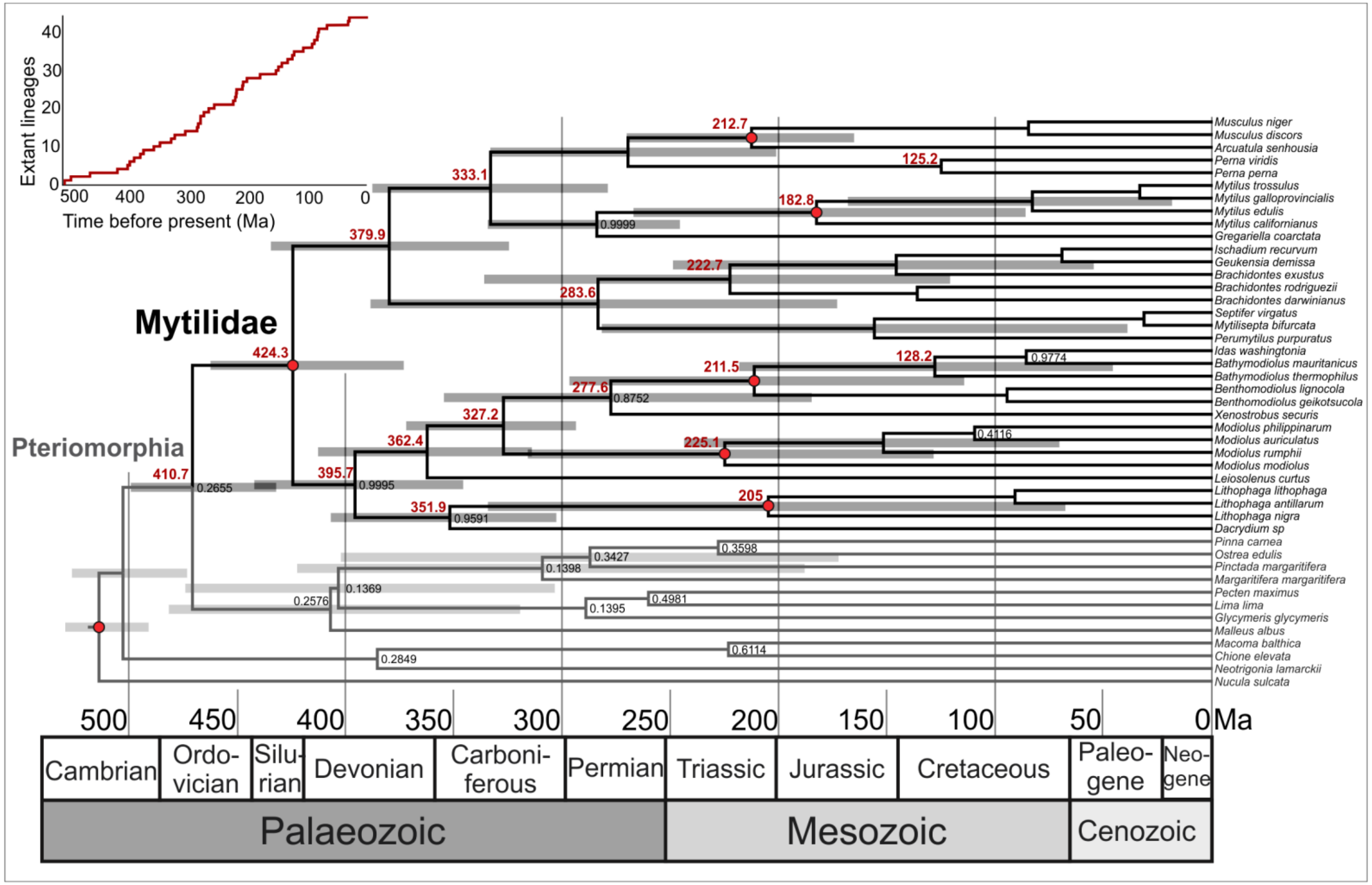

Figure 5. **Time-calibrated phylogeny of Mytilidae.** Divergence time analysis under Bayesian Inference based on five genes (16S rRNA, 18S rRNA, 28S rRNA, COI, and H3) and seven fossils used to calibrate internal nodes (red circles). Red numbers indicate median ages on respective nodes. Bars indicate 95% highest posterior density intervals (HPD) for nodes of interest. Posterior probabilities different than 1.0 are indicated on nodes. A lineages-through-time plot is represented on the upper left.

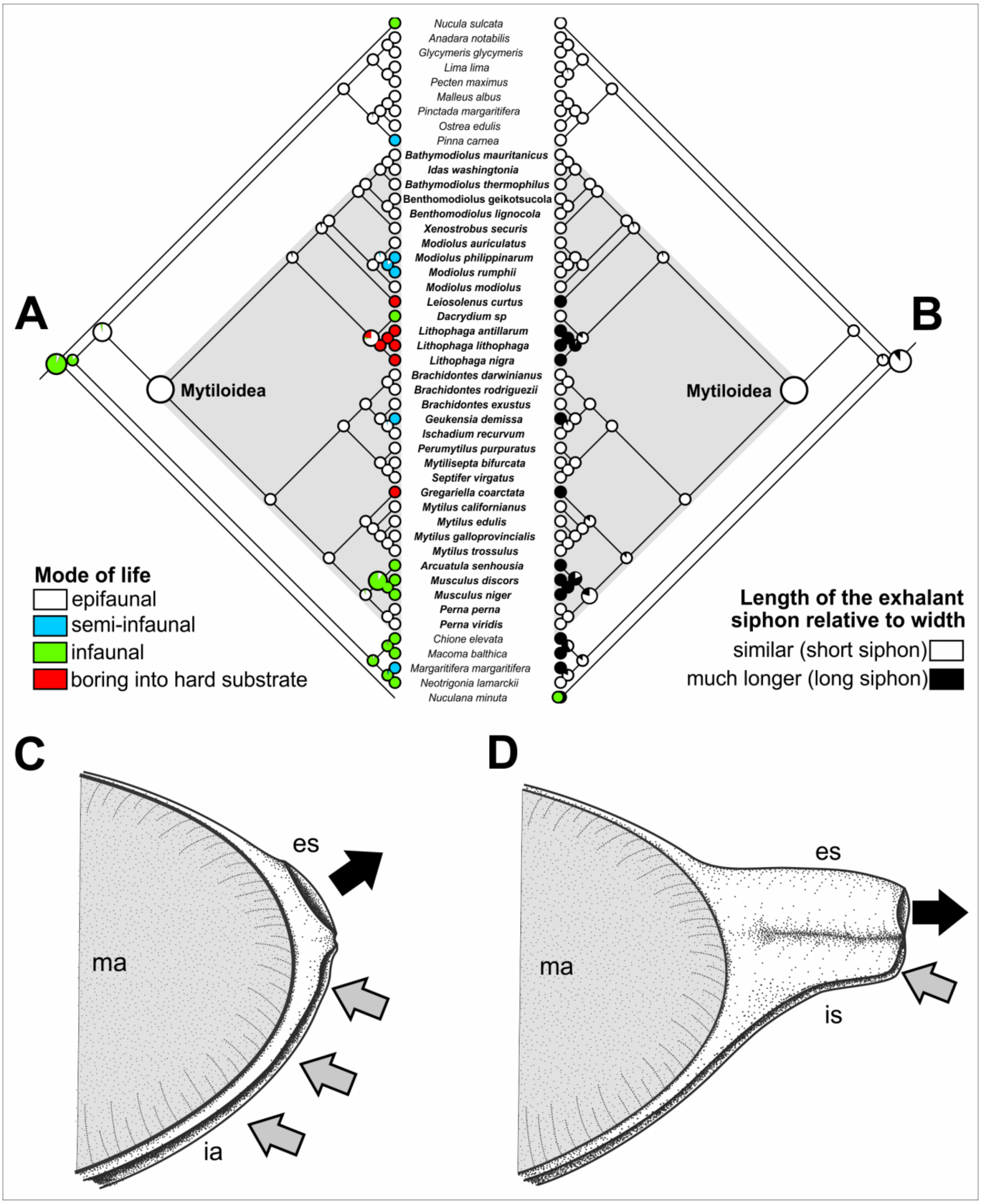

Figure 6. Evolution of siphons and lifestyles in Mytilidae. Ancestral state reconstruction of (**A**) and mode of life and (**B**) length of the exhalant siphon relative to width in Mytilidae under maximum likelihood approach with MK1 model. The convergent evolution of long siphons is closely associated with transitions to semi-infaunal, infaunal, and boring habits. C-D. Lateral view of the posterior mantle region depicting short (C) and long (D) siphons, respectively. Black arrows indicate exhalant currents and grey arrows indicate inhalant currents of water. Abbreviations: es, exhalant siphon; ia, inhalant aperture; inhalant siphon; ma, mantle.

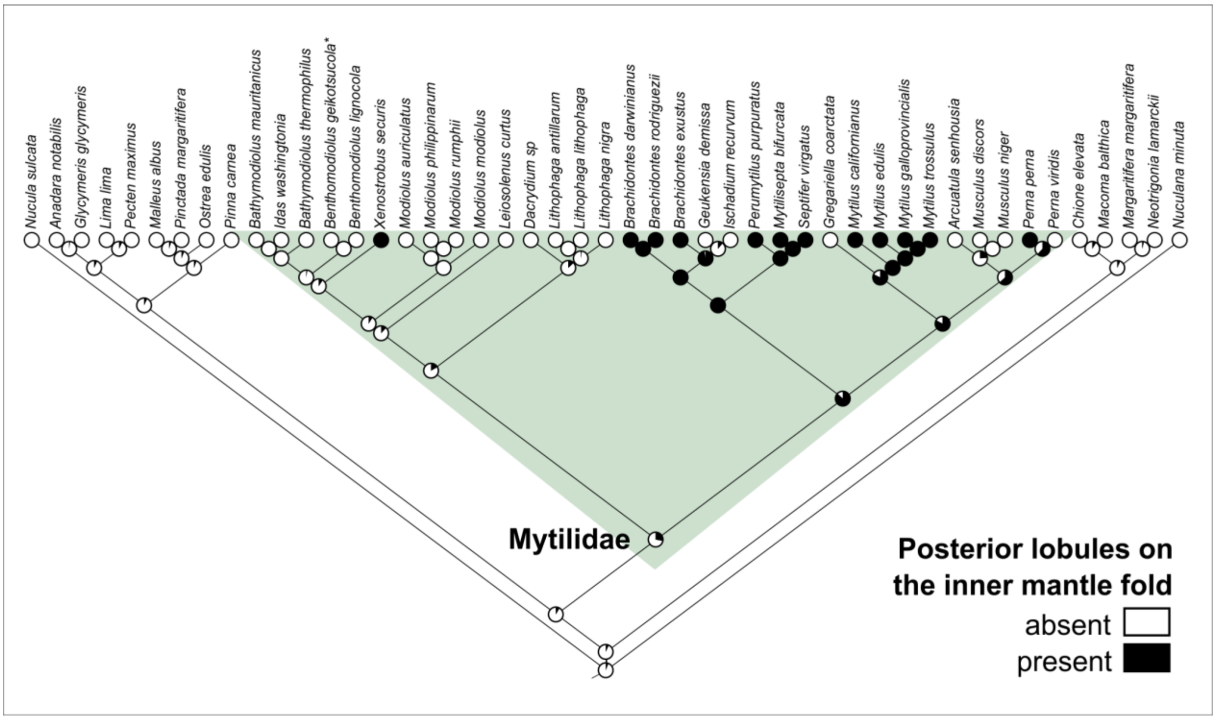

Figure 7. Origin of posterior lobules on the inner mantle fold. Ancestral state reconstruction under maximum likelihood approach with AsymmMK model. The results suggest gain of posterior lobules in the clade including *Brachidontes*, *Mytilisepta*, *Mytilus*, *Perna*, *Perymytilus*, and *Septifer*, with a likely convergent gain for *Xenostrobus securis*. Multiple losses of posterior lobules are associated with lifestyle shifts from epifaunal to semi-infaunal/infaunal, such as in *Arcuatula*, *Gregariella*, *Geukensia*, and *Musculus*.

Table 1. Taxa included in the analyses. Only sequenced species were included in the phylogenetic analysis while congeneric or additional species were observed for morphology. Collection catalog numbers and accession numbers in *GenBank* database are listed. Abbreviations: Museum of Comparative Zoology (MCZ), Museum of Zoology “Prof. Adão José Cardoso” of the University of Campinas (ZUECBIV), Museum of Zoology of the University of São Paulo (MZSP), Smithsonian National Museum of Natural History (USNM), and Santa Barbara Museum of Natural History (SBMNH).

Species	**Author**	**16S**	**18S**	**28S**	**COI**	**Histone H3**	**Catalog number and collection**
Adula diegensis	(Dall, 1911)						SBMNH83588
Arcuatula senhousia	(Benson, 1842)		AB201231		HQ891093		MCZ359059
Aulacomya atra	(Molina, 1782)						USNM869293, MCZ288117
Bathymodiolus brooksi	Gustafson, Turner, Lutz & Vrijenhoek, 1998						USNM1175390
Bathymodiolus childressi	Gustafson, Turner, Lutz & Vrijenhoek, 1998						USNM1263668
Bathymodiolus mauritanicus	Cosel, 2002	HF545083	AY649828	FJ890504	FJ890502	HF545126	
Bathymodiolus thermophilus	Kenk & B. R. Wilson, 1985	KF611760	AF221638	GU966640	GQ473715	KF720623	SBMNH350528
Benthomodiolus geikotsucola	Okutani & Miyazaki, 2007	HF545049	AB679345	HF545023	AB679346	HF545149	
Benthomodiolus lignocola	Dell, 1987	KF611733	AF221648		AY275545	HF545156	
Brachidontes adamsianus	(Dunker, 1857)						USNM802545
Brachidontes darwinianus	(d'Orbigny, 1842)			KC844370	KC844414		
Brachidontes exustus	(Linnaeus, 1758)	KX71319	KT757791	KT757838	AY621838		USNM760843, SBMNH83454
Brachidontes rodriguezii	(d'Orbigny, 1842)		DQ640530	KC844362	KC844477		MZSP115160
Crenella decussata	(Montagu, 1808)						USNM803487
Dacrydium albidum	Pelseneer, 1903						USNM886223
Dacrydium sp.	Torell, 1859	KX713210	KX713285	KX713372	KX713456	KX713529	
Dacrydium vitreum	(Møller, 1842)						USNM831489
Geukensia demissa	(Dillwyn, 1817)	U68772	L33450	AY622004	GQ282963	U68772	SBMNH95794
Gregariella coarctata	(Carpenter, 1857)		AJ414641	AJ307538			

Species	**Author**	**16S**	**18S**	**28S**	**COI**	**Histone H3**	**Catalog number and collection**
Gregariella coralliophaga	(Gmelin, 1791)						MZSP96956, ZUECBIV4844
Idas argentea	(Jeffreys, 1876)						MCZ359142
Idas washingtonius	(Bernard, 1978)	HF545073	AF221645		AY275546		
Ischadium recurvum	(Rafinesque, 1820)	KT959477		AY622009	AY621933		USNM1286864, 1286716
Leiosolenus aristatus	(Dillwyn, 1817)						USNM803979
Leiosolenus bisulcatus	(d'Orbigny, 1853)						USNM803980
Leiosolenus curtus	(Lischke, 1874)	JQ267791	AB201235	AB103123	AB076944	LC004203	
Leiosolenus malaccanus	(Reeve, 1857)						SBMNH452667
Leiosolenus plumula	(Hanley, 1843)						SBMNH213239
Lioberus castaneus	*(Say, 1822)*						USNM833820
Lithophaga antillarum	(d'Orbigny, 1853)	KX713229	KX713308	KX713397		KX713550	USNM847935
Lithophaga lithophaga	(Linnaeus, 1758)	JF496757	AF120530		AF120644		USNM754499, MCZ271738
Lithophaga nigra	(d'Orbigny, 1853)		AF124209	AB103127			USNM833842, MZSP105742
Modiolus americanus	(Leach, 1815)						USNM833854, MZSP104167
Modiolus auriculatus	Kraus, 1848		AJ389644	AJ307537	GQ480317		USNM836901
Modiolus carpenteri	Soot-Ryen, 1963						USNM802553
Modiolus carvalhoi	Klappenbach, 1966						ZUECBIV1134
Modiolus modiolus	(Linnaeus, 1758)	KF611732	AF124210	EF526455	HM884246		SBMNH361489
Modiolus philippinarum	(Hanley, 1843)	KY705073	AB201232		KY705073	LC004218	
Modiolus rumphii	(Philippi, 1847)	KC429248	KC429330	KC429423	KC429094	KC429165	
Musculus discors	(Linnaeus, 1767)	KR827553	AF124206		KF643642	KP113647	USNM832507, MCZ358965
Musculus niger	(J.E. Gray, 1824)		KX713316	KX713404	KF644120		USNM847946
Mytella charruana	(d'Orbigny, 1842)						ZUECBIV2177
Mytilisepta bifurcata	(Conrad, 1837)		KJ453815	KJ453831			USNM802550, SBMNH80853
Mytilus californianus	Conrad, 1837	AF317544	L33449		U68777	AY267745	USNM802552
Mytilus edulis	Linnaeus, 1758	KC429249	KC429331	KC429424	KF644190	KC429166	MZSP120321

Species	Author	16S	18S	28S	COI	Histone H3	Catalog number and collection
Mytilus galloprovincialis	(Lamarck, 1819)	AF317543	L33452	AB105357	AB076943	AY267748	USNM857641, MCZ251341
Mytilus trossulus	Gould, 1850	U22879	L33453		KF643612	AY267747	SBMNH235094
Perna perna	(Linnaeus, 1758)	DQ923882	DQ640520		KU743163		MZSP107780
Perna viridis	(Linnaeus, 1758)	AB265680	EF613234		DQ917584		MZSP55599
Perumytilus purpuratus	(Lamarck, 1819)	JQ390293	KJ453820	KJ598046	KF661934		MZSP92756, USNM869289
Septifer bilocularis	(Linnaeus, 1758)						MZSP 55012, USNM747766, 746371, MCZ301874
Septifer virgatus	(Wiegmann, 1837)	AB372228	KJ453817	KJ453832	AB076941		
Vilasina seminuda	(Dall, 1897)						SBMNH85093
Xenostrobus pulex	(Lamarck, 1819)						SBMNH140005
Xenostrobus securis	(Lamarck, 1819)	AB372227	EF186014		JF430154		
Outgroup							
Anadara notabilis	(Röding, 1798)		KT757768	KT757816	AF416828	KT757863	MZSP84987, 84886
Chione elevata	(Say, 1822)	KC429298	KC429387	KC429495	KC429136	KC429219	
Glycymeris glycymeris	(Linnaeus, 1758)	KC429246	KC429328	KC429421	KC429093	KC429163	USNM794960
Lima lima	(Linnaeus, 1758)	KC429257	KC429339	KC429434	KC429101	KC429174	USNM754383
Macoma balthica	(Linnaeus, 1758)	KC429303	KC429393	KC429501	KC429141	KC429224	
Malleus albus	Lamarck, 1819	KC429252	KC429334	HQ329464	KC429097	KC429169	MZSP55595
Margaritifera margaritifera	(Linnaeus, 1758)	KC429265	AF229612	KC429443	AF303316	KC429185	
Neotrigonia lamarckii	(Gray, 1838)	KC429262	KC429345	KC429443	KC429105	KC429182	
Nucula sulcata	Bronn, 1831	KC984679	AF207642	KC984815	KC984746	KC984777	
Ostrea edulis	Linnaeus, 1758	AF052068	L49052	AF137047	AF120651	AY070151	USNM836256
Pecten maximus	(Linnaeus, 1758)	KC429258	L49053	HM630545	KC429102	EU379508	
Pinctada margaritifera	(Linnaeus, 1758)	HQ329425	AB214451	AB214466	AB259166	HQ329296	USNM836493
Pinna carnea	Gmelin, 1791	KC429255	HQ329375	KJ366067	KJ366325	KC429172	MZSP29040

Table 2. Mantle margin morphology and habits of life in Mytilidae species investigated in the present study, grouped according putative subfamilies (Huber, 2010, 2015). References for ecological information and habits are listed in the supplementary material Table S1.

MYTILIDAE	**Posterior lobules**	**Septum**	**Siphons**	**Lifestyle**
Arcuatulinae				
Arcuatula senhousia	absent	short with callus	long	infaunal in sand and mudflats (byssal nest)
Mytella charruana	large and folded	short	short	semi-infaunal in mudflats
Xenostrobus pulex	large and folded	short	short	epifaunal on hard substrate
Bathymodiolinae				
Bathymodiolus brooksi	absent	short	short	epifaunal on seeps
Bathymodiolus childressi	absent	short	short	epifaunal on seeps
Bathymodiolus termophilus	absent	long with flap and papillae	short	epifaunal on hydrothermal vent
Idas argenteus	absent	short	short	epifaunal on whale bones and sunken wood
Brachidontinae				
Brachidontes adamsianus	short and sparse	long with callus	short	epifaunal on hard substrate
Brachidontes exustus	short and sparse	short with a callus	short	epifaunal on hard substrate
Brachidontes rodriguezii	short and sparse	long with a callus	short	epifaunal on hard substrate
Geukensia demissa	absent	long with flap	long	semi-infaunal in mudflats
Perumytilus purpuratus	short and sparse	long	short	epifaunal on hard substrate
Crenellinae				
Crenella decussata	absent	short	short	infaunal in soft substrate
Vilasina seminuda	absent	unknown	short	unknown
Dacrydinae				
Dacrydium albidum	absent	short	short	infaunal in mud
Dacrydium vitreum	absent	short	short	infaunal in mud
Lithophaginae				
Adula diengensis	absent	long	long	epifaunal in crevices
Leiosolenus aristatus	absent	long with callus and papillae	long	boring into bivalve shells and corals
Leiosolenus bisulcatus	absent	long with callus and papillae	long	boring into bivalve shells and corals
Leiosolenus malaccanus	absent	short with callus	long	boring into bivalve shells and corals
Leiosolenus plumula	absent	long with flap and papillae	long	boring into bivalve shells and calcareous rocks
Lithophaga antillarum	absent	long with flap and papillae	long	boring into calcareous rocks and corals
Lithophaga lithophaga	absent	long with flap and papillae	long	boring into calcareous rocks
Lithophaga nigra	absent	long with flap	long	boring into calcareous rocks and corals

MYTILIDAE	Posterior lobules	Septum	Siphons	Lifestyle
Modiolinae				
Lioberus castaneus	absent	short with papillae	short	epifaunal on hard substrates
Modiolus americanus	absent	short with callus	short	epifaunal or semi-infaunal in a variety of substrates
Modiolus auriculatus	absent	long with callus	short	epifaunal on hard substrates
Modiolus carpenteri	absent	short	short	epifaunal on hard substrates
Modiolus carvalhoi	absent	short	short	epifaunal on hard substrates
Modiolus modiolus	absent	unknown	short	epifaunal or semi-infaunal in a variety of substrates
Mytilinae				
Aulacomya atra	large and folded	short	short	epifaunal on hard substrates
Ischadium recurvum	absent	short with flap	short	epifaunal on hard substrates
Mytilus californianus	large and folded	short with callus	short	epifaunal on hard substrates
Mytilus edulis	large and folded	short	short	epifaunal on hard substrates
Mytilus galloprovincialis	large and folded	short	short	epifaunal on hard substrates
Mytilus trossulus	large and folded	short with callus	short	epifaunal on hard substrates
Perna perna	large and folded	short	short	epifaunal on hard substrates
Perna viridis	absent	short with callus	short	epifaunal on hard substrates
Musculinae				
Gregariella coralliophaga	absent	long with callus	long	semi-infaunal or boring into hard substrates
Musculus discors	absent	short	long	infaunal in sand, mud or algae (byssal nest)
Musculus niger	absent	short	long	infaunal in sand (byssal nest)
Septiferinae				
Mytilisepta bifurcata	large and folded	short	short	epifaunal on hard substrates
Septifer bilocularis	short and sparse	short	short	epifaunal on hard substrates

Supplementary materials

Table S1. References used for compiling habits of life in Mytilidae. Abbreviations: BO=Boring into hard substrate, EF=Epifaunal, IF=Infaunal, SF=Semi-infaunal.

Mytilidae	Habit of life	Substrate	References
Adula diengensis	EF	free-living, mud flats, crevices	Soot-Ryen 1955, Ockelmann and Dinesen 2009
Amygdalum watsoni	IF	soft mud, byssal nest	Lee and Morton 1985
Arcuatula elegans	IF	mud, in a gelatinous byssal net	Morton 1980, Lee and Morton 1985, Ong Cge and Morton 1991, Leung and Morton 1997, 2000
Arcuatula senhousia	IF	sand and mudflats, in a byssal nest	Morton 1974
Aulacomya atra	EF	rocks and mussels	Soot-Ryen 1955
Bathymodiolus brooksi	EF	cold seeps	Duperron et al. 2007
Bathymodiolus childressi	EF	cold seeps	Duperron et al. 2007
Bathymodiolus mauritanicus	EF	hydrocarbon seeps	Turgeon et al. 2009, Lorion et al. 2010
Bathymodiolus thermophilus	EF	hydrothermal vents	Lorion et al. 2010
Benthomodiolus geikotsucola	EF	bone	Lorion et al. 2010
Benthomodiolus lignocola	EF	bone, wood	Lorion et al. 2010
Botula fusca	BO	dead coral	Lee and Morton 1985, Huang et al. 1992, Turgeon et al. 2009
Brachidontes darwinianus	EF	hard substrate, rocks	Tanaka 2005, Trovant et al. 2013
Brachidontes exustus	EF	hard substrate	Turgeon et al. 2009
Brachidontes rodriguezii	EF	hard substrate	Trovant et al. 2013
Crenella decussata	IF	soft substrate	Turgeon et al. 2009, Morton 1974
Dacrydium elegantulum	IF	nest of sand grains, bottom materials, mud	Turgeon et al. 2009, Mattson and Waren 1977, Salas 1996
Geukensia demissa	SF	mud	Owada 2007
Gregariella coralliophaga	BO	rock pools, clusters of *Brachidontes*, vacated bore holes in dead corals	Scott 1980, Morton 1982, Tsi and Ma 1982, Lee and Morton 1985, Turgeon et al. 2009
Idas washingtonia	EF	sunken wood	Samadi et al. 2007
Ischadium recurvum	EF	hard substrate, oyster reefs	Turgeon et al. 2009

Leiosolenus curtus	BO	dead shells, calcareous sandstone	Owada 2015
Lioberus castaneus	EF	hard substrate	Turgeon et al. 2009
Lithophaga antillarum	BO	coral, limestone	Turgeon et al. 2009
Lithophaga lithophaga	BO	limestone	Morton and Scott 1980
Lithophaga nigra	BO	coral, limestone	Turgeon et al. 2009
Modiolus americanus	EF/SF	hard substrate, seagrass	Stanley 1970, Strömgren 1976, Savazzi 1994, Turgeon et al. 2009
Modiolus auriculatus	EF	rocks, rocky sand, seagrass, pilings	Huang et al 1992, Hazek et al. 2014
Modiolus modiolus	EF/SF	sand, mud and rocks	Stanley 1972, Dinesen and Morton 2014,
Modiolus philippinarum	SF	sand and mudflats	Savazzi 1984, Lee and Morton 1995, Sanpanich 2011
Modiolus rumphii	SF	sand	Stanley 1972
Musculus discors	IF	sandy mud, byssal nest among algae	Aitken and Fournier 1993, Merrill and Turner 1963
Musculus lateralis	EF/SF	coarse silt, hard substrate, byssal nest	Pires-Vanin et al. 2014, Turgeon et al. 2009, Bertran 1971
Musculus niger	IF	silty sand, byssal nest	Aitken and Fournier, 1993
Mytilisepta bifurcata	EF	hard substrate, rocks	Seed and Richardson 1999
Mytilus edulis	EF	hard substrate	Stanley 1972
Mytilus galloprovincialis	EF	rocks and pilings	Britton 1990, Lee and Morton 1985, Morton 1987
Mytilus trossulus	EF	hard substrate, rocks	Braby and Somero 2006
Perna perna	EF	hard substrate	Turgeon et al. 2009
Perna viridis	EF	hard substrate, rocks and pilings	Tsi and Ma 1982, Lee and Morton 1985, Morton 1986, Taylor 1993, Leung and Morton 2000
Perumytilus purpuratus	EF	hard substrate	Trovant et al. 2013
Septifer bilocularis	EF	dead corals, on pilings, rocks	Lee and Morton 1995, Huang et al 1992, Sanpanich 2011
Septifer virgatus	EF	corals heads, rocks	Dudgeon and Morton 1982, Lee and Morton 1985, Huang et al 1992, Taylor and Morton 1996
Xenostrobus securis	EF	rocky substrates	Colgan and Costa 2013

Table S2. Phenotypical matrix used to reconstruct ancestral states of key mantle characters and lifestyles.

1. Posterior lobules on the inner mantle fold: (0) absent, (1) present;
2. Exhalant siphon length relative to width: (0) similar or shorter, (2) longer;
3. Mode of life, position relative to substrate: (0) epifaunal, (1) semi-infaunal, (2) infaunal, (3) boring into hard substrate
4. Mode of life, position relative to substrate (binary): (0) epifaunal, (1) semi-infaunal/infaunal/borer

Taxa	**1234**
Anadara notabilis	0000
Bathymodiolus mauritanicus	0000
Bathymodiolus thermophilus	0000
Benthomodiolus geikotsucola	0000
Benthomodiolus lignocola	0000
Brachidontes darwinianus	1000
Brachidontes exustus	1000
Brachidontes rodriguezii	1000
Chione elevata	0121
Dacrydium sp	0021
Geukensia demissa	0111
Glycymeris glycymeris	0000
Gregariella coarctata	0131
Idas washingtonia	0000
Ischadium recurvum	0000
Leiosolenus curtus	0131
Lima lima	0000
Lithophaga antillarum	0131
Lithophaga lithophaga	0131
Lithophaga nigra	0131
Macoma balthica	0121
Malleus albus	0000
Margaritifera margaritifera	0111
Modiolus auriculatus	0000
Modiolus modiolus	0000
Modiolus philippinarum	0011
Modiolus rumphii	0011
Musculista senhousia	0121
Musculus discors	0121
Musculus niger	0121
Mytilus californianus	1000
Mytilus edulis	1000
Mytilus galloprovincialis	1000
Mytilus trossulus	1000
Neotrigonia lamarckii	0021
Nuculana minuta	0121
Nucula sulcata	0021
Ostrea edulis	0000
Pecten maximus	0000
Perna perna	1000
Perna viridis	0000
Perumytilus purpuratus	1000
Pinctada margaritifera	0000
Pinna carnea	0011
Septifer bifurcatus	1000
Septifer virgatus	1000
Xenostrobus securis	1000

CHAPTER 8

Detailed and comparative anatomy reveal further unusual mantle specializations in pen shells (Mollusca: Bivalvia: Pinnidae)

CHAPTER 8

Detailed and comparative anatomy reveal further unusual mantle specializations in pen shells (Mollusca: Bivalvia: Pinnidae)

Abstract

Pinnids are semi-infaunal bivalves with several unusual morphological features, some of them regarded as adaptations to environments with high concentration of suspended sediments. The presence of a waste canal on the mantle wall, for example, helps rejecting surplus sediments from the mantle cavity. The pallial organ, located within the mantle cavity, is thought to be involved in opportunistic prey capture through acid secretion. Despite being such anatomically intriguing bivalves, detailed comparative morphology studies are still scarce. To gain further insights into the functional anatomy of pinnids, we thoroughly investigated the mantle of *Pinna carnea* Gmelin, 1791 by means of scanning electron and light microscopy, including the application of histochemical staining methods. The mantle was also analyzed in nine pinnids from the genera *Atrina*, *Pinna*, and *Streptopinna*, based on archived specimens. Comparative morphology shows a uniform organization of the mantle in Pinnidae, but with variation in pigmentation, presence of commarginal folds, and papillae. Our results revealed intense secretory activity in the inner mantle fold, inner mantle epithelium, and waste canal, including at least three secretory cell types. Secretions are diverse and comprise mainly acidic mucosubstances on the mantle margin, while the waste canal secretes abundant acidophilic material apparently composed of basic proteins, and also possibly lipid content. Based on these results, we hypothesize that efficient mucociliary transportation is achieved in a hydrophobic environment provided by the waste canal, rapidly agglutinating and removing large amounts of sediment from the mantle. Discoid glands secreting protein-rich content were found on the middle mantle fold of *Pinna carnea* and *Streptopinna saccata*. Surprisingly, these organs have hitherto not been recorded in the Bivalvia, therefore representing another unique morphological feature within the Pinnidae.

Keywords: microscopy, mucus, pen shells, secretion, semi-infaunal

Introduction

The family Pinnidae Leach, 1819 comprises subtidal and coastal bivalves often called pen shells, fan shells, or even fan mussels. Pinnids are semi-infaunal bivalves living in sandy and muddy sediments, mainly seagrass beds, but also embedded in coral reefs (Rosewater, 1961). The body is vertically positioned in the sediment with the anterior region deeply buried and anchored by a strong byssus attached to surrounding materials, leaving the enlarged posterior region exposed above the sediment (Grave, 1911; Yonge, 1953).

The fossil record indicates the family Pinnidae dates back to the Lower Carboniferous (330.9–358.9 Ma) with abundant fossil species (Turner & Rosewater, 1958; Cox & Hertlein, 1969). Comparative morphology of shell and muscle scars among fossil and living species suggests an epifaunal origin for the family with a subsequent transition to the infaunal habit (Stanley, 1972). The recent diversity of pinnids encompasses around 55 species in three genera, i.e., *Atrina, Pinna,* and *Streptopinna* (Schultz & Huber, 2013). Based on a very comprehensive taxonomic sampling, a phylogenic study of Pinnidae supported the monophyly of the genera *Atrina* and *Pinna*; however, *Streptopinna* is nested within *Pinna* (Lemer *et al.*, 2014).

Pinnids are distributed in all oceans, occupying shallow waters in temperate to tropical environments (Turner & Rosewater, 1958). Recent investigations have suggested that features related to shell size and shape, as well as boring depth, are habitat adaptations possibly related to bathymetry and sediment composition (Printrakoon, Roopnarine, & Yeemin, 2019). Pinnids are also known to host many commensal organisms, particularly small crustaceans, that find both refuge in the mantle cavity and food supplies in the rejected sediment trapped by the bivalve mucus (Turner & Rosewater, 1958; Sastry & Menzel, 1962; Richardson *et al.*, 1997; Rabaoui, Zouari, & Hassine, 2008; Aucoin & Himmelman, 2010).

The biology and anatomy of Pinnidae were thoroughly investigated in a few species, such as *Atrina fragilis*, *A. rigida*, *Pinna carnea*, and *P. nobilis*, including studies focused on the structure of the shell and the functional anatomy of ctenidia and stomach (Grave, 1911; Atkins, 1938; Yonge, 1953; Purchon, 1957; Turner & Rosewater, 1958; Rosewater, 1961). In addition, the mantle of pinnids has attracted great attention of morphologists because of two specialized structures uniquely found in this family: the pallial organ and the waste canal.

The pallial organ is an elongated structure located in the suprabranchial chamber, dorsal to the anus and extending posteriorly (Grave, 1911). The organ comprises a proximal stalk and a distal, swollen head, which was initially assumed to clean the suprabranchial cavity and remove shell fragments (Yonge, 1953). Later, detailed investigations of *Atrina pectinata* and *Pinna nobilis* revealed that the pallial organ head secretes sulphuric acid, and that these bivalves feed on microcrustaceans (Liang & Morton, 1988; Morton & Puljas, 2018). The pallial organ is thus thought to be involved in opportunistic prey capture, using acidic secretion to stun or kill their prey, which would then be transported by the strong inhalant stream to the gill ciliary tracts and mouth (Morton & Puljas, 2018).

The waste canal was originally described for *Pinna nobilis* (Stenta, 1903) and *Atrina rigida* (Grave, 1911) as a specialization of the mantle that continuously removes pseudofaeces from the mantle cavity. In combination with the posterior extension of the mantle, the waste canal is regarded as a major adaptation for cleansing, strongly associated with the evolution of the pinnid semi-infaunal habit (Yonge, 1953). The canal was described as a ciliated epithelium with mucous glands in *Pinna carnea* (Yonge, 1953). Nevertheless, the nature of their secretions and the distribution of secretory cells along the mantle are still unknown. Similarly, comparative information on mantle morphology is still lacking for the family.

Pinnids are generally found in environments with a high concentration of suspended sediments (Grave, 1911; Yonge, 1953). Given that they are suspension-feeders that use their ciliated gills (i.e., ctenidia) to obtain food particles, they are often faced with the challenge of keeping their mantle cavity clean of surplus sediment that would otherwise obstruct their ctenidial filaments. Further information on mantle anatomy and secretory activity should provide additional evidence to understand pinnid adaptations to live in environments with high concentration of suspended sediments.

The present study investigated in detail the mantle margin of *Pinna carnea* Gmelin, 1791 to gain insights into its anatomy and further investigate its functions. We focused on the secretory activity of the mantle margin and waste canal to elucidate possible roles associated with the infaunal lifestyle. In addition, we comparatively analyzed the anatomy of archived specimens of selected pinnid species to check for patterns in mantle morphology.

Material and Methods

Specimens of *Pinna carnea* were found partially buried in the sand and among debris in Ilhabela (São Sebastião Island, State of São Paulo, Brazil). Prior to fixation, anesthesia was performed with a 7.5% solution of $MgCl_2$, which was slowly added into the seawater container holding the specimen; complete anesthesia was achieved after 3 h. This procedure was adopted to prevent undesired reflexes, such as shell closure, and to allow a gradual anesthesia, thus reducing the chances of muscular contraction. Subsequently, mantle samples were dissected for microscopy procedures, fixed for 3 h at 4 °C in a modified Karnovsky solution (Marian, 2012), and stored in cacodylate buffer.

Mantle morphology was also examined in other nine pinnid species, based on archived specimens of the following collections (Table 1): Museum of Comparative Zoology (MCZ), Museum of Zoology "Prof. Adão José Cardoso" of the University of Campinas (ZUEC-BIV), Museum of Zoology of the University of São Paulo (MZSP), and Smithsonian National Museum of Natural History (USNM). These specimens have originally been preserved in ethanol, and during our survey they were dissected and analyzed under a stereomicroscope.

Histological investigation

Mantle samples of *P. carnea* were completely dehydrated in a graded ethanol series, embedded in resin (Leica Historesin Kit, Germany) and serial sectioned into 4-μm-thick sections. The following staining methods were applied to describe the nature of secretions from different mantle structures (Humason, 1962; Behmer, Tolosa, & Freitas Neto, 1976; Bancroft & Stevens, 1982; Pearse, 1985): hematoxylin and eosin (HE) and toluidine blue and basic fuchsin (TF) were applied for general histological study; Gomori trichrome (GO) and Mallory's trichrome (MA) were used for general investigation and for detection of secretory cells; bromophenol blue (BB) and naphthol yellow (NY) were used to evidence protein aggregates; Sudan black B (SB) was applied to identify neutral lipids; alcian blue (AB) and periodic acid-Schiff stain (PAS) were used to detect mucosubstances in secretory cells, including glycoconjugates with acidic or neutral carbohydrates, respectively.

Scanning Electron Microscopy

Mantle samples were post-fixed, dehydrated, critical point dried, mounted on stubs, coated with gold, and analyzed as described in Audino *et al.* (2015).

Results

Functional pallial anatomy in Pinna carnea

The mantle is a very extensible organ in *Pinna carnea*, being greatly enlarged posteriorly (Fig. 1A). Within the infrabranchial (inhalant) chamber, the inner surface of each mantle lobe bears a waste canal (Fig. 1A, B). Each waste canal is formed by two parallel folds that run from the anterior to the dorso-posterior region where the ctenidia attach to the mantle margin (Fig. 1A, B). The mantle margin is comprised by outer, middle, and inner folds (Fig. 1B). While all marginal folds have similar size along the antero-ventral region, the inner mantle fold becomes much longer and enlarged posteriorly, where it also bears marginal tentacles (Fig. 1A). The middle and outer folds remain similar along the whole mantle margin extension, although in the posterior region brown pigmentation is present on the outer fold. The inner mantle surface varies from whitish to translucent, containing large muscle fibers that form the mantle retractor system (Fig. 1A). In the suprabranchial (exhalant) chamber, numerous commarginal folds are distributed on both mantle lobes (Fig. 1A).

Scanning electron microscopy showed that the whole mantle epithelium is covered with abundant cilia. The middle fold is covered by long and densely distributed cilia on both inner and outer surfaces; putative sensory structures were not found on this fold (Fig. 2A). Longer and more densely distributed cilia are present on the inner mantle fold (Fig. 2B), as well as numerous droplets of possible mucosubstances interspersed with cilia (Fig. 2C). The comarginal folds are also ciliated (Fig. 2D), with cilia organized in bands and patches (Fig. 2E). In general, the inner mantle epithelium is also densely ciliated, particularly between the inner mantle fold and the waste canal (Fig. 2F). Similar to the inner mantle fold, the outer and inner folds of the waste canal have dense, long cilia sometimes interspersed with abundant droplets of possible mucosubstances (Fig. 2G-I).

Three secretory cell types were identified in the mantle epithelium based on their morphological appearance and staining affinities (Table 2). Type I corresponds to secretory cells containing vesicles with fine granular content stained strongly with AB and slightly with MA (in light blue), PAS, SB, and TF (Fig. 3A-E). These cells are abundant on the epithelium of the middle and inner mantle folds, being also present in the inner mantle epithelium and waste canal. Type II secretory cells have large granules with strong affinity for eosin (in pink), MA (in orange), GO (in red), BB and NY (Fig. 3E-L). They are distributed in all mantle regions, but mostly in the inner mantle epithelium and waste canal. Type III secretory cells have very fine granular content that stained slightly with AB, MA (in blue, Fig. 3L), and PAS, and strongly with TF (in pink) and SB (Fig. 3M-O). Beside the inner mantle epithelium, type III secretory cells are very abundant in both folds of the waste canal.

In the posterior region, the middle mantle fold bears numerous discoid structures distributed on its inner surface, at the base of the fold (Fig. 4). After histological investigation, they were identified as a concentration of secretory cells, therefore justifying the term “discoid gland”. Each organ has a cap-like morphology in section and is attached to the middle fold by a short connection (Fig. 4B). Their secretory cells are very elongate; the nuclei are basal and the vesiculated content runs from the base to the apical region, where it is supposedly released. The content had no affinity for AB and PAS, weak affinity for TF (in pink; Fig. 4D), and strong affinity for eosin (Fig. 4C), NY (Fig. 4E), BB (Fig. 4F), MA (in orange) and GO (in red).

Comparative mantle morphology in Pinnidae

The three genera of Pinnidae, *i.e.*, *Atrina*, *Pinna*, and *Streptopinna*, share great similarity in mantle organization (Table 1; Fig. 5). The waste canal is present in all studied species as an enlarged structure in the suprabranchial region (Fig. 5, arrows), frequently exhibiting sediment and agglutinated particles along its extension. The mantle margin has a very elongated inner fold in the posterior region, also bearing abundant marginal tentacles of similar sizes (Fig. 5B, D, I). Pigmentation varies greatly among species, being frequent on the outer and inner folds, with different patterns of spots and bands, ranging from light yellow to dark brown. In *Atrina* (Fig. 5A-H), white papillae can occur on the inner mantle epithelium, as observed in *Atrina seminuda* (Fig. 5A). Multiple commarginal folds are only present in *Pinna* and *Streptopinna* (Fig. 5J, M), located in the suprabranchial chamber of both mantle lobes. Discoid glands were found only in *Pinna carnea* and *Streptopinna saccata* (Table 1; Fig. 4).

Discussion

The functional pallial anatomy of Pinna carnea

Our results with *Pinna carnea* contribute to expand the knowledge of the pinnid mantle structure and function, previously settled by classical anatomical investigations conducted with *Atrina rigida*, *P. carnea* and *P. nobilis* (Stenta, 1903; Grave, 1911). The waste canal is a remarkable feature acting in mantle cleansing, bearing cilia and numerous mucous glands (Yonge, 1953). Cilia type and distribution are in accordance with the conditions required for mucociliary transportation (Sleigh, 1989). Also, the ciliated inner mantle epithelium and waste canal surface of *P. carnea* possibly play an analogous condition to mantle ciliary tracts involved in rejecting particles in other bivalves (Yonge, 1953; Turner & Rosewater, 1958). For instance, particles can be bounded in sticky mucus secreted by mantle glands to be subsequently carried by ciliated rejecting tracts and expelled from the mantle cavity (e.g., Morton, 1977; Sartori & Domaneschi, 2005). In Pinnidae, a string of rejected material is formed within the waste canal and is carried vertically upward until elimination

(Turner & Rosewater, 1958). Dense distribution of long cilia in a large canal possibly facilitates the rapid agglutination of sediment and undesirable particles of various sizes for continuous transport out of the mantle cavity. Correspondingly, the diversity of mantle secretions in *P. carnea* should also play a major role in the efficiency of the cleaning mechanism.

Secretory activity has been intensely studied for the bivalve mantle, mainly focused on mucin producing cells that contain different combinations of polysaccharides and glycoproteins resulting in a viscous fluid (Denny, 1983; Prezant, 1990; Beninger, Veniot, & Poussart, 1999). A previous study conducted with different bivalve species demonstrated the abundance of viscous acid or acid-dominant mucopolysaccharides for particle transport on mantle surfaces (Beninger & St-Jean, 1997). Mucous secreting cells are abundant in the mantle epithelium of scallops (Pectinidae), oysters (Ostreidae), and pearl oysters (Pteriidae), as well as in the mantle margin of ark clams (Arcidae) (Richardson, Runham, & Crisp, 1981; Jabbour-Zahab *et al.*, 1992; Beninger & St-Jean, 1997; Audino & Marian, 2018). A remarkable difference was noted herein for *P. carnea*, in which mantle secretion is performed exclusively by epithelial cells, in contrast to numerous subepithelial secretory cells present in most studied bivalves (Jabbour-Zahab *et al.*, 1992; Beninger & St-Jean, 1997; Audino & Marian, 2018).

Type I secretory cells are probably composed of acidic mucosubstances (AB-positive; Bancroft & Stevens, 1982), which were previously detected in the waste canal epithelium of *Pinna carnea* (Yonge, 1953). Type II secretory cells are highly acidophilic and probably largely composed by basic proteins (BB and NF positive; Pearse, 1985). At higher mucin concentration, cross-links between proteins and polysaccharides molecules cause the formation of a gel network with enhanced viscoelastic properties (Denny, 1983). For instance, in marine snails, biomechanical differences between adhesive and trail mucus (used for locomotion) includes much larger amounts of glycoproteins in the adhesive mucous, suggesting an important role in adhesion by interactions of these macromolecules (Smith & Morin, 2002). In addition, adhesive force and gel formation in snail mucus are known to be enhanced in association with glycoprotein complex and amino acid composition (Zhong *et al.*, 2018).The fact that abundant secretory cells of types I and II were found in the inner mantle surface may indicate that, in addition to lubrication of the epithelia, the resulting mucus of *P. carnea* may have its viscosity and adhesive properties increased, which would explain the rapid and continuous rejection of sediment pellets (Grave, 1911; Yonge, 1953).

Type III secretory cells probably correspond to neutral to acidic mucins (stained slightly with PAS, AB, and MA in light blue; Bancroft & Stevens, 1982). The fact that type III cells also stained with SB in the waste canal of *P. carnea* is certainly striking, because this result suggests the secretion of lipid molecules. Lipid droplets were detected in mucin-secreting glands on the sensory tentacles of a terrestrial snail, but their functions are unknown (Chase & Tolloczko, 1985). Different types of mucin glycoproteins secreted by animal epithelial cells were demonstrated to be extremely hydrophobic and associated with a variety of lipids, which could also increase the gel-forming capability and viscosity of the mucus by enhancing the intermolecular hydrophobic interactions (Kim & Singh, 1990; Rogunova *et al.*, 1997). Therefore, lipid secretion in *P. carnea* could provide a hydrophobic environment along the waste canal, contributing to bound sediment particles within the secretion possibly comprised by highly hydrophobic mucins. However, the lack of specificity of SB for lipids has already been pointed out in previous histochemical studies (Pfüller, Franz, & Preiß, 1977), so the presence of lipids in *P. carnea* should be confirmed in the future with more detailed protocols.

Pinnid mantle margin and discoid glands

The mantle margin in Pinnidae shows great similarity among species, including middle and outer folds relatively small in comparison to the very enlarged inner fold. A major difference is represented by the presence of commarginal folds in the suprabranchial chamber, which are absent in *Atrina* but present in *Pinna* and *Streptopinna*. These structures were previously observed in the posterior mantle lobes of *P. carnea* (Simone, Mikkelsen, & Bieler, 2015). The presence of commarginal folds in *Pinn*a and *Streptopinna* suggests a shared morphological feature, which is in accordance with the phylogenetic history inferred for Pinnidae, composed of two main clades: *Atrina* and *Pinna* (including *Streptopinna*) (Lemer *et al.*, 2014).

In contrast to many pteriomorphian bivalves (Yonge, 1983; Audino & Marian, 2016), sensory structures were not detected on the middle fold of Pinnidae. However, the middle fold of *S. saccata* and *P. carnea* bears discoid glands, which, surprisingly, have hitherto not been recorded in the Bivalvia. While most studied bivalve species exhibit abundant epithelial and subepithelial secretory cells spread on the mantle, the discoid glands of *S. saccata* and *P. carnea* are concentrated in patches along the posterior mantle margin. The secretion of discoid glands is highly acidophilic and likely composed of basic proteins. It is difficult to envisage the role of these glands. Although lubrication of the mantle folds could be a function for their secretion, such role is generally performed by mucous secreting cells diffused throughout the epithelium of the mantle, as already reported for many bivalves (Richardson *et al.*, 1981; Beninger & St-Jean, 1997; Audino & Marian, 2018). Therefore, we hypothesize they are involved with other functions.

Pinnids are known to host many different species of crustaceans, such as Pontoniine shrimps and Pinnotheridae pea crabs (Turner & Rosewater, 1958; Sastry & Menzel, 1962; Aucoin & Himmelman, 2010). Commensal crustaceans live within the mantle cavity of pinnid species, including *P. carnea*, where they found refuge from predators, shelter, and food from particles trapped in mucus of the rejection currents of the host (Johnson & Liang, 1966; Courtney & Couch, 1981; Richardson *et al.*, 1997). By their turn, the behavior of the commensal crustaceans is thought to act as an alarm signal against predators, contributing to pinnid protection by stimulating shell closure (Yonge, 1953; Rabaoui *et al.*, 2008). In addition, several lines of evidence suggest a long-term association between Pontoniine shrimp and pinnids (Aucoin & Himmelman, 2010; Góngora-Gómez *et al.*, 2015). Considering the reported commensalism between pinnids and some crustaceans, and also that crustaceans largely depend on chemical communication (Breithaupt & Thiel, 2010), one hypothesis for the function of discoid glands would be attraction of shrimps by chemotaxis. Surface-bound glycoprotein and peptides are known to act as pheromones in crustacean chemical communication and recognition (Rittschof & Cohen, 2004; Derby & Weissburg, 2014). In addition, experimental studies have demonstrated that pinnotherid crabs are able to chemically recognize their hosts (Sastry & Menzel, 1962; Derby & Atema, 1980). Therefore, the protein secretory content observed in the discoid glands could presumptively serve to attract commensal individuals to the mantle cavity.

Another type of function that could be ascribed to these glands could be protection. Pinnids are prey for a variety of animals, such as sea urchins, crabs, gastropods, and fishes (Wu & Shin, 1998; Printrakoon *et al.*, 2019), yet they have thin, fragile shells and keep their posterior region constantly exposed above the substrate (Yonge, 1953). Given that discoid glands were found only on the posterior region of the mantle, we also speculate that they could be involved in the production of some sort of defensive secretion, e.g., to repel predators. Other bivalves are also known to produce defensive secretions. For example, the mantle margins of *Limaria hians* (Limidae) and *Galeomma takii* (Galeommatidae) secrete noxious substances possibly involved with avoiding predation (Gilmour, 1967; Morton, 1973). Regardless of their function, the discovery of such intriguing organs clearly adds to the unusual specializations of pen shells, and should stimulate further studies to elucidate their roles.

Acknowledgements

The authors acknowledge the grants 2015/09519-4 and 2017/01365-3, São Paulo Research Foundation (FAPESP). This study was financed in part by the Coordenação de Aperfeiçoamento de Pessoal de Nível Superior - Brasil (CAPES) - Finance Code 001. This study is part of the first author's Doctorate's thesis through the Graduate Program in Zoology of the Institute of Biosciences (University of São Paulo). The authors thank the following institutions that provided materials for the development of this study: Museum of Comparative Zoology (MCZ), Museum of Zoology "Prof. Adão José Cardoso" of the University of Campinas (ZUEC), Museum of Zoology of the University of São Paulo (MZSP), Santa Barbara Museum of Natural History (SBMNH), and Smithsonian National Museum of Natural History (USNM). The authors also thank the Center for Marine Biology (CEBIMar–USP), the technical staff, and Prof. Alvaro Migotto for the invaluable support in the collection and analysis of live specimens used in this study. This is a contribution of NP-BioMar (Research Center for Marine Biodiversity – USP).

References

Atkins D. 1938. On the ciliary mechanisms and interrelationships of lamellibranchs: Latero-frontal cilia of the gill filaments and their phylogenetic value. *Journal of Cell Science* 2: 345–435.

Aucoin S, Himmelman JH. 2010. A first report on the shrimp *Pontonia sp*. and other potential symbionts in the mantle cavity of the penshell *Pinna carnea* in the Dominican Republic. *Symbiosis* 50: 135–141.

Audino JA, Marian JEAR. 2016. On the evolutionary significance of the mantle margin in pteriomorphian bivalves. *American Malacological Bulletin* 34: 148–159.

Audino JA, Marian JEAR. 2018. Comparative and functional anatomy of the mantle margin in ark clams and their relatives (Bivalvia: Arcoidea) supports association between morphology and life habits. *Journal of Zoology* 305: 149–162.

Audino JA, Marian JEAR, Wanninger A, Lopes SGBC. 2015. Anatomy of the pallial tentacular organs of the scallop *Nodipecten nodosus* (Linnaeus, 1758) (Bivalvia: Pectinidae). *Zoologischer Anzeiger - A Journal of Comparative Zoology* 258: 39–46.

Bancroft J, Stevens A. 1982. *Theory and Practice of Histological Techniques*. New York, NY: Churchill Livingstone.

Behmer OA, Tolosa EMC, Freitas Neto AG. 1976. *Manual de técnicas para microscopia normal e patológica*. São Paulo: Edusp.

Beninger PG, St-Jean SD. 1997. The role of mucus in particle processing by suspension-feeding marine bivalves: unifying principles. *Marine Biology* 129: 389–397.

Beninger P, Veniot A, Poussart Y. 1999. Principles of pseudofeces rejection on the bivalve mantle: Integration in particle processing. *Marine Ecology Progress Series* 178: 259–269.

Breithaupt T, Thiel M. 2010. *Chemical communication in crustaceans*. New York, NY: Springer.

Chase R, Tolloczko B. 1985. Secretory glands of the snail tentacle and their relation to the olfactory organ (Mollusca, Gastropoda). *Zoomorphology* 105: 60–67.

Courtney LA, Couch JA. 1981. Aspects of the host-commensal relationship between a palaemonid shrimp (*Pontonia domestica*) and the pen shell (*Atrina rigida*). *Gulf of Mexico Science* 5: 7.

Cox LR, Hertlein LG. 1969. Superfamily Pinnacea Leach, 1819. *Treatise on Invertebrate Paleontology, Part N, Mollusca 6*. Lawrence: Geological Society of America and University of Kansas Press, N281–N285.

Denny M. 1983. Molecular biomechanics of molluscan mucous secretions. In: Hochachka PW, ed. *Metabolic Biochemistry and Molecular Biomechanics*. Academic Press, 431–465.

Derby CD, Atema J. 1980. Induced host odor attraction in the pea crab *Pinnotheres maculatus*. *The Biological Bulletin* 158: 26–33.

Derby CD, Weissburg MJ. 2014. The chemical senses and chemosensory ecology of crustaceans. In: Derby CD, Thiel M, eds. *The natural history of Crustacea. Nervous systems and control of behavior*. New York, NY: Oxford University Press, 263–93.

Gilmour THJ. 1967. The defensive adaptations of *Lima hians* (Mollusca, Bivalvia). *Journal of the Marine Biological Association of the United Kingdom* 47: 209–221.

Góngora-Gómez AM, Muñoz-Sevilla NP, Hernández-Sepúlveda JA, García-Ulloa M. 2015. Association between the pen shell *Atrina tuberculosa* and the shrimp *Pontonia margarita*. *Symbiosis* 66: 107–110.

Grave BH. 1911. Anatomy and physiology of the wing-shell, *Atrina rigida*. *Bulletin of the Bureau of Fisheries (United States Bureau of Fisheries)* 29: 409–439.

Humason GL. 1962. *Animal tissue techniques*. San Francisco & London: W. H. Freeman and Company.

Jabbour-Zahab R, Chagot D, Blanc F, Grizel H. 1992. Mantle histology, histochemistry and ultrastructure of the pearl oyster *Pinctada margaritifera* (L.). *Aquatic Living Resources* 5: 287–298.

Johnson DS, Liang M. 1966. On the biology of the Watchman prawn, *Anchistus custos* (Crustacea; Decapoda; Palaemonidae), an Indo-West Pacific commensal of the bivale *Pinna*. *Journal of Zoology* 150: 433–435.

Kim KC, Singh BN. 1990. Hydrophobicity of mucin-like glycoproteins secreted by cultured tracheal epithelial cells: Association with lipids. *Experimental Lung Research* 16: 279–292.

Lemer S, Buge B, Bemis A, Giribet G. 2014. First molecular phylogeny of the circumtropical bivalve family Pinnidae (Mollusca, Bivalvia): Evidence for high levels of cryptic species diversity. *Molecular Phylogenetics and Evolution* 75: 11–23.

Liang XY, Morton B. 1988. The pallial organ of *Atrina pectinata* (Bivalvia: Pinnidae): its structure and function. *Journal of Zoology* 216: 469–477.

Marian JEAR. 2012. Spermatophoric reaction reappraised: Novel insights into the functioning of the loliginid spermatophore based on *Doryteuthis plei* (Mollusca: Cephalopoda). *Journal of Morphology* 273: 248–278.

Morton B. 1973. The biology and functional morphology of *Galeomma (Paralepida*) *takii* (Bivalvia: Leptonacea). *Journal of Zoology* 169: 133–150.

Morton B. 1977. The hypobranchial gland in the Bivalvia. *Canadian Journal of Zoology* 55: 1225–1234.

Morton B, Puljas S. 2018. An improbable opportunistic predator: the functional morphology of *Pinna nobilis* (Bivalvia: Pterioida: Pinnidae). *Journal of the Marine Biological Association of the United Kingdom*: 1–15.

Pearse AGE. 1985. *Histochemistry, theoretical and applied*. London: Churchill Livingstone.

Pfüller U, Franz H, Preiß A. 1977. Sudan Black B: Chemical structure and histochemistry of the blue main components. *Histochemistry* 54: 237–250.

Prezant RS. 1990. Form, function and phylogeny of bivalve mucins. *The Bivalvia—The Proceedings of a Memorial Symposium in Honour of Sir Charles Maurice Yonge*. Hong Kong: Hong Kong University Press, 83–95.

Printrakoon C, Roopnarine PD, Yeemin T. 2019. Ecology of Pinnidae (Mollusca: Bivalvia) from the Gulf of Thailand. *Acta Oceanologica Sinica*: 1–18.

Purchon RD. 1957. *The stomach in the Filibranchia and Pseudolamellibranchia*. Oxford: Blackwell Publishing Ltd.

Rabaoui L, Zouari ST, Hassine OKB. 2008. Two species of Crustacea (Decapoda) associated with the fan mussel, *Pinna nobilis* Linnaeus, 1758 (Mollusca, Bivalvia). *Crustaceana*: 433–446.

Richardson CA, Kennedy H, Duarte CM, Proud SV. 1997. The occurrence of *Pontonia pinnophylax* (Decapoda: Natantia: Pontoninae) in *Pinna nobilis* (Mollusca: Bivalvia: Pinnidae) from the Mediterranean. *Journal of the Marine Biological Association of the United Kingdom* 77: 1227–1230.

Richardson CA, Runham NW, Crisp DJ. 1981. A histological and ultrastructural study of the cells of the mantle edge of a marine bivalve, *Cerastoderma edule*. *Tissue and Cell* 13: 715–730.

Rittschof D, Cohen JH. 2004. Crustacean peptide and peptide-like pheromones and kairomones. *Peptides* 25: 1503–1516.

Rogunova MA, Blackwell J, Jamieson AM, Pasumar-Thy M, Gerken TA. 1997. Effect of lipids on the structure and rheology of gels formed by canine submaxillary mucin. *Biorheology* 34: 295–308.

Rosewater J. 1961. The family Pinnidae in the Indo-Pacific. *Indo-Pacific Mollusca* 1: 175–226.

Sartori AF, Domaneschi O. 2005. The functional morphology of the Antarctic bivalve *Thracia meridionalis* Smith, 1885 (Anomalodesmata: Thraciidae). *Journal of Molluscan Studies* 71: 199–210.

Sastry AN, Menzel RW. 1962. Influence of hosts on the behavior of the commensal crab *Pinnotheres maculatus* Say. *The Biological Bulletin* 123: 388–395.

Schultz PW, Huber M. 2013. *Revision of the worldwide Recent Pinnidae and some remarks on fossil European Pinnidae*. ConchBooks.

Simone LRL, Mikkelsen PM, Bieler R. 2015. Comparative anatomy of selected marine bivalves from the Florida Keys, with notes on Brazilian congeners (Mollusca: Bivalvia). *Malacologia* 58: 1–127.

Sleigh MA. 1989. Adaptations of ciliary systems for the propulsion of water and mucus. *Comparative Biochemistry and Physiology Part A: Physiology* 94: 359–364.

Smith AM, Morin MC. 2002. Biochemical differences between trail mucus and adhesive mucus from marsh periwinkle snails. *The Biological Bulletin* 203: 338–346.

Stanley SM. 1972. Functional morphology and evolution of byssally attached bivalve mollusks. *Journal of Paleontology* 46: 165–212.

Stenta M. 1903. Zur Kenntniss der Strömungen im Mantelraume der Lamellibranchiaten. *Arb. Zool. Inst. Univ. Wien* 14: 211–240.

Turner RD, Rosewater J. 1958. The family Pinnidae in the western Atlantic. *Johnsonia* 3: 285–326.

Wu RSS, Shin PKS. 1998. Transplant experiments on growth and mortality of the fan mussel Pinna bicolor. *Aquaculture* 163: 47–62.

Yonge CM. 1953. Form and habit in *Pinna carnea* Gmelin. *Philosophical Transactions of the Royal Society B: Biological Sciences* 237: 335–374.

Yonge CM. 1983. Symmetries and the role of the mantle margins in the bivalve Mollusca. *Malacological Review* 16: 1–10.

Zhong T, Min L, Wang Z, Zhang F, Zuo B. 2018. Controlled self-assembly of glycoprotein complex in snail mucus from lubricating liquid to elastic fiber. *RSC Advances* 8: 13806–13812.

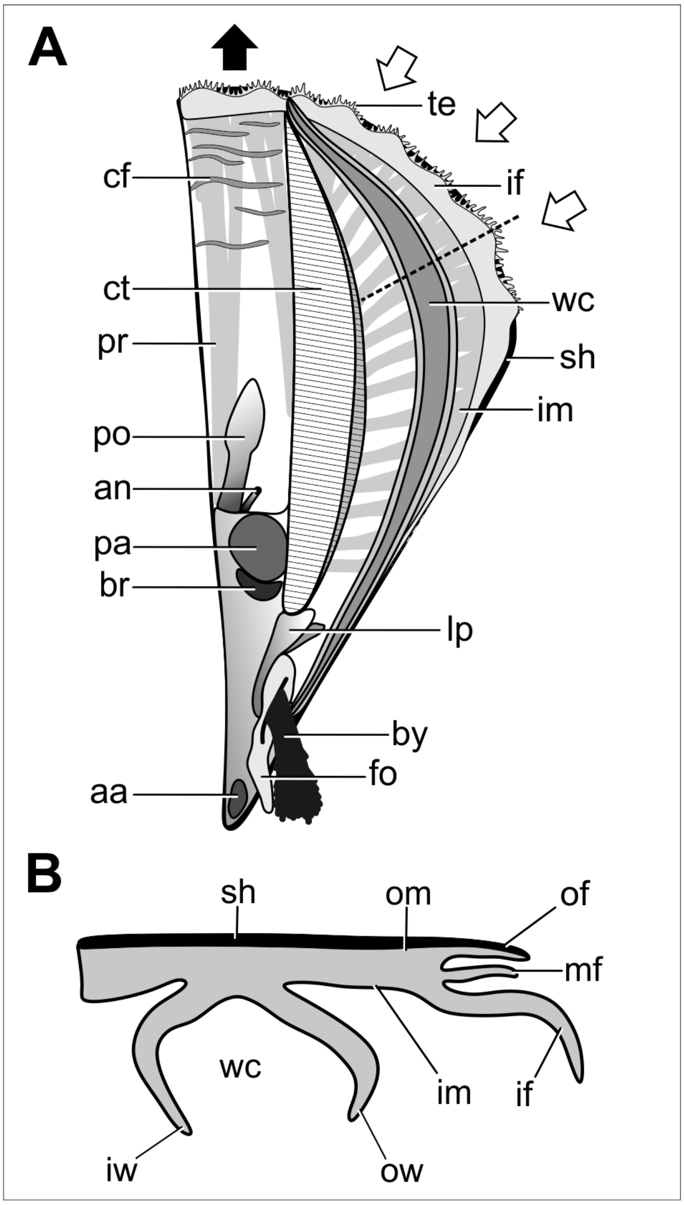

Figure 1. Mantle anatomy of *Pinna carnea*. **A.** Schematic representation of an individual with the left mantle lobe removed to evidence the waste canal; lateral view, ventral to the right and posterior to the top. Water flow is indicated by inhalant streams (white arrows) to the infrabranchial chamber and exhalant stream (black arrow) out of the suprabranchial chamber. The dashed line represents the region of the section illustrated in B. **B.** Schematic section of the mantle (dashed line in A) showing the mantle margin, mantle folds, and the waste canal; distal to the right. Abbreviations: aa, anterior adductor muscle; an, anus; br, byssal retractor muscle; by, byssus; cf, commarginal mantle folds; ct, ctenidium; fo, foot; if, inner mantle fold; im, inner mantle epithelium; iw, inner waste canal fold; lp, labial palps; mf, middle mantle fold; of, outer mantle fold; om, outer mantle epithelium; ow, outer waste canal fold; pa, posterior adductor muscle; po, pallial organ; pr, mantle retractor muscle; sh, shell; te, tentacle; wc, waste canal.

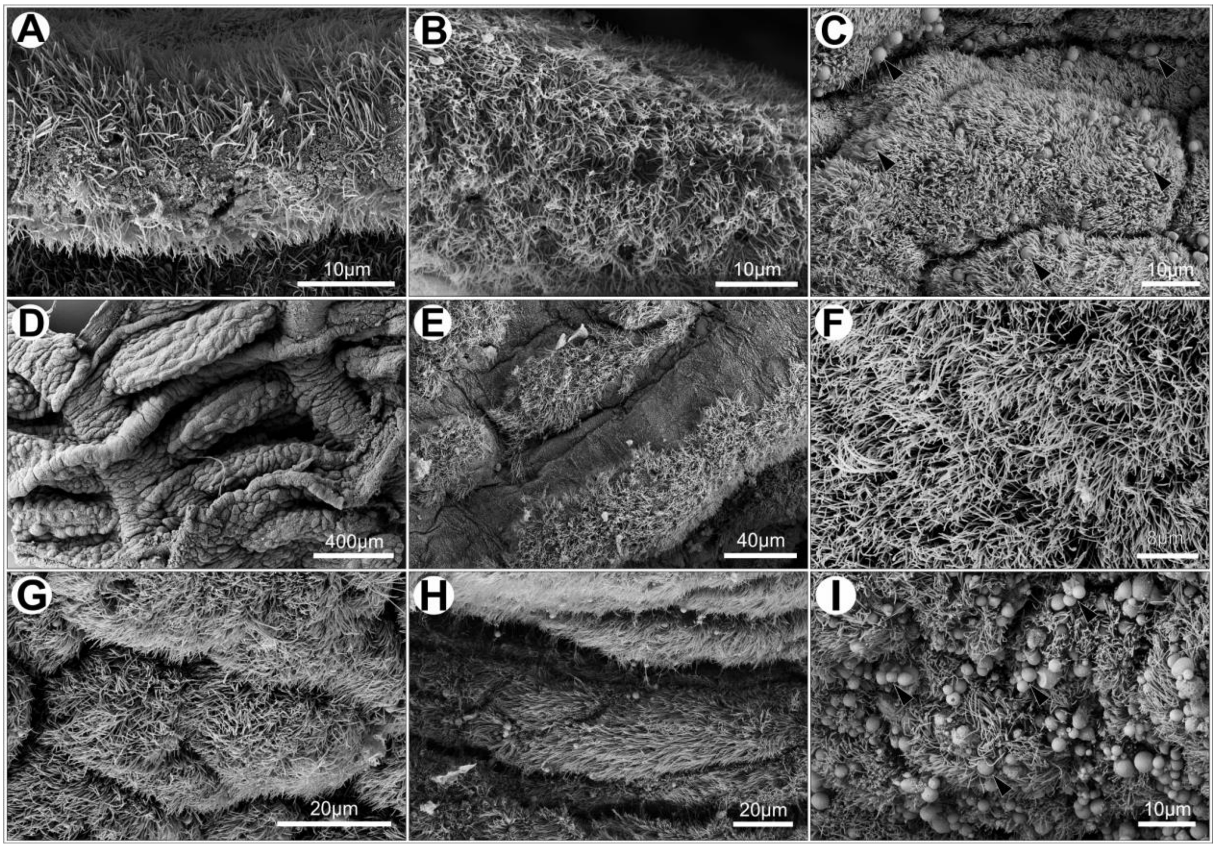

Figure 2. Mantle epithelium of *Pinna carnea*. Scanning electron micrographs. **A.** Cilia distribution on the middle mantle fold. **B.** Cilia distribution on the inner mantle fold. **E.** Detail of the ciliated epithelium of the inner fold, including abundant droplets of secretion (arrowheads). **D.** Commarginal folds in the suprabranchial chamber. **E.** Cilia distribution on the commarginal folds. **F.** Cilia on the inner mantle epithelium. **G.** Ciliated epithelium of the inner fold of the waste canal. **H.** Ciliated epithelium of the outer fold of the waste canal. **I.** Detail of dense ciliary distribution of the waster canal, with abundant droplets of mucosubstances.

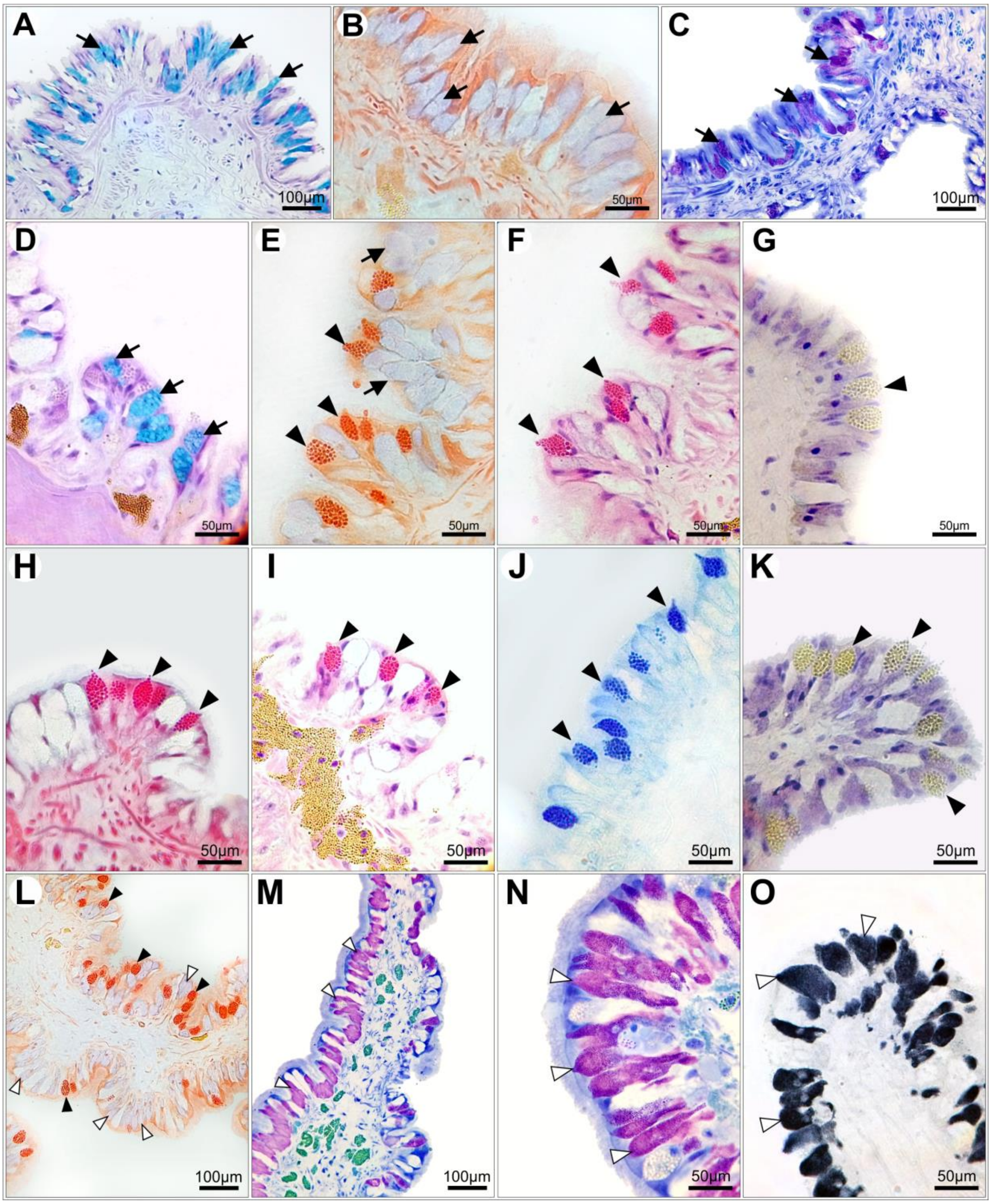

Figure 3. Mantle secretory activity of *Pinna carnea*. Histological sections of the inner mantle fold in A-C, inner mantle epithelium in D-G, and waste canal in H-O. Type I secretory cells is indicated by arrows, type II by black arrowheads, and type III by white arrowheads. **A.** Type I secretory cells, with acidic mucosubstances stained with alcian blue (AB). **B.** Same as A, but stained in light blue with Mallory's trichrome (MA). **C.** Granular content stained in dark purple with toluidine blue and fuchsin (TF). **D.** Periodic acid-Schiff (PAS) and alcian blue (AB); type I secretory cells have strong affinity for AB. **E.** Type I secretory cells are slightly stained in light blue (MA), while type II cells in orange (MA). **F-K.** Type II secretory cells showing strong affinity for HE (pink staining; F and I), naphthol yellow (G and K), Gomori's Trichrome (red staining; H), and bromophenol blue (J). **L.** Type II (orange staining) and type III (light blue staining) secretory cells; MA. **M.** TF staining showing most type III secretory cells distributed on the surface of the canal. **N.** Detail of type III cells stained with TF. **O.** Type III secretory cells showing affinity for Sudan black B.

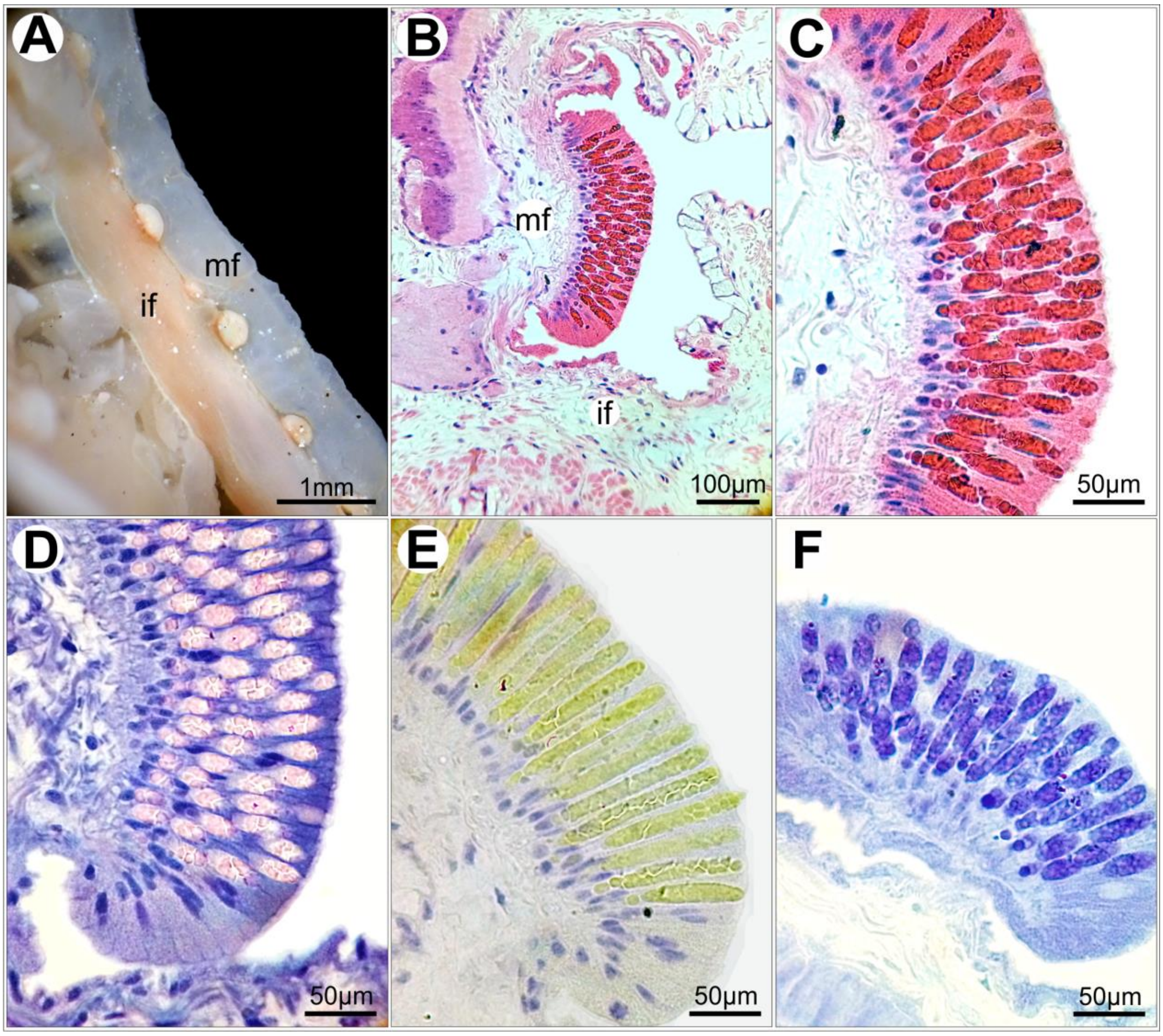

Figure 4. Discoid glands on the middle fold of *Streptopinna sacatta* (A, stereomicrograph) and *Pinna carnea* (B-F, histological sections). **A.** Glands regularly distributed on the inner surface of the fold. **B.** Section of the discoid gland showing its attachment position at the base of the middle mantle fold. **C.** Secretory content organized in vesicles and strongly stained by eosin. **D.** Secretory cells slightly stained by toluidine blue and fuchsin. **E.** Positive reaction to naphthol yellow. **F.** Positive reaction to bromophenol blue. Abbreviations: if, inner mantle fold; mf, middle mantle fold.

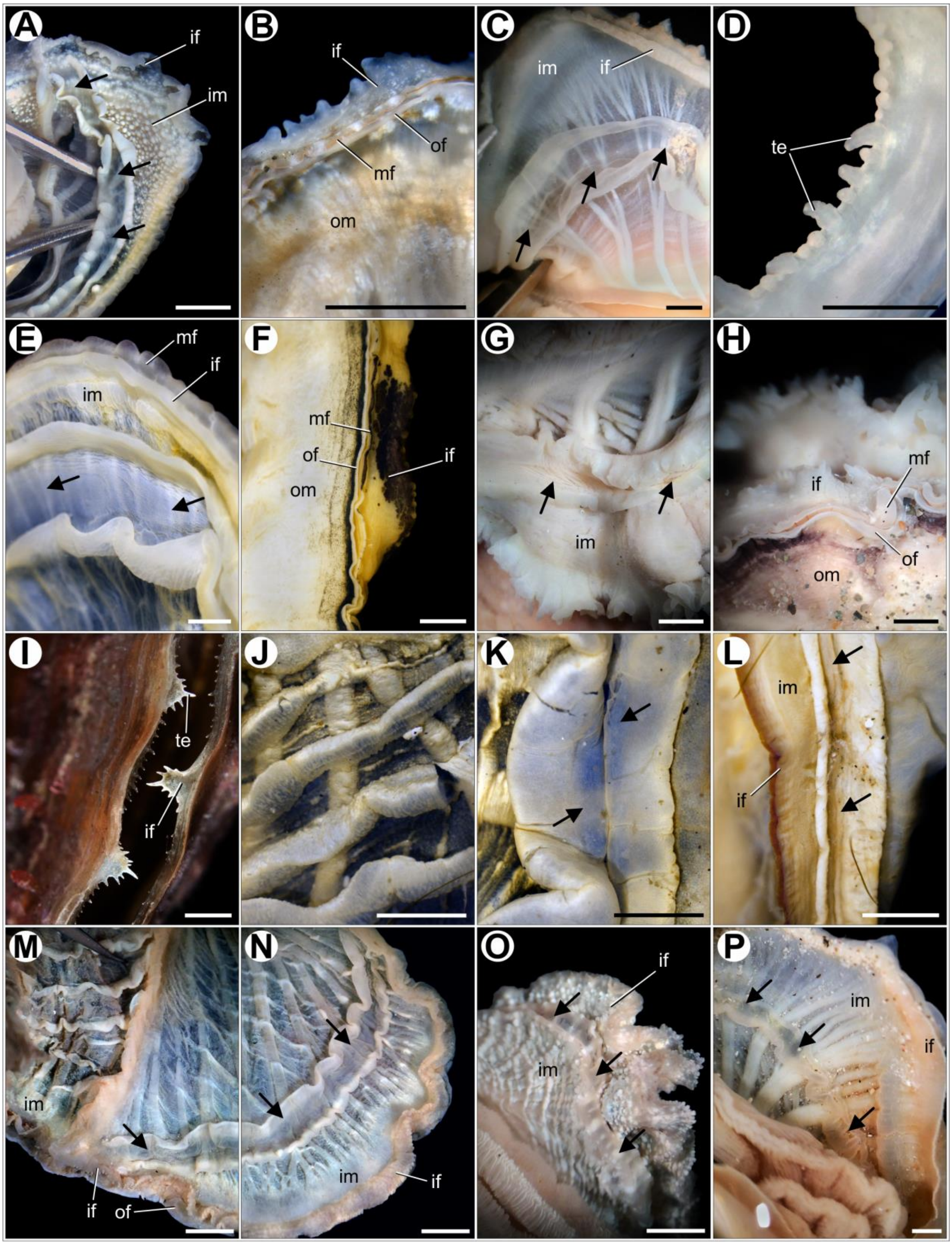

Figure 5. Mantle morphology in Pinnidae. Species of *Atrina* (A-H), *Pinna* (I-O), and *Streptopinna* (P). Detail of the posterior mantle margin in B, D, G, and I; lateral view of the inner mantle surface in the remaining. The waste canal is indicated by arrows. Scale bars=2mm. **A.** *Atrina seminuda* (ZUEC-BIV 2135). **B.** *Atrina seminuda* (ZUEC-BIV 2135). **C.** *Atrina serrata* (USNM 801651). **D.** *Atrina serrata* (USNM 801651). **E.** *Atrina inflata* (MZSP 55029). **F.** *Atrina inflata* (MZSP 55029). **G.** *Atrina rigida* (USNM 847971). **H.** *Atrina rigida* (USNM 847971). **I.** *Pinna carnea* (collected specimen).

J. *Pinna carnea* (MZSP 29040). **K.** *Pinna carnea* (MZSP 29040). **L.** *Pinna rudis* (MZSP 114038). **M.** *Pinna muricata* (MCZ 238056); posterodorsal. Commarginal folds are located in the suprabranchial chamber (left side) **N.** *Pinna muricata* (MCZ 238056); posteroventral region. **O.** *Pinna muricata* (USNM 836526). **P.** *Streptopinna saccata* (USNM 793744). Abbreviations: if, inner mantle fold; im, inner mantle epithelium; mf, middle mantle fold; of, outer mantle fold; om, outer mantle epithelium; te, tentacle.

Table 1. Species of Pinnidae included in the morphological investigation of the mantle, with respective collection and catalog numbers for observed specimens. Presence and absence of the following structures are indicated by + and –, respectively: (1) waste canal, (2) marginal tentacles on the inner mantle fold, (3) comarginal folds on the mantle epithelium of the suprabranchial chamber, (4) discoid glands on the middle fold. Collections: MCZ: Museum of Comparative Zoology; MZSP: Museum of Zoology of the University of São Paulo; USNM: Smithsonian National Museum of Natural History; ZUEC-BIV: Museum of Zoology “Prof. Adão José Cardoso” of the University of Campinas.

Species	**Authority**	**Catalog number**	**1**	**2**	**3**	**4**
Atrina inflata	(Dillwyn, 1817)	MZSP 55029	+	+	–	–
Atrina maura	(G. B. Sowerby I, 1835)	USNM 828614	+	+	–	–
Atrina rigida	(Lamarck, 1819)	USNM 847971	+	+	–	–
Atrina seminuda	(Lamarck, 1819)	ZUEC-BIV 2135	+	+	–	–
Atrina serrata	(G. B. Sowerby I, 1825)	USNM 801651	+	+	–	–
Atrina vexillum	(Born, 1778)	USNM 793718	+	+	–	–
Pinna carnea	Gmelin, 1791	MZSP 29040 USNM 804284	+	+	+	+
Pinna muricata	Linnaeus, 1758	USNM 836526 MCZ 238056	+	+	+	–
Pinna rudis	Linnaeus, 1758	MZSP 114038	+	+	+	–
Streptopinna saccata	(Linnaeus, 1758)	USNM 793744 USNM 780031	+	+	–	+

Table 2. Histochemical affinities of the three secretory cell types found in the mantle epithelium of *Pinna carnea*. Positive and strongly positive reactions to different staining methods are indicated by (+) and (++), respectively, while lack of affinity is denoted by (–). Mantle regions: IM, inner mantle epithelium; IF, inner mantle fold; MF, middle mantle fold; WC, waste canal. Please see Fig. 1B for locations of mantle regions.

Staining method	**Type I**	**Type II**	**Type III**
Alcian Blue	++	–	+
Bromophenol blue	–	++	–
Gomori trichrome (red staining)	–	++	–
Hematoxylin and eosin (pink staining)	–	++	–
Mallory’s trichrome (blue staining)	+	–	+
Mallory’s trichrome (orange staining)	–	++	–
Naphthol yellow	–	++	–
PAS	+	+	+
Sudan black B	+	–	++
Toluidine blue and fuchsin (pink staining)	+	–	++
Regions of higher abundance	IF, MF	IM, WC	IM, WC

CONSIDERAÇÕES FINAIS

CONSIDERAÇÕES FINAIS

O emprego de diferentes abordagens e a análise conjunta dos dados obtidos permitiram ampla investigação sobre a margem do manto em Pteriomorphia, contemplando os objetivos da pesquisa proposta. O conjunto de questões e resultados levantados com este trabalho é inédito para bivalves e não somente amplia o conhecimento sobre Pteriomorphia, como também contribui para o entendimento de questões que extrapolam o grupo-modelo, como irradiações evolutivas, correlação fenótipo-ambiente, convergências evolutivas e adaptação.

A hipótese filogenética de Pteriomorphia foi inferida com base em ampla amostragem taxonômica e até cinco genes. O clado foi recuperado como monofilético, assim como previamente sugerido em estudos filogenéticos de Bivalvia (Steiner & Hammer, 2000; Giribet & Wheeler, 2002; Bieler *et al.*, 2014; Gonzalez *et al.*, 2015; Combosch *et al.*, 2017; Ozawa *et al.*, 2017). Na presente análise, Pteriomorphia está organizada em quatro ordens contidas em dois clados principais (Arcida+Pectinida e Ostreida+Mytilida).

As relações de parentesco entre famílias e ordens, principalmente Mytilida e Arcida, revelaram-se pouco consensuais na literatura, gerando hipóteses conflitantes (Matsumoto, 2003; Bieler *et al.*, 2014; Lemer *et al.*, 2016; Sun & Gao, 2017). Estudos prévios com Arcida, por exemplo, revelaram ampla sensibilidade à amostragem taxonômica e conjunto de dados (Feng, Li, & Kong, 2015; Combosch & Giribet, 2016), o que também foi constatado na presente investigação. A ordem é composta por duas superfamílias, Arcoidea e Limopsoidea, e os dados sugerem que a família Arcidae não é monofilética.

A ordem Pectinida inclui as superfamílias Anomioidea, Dimyoidea, Limoidea, Pectinoidea e Plicatuloidea. Os resultados sugerem o posicionamento de Limoidea como grupo-irmão de Pectinoidea, assim como sugerido em um estudo prévio (Combosch *et al.*, 2017). Entretanto, esse resultado refuta a ordem Limida *sensu* Bieler *et al*. (2014), composta por Limoidea como grupo-irmão de Pectinoidea, Anomioidea, Dimyoidea e Plicatuloidea (Bieler *et al.*, 2014; Lemer *et al.*, 2016). Entre as famílias atualmente reconhecidas dentro de Pectinida, apenas Propeamussiidae não foi recuperada como monofilética.

Nossas análises corroboram a ordem Ostreida sendo composta pelas superfamílias Ostreoidea, Pinnoidea e Pterioidea, bem como o clado Ostreoidea+Pterioidea (Matsumoto, 2003; Lemer *et al.*, 2016). As relações dos gêneros dentro das respectivas superfamílias também estão de acordo com propostas anteriores (Tëmkin, 2010; Lemer *et al.*, 2014; Salvi, Macali, & Mariottini, 2014).

A ordem Mytilida compreende apenas a família Mytilidae, que inclui atualmente dez subfamílias e, de acordo com a análise filogenética, está organizada em dois clados. O presente estudo representa um avanço no conhecimento filogenético do grupo, uma vez que análises prévias da família não abrangiam a diversidade do clado ou eram restritas a grupos particulares, como mexilhões de águas profundas e mitilídeos perfuradores (Owada, 2007; Lorion *et al.*, 2013; Liu, Liu, & Zhang, 2018).

A margem do manto em Pteriomorphia representa uma região anatômica de ampla plasticidade fenotípica e complexa evolução, como demonstrado pelos dados obtidos na presente Tese. Por exemplo, órgãos fotorreceptores da margem do manto surgiram ao menos seis vezes de modo independente, exclusivamente em linhagens epifaunais de Pteriomorphia. Ao todo, cinco tipos morfofuncionais de ocelos paliais (Morton, 2008) ocorrem em 11 famílias do clado. Dados a respeito de hábitos de vida também foram analisados, indicando possível associação entre evolução de ocelos e transição para o hábito epifaunal de ocupação de fendas. Além disso, a perda de ocelos ocorreu múltiplas vezes, principalmente em linhagens que adotaram hábitos infaunais ou semi-infaunais. Em conjunto, os dados levantam novas hipóteses para o surgimento e evolução de órgãos fotorreceptores em Bivalvia, fornecendo evidências para explorar padrões evolutivos e ecológicos de fotorrecepção no bentos marinho.

Órgãos sensoriais, células secretoras e distintos conjuntos musculares estão amplamente distribuídos na margem do manto dos bivalves (Yonge, 1983). O presente estudo caracterizou a inervação, musculatura, atividade secretora e ciliação da margem do manto em representantes das principais famílias de Pteriomorphia, possibilitando a inferência de funções associadas às estruturas paliais. Os diferentes tipos de ocelos são responsáveis por fotorrecepção direcional, ou mesmo formação de imagens de baixa resolução, e estão possivelmente associados à comportamentos de fototaxia, posicionamento do corpo no substrato e alarme contra predadores (Nilsson & Bok, 2017). Outras funções sensoriais também estão presentes, principalmente nos tentáculos de Pectinida e Ostreida, que concentram receptores ciliados e inervados. Tentáculos também protegem a abertura da cavidade do manto, principalmente na região inalante dos representantes de Ostreida e Mytilida. Uma grande diversidade de células secretoras está presente nas pregas paliais, principalmente na prega interna, atuando na lubrificação e limpeza da margem do manto.

A integração dos dados filogenéticos, de morfologia comparada e de anatomia funcional permitiram o reconhecimento de padrões evolutivos em Pteriomorphia. Os dados obtidos sugerem a evolução independente de estruturas paliais, como tentáculos, ocelos, e pregas hipertrofiadas, caracterizando ampla ocorrência de convergências evolutivas em diferentes níveis taxonômicos. Por exemplo, tentáculos surgiram em Pteriomorphia de modo independente ao menos quatro vezes na prega interna do manto e duas vezes na prega mediana. Esses resultados evidenciam a plasticidade do corpo dos moluscos bivalves (Giribet, 2008; Wanninger *et al.*, 2008) e demonstram que convergências evolutivas foram frequentes na irradiação do grupo, assim como sugerido por estudos focados em outras características ecológicas e morfológicas (Distel, 2000; Oliver & Holmes, 2006; Alejandrino, Puslednik, & Serb, 2011; Lorion *et al.*, 2013; Li, Ó Foighil, & Strong, 2016; Serb *et al.*, 2017).

O estudo da evolução da margem do manto em conjunto com mudanças nos hábitos de vida também foi fundamental para explorar mais a fundo questões macroecológicas na irradiação de Pteriomorphia. Em Arcida, por exemplo, convergências evolutivas, como perda de ocelos, redução da prega mediana e hipertrofia da prega interna, estão correlacionadas a múltiplas transições para o hábito de vida infaunal. Tais evidências corroboram a importância do reconhecimento de homoplasias para a compreensão da irradiação do grupo (Oliver & Holmes, 2006), além de levantarem novas hipóteses a respeito da diversificação de Pteriomorphia ao longo do Mesozoico (Stanley, 1972; Vermeij, 1977). Em Mytilidae, a evolução convergente de sifões longos em linhagens que substituíram o hábito epifaunal pelo hábito perfurador ou infaunal representa outro exemplo de correlação evolutiva entre fenótipo e ambiente. De modo geral, os resultados obtidos contribuem para a compreensão da evolução de fenótipos similares em resposta a pressões seletivas e condições ecológicas semelhantes (Schluter, 2000; Losos & Mahler, 2010; Losos, 2011), além de fornecer evidências para compreensão de adaptações em invertebrados bentônicos.

Referências bibliográficas

Alejandrino A, Puslednik L, Serb JM. 2011. Convergent and parallel evolution in life habit of the scallops (Bivalvia: Pectinidae). *BMC Evolutionary Biology* 11.

Bieler R, Mikkelsen PM, Collins TM, Glover EA, González VL, Graf DL, Harper EM, Healy J, Kawauchi GY, Sharma PP, Staubach S, Strong EE, Taylor JD, Tëmkin I, Zardus JD, Clark S, Guzmán A, McIntyre E, Sharp P, Giribet G. 2014. Investigating the Bivalve Tree of Life – an exemplar-based approach combining molecular and novel morphological characters. *Invertebrate Systematics* 28: 32.

Combosch DJ, Collins TM, Glover EA, Graf DL, Harper EM, Healy JM, Kawauchi GY, Lemer S, McIntyre E, Strong EE, Taylor JD, Zardus JD, Mikkelsen PM, Giribet G, Bieler R. 2017. A family-level Tree of Life for bivalves based on a Sanger-sequencing approach. *Molecular Phylogenetics and Evolution* 107: 191–208.

Combosch DJ, Giribet G. 2016. Clarifying phylogenetic relationships and the evolutionary history of the bivalve order Arcida (Mollusca: Bivalvia: Pteriomorphia). *Molecular Phylogenetics and Evolution* 94: 298–312.

Distel DL. 2000. Phylogenetic relationships among Mytilidae (Bivalvia): 18S rRNA data suggest convergence in mytilid body plans. *Molecular Phylogenetics and Evolution* 15: 25–33.

Feng Y, Li Q, Kong L. 2015. Molecular phylogeny of Arcoidea with emphasis on Arcidae species (Bivalvia: Pteriomorphia) along the coast of China: Challenges to current classification of arcoids. *Molecular Phylogenetics and Evolution* 85: 189–196.

Giribet G. 2008. Bivalvia. *Phylogeny and Evolution of the Mollusca*. Berkeley: University of California Press, 105–141.

Giribet G, Wheeler W. 2002. On bivalve phylogeny: a high-level analysis of the Bivalvia (Mollusca) based on combined morphology and DNA sequence data. *Invertebrate Biology* 121: 271–324.

Gonzalez VL, Andrade SCS, Bieler R, Collins TM, Dunn CW, Mikkelsen PM, Taylor JD, Giribet G. 2015. A phylogenetic backbone for Bivalvia: an RNA-seq approach. *Proceedings of the Royal Society B: Biological Sciences* 282: 20142332–20142332.

Lemer S, Buge B, Bemis A, Giribet G. 2014. First molecular phylogeny of the circumtropical bivalve family Pinnidae (Mollusca, Bivalvia): Evidence for high levels of cryptic species diversity. *Molecular Phylogenetics and Evolution* 75: 11–23.

Lemer S, González VL, Bieler R, Giribet G. 2016. Cementing mussels to oysters in the pteriomorphian tree: A phylogenomic approach. *Proceedings of the Royal Society B: Biological Sciences* 283: 20160857.

Li J, Ó Foighil D, Strong EE. 2016. Commensal associations and benthic habitats shape macroevolution of the bivalve clade Galeommatoidea. *Proceedings of the Royal Society B: Biological Sciences* 283: 20161006.

Liu J, Liu H, Zhang H. 2018. Phylogeny and evolutionary radiation of the marine mussels (Bivalvia: Mytilidae) based on mitochondrial and nuclear genes. *Molecular Phylogenetics and Evolution* 126: 233–240.

Lorion J, Kiel S, Faure B, Kawato M, Ho SYW, Marshall B, Tsuchida S, Miyazaki JI, Fujiwara Y. 2013. Adaptive radiation of chemosymbiotic deep-sea mussels. *Proceedings of the Royal Society B: Biological Sciences* 280: 20131243–20131243.

Losos JB. 2011. Convergence, adaptation, and constraint. *Evolution* 65: 1827–1840.

Losos JB, Mahler DL. 2010. Adaptive radiation: the interaction of ecological opportunity, adaptation, and speciation. *Evolution after Darwin: the first 150 years*. Sunderland, MA: Sinauer.

Matsumoto M. 2003. Phylogenetic analysis of the subclass Pteriomorphia (Bivalvia) from mtDNA COI sequences. *Molecular Phylogenetics and Evolution* 27: 429–440.

Morton B. 2008. The evolution of eyes in the Bivalvia: New insights. *American Malacological Bulletin* 26: 35–45.

Nilsson DE, Bok MJ. 2017. Low-resolution vision – at the hub of eye evolution. *Integrative and Comparative Biology* 57: 1066–1070.

Oliver PG, Holmes AM. 2006. The Arcoidea (Mollusca: Bivalvia): a review of the current phenetic-based systematics. *Zoological Journal of the Linnean Society* 148: 237–251.

Owada M. 2007. Functional morphology and phylogeny of the rock-boring bivalves *Leiosolenus* and *Lithophaga* (Bivalvia: Mytilidae): a third functional clade. *Marine Biology* 150: 853–860.

Ozawa G, Shimamura S, Takaki Y, Yokobori S ichi, Ohara Y, Takishita K, Maruyama T, Fujikura K, Yoshida T. 2017. Updated mitochondrial phylogeny of Pteriomorph and Heterodont Bivalvia, including deep-sea chemosymbiotic *Bathymodiolus* mussels, vesicomyid clams and the thyasirid clam *Conchocele cf. bisecta. Marine Genomics* 31: 43–52.

Salvi D, Macali A, Mariottini P. 2014. Molecular phylogenetics and systematics of the bivalve family Ostreidae based on rRNA sequence-structure models and multilocus species tree (V Ketmaier, Ed.). *PLoS ONE* 9: e108696.

Schluter D. 2000. *The ecology of adaptive radiation*. Oxford: Oxford University Press.

Serb JM, Sherratt E, Alejandrino A, Adams DC. 2017. Phylogenetic convergence and multiple shell shape optima for gliding scallops (Bivalvia: Pectinidae). *Journal of Evolutionary Biology* 30: 1736–1747.

Stanley SM. 1972. Functional morphology and evolution of byssally attached bivalve mollusks. *Journal of Paleontology* 46: 165–212.

Steiner G, Hammer S. 2000. Molecular phylogeny of the Bivalvia inferred from 18S rDNA sequences with particular reference to the Pteriomorphia. *Geological Society, London, Special Publications* 177: 11–29.

Sun W, Gao L. 2017. Phylogeny and comparative genomic analysis of Pteriomorphia (Mollusca: Bivalvia) based on complete mitochondrial genomes. *Marine Biology Research* 13: 255–268.

Tëmkin I. 2010. Molecular phylogeny of pearl oysters and their relatives (Mollusca, Bivalvia, Pterioidea). *BMC Evolutionary Biology* 10: 342.

Vermeij GJ. 1977. The Mesozoic Marine Revolution: Evidence from snails, predators and grazers. *Paleobiology* 3: 245–258.

Wanninger A, Koop D, Moshel-Lynch S, Degnan BM. 2008. Molluscan evolutionary development. *Phylogeny and Evolution of the Mollusca* 16.

Yonge CM. 1983. Symmetries and the role of the mantle margins in the bivalve Mollusca. *Malacological Review* 16: 1–10.

RESUMO

Nos moluscos da classe Bivalvia, a margem do manto (ou palial) é geralmente organizada em três pregas e representa um ponto chave na compreensão da irradiação evolutiva do grupo e na conquista de novos nichos ecológicos. Na subclasse Pteriomorphia, agrupamento que reúne bivalves como ostras, vieiras e mexilhões, a margem do manto é amplamente diversa. Além disso, algumas linhas de evidência apontam para a associação entre estruturas paliais e diversificação de hábitos de vida, de modo que essa região anatômica representa uma importante fonte de dados para estudos de adaptação e correlação fenótipo-ambiente. A pesquisa desenvolvida investigou a diversidade morfológica da margem do manto em Pteriomorphia, por meio de abordagens comparativas e funcionais, a fim de inferir a evolução dessa região anatômica e testar hipóteses de homologia, convergência e correlação. A metodologia abrangeu: (1) inferência filogenética de Pteriomorphia com base em 187 espécies e até cinco genes; (2) morfologia comparada de 209 espécies utilizando-se espécimes depositados em coleções científicas, levantamento de caracteres chave do manto e emprego de métodos filogenéticos comparativos; e (3) anatomia detalhada da margem do manto em representantes de 12 espécies das principais famílias de Pteriomorphia, que foram coletados e analisados por meio de histologia, microscopia eletrônica de varredura e microscopia confocal. A análise filogenética de Pteriomorphia indica que o grupo é monofilético e organizado em quatro ordens contidas em dois clados principais (Arcida+Pectinida e Ostreida+Mytilida). A evolução da margem do manto abrange o surgimento de cinco tipos de órgãos fotorreceptores em diferentes linhagens epifaunais, com subsequente perda desses órgãos principalmente em grupos que se tornaram infaunais. Convergências evolutivas foram recorrentes na irradiação dos Pteriomorphia, como é o caso dos tentáculos paliais. Algumas dessas convergências estão correlacionadas a transições para o hábito de vida infaunal, como demonstrado pela hipertrofia da prega interna do manto em representantes de Arcida e Mytilida. A caracterização da inervação, musculatura, atividade secretora e ciliação da margem do manto contribuiu para a compreensão da anatomia funcional das pregas, ocelos, tentáculos, glândulas e demais estruturas associadas. Em suma, os resultados obtidos permitem compreender a evolução da margem do manto em Pteriomorphia associada a mudanças nos hábitos de vida, fornecendo evidências importantes para se explorar questões macroecológicas na irradiação dos bivalves e do bentos marinho como um todo.

Palavras-chave: bivalves, convergência evolutiva, filogenia, microscopia, ocelos, tentáculos

ABSTRACT

The mantle margin in bivalve mollusks typically comprises three folds, being considered a key element in the evolutionary radiation of the class and occupancy of novel ecological niches. In the subclass Pteriomorphia, which includes oysters, scallops, and mussels, the mantle margin is significantly diverse. In addition, several lines of evidence suggest the association between mantle structures and diversification of lifestyles, making the mantle margin a suitable anatomical region for studies focused on adaptations and phenotype-environment correlations. The present investigation evaluated the morphological diversity of the mantle margin in Pteriomorphia, by means of comparative and functional approaches, to infer the evolution of this anatomical region, and test hypotheses of homology, convergence and correlation. The methodology included: (1) phylogenetic inference of Pteriomorphia based on 187 taxa and up to five genes; (2) comparative morphology of 209 species based on observations of archived specimens, survey of key mantle traits and subsequent use of phylogenetic comparative methods; and (3) detailed anatomy of the mantle margin in representatives of 12 species from the most diverse pteriomorphian families, which were collected and analyzed by means of histology, scanning electron microscopy and confocal microscopy. Phylogenetic analyses of Pteriomorphia corroborate its monophyly and indicate it is comprised of four orders divided in two main clades (Arcida+Pectinida and Ostreida+Mytilida). The inferred evolution of the mantle margin suggests the origin of five types of photoreceptor organs in independent epifaunal lineages, with subsequent loss of eyespots mostly in groups that became infaunal. Evolutionary convergences were pervasive in pteriomorphian radiation, as illustrated by multiple gains of mantle tentacles. Some convergences are correlated with transitions to infaunal lifestyles, as demonstrated by the hypertrophy of the inner mantle fold in lineages within Arcida and Mytilida. In addition, the detailed investigation of musculature, innervation, secretory activity and cilia of the mantle margin permitted inferring possible functions performed by mantle folds, eyespots, tentacles, glands and further associated structures. Altogether, the results shed light on the evolution of the mantle margin in Pteriomorphia in association with lifestyle shifts, therefore providing bases to explore macroecological questions in the evolutionary radiation of bivalves and the marine benthos as a whole.

Keywords: bivalves, evolutionary convergence, phylogeny, microscopy, eyespots, tentacles